Structure & Properties of Particulate and Fibre Reinforced Dental Composites

A thesis submitted to The University of Manchester for the degree of
Doctor of Philosophy
in the Faculty of Biology, Medicine and Health

2020

Abdulrahman AlShabib

Division of Dentistry
School of Medical Sciences

Table of Content

Word count ≈ 42000

List of Figures

List of Tables

List of Abbreviation

- **List of Chemical and Materials**

ASTM	American Standard for Testing and Materials
Au/Pd	Gold/Palladium
BisGMA	Bisphenol A Glycidyl Methacrylate
C=C	Carbon double bonds
CQ	Camphorquinone
DMAEMA	Dimethylamino ethylmethacrylate
E-glass	Electrically corrosive resistance glass
GIC	Glass ionomer cement
H_2O	Water
nHAP	Nano-hydroxyapatite
ORMOCERS	Organically-modified ceramics
BaSi	Barium borosilicate glass
TEGDMA	Triethylenglycol dimethacrylate
UDMA	Urethane diacrylates
BisEMA	Ethoxylated bisphenol-A dimethacrylate
PMMA	Polymethyl methyl methacrylate
3-MPS	3-Trimethoxysilyl Propyl methacrylate
THF	Tetrahydrofuran

- **List of Units**

Time

w	Week
d	Day
h	Hour
min	Minute
s	Second

Weight

g	Gram
mg	Milligram
μg	Microgram
Wt%	Weight percentage

Length and distance

m	Meter
cm	Centimeter (10^{-2} m)
mm	Millimeters (10^{-3} m)
μm	Micrometers (10^{-6} m)
nm	Nanometer (10^{-9} m)

Volume

L	Liter
ml	Milliliter
M	Mole

Temperature

°C	Celsius
°F	Fahrenheit

Concentration

ppm	Part per million

Force

N	Newton
GPa	Gigapascal
MPa	Megapascal

- **Other Abbreviations**

DC%	Degree of conversion
DoC	Depth of cure
FTIR	Fourier-Transform Infrared Spectroscopy
ISO	International organization for standardization
LCU	Light cure unit
LSM	Laser scanning micrometer
rpm	Revolutions per minute
SEM	Scanning electron microscope
VHN	Vickers hardness
FT	Fracture toughness
FS	Flexural strength
RI	Refractive index

Abstract

The traditional restorative materials based on amalgam are being replaced by resin composite materials. The wide acceptance of this material is due to several characteristics: it is easy to use, aesthetically pleasing and requires less cavity preparation. Furthermore, it carries fewer environmental risks. Concerns about the use of this material and its performance in the long term are due to issues such as recurring caries and bulk fracture. Clinical data suggest that the most common problems are restoration fracture and secondary caries, therefore these issues deserve investigation. This will require an in-depth exploration of the factors that influence degradation resistance in photo cured fibre reinforced composites. This question is investigated in this thesis, which focuses on the polymeric phase of fibre reinforced composites.

This thesis comprises of four expermintal chapters. In chapter 4 and 5, Three resin-composites incorporating fibres, additional to particle reinforcement, were examined: everX™, NovoPro Fill™ and NovoPro Flow™. Four composites were used as controls, with only particle reinforcement: Filtek bulk Fill™, Filtek bulk one™, Filtek XTE™, and Filtek Flow XTE™. For hardness measurement, specimens were stored dry for 1 h and then in either water or 75% ethanol/water for 1 h, 1 d and 30 d at 37 ± 1°C. VHN decreased for all composites with storage time in both solvents, but more appreciably in 75% ethanol/water. For fracture toughness (K_{IC}) measurements, single-edge-notched specimens were prepared and stored for 1 and 7 d in water at 37°C. K_{IC} ranged from 2.14 (everX Posterior) to 0.96 NovoPro Flow) MPa.m$^{0.5}$.

For sorption and solubility measurements: Over a period of 140 d specimens were weighed at predetermined time intervals, then they were dried for a further 42 days at 37±1°C, to assess the desorption. After 140 days in storage, the water sorption values were found to range between 19.96 and 30.11 µg/mm. XTF exhibited the highest sorption, followed by EVX and NPF, for which both results were similar. In terms of solubility, the range was between -1.49 to 5.28 µg/mm; NPF and XTF were found to have the highest solubility levels, with EVX demonstrating a negative solubility value at -1.49 µg/mm. The hygroscopic expansions at 140 days exhibited results between

1.40 and 2.21%. everX had the highest expansion (2.21%), while NovoPro Fill had the lowest expansion (1.40%).

Within chapters 6, and 7 five experimental fibre-reinforced resin composite materials were evaluated. Controlled changes were made to its matrix chemistry in order to determine how the material's mechanical and physical properties were affected.The following monomer mass fractions were mixed: 50% bis-GMA plus 50% of different ratios of Bis-EMA+UDMA to produce consistent formulations (Groups B-E) of workable viscosities. As control (Group A), a monomer mixture with mass fractions: 60% Bis-GMA, 30% TEGDMA, 10% PMMA (typical FRC monomers) was also studied.

Surface micro-hardness profiles were used as an indirect method to assess the depth of cure (DoC) of experimental fibre reinforced composites. The depth corresponding to 80% of max. VHN, ranged from 3.4 to 4.4 mm. Group B (highest amounts of Bis-EMA) had the greatest DoC (4.4 mm) while group E (lowest Bis-EMA content) had the lowest (3.4 mm). To assess the degree of conversion (DC) moulds with clinically relevant depths (2 mm and 4 mm) were used over the crystal of an (FTIR) spectrometer. DC was measured immediately post-cure. At 2 mm thickness, the lowest DC values were found in group D and E. While, the highest DC values were observed in group A and B, which were significantly higher than other groups. Similar patterns were also observed in the other specimens at 4 mm thicknesses.

For FS measurement, materials were cured in 2 x 2x 25 mm by a LED source. Specimens were stored in water for 1 d, 7 d and 30 d at 37 ± 1°C. For K_{IC} measurements, single-edge-notched (SEN) specimens were prepared: 32 x 6 x 3 mm for 3-point bending and stored for 1, 7 d, and 30 d in water at 37°C. FS decreased for all composites with storage time in water, but more appreciably in group A after 30 d of storage. While for K_{IC} no significant difference was found for each group stored at different intervals (1d, 7 d, and 30 d). At 30 d storage, the experimental composites showed FS, K_{IC} values not significantly different from each other ($P>0.05$).

The results from this study have shown that Bis-GMA/TEGDMA-PMMA and Bis-GMA/Bis-EMA-UDMA based fibre reinforced composite have varying levels of

water sorption and solubility, depending on the type and amount of monomer used. The sorption value of the control group was the highest at 37.8 μg/mm³ and that of experimental composite (group C) was the lowest at 22.6 μg/mm³. This suggests that water storage has a significant effect on the properties of these polymeric matrices.

Declaration

No portion of the work referred to in the thesis has been submitted in support of an application for another degree or qualification of this or any other university or other institute of learning.

Conflicts of interest

The authors do not have any financial interest in the company whose materials are studied.

Abdulrahman AlShabib 2020

Copyright Statement

Dedication

In the name of God, the most gracious the most merciful,

This thesis is dedicated to my family. Special gratitude to my grandmother, mother and my father for their endless care, love and support. Also, to my lovely wife Hanan this work couldn't be done without her unfailing support. This thesis is also dedicated to my brother Meshal, and beloved sisters Haifa, Sarah, Sadeem and Norah.

Acknowledgments

It is impossible to recognize everyone who has lend a hand during my six years training period at University of Southern California and the University of Manchester. Even so, I would like to take note of the following persons for their unrelenting support toward my two degrees and demanding research project. Firstly, I will forever be indebted to my father Nasser and my mother Maha for their love and support throughout my life. Thank you both for giving me strength to chase my dreams, Professors David Watts and Nick Silikas whom accepted my application to the biomaterials program, and guided me throughout my research project. I would also like to thank Dr. Chen for her continuous support as my academic advisor. Equal gratitude goes to the faculty and staff in the Department of Dental Materials, who have made my stay in Manchester enjoyable. Their input goes beyond the support, guidance, and training they provided to bearing with me during the times when I was at my lowest. Also, I would like to recognize the special input of King Saud University for their support which enabled me to conduct the research project.

It has been one of my greatest honours to be acquainted with fellow students, faculty staff, and visiting scientists. While it is impossible to recognize all of them for their special contribution, I am obliged to mention just but a few with who I have worked closely. They are: Dr. Mahir Mirah, Dr. Ahmed Almokhadeb, Dr. Khalid Althagafi, Dr.Maryam Almansour, Dr.Abdulaziz AlHotan and Dr.Hamad Algumiah. Finally, special appreciation goes to my very supportive wife Hanan, who has had the patience and courage to walk the journey with me. It was her unqualified patience and affection that kept me going during my darkest moments. For this, I am forever indebted to her.

The Author

I graduated from King Saud University (2011, Riyadh, KSA), gaining a BDS degree. I currently work as a teaching assistant in the dental restorative department at King Saud University. In 2014, I was awarded a scholarship by the university to continue my postgraduate studies and I became a member of the full-time 27 months clinical training in Operative and Aesthetic dentistry programme at the University of Southern California (Los Angeles, USA). In September 2016, I began a full-time four-year clinical PhD course leading to Doctor of Clinical Dental Science in Restorative Dentistry at the University of Manchester.

During my residency I've been acting as enquiry-based learning and clinical tutor for undergraduate dental students at the University of Southern California and the University of Manchester. I am also a reviewer for the journal of Dental Materials.

Throughout my residency I had the chance to published the following papers:

- **Alshabib, A**., N. Silikas, and D.C. Watts, *Hardness and fracture toughness of resin-composite materials with and without fibers.* Dent Mater, 2019. 35(8): p. 1194-1203.
- Jurado, C. A., Tsujimoto, A., Alhotan, A., Villalobos-Tinoco, J., & **AlShabib, A**. (2020). Digitally Fabricated Immediate Complete Dentures: Case Reports of Milled and Printed Dentures. *The International Journal of Prosthodontics*, *33*(2), 232-241.
- Tinoco, Jose Villalobos, Jurado, C., **AlShabib, A**. & Tsujimoto, A.,"Conservative approach for management of fractured maxillary central incisors in young adults." *Clinical Case Reports*. (accepted)
- **Alshabib, A**., N. Silikas, and D.C. Watts, *Material behaviour of resin-composites with and without fibres after extended water storage.* Dent. Mater. J (accepted)
- **Alshabib, A**., S Brindley and JD Satterthwaite*, Evaluation of the efficacy of two fibre-reinforced post removal techniques.* EJPRD (accepted)

Chapter One

Introduction

1.1 Dental caries

Caries can be defined as a pathological process that results in dissolution of tooth tissues by the by-products of microorganisms [1]. When looking into the pathobiology of dental caries, multifactorial aetiology has been proven [2] in which three essential elements are required to initiate the process: acidogenic bacteria, a fermentable carbohydrate, and tooth surface (Figure 1-1).

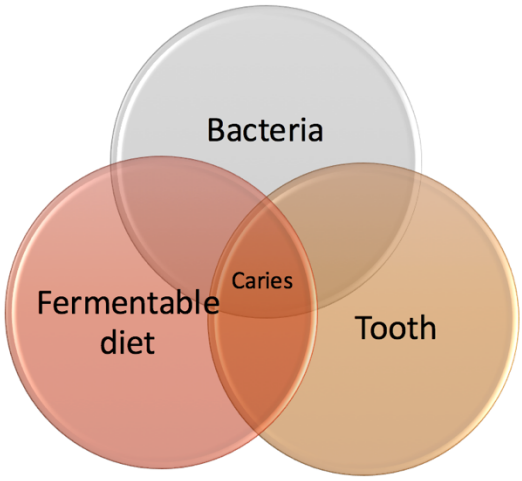

Figure 1-1: Essential etiological factors of dental caries [3]

Dental caries is estimated to be the most common oral disease globally, and a principal cause of tooth loss [4, 5]. It is estimated that approximately 60-90% of children and almost 100% of adults have teeth affected by dental caries [4]. Indeed, dental caries is considered to be the most common infectious disease of childhood [6].

Management of carious teeth is necessary and follows a multilevel approach, comprising early interventions such as topical fluoride application, to more aggressive treatments including the replacement of lost tooth structure by restorative measures. With such a high prevalence of the disease, the overall cost of treatment met by health authorities has been found to range from between 5% and 10% of total health care expenditure. In the United States, for example, spending on dental services was over US$ 124 billion in 2016 [7]. This increased demand for dental treatment has

encouraged researchers to address the limitations and to look for innovative and superior dental restorative materials.

1.2 Direct restorative materials

Remineralisation of incipient lesions may occur as long as good dental hygiene is maintained at an appropriate level. However, cavitated lesions are unlikely to be self-repaired by the remineralisation process; in such cases, surgical intervention is required in order to restore and preserve the remaining tooth from further destruction [8]. Various materials have been introduced as artificial replacements for the lost tooth structure; materials which aim to mimic the tooth's natural structure. Ideal properties for direct restorative material are listed in Table 1-1.

Table 1-1: Requirements of an ideal restorative material [9].

Biological	Mechanical	Miscellaneous
Anti-bacteria	High strength	Tooth coloured
Promote remineralization	Low wear	Bonds to enamel and dentine
Nontoxic/ Non irritant	Dimensional stable	Radiopaque

1.2.1 Amalgam

Dental amalgam was introduced more than 150 years ago as direct restorative material. It consists of a mixture of a silver alloy with mercury [10]. The alloy is composed of fine particles of silver, tin, copper, and traces of zinc. Over the years, dental amalgam has gained the trust of both dentists and patients with outstanding performance as a direct restorative material. Lately, however, concerns regarding the hazards of mercury in dental amalgams to patients and dental staff have led to a decrease in its use. A report was published by the United Nations (UN) in 2002 that illustrated the harmful effects that mercury could have both on people and the environment [11]. The

UN Minamata Convention on Mercury resolved to take action to minimise, control and eliminate the use of mercury by 2020 [12].

1.2.2 Glass ionomer cements

Glass ionomer cement was introduced in 1968 by Wilson and Kent [13]. The cement is composed of a calcium aluminosilicate glass powder and an aqueous solution of an acrylic acid. Glass-ionomer cement has two main advantages over any direct restorative materials. The first advantage is having a reliable chemical adhesion to the mineralised tooth's surface [14]. Moreover, it also has the advantage of an anticariogenic capacity by releasing fluoride ions, together with the capability of fluoride uptake (rechargeability) [15]. Unfortunately, marginal integrity after aging reveals inferior adhesion to enamel surface with greater marginal gaps when compared to resin composites [16], furthermore this cement has inferior mechanical properties, which mostly limits its clinical use for permanent fillings to an interim restorative material [17].

1.2.3 Resin composite

Glossary of Prosthodontics Term defined resin composite as a "highly cross-linked polymeric material reinforced by a dispersion phase of amorphous silica, glass, crystalline or organic resin filler particles and/or short fibres bonded to the matrix by a coupling agent" [18].

Polymethylmethacrylate (PMMA) was introduced in the early 1950s in order to improve tooth coloured restorations which, at that time, were limited to silicate based materials [19], such materials are known to have a composite structure, which is a combination of two (or more) elements producing a new material with desirable properties different from the original components.

Since that time, both the physical and optical properties of dental composites have significantly improved [20]. Such improvements can be attributed to advancements in the fields of both engineering and medical sciences. Another important improvement is the enhancement of both the loading and arrangement of the fillers within the resin

matrix. This development has, in turn, led to significant improvements in composites' physical and mechanical properties.

1.3 Composition of resin composites

Resin composites have three main components:

- Resin matrix (organic phase).
- Coupling agent.
- Fillers (inorganic phase).

1.3.1 Resin matrix

The resin matrix acts as a backbone of dental composite, providing the basis for a complex structure, and therefore influencing the physical and mechanical properties of the restoration [21]. Ideal properties for resin matrix are listed in Table 1-2.

Table 1-2: Ideal requirements for resin matrix [22]

Ideal requirements for dental monomers
Non toxic
Low polymerization shrinkage
High degree of polymerization and cross-linking
Low sorption and solubility
High mechanical properties

1.3.1.1 Dimethacrylate

Bis-GMA 2,2-bis[4-[2-hydroxy-3-(methacryloyloxy)propyl]phenyl] (Figure 1-2) monomer was devolved by Bowen in 1960 [19]; up to this time, Bis-GMA is the most commonly used organic matrix in dental composite. One drawback of this monomer is its high viscosity. To address this issue, manufacturers diluted the Bis-GMA with triethylene glycol dimethacrylate (TEGDMA) as a viscosity modifier (Figure 1-3), in

order to properly disperse the inorganic content into the matrix and to improve the overall handling properties. However, due to the small molecular size, as well as the higher amounts of double bond in (TEGDMA), the material is prone to higher polymerisation shrinkage and water uptake which negatively influences the overall quality of the restoration .

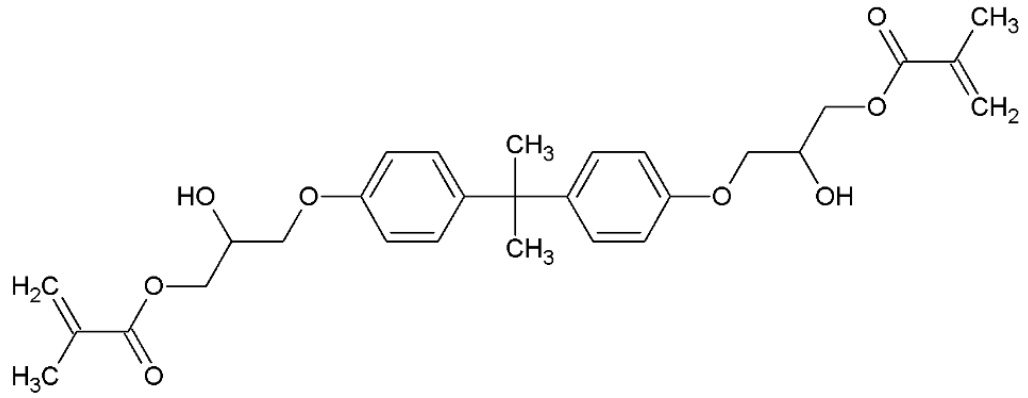

Figure 1-2: Chemical structure of Bis-GMA

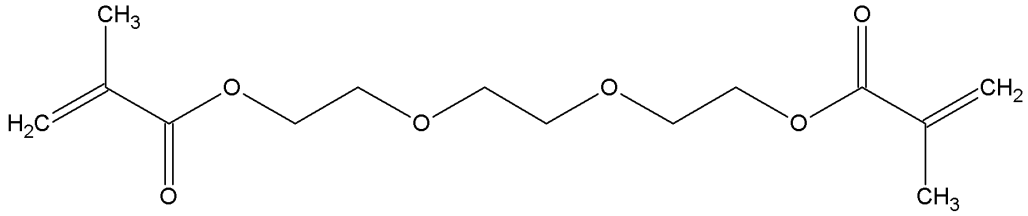

Figure 1-3: Chemical structure of TEGDMA

Other resin composite formulations contains urethane dimethacrylate monomers (UDMA) (Figure 1-4). When looking into this monomer in particular, it can be seen to have lower viscosity compared to the Bis-GMA [9, 23].

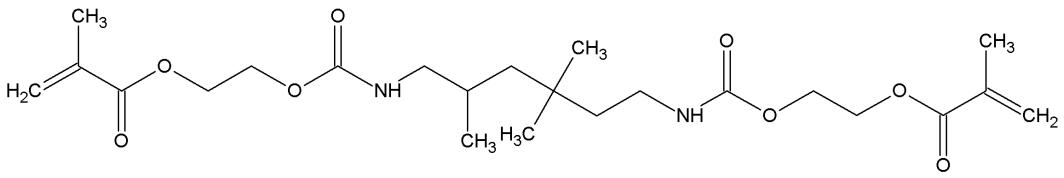

Figure 1-4: Chemical structure of UDMA

The efficiency of polymerisation can be affected significantly by the monomer molecular structure (stiffness, weight etc.) and the ratio of specific monomers within the mixures. The final degree of conversion (DC) of pure Bis-GMA is no higher than 30%. On the other hand, the final DC of pure TEGDMA is more than 60%. The values of combinations of these monomers lie somewhere between these points [24]. Based on the above, we can infer that a different dimethacrylate monomer with a different viscosity will also affect the efficiency of polymerisation. For instance, the ethoxylated versions of Bis-GMA (Bis-EMA), which is commonly employed to limit the shrinkage during polymerisation, have a high molecular weight but their viscosity is relatively low [21, 25, 26].

In the field of dentistry, Bis-EMA is used as a generic term for a large homologous series of ethoxylated bisphenol-A-based dimethacrylate molecules. It is therefore not a single monomer like Bis-GMA or TEGDMA. The index N or M (see Fig.1-5) indicates the degree of ethoxylation (bis-EMA $_{(4)}$ means n + m= 4) (Figure 1-5). There are various Bis-EMAs with different molar weights; these weights are determined by the length of the ethylene oxide chain between the aromatic core and the functional methacrylate groups. If the degree of ethoxylation of Bis-EMA is increased, the viscosity decreases but the conversion increases. However, this also increases water sorption and reduces the flexural strength and modulus [25, 27].

Bis-EMA shares most structural features with Bis-GMA, but without either of the pendant hydroxyl groups (Figure 1-5). Bis-EMA decreases the water sorption of resin, thus allowing its utilisation for complete or partial substitution of Bis-GMA in more recent dental composite materials. UDMA has higher viscosity than Bis-EMA and TEGDMA on account of the hydrogen bond between C=O and -NH groups. Conversely, UDMA has a lower viscosity than Bis-GMA because the hydrogen bonds between amino groups are weaker than in hydroxyl groups [28]. Monomers such as Bis-EMA and UDMA can be combined to lower the viscosity of the composite and reduce polymerisation shrinkage and water sorption [29].

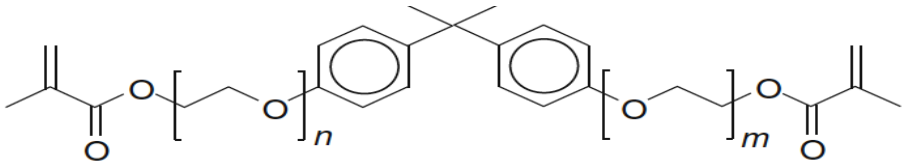

Figure 1-5: Chemical structure of Bis-EMA, n and m are the numbers of the ethoxy structure.

1.3.1.2 Non-Dimethacrylate

- **Organically Modified Ceramics-based Composite (Ormocers)**

A hybrid matrix was introduced in which a certain amount of the conventional resin has been substituted with a chain of polymerised SiO_2 molecules (Ormocers). This type of hybrid matrix was developed at The Fraunhofer Institute for Silicate Research in Wurzburg, Germany, in 1990. This inorganic–organic hybrid polymer was presented as an alternative to the organic resin matrices, to overcome the possible toxic effects of dimethacrylate [30].

The Ormocers-based composite was introduced in 1998, but the research carried out on this composite has reported contrasting results. For example, in comparison to conventional resin composites, a systematic review showed that Ormocers composite materials performed less well [31]. On the other hand, Cavalcante *et al*. published results supporting the use of Ormocers composites. In their *in vitro* study, the surface hardness of two Ormocers resin composite materials and two nano-hybrids were evaluated following different light curing modes and three different storage conditions. Their results showed that a pure Ormocers composite with no additional acrylate-based monomers was better at maintaining surface integrity and its hardness was the least affected by being stored in ethanol or water for seven days, compared to a partial Ormocers or a conventional resin composites [32]. Further research is needed to establish the long-term performance of the Ormocers that are currently being used.

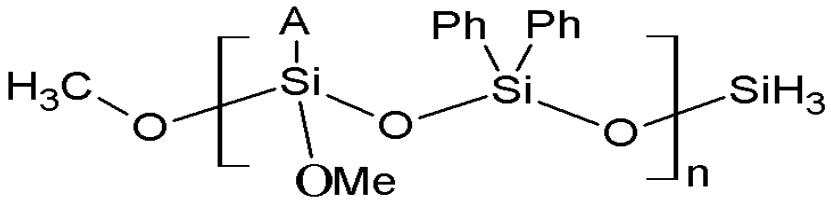

Figure 1-6: Chemical structures of Ormocer

- **Oxirane-Based Composite (Silorane)**

To overcome the problem of polymerisation shrinkage, recent developments in the field of dental composite have been directed to the use of ring-opening systems as a matrix for the dental composite. Oxirane-based resins have shown many desirable properties, such as high flexural strength and fracture toughness [33]. Most importantly, these resins have reduced the material shrinkage associated with polymerisation, and subsequently less polymerisation stress is evident when compared with methacrylate-based resin composite [34, 35]. Despite the significant advantages of silorane-based composite, major problems have been associated colour change and from surface degradation when compared to dimethacrylate-based composite [36].

1.3.2 Polymerization reactions

Resin composites are polymerised through a series of chemical reactions between dimethacrylate resin monomers. The final outcome of the reaction establishes a cross-linked polymer network entailing the filler particles. The process of a polymerisation reaction can be explained through the following steps (Figure 1-7): Free radicals are created either through chemical reaction, light or heat (*Activation)*. Free radicals attack the bonds between two carbon atoms (*Initiation*), thereby forming a strong covalent bond to one of the atoms; this leaves the other carbon atom with an unpaired electron, allowing the reaction to go on and form the polymer chain (*Propagation*). Termination of the process, which can occur for several reasons, for example increase the viscosity of the polymer limiting chain movement (*Termination*) [37].

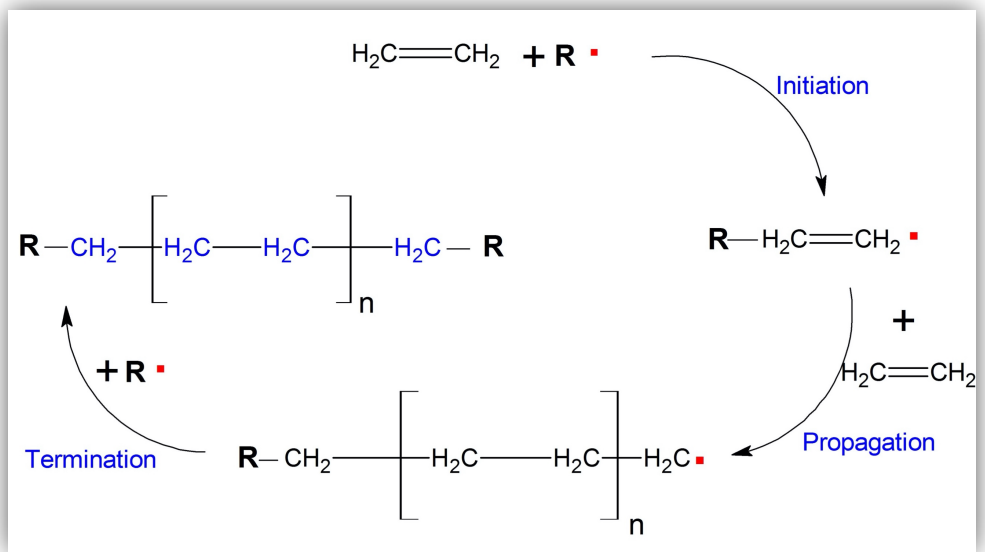

Figure 1-7: Schematic drawing of the free-radical photo-polymerisation process. Red dot represents free radicals.

1.3.2.1 Chemically Activated Resins

Chemically cured resins are supplied in two tubes; one tube contains the initiator (Benzoyl peroxide), with the co-initiator (Tertiary amine) in the other tube. A setting reaction will be triggered with the admixture of both tubes. The shelf lives of these resins were rather restricted, although refrigeration extended them slightly; however, the main challenge is to combine the two pastes into one homogeneous mass which would set satisfactorily in a uniform manner [9].

1.3.2.2 Light-Activated Resins

The idea of developing light-cured resin materials was triggered by the challenges associated with the mixing of chemical cure resins. Light-cured resin comes in a single tube which contains all the constituent elements and chemicals which include initiators and activators. The benefits associated with the resins include time effectiveness since the resinous material can be set within a short time, and a reduced likelihood of air inclusion in the set material since mixing is not necessary.

Camphorquinone (CQ) / amine is the most commonly used photo-initiator system; it has an extended photo-initiation capability, absorbing wavelengths from 360-510 nm,

with peak absorption of 470 nm [38, 39]. However, when the concentrations of CQ/amine are raised beyond their optimum values (between 0.4 and 1.6 wt. %), hardness and degree of conversion reduces [38, 40, 41]. This is probably because there is an excessive absorption of light in the superficial regions, which means that less light is transmitted to the deeper layers, and polymerisation is therefore below optimal levels [41]. Moreover, the lack of colour stability which gives it a tendency to become yellower limiting its use in anterior composites (particularly in enamel shades) [42, 43].

For these reasons, especially due to the yellowing potential of CQ on composites, different photo-initiators have been adopted, such as 1-phenyl-1, 2-propanedione (PPD) and Lucirin TPO. These initiators have absorption peaks near 410 nm and at 390 nm respectively, and have been used as alternatives to CQ.

For optimal polymerisation of light-activated resins, the distance between the light source and the composite should be kept at a minimum distance, regardless of the type of photo-initiator used. Also, the angle of the light curing unit's tip plays a significant role in the quality of the transmitted light energy. Therefore, it should be kept at an angle of 90 degrees over the restoration to optimize light transmission through the depth of the material [9, 44].

1.3.2.3 Dual Cured

In a resin composite where light is used for curing, free radicals are formed where there are photons within the material, and this only occurs up to a certain depth. This contrasts with chemical curing, where the formation of free radicals occurs throughout the material. Whenever the process of light irradiation might be obstructed from reaching the resin, a dual cure resin could be a wiser choice to ensure sufficient polymerisation. They are supplied in two pastes (base paste and catalyst paste); the base contains the photo-initiation system required for visible light activation, with the chemical initiator in the other paste. Chemical polymerisation initially occurs at a slow rate when the two pastes are mixed together [45]. Light-curing acts to speed up the curing rate.

Products that are dual cured continue to be used mainly for luting indirect restorations. They have one main advantage as a luting agent; they have a low viscosity, so can be spread very thinly to make a thin film beneath the crown. Their filler content is therefore much lower than that of similar products used for restorations. Nonetheless, in order to function effectively, care must be taken to ensure that they are mixed properly [45].

1.3.3 Inhibitors

Manufacturers add polymerisation inhibitors to avoid any unintentional polymerisation happening to the resin-based composites, thus affecting their shelf life. Hydroquinone or Butylhydroxytoluene are among of the most frequently used inhibitors for this purpose [9].

1.3.4 Pigment (shade modifiers)

The main advantage of a resin-based composite is its ability to have a close or even exact shade match to the tooth structure. This advantage is mainly attributed to the ability of the metal oxides (pigments) to blend within a complex mixture of an organic and non-organic components [46].

1.3.5 Coupling Agent

One important factor for a successful composite restoration is a strong bond between the inorganic particles and the organic matrix. The greater the disparity between the elastic modulus of the fillers and the resin the more the matrix will deform when subjected to stress [37]. This can have a number of detrimental effects, such as hindering the adhesion between the particles and the resin. Fillers are silanized, to facilitate interaction between the inorganic and organic phases. Silanization is the process of treating a surface with an organofunctional molecule [47]. This process is done to enhance the stress distribution between the resin matrix and the filler particles [48, 49]. The bi-functional molecule attaches to the filler, via a silanol group by a hydrolysis/condensation reaction, so forming a stable covalent bond. While on the other end of the organofunctional molecule, the methacrylate group co-polymerizes

with the methacrylate-based dental resin, forming a strong covalent bond. Several coupling agents are used in dental composites, the most common being 3-methacryloxypropyl-trimethoxysilane (3-MPS) [50].

1.3.6 Fillers

Fillers were first added to resins in the early 1950s [19]. In an attempt to improve their physical properties such as strength and modulus of elasticity, and reduce the polymerisation shrinkage and water sorption, moreover fillers also had an effect on the coefficient of thermal expansion (CTE) by improving it to be closer to the tooth structure. It has been reported that an inverse linear relationship exists between coefficient of thermal expansion (CTE) and filler volume fraction, which suggests a lower CTE value with highly filled materials [51]. This relationship has been observed by researchers whilst investigating the thermal properties of various resin composite [52, 53]. With the recent developments in nanoscience, filler particles that are incorporated into the resin matrix have significantly decreased in size [40]. This improvement has led to the enhancement of the physical properties of a composite resin and the minimising of the undesirable effect of the polymerisation shrinkage. Moreover, increasing the filler content has a desirable effect on the resin's optical and handling properties. The most commonly used fillers in dental composites are quartz, silica, barium borosilicate glass, and zirconium oxide. Filler particles can also be pre-polymerized. These specialized fillers are produced by adding very high concentrations of inorganic micro- or nanofillers to a resin monomer and polymerized under high heat and pressure. After they are polymerized, filler blocks are made by milling the resultant blocks.

Filler load can be represented as a percentage of volume (vol%) or weight (wt%). While higher filler loads correlate with enhanced properties, there is an upper limit after which any further addition of the filler will have the opposite effect, which is between 60 and 70 vol% [54, 55]. Filler particles disperse the smaller forces into the components, leading to adverse conditions for crack propagation. Thus, as posited by Lien , if there is an increase in the number of filler particles, there is a consequential increase in the number of obstacles which can disperse the components of the force

between particles, enabling the crack front to curve [56]. Put simply, a higher filler load increases potential energy loss and crack deflection. Dental composite manufacturer data about filler load should be considered as a guide only, as there is currently no set standard for identifying filler's wt%. A particular point to note is that some manufacturers weigh their fillers before the silanization process, and others after. These differences have been known to give final weight readings with differences of between 2.8 and 9 wt% [57].

When selecting a filler, it is important to consider the composite's optical characteristics. In the composites used in dental field, the monomers usually possess a refractive index of around 1.55 [37]. If the refractive index of the fillers is too far from this value, the composite will become opaque, which limits its depth of cure and it is not as aesthetically pleasing. This is a variable that must be taken into consideration when selecting a filler for use in dental composites.

Table 1-3: Chemical composition of dental resin composite

Component	Example	Purpose
Main Monomer	Bis-GMA, UDMA	Forms The polymer matrix.
Diluent Monomer	TEGDMA	Reduce the viscosity of the polymer matrix.
Inorganic Fillers	Glass, Ceramics, Zirconium, Hydroxyapatite	Improve the physical properties.
Coupling Agent	3-Methacryloxypropyl trimethoxysilane (MPTMS)	Bonds the inorganic component to the resin matrix to the
Photo initiators	Camphoroquinone, ivocerin, 1-phenyl-1,2-propanedione	Initiate the setting reaction
Stabilizers	Hydroquinone monomethylether	Inhibit self-polymerization
Radiopacifier	Barium salts, Strontium	Allow the composite to be evaluated radiographically
Pigments	Iron an titanium oxides	Improves the shade match

1.4 Classification of resin composites

The classification of dental resin composites has been done in various ways, looking into the amount, the size of filler, as well as the method of application of the composite. At present, Luts and Philips classification is the most commonly used classification which is based on the particle size of the inorganic filler [58]. Dental resin composites within this classification are grouped into: microfiller composite, macrofiller composite, hybrid filler composite (a combination of fillers with various particle sizes).

1.4.1 Macro-filled resin composites

Macro-filled composites, also known as conventional composites, were introduced in 1950 [45]. They are obtained through grinding larger quartz and strontium particles into smaller particles ranging from between 15 and 100 μm. Despite the superior physical properties when compared to non-filled resin, there were significant shortcomings with utilising macro-particulate as fillers. In particular, there was a loss of the filler particles, which could be explained by the limited contact area between the filler and the matrix influencing the bonding interface negatively, which eventually adversely affects the polishability of the restoration [59].

1.4.2 Micro-filled resin composites

Micro-filled composite resins show adequate aesthetic qualities due to their excellent polishability and capacity to retain their surface gloss over time. Microfilled composite resins have an average filler size of 40 to 1,200 nm, and relatively low filler content of 30% to 60% by volume [30]. In this class of composite, splintered pre-polymerised resin-**composite** chips are incorporated and mixed in with further monomer to make the composite paste. There are therefore two very different sizes of particles: the original (almost nano) particles *within* the chips as viewed in Fig 1.8 and the sizes of the chips themselves, which could be up to 100 micrometres or more.

These types of materials are not recommended for stress-bearing restorations due to their poor mechanical properties [55]. Moreover, the large amount of organic content and lower filler concentration makes microfilled composite resins more susceptible to water sorption and wear [60].

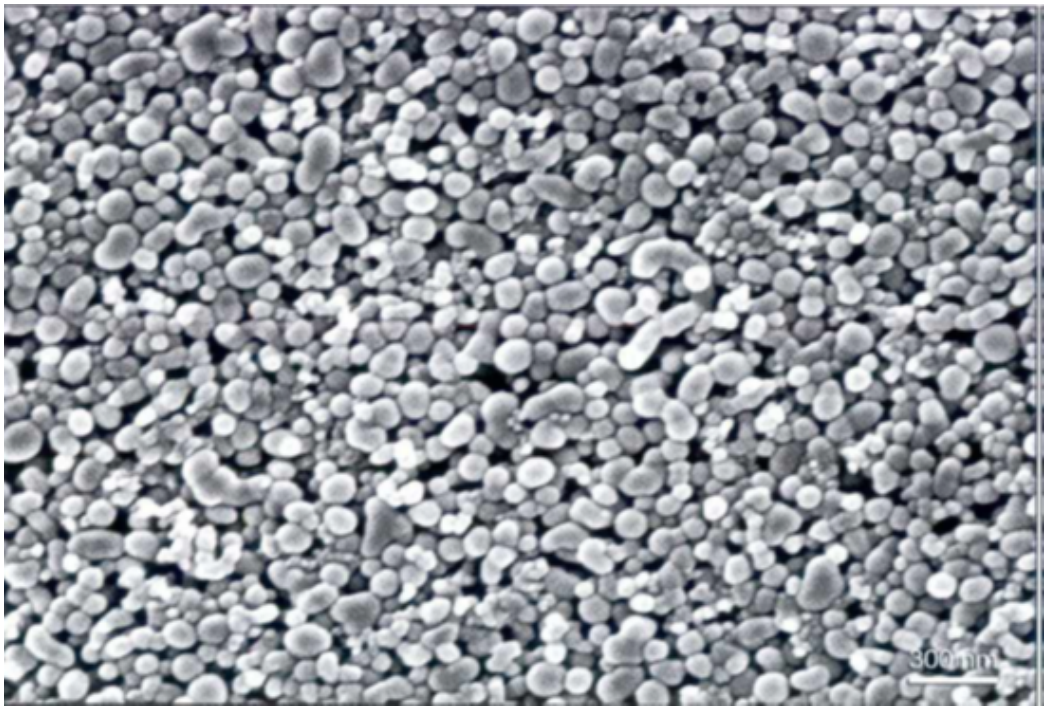

Figure 1-8: SEM image showing fillers of micro-filled composite resins: Durafill™ (magnification x65,000) *[61]*.

1.4.3 Hybrid resin composites

Hybrid composite resins make up a large majority of the available composite resins. They are reinforced by inorganic fillers of different compositions and shapes, with two or more distinct size ranges [62].

Most hybrid composite resins present a filler ratio of 60% to 70% by volume, which leads to significantly improved physical properties when compared to those of micro-filled composite resins. Hybrid composite resins can be sub-classified into three groups according to the filler size:

1.4.3.1 Hybrids

Hybrid composite resins have an average filler size of ≥ 600 nm and an adequate filler ratio, thus supporting their use in stress-bearing areas. They are characterised by irregular shaped fillers with sharp edges that make proper polishing and long-term gloss retention more difficult [30]. Hybrid composite resins are indicated to restore both anterior and posterior teeth; however, they are not ideal for highly aesthetic areas such as the facial surfaces of anterior teeth. An example of a hybrid composite filler is presented in Figure 1-9

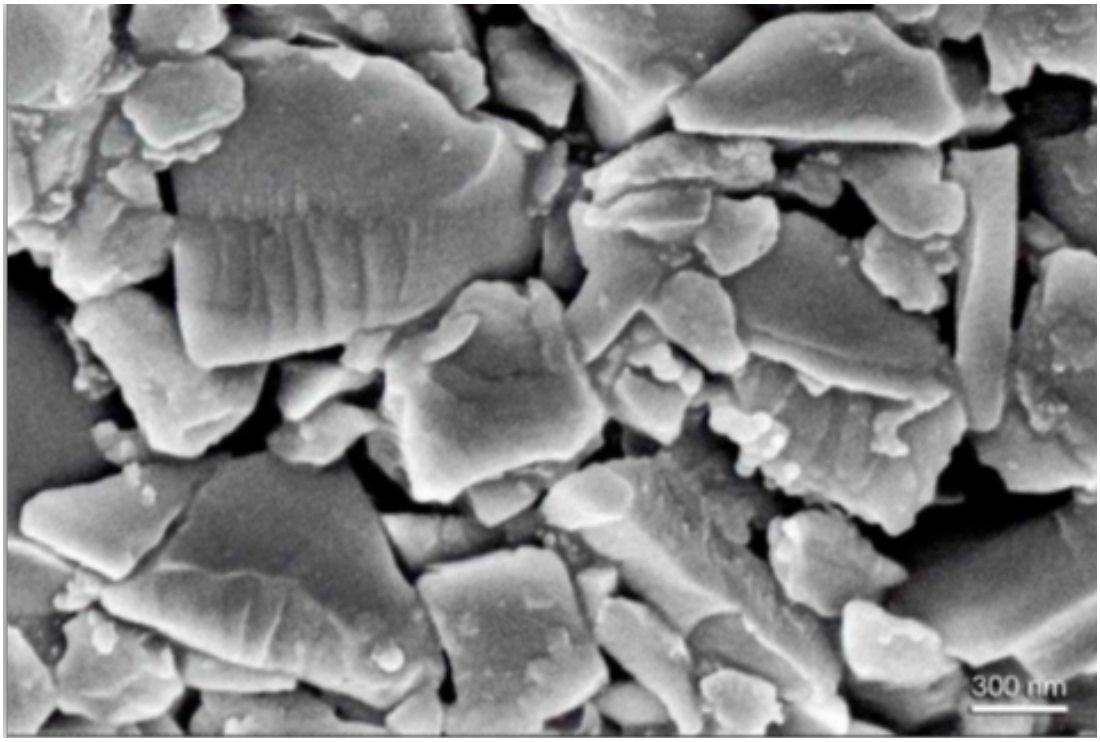

Figure 1-9**:** SEM image showing fillers of hybrid composite resins: Herculite XRV™ (magnification x65,000) *[61]*.

1.4.3.2 Micro-hybrids

Enhanced milling and grinding techniques allowed the formation of submicron particles with sizes averaging 400 to 1,000 nm [62]. Micro-hybrid composite can be effectively used to restore both anterior and posterior teeth [30]. One of the major benefits of micro-hybrids is the incorporation of more rounded filler particles,

therefore improving the surface smoothness and long term gloss retention [61]. An example of a Microhybrid composite filler is presented in Figure 1-10.

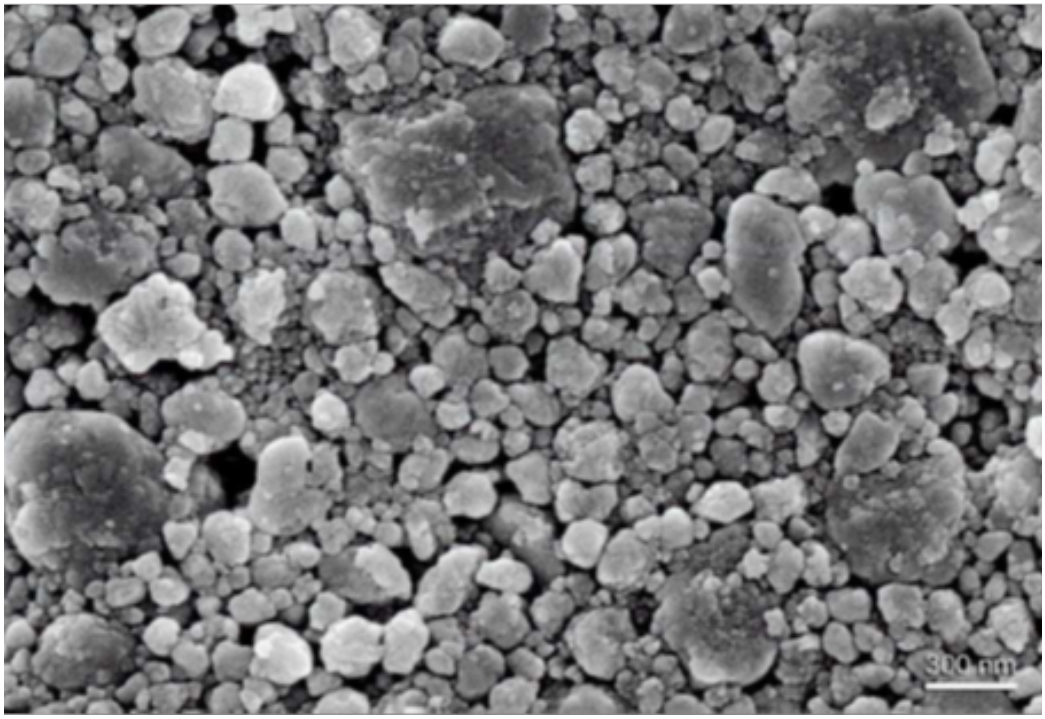

Figure 1-10: SEM image showing fillers of microhybrid composite resins: Filtek Z250™ (magnification x65,000) [61].

1.4.3.3 Nanohybrids

Today, most manufacturers have improved their composite resin formulations to include nanoparticles, prepolymerised, or clusters of nanofillers. These composite resins are classified as nanohybrids. They have an average filler size ranging from 200 to 300 nm [63]. An example of a nanohybrid composite filler is presented in Figure 1-11.

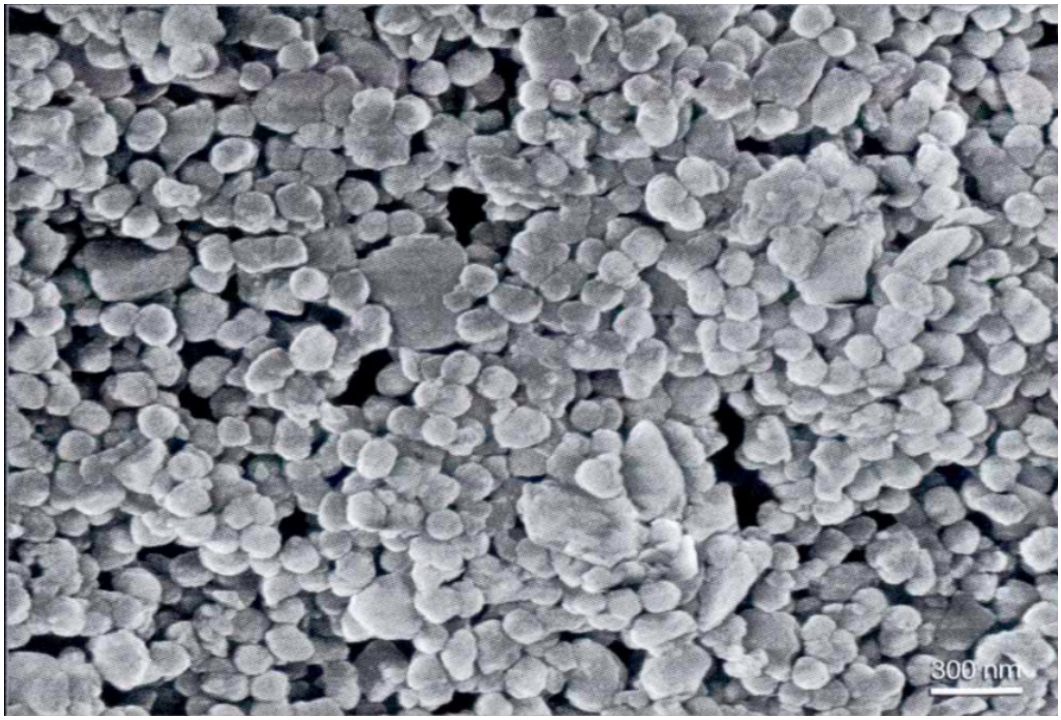

Figure 1-11: SEM image showing fillers of nanohybrid composite resins: IPS Empress Direct™ (magnification x65,000) *[61]*.

1.4.4 Toughening mechanism of particulate filled composite (PFC)

The toughening mechanism is designed to effectively transfer stress to the filler particles from the matrix, which mandates a good filler/matrix coupling and optimal filler content. Fillers would improve fracture toughness through different mechanisms such as crack branching, crack pinning, crack-deflection, and micro-crack induced toughening mechanisms; all of these mechanisms have been covered in detail by a number of studies [64-67].

The tip of a crack curves when it affronts filler, and in this process, the inter-particle space plays the biggest role. If filler particles are closely packed together with very little inter-particle space, then the pattern of crack propagation may be changed since more filler particles interrupt the path of the crack (Figure 1-12). Once critical spacing is reached, this initiates an optional mechanism for passing a particle filler – this

mechanism sets off particle decohesion at the tip of the crack. This is known as the crack pinning effect (Figure 1-13).

A crack does not lead immediately to failure, as there is often a micro-crack which occurs first which lessens the stress and enhances fracture toughness in an effect known as micro-crack-induced toughening. A toughening mechanism is also provided by the matrix-filler interface, due to the plastic deformation around the fillers in the composite matrix.

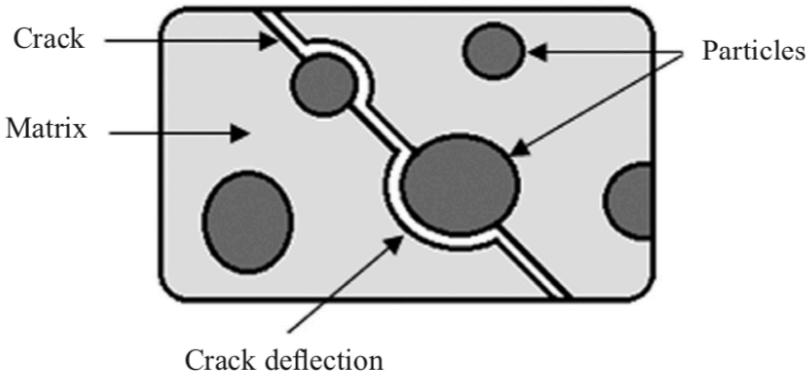

Figure 1-12: Schematic drawing of crack deflection [68].

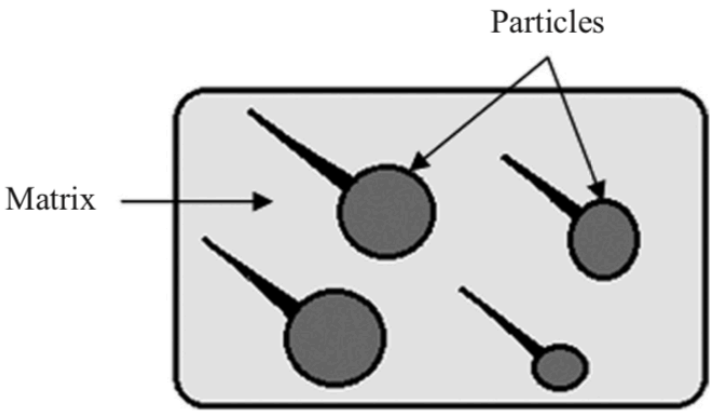

Figure 1-13: Schematic drawing of crack pinning [68].

Filler additives

1.4.5 Fibre Reinforced Resin Composite (FRC)

Several reports have found that in high bearing areas such as cusps of first molars, resin composite might not be an appropriate choice [68-71]. This conclusion is mainly

due to the mismatch between the hardness of the fillers and the resin matrix, in which the forces will be concentrated on the filler particles and this focus will lead to the initiation of cracks within the resin matrix [72, 73]. In order to improve the mechanical properties and load bearing capacity of resin composite, attempts have been made to reinforce the resin with fibres [20]. These fibres enhance composite properties by acting mainly as crack stoppers [70, 74]. This approach was first reported to be used as a reinforcement to polymethylmethacrylate (PMMA), which was later utilised in a different aspect of clinical dentistry [20, 75, 76]. Furthermore, reinforcing the resin with fibres improves the capacity of distributing the stress more efficiently when the loads are concentrated on the restoration [74]. It has also been established that when combining both particulate and fibres as a method of reinforcement, improvements were recognised for both physical and mechanical properties in comparison to particulate-only filled composite [74, 77]. Having said this, several other factors play an important role in ensuring the efficiency of the fibre reinforcement, such as the type of fibre and orientation, distribution, aspect ratio, volume fraction and also the nature of chemical bonding between the fibre and the resin matrix [78].

In clinical dentistry, several fibres have been used as reinforcement; carbon, for example, has been utilised in post and core systems. Unfortunately, the dark colour of the fibres restricts their clinical usage as a tooth-coloured restorative material [79, 80]. On the other hand, glass have favourable aesthetic and chemical properties. Thus, glass fibres have been used as reinforcement for direct restorations [81]. Electrical/E-glass is the most commonly used glass fibre due to its low cost among other glass fibres. It offers a chemical stability at a pH range 4-11 [82]. It consists of 54.5 wt% SiO_2, 14.5 wt% Al_2O_3, 17 wt% CaO, 4.5 wt% MgO, 8.5 wt% B_2O_3 and 0.5 wt% Na_2O. The most common used fibres with their properties are given in **Table 1-4**.

Table 1-4: The most common used fibres with their properties

Fibres	Properties	Reference
Carbon	Excellent fatigue and tensile strength, colour is a major limitation	[79]
Ultra-high molecular weight polyethylene	Adhesion to the resin matrix is questionable, limiting the reinforcement capacity.	[80]
Glass	Good aesthetic properties, adequate physical and mechanical properties.	[81, 83]
Hydroxyapatite	Biocompatible, questionable fatigue properties	[84, 85]

1.4.5.1 Fibre-Related Properties

A number of factors influence the mechanical properties of discontinuous-FRCs, either by enhancing or impairing them. Examples of these factors are the length and orientation of the fibres, the aspect ratio, fibre loading and fibre matrix interaction [78].

1.4.5.1.1 Aspect Ratio & Critical Fibre Length

The influence of the aspect ratio of fibres is closely linked to the subject of critical fibre length. This length may be defined as the measurement of the of the minimum fibre length required for optimal stress transfer within the resin matrix [86]. This length represents the minimum length at which a fibre will fail, midway along its length in an FRC, rather than as interfacial fracture between the matrix and the fibre [87]. It has been found that in fibre reinforced resin composite, the critical fibre length should be 50 times greater than the diameter of the fibre, in order to allow homogenous stress transfer within the resin matrix [87].

Aspect ratio refers to the fibre length to fibre diameter ratio (l/d). Aspect ratio has an effect on the reinforcing efficiency of the fibre reinforced composites (FRC) [88]. In the case of E-glass fibres, the diameter ranges between 8 and 20 μm, averaging between 15 and 17 μm [89]. For the provision of actual reinforcement of the resin

materials in which it is included, it is crucial that the fibre length surpasses the critical fibre length. In most glass systems, this critical length is approximately between 50 and 150 times of the fibre diameter; this fibre length is the smallest fibre length that can allow tensile failure of the fibre, and reduce the likelihood of shear failure of the matrix or the interface [89]. According to Callister et al, short fibres with a subcritical length are not effective, and significantly lower the capacity of any resin containing such short fibres to reinforce sufficiently [90]. Such fibres are unable to achieve maximum failure stress, and are more likely to exhibit deformation of the matrix with low shear stress transfer. As a result, these materials behave as particulate fillers [90].

1.4.5.1.2 **Fibre Loading**

Fibre loading is a measure of how many fibres a material contains. Up to a point, fracture resistance can be improved by increasing the number of fibres embedded in a composite, but then as fibres are added to the resin it raises the materials viscosity and this limits the number of fibres that can be incorporated further. Furthermore, a large number of fibres increases the chances of poor fibre wetting occurring [91], and the composite's workability and handling properties may be negatively affected. The fibres could then cluster together therefore increasing the incidences of voids with in the resin which can act as a reservoir for oxygen [92, 93].

1.4.5.1.3 **Fibre Orientation**

The fibre orientation within the resin composite can be categorised as short discontinuous: random or unidirectional or long continuous: unidirectional or bidirectional. When looking at the influence of the fibre orientation within dental resin, unidirectional fibre arrangements can be either in a continuous or discontinuous course. In this situation both arrangements will show an anisotropic property; while for discontinuous, random fibres, the properties are isotropic [86]. The Krenchel factor (K_θ) is used to describe the efficiency of the reinforcement of FRC, loaded at various levels [94, 95]. If the fibres are unidirectional (all set in one direction), FRC can be said to have K_θ =1 (100%) – the maximum reinforcement level in that direction. Because of the anisotropy produced, however, other loading directions give differing

properties with $K_\theta = 0$. If the fibres are bidirectional (the fibres are set perpendicular to one another), the efficiency is then halved and gives a value of $K_\theta = 0.5$, thus giving equal reinforcement in either direction as well as in orthotropic properties. FRCs which are strengthened using randomly-oriented fibres have $K_\theta = 0.38$ providing they are within flat surfaces, although in three-dimensional structures the efficiency of reinforcement is lowered ($K_\theta = 0.20$) (Figure 1-14) [78, 95].

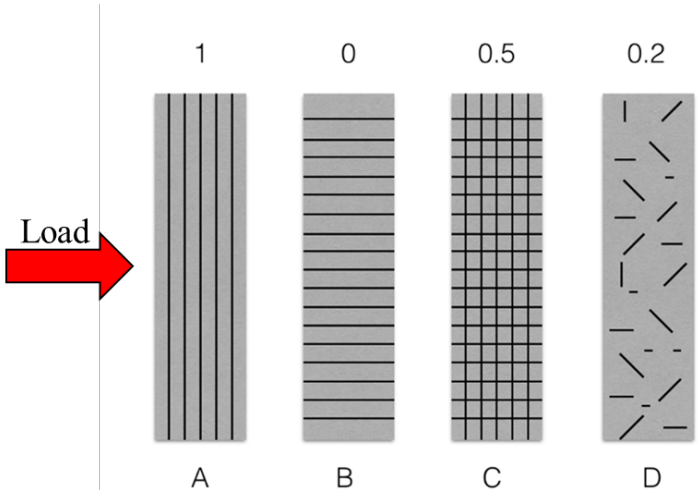

Figure 1-14: Reinforcing efficiency (Krenchel's factor K_θ) of fibres with different orientation . **A:** Unidirectional fibre orientation with reinforcing capacity of 1, **B:** Unidirectional fibre orientation with reinforcing capacity of 0, **C**: Bidirectional fibre orientation with reinforcing capacity of 0.5, **D**: Random fibres orientation with reinforcing capacity of 0.2 in 3D.

The placement of composite in a cavity may result in changing the fibre orientation, which clinically impact alignment of fibres. For instance, the filling technique can contribute to fibre arrangement from the random orientation direction to in-one-plane orientation that causes anisotropic reinforcement. The length of the fibres and size of the cavity influences the discontinuous-FRC. When cavities have smaller width compared to the length of fibres during composite placement, the fibres are arranged in the cavity plane; hence leading to anisotropic features. Multidirectional arrangements of the fibre leading to isotropic properties are enhanced by shorter-scale fibres. Conversely, longer millimetre-scale fibres have the potential for in-one-plane direction providing anisotropic reinforcement.

1.4.5.1.4 Fibre-Resin Adhesion

With regard to clinical longevity, one of the key characteristics is the level of adhesion between the fibres and polymer matrix. This can be an issue because there can be significant differences between deformation behaviour between the two constituents. This leads to high stress levels close to the interface between the two materials [50, 96]. If adhesion is weak, the mechanical properties can be compromised; strong adhesion is required for the material to possess high modulus and strength. The majority of discontinuous fibres employed in dentist work are inorganic and they generally form weak bonds with organic resin matrices [97]. Fibres must therefore be treated with a silane coupling agent in order to increase the bonding between the fibres and resin matrix [50].

1.4.5.2 Performance of Commercially Available FRC

There are currently seven dental discontinuous-FRCs available, namely Alert™, Nulite F™, Restolux™, everX™, everX flow™, NovoProFill™, NovoProFlow™ (Table 1-5). Two of these products Alert™ and Nulite F™ were evaluated clinically by van Dijken who observed that both are linked with non-uniform fibre distribution and surface roughness leading to progressive wear. Van Dijken highlighted differences between materials and suggested that these are associated with the size and quantity of glass fibres, the geometry of the fibres, and the fibre-matrix bond [98]. In the case of Restolux, this product has recently been withdrawn from use; however, several studies demonstrate its behaviour in vitro. Good fatigue resistance is enabled with the presence of a fibre, although the length of the fibres was not sufficient for any improvement in mechanical properties [99-101].

Alert™, Nulite F™, Restolux™ all are considered to low aspect ratio composites, with lengths varying between 60 μm and 200 μm and diameters from 6 μm to 15 μm (**Table 1-5**). Which could explain their limited reinforcing capability. Garoushi demonstrated that with high aspect ratio E-glass fibre reinforced composite, there was notable improvement in flexural strength when compared to the non-fibre filled resin composite [69]. Other reports confirmed this and showed improvements in the

composites' mechanical properties such as stiffness, strength, toughness, and fatigue resistance [102]. Based on these positive findings, GC Corp developed two commercially available short fibre resin composites (everX Posterior ™; everX Flow ™). These products are composed of short E-glass fibre and particulate barium glass fillers, with an average fibre diameter of 17 μm and a length ranging from 1.3 to 2 mm for everX Posterior in a Bis-GMA, TEGDMA, and PMMA matrix, and 300 to 400 μm with diameter of 7 μm for everX Flow in a Bis-EMA, TEGDMA, and UDMA matrix [83, 103].

Improved resistance to crack propagation was seen in both everX Posterior and in everX flow, evidently due to this material's fibre and matrix-related properties. Both materials contain fibres which are longer than the critical fibre length [103-106] which are more effective in transferring stress from the matrix. According to its *Instructions for Use* everX posterior and everX flow should only be used as dentine replacement and thus should be covered by a conventional particulate filled composite. However, in certain clinical situations such a procedure may not be feasible [107, 108]. In such situations water or saliva, can come into contact with glass fibre by exposing the glass fibres during finishing the restoration, by cracks in the composite, the proceeding of the saliva and water along the interface is much greater than the diffusion through the polymer matrix. This is due to the capillary effect of the glass fibre.

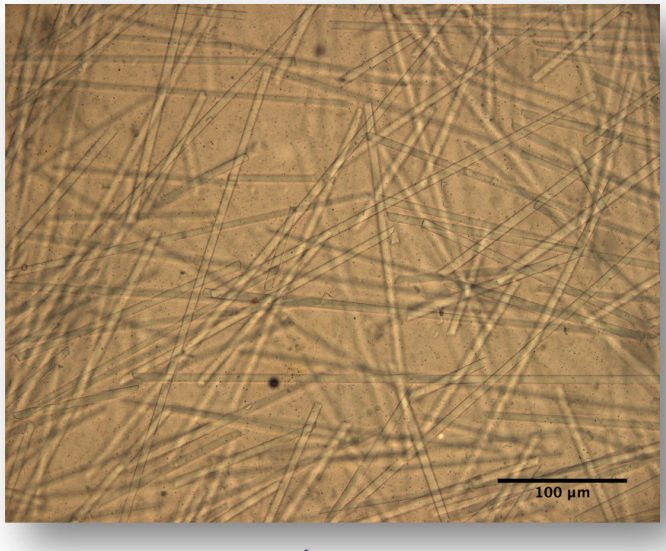

A

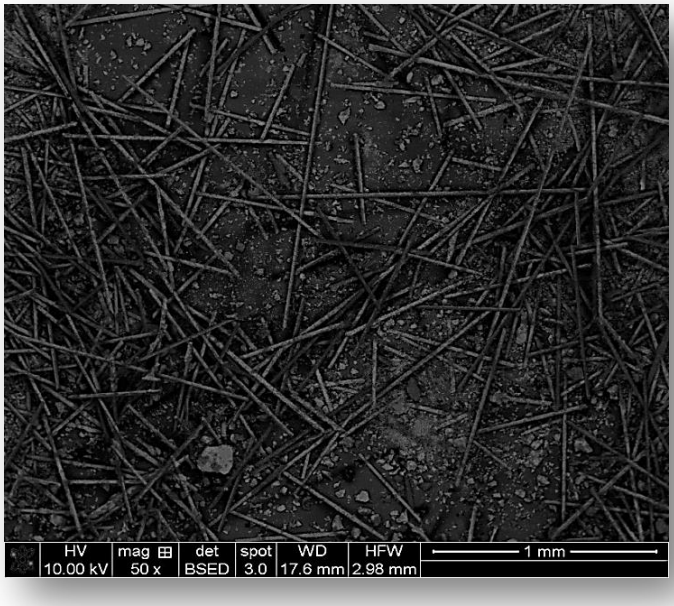

B

Figure 1-15: **A**: Optical microscopic images (x10) of randomly aligned short glass Fibres (everX posterior ™) **B**: Scanning electron microscopy (SEM) images obtained in back scattered electrons mode (x50) of extracted short glass Fibres from the same material.

Table 1-5: Commercially available Discontinuous-FRCs

Material	Fibre length	Fibre diameter	Aspect ratio	Filler type	Filler loading Wt%	Manufacturer	Reference
Alert	60-80 µm	6-10 µm	6-13	Crushed and chopped glass fibre	84%	Jeneric/ Pentron, Wallingford, CT, USA	[101]
Nulite F	150-200 µm	9 µm	16-22	Micro-rod glass	83%	Nulite System International PTY Ltd, Hornsby, Australia	[98]
Restolux	80-120 µm	10-15 µm	5-12	Chopped	85%	Lee Pharmaceutical, South El Monthem	[98]
everX Posterior	0.3-2 mm	17 µm	18-125	E-Glass fibre	74.4%	GC corporation, Tokyo, Japan	[83]
everX Flow	300-400 µm	7 µm	43-57	E-Glass fibre	70.0%	GC corporation, Tokyo, Japan	[103]
NovaPro Universal	Not available	Not available	Not available	Hydroxyapatite fibres	77%	Nanova Inc., Missouri, USA	Manufacture information
NovaFlow	Not available	Not available	Not available	Hydroxyapatite fibres	77%	Nanova Inc., Missouri, USA	Manufacture information

The employment of nanoscale fibres is expected to outperform microscale fibres as the reinforcement material of choice for dental composites. A major advantage of this arrangement is the high strength of the nanofibres, which will provide additional support for the resin composite in terms of physical and mechanical properties, as it will act as a stopper for any crack propagation.

Due to the biocompatibility of hydroxyapatite [84], researchers were able to utilise hydroxyapatite as a reinforcement in dental resins to improve their mechanical properties. The material could be employed in various forms, such as particulate fillers [109] or fibres [85]. Chen et al. have found that when using hydroxyapatite nanofibres

with high aspect ratios of from 600 to 800, significant improvements were noticed in the biaxial flexural strength with 10 wt% hydroxyapatite nanofibres. However, the authors noticed that with increasing the load of hydroxyapatite nanofibres up to 40 wt%, the mechanical performance was negatively affected. They attributed this outcome to the clustering of the nanofibres within the dental resin and therefore concluded that at a certain loading limit (10 wt%), further loading of the resin with the nanofibres would have a negative influence [85].

With the evidence of the positive influence of nanofibres on resin composites [85, 110], a nanohybrid resin composite reinforced with hydroxyapatite nanofibres (NovoPro Fill ™) was recently introduced on the market by Nanova Biomaterials [111] (Figure 1-16). However a recent study looked into the efficacy of the reinforcement provided by the nano-hydroxyapatite fibres found that short (millimetre scale) e-glass fibre reinforced composite had significantly higher fracture toughness values [77].

It should be taken into account that it is instructed that FRC's to be used as dentine replacement and should not be used as final fillings, except for Novopro Universal and Novopro flow as they can be used as enamel replacement as well.

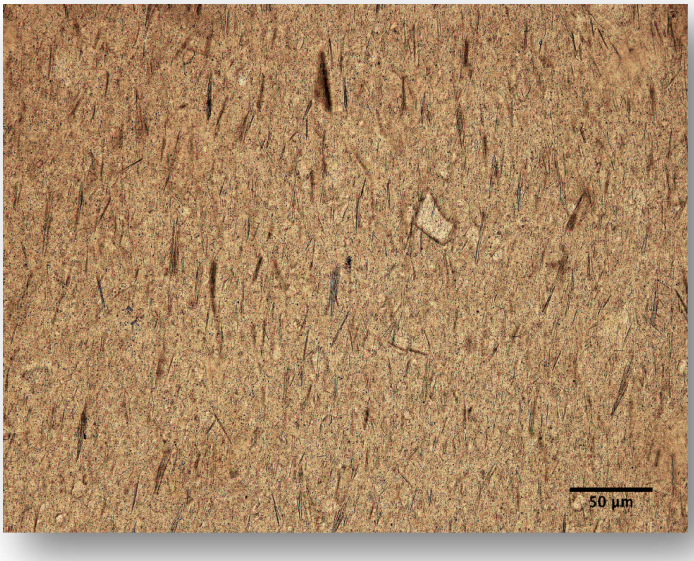

A

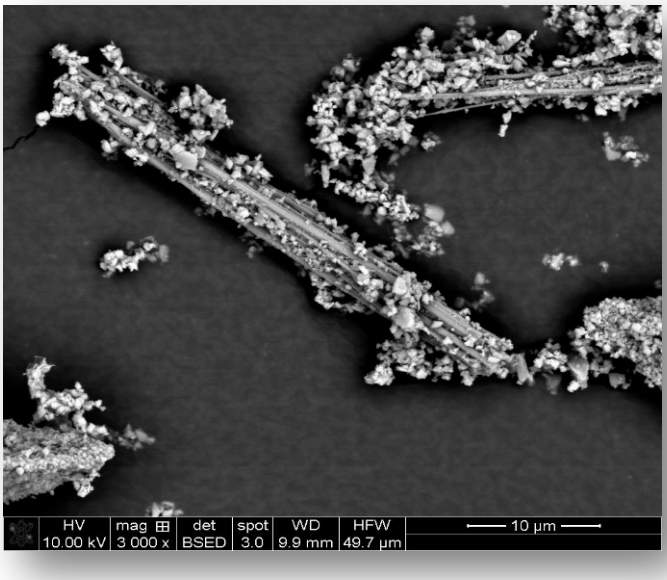

B

Figure 1-16: **A:** Optical microscopic images (x10) of randomly aligned hydroxyapatite fibre bundles in fibre reinforced resin composite (Novopro-fill™). **B:** Scanning electron microscopy (SEM) images (x 3000) of of extracted hydroxyapatite fibre bundles from fibre reinforced resin composite (Novopro-fill™).

1.4.6 Nanotubes

Due to the favourable structure of a nanotube, which offers a high capacity of reinforcement for dental composites, several studies addressed their usage. Zhang and his co-workers utilised carbon nanotubes as reinforcement for urethane dimethacrylate resin. They reported notable improvements in the mechanical properties of the dental resin. However, as a side effect of adding carbon nanotubes, the resin became discoloured which would limit their usage as an aesthetically appropriate tooth-coloured restorative [112].

Titanium oxide nanotubes have been widely used as a substrate for bone regeneration due to the substrate's excellent biocompatibility and due to its favourable whitish colour [113]. These nanotubes, as a potential reinforcement for dental resin, have a unique structure which allows intertwining of both internal and external aspects of the nanotube with the resin matrix [114]. Khaled et al looked into the mechanical performance of resin cement when adding titanium nanotubes and he reported an improvement in the mechanical properties of the luting agent [115]. Dafar and her co-workers looked into reinforcing a flowable composite with titanium dioxide nanotubes; they found improvements in both Young's modulus and the fracture toughness of such resin. The findings from both studies were attributed to the efficient stress distribution within the composite because of the reliable resin- nanotube interlocking mechanism [115, 116].

1.4.7 Fibre toughening mechanisms

Fibre toughening mechanisms rely on the fibres' ability to deflect crack propagation, to stretch, bridge and resist the opening and further spreading of the crack. These properties induce a closure force onto the crack itself [117]. Due to the stretchiness of the fibres, crack blunting and crack bridging mechanisms can take place. In crack bridging, short fibres stretch along the sides of the crack; this stretching near the crack tip during propagation blunts the crack tip [118]. This action subsequently lowers the stress concentration at the tip of the crack, thus slowing or preventing further progression. Moreover, when a fibre composite fails, the fibres will tend to break at

different points along the length of the material. This will not only create a complex crack path, but will also mean that fibres will need to slide passed each other in order for a crack to be opened up. This absorbs energy, since there is usually a frictional force resisting this 'pull out' (Figure 1-17).

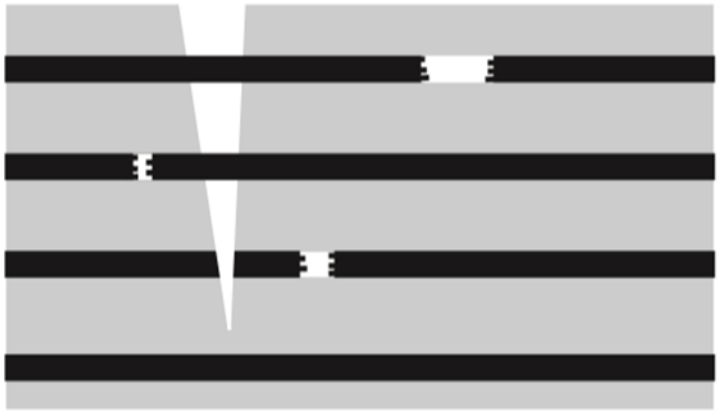

Figure 1-17: Schematic of fibre pull out in a composite.

1.5 Properties of resin composites

When materials are tested within clinical studies there is often a lack of standardization, which leads to more variability and the risk of a number of different biases. This variation may be due to patient-related factors, the skills of the practitioner, the complexity of the procedure, treated teeth, the type of outcome assessed and the methods used for this assessment.

A number of positive correlations were found between the clinical and laboratory outcomes, with a few of the results being significant. Two of the correlations found were between the fracture toughness of a material and the fracture of restorations, and between flexural strength and clinical wear [119]. However, we must treat these conclusions with caution, given that they are founded on a large number of variable studies that in some cases have high risks of bias or a lack of detailed descriptions [119].

An initiative was introduced in 2017 by the Academy of Dental Materials with the aim of critically appraising a range of available laboratory testing methodologies that had

been used to assess the technique sensitivity and mechanical performance of resin composites [120, 121]. This appraisal then led to the development of a set of guidelines for the evaluation of in vitro composites. The testing methodologies were assessed on the importance of the property, and on the methods employed. This initiative focused on what were considered to be the highest priority methods, i.e. those that were supported by the literature, were considered to be the most useful and applicable in practice, and those with clinical correlation. The purpose of these guidelines was to assist researchers with their choice of method so that they could select the most appropriate for evaluating the key properties of dental resin composites in terms of their technique sensitivity and mechanical behaviour.

1.5.1 Properties of unset resin composites

1.5.1.1 Viscosity

The definition of viscosity is "a measure of a liquid's resistance to forces that tend to cause it to flow" [122]. It is key factor for the adhesion to tooth structure; and it is a key determinant of the restoration's quality as well as how long is required to complete the restoration [123].

There are several factors that can affect the viscosity of a resin composite, for example the ratio and type of the resin matrix, and the composition, shape and size of the inorganic filler [124]. The flowability of a resin composite before it sets is largely affected by the inherent rheology of the monomers in the matrix [122]. For example, at room temperature the viscosity of the Bis-GMA is high; therefore, low viscosity monomers such as triethyleneglycol dimethacrylate (TEGDMA) are added in order to provide better handling properties. This makes it easier to mix and to carry it to the cavity [125].

In practical use, it is easier to handle amalgam than resin composites. Researchers have therefore looked at ways of improving the handling of these materials, with the aim of producing a material that can is easily manipulated while recreating the contact point, in particular for posterior teeth. With this aim in mind, a high viscosity resin composite has been developed that fulfils these criteria [126]. However, it must be borne in mind

that having a higher viscosity can result in voids within the restoration, which would reduce the physical properties of the composite as well as the adhesion between the composite and the tooth [127].

In contrast, flowable composites have also been developed, with the aim of facilitating the adaptation of small cavity restorations, and the adaptation at the base of large cavities. As they usually have lower filler loading, the mechanical properties of these flowable composites are generally lower than in conventional composites, which means that they are not suitable for applications that include load-bearing areas [128].

1.5.2 Properties of resin composites post irradiation

1.5.2.1 Refractive index:

For any material, the refractive index (n) can be defined as the ratio of the velocity of light in a vacuum (or air) to its velocity in the material. Dental composite contains a number of phases, each of which is likely to have a different index of refraction.

For aesthetic reasons, it is important that the translucency of the restored tooth and that of a composite are similar. This means that the filler's refractive index should be very close to that of the resin. The indices of refraction for bis-GMA and TEGDMA are around 1.55 and 1.46 respectively; therefore a compound that comprises equal amounts of both of these by weight has an index of refraction of approximately 1.50 [37]. The refractive index of the majority of glasses utilised as fillers is around 1.50, which provides a sufficient level of translucency. It is also important to note the effect of the materials translucency on light transmission, and its influence on the depth of cure.

A number of different methods have been employed to explore the refractive index (RI) of uncured monomers and cured polymers. An Abbe Refractometer is typically used to measure the RI [129].

In an Abbe refractometer, the sample is positioned underneath a microscope between right angled prisms. A monochromatic light is refracted through "the first prism, sample, and second prism" and a scale on the refractometer is used to calculate the RI

[130]. Monochromatic light is used for this process, usually yellow sodium light (589 nm), at a temperature of 23^{o}C. The reason why monochromatic light is used is that this prevents light dispersion and thus ensures that the critical angle is formed. The limitation of the Abbe Refractometer is that it can only be used to take RI measurements of materials that are transparent materials and either in a liquid state, or bulk cured.

1.5.2.2 Degree of conversion:

The ratio of converted carbon-carbon double bonds to new single carbon-carbon bonds in order to form a polymeric chain is defined as the degree of conversion (DC) [131]. In a clinical situation, the overall degree of conversion of dental resin cannot reach 100% due to several factors that lead to the presence of unreacted monomers [132], for example oxygen. It will form an inhibiting layer over the resin, thereby preventing the monomers from full polymerisation. Initiators, and their concentration in the composite, would also have a significant influence on the degree of conversion [133]. Light activated dental resins usually achieves a DC of 40-75% after the end of the light irradiation [134-136]. The unreacted monomers carry toxic concerns to the human tissues, such as pulpal irritation, mucosal allergic reaction or even carcinogenic effects [137, 138].

A high DC implies that when a polymeric network is formed, a high number of double bonds were consumed. This leaves a smaller amount of unreacted monomer that can plasticise the structure of the network [139]. These two factors enhance the mechanical properties of the material, for example elastic modulus, and strength [140, 141]. However, this relationship between mechanical properties and DC is not applicable to all resin composites as these properties are not merely dependent on the DC but a range of other factors, in particular the composition of the resin and the filler load [142, 143]. Moreover, higher degrees of conversion usually leads to higher shrinkage stresses. As it was found that with higher conversion levels, increase in stress-development within the composite [144].

There are various methods to measure the degree of conversion of resin composites; among them is Fourier transform infrared spectroscopy (FTIR), which is the most

commonly used method. There are other indirect methods for determining the extent of conversion, such as thermal analysis (DTA) [145, 146], and surface hardness [147]. However, the progress of the polymerisation can be difficult to assess indirectly as it can be affected by a number of factors. These properties (DTA and hardness) can therefore only be used to make an estimation of the degree of polymerisation.

The basis of FTIR spectroscopy is the interaction between electromagnetic radiation in the infrared (IR) area and the chemical bonds between a material's atoms. When IR radiation comes into contact with a material, some of that IR energy is absorbed before the rest is transmitted.

When a resin composite is polymerised, monitoring of the intensity between the C=C bonds can take place using FTIR, thus enabling assessment of the degree of monomer conversion [148]. The absorption bands generated by C=C double bonds in the FTIR spectra are very distinctive. For example, the absorption band of the aliphatic methacrylate C=C double bond stretch occurs in the mid-IR region at 1638 cm^{-1}[149]. In order to use a spectrograph to evaluate the concentration of C=C, a calibration curve must be used to establish the relationship between peak height (or area) change and the C=C concentration. Any changes in band absorption can, alternatively, be related to another band's absorption rate in the spectrograph, which does not exhibit change during polymerisation: an internal standard.

The DC of polymers is calculated using an internal standard in cases where a non-reactive bond's absorption band can be determined. In the case of BisGMA-based resins, the internal standard reference is normally the absorption band of an aromatic C=C, found at 1608 cm^{-1} [150]. For UDMA-based resins, which do not contain the aromatic C=C, the reference is usually the carbonyl C=O absorption band at 1720 cm^{-1} [151]. One issue with this is that the carbonyl absorption band's intensity and position can alter during polymerisation [152]. Before curing, the carbonyl group is conjugated with the C=C bond, and this conjugation is lost after polymerisation. As a result, the carbonyl absorption band moves to a higher frequency once the bond stiffens after curing. In addition, the absorption intensity of this band is significantly reduced [28]. A reliable absorption band to use as an internal standard is the amide (N-H) bond at

1537 cm^{-1}, which can be used to calculate the DC of UDMA resin composites that do not contain BisGMA [153].

1.5.2.3 Depth of Cure (DoC)

It is generally acknowledged that 2 mm increment should be used for the placement of conventional resin composites. This permits adequate conversion of the resin composite [154]. However, the actual depth of cure that is achieved varies with the translucency and shade of the material being used – the depth of cure for darker, opaque shades is less than for lighter more translucent resins.

The DoC is defined as "the maximum thickness of a composite material that can be adequately cured in a single layer" [155]. The term "adequately" can be interpreted in different ways, which has led to a great deal of dispute, so there is a lack of consensus over the concept of DoC. The cure can therefore be said to be adequate if micro-hardness greater than 80% of the maximum value are achieved [120]. Such a concept (hardness profiles) has been criticized saying that the cut-off values have been determined in a totally arbitrary way that does not correlate with any actual level of change within the composite's properties, so they have no physical meaning. However, although there seems to be no physical foundation for this cut-off point, surface hardness profiles continues to be used for the assessment of curing efficiency, many studies have cited 80% of the maximum micro-hardness value as an indication of adequate cure [156, 157].

Following the Beer-Lambert Law, the deeper we go into the irradiated material, the less effective curing is, meaning that sufficient curing can only be achieved with longer irradiation times. This effect is intensified with increased photo-initiators concentrations [37]. However, there are other factors to consider besides absorption. The intensity of the light may decrease faster than expected with depth due to filler particle and void scattering. Products can therefore vary widely due to differences in the volume fraction of the filler, and particle size and distribution.

This has important clinical implications because for a given exposure (intensity × time) at the surface of the material, the curing process will only take place up to a certain depth.

Most of the commercially available bulk-fill materials are cured with light only, although some dual-cure materials are available. A number of methods have been employed by manufacturers to improve depth of cure. These include:

- Using fillers with larger particle size [158].
- Decreasing the filler content [158]
- The use of different photo-initiators [159].
- Matching the refractive indices of fillers and resin.

If the filler content is reduced and the filler size increased, there is less light scattering at the resin-filler interface and therefore more absorbed light can activate the photo-initiator. Tetric EvoCeram Bulk-fill for example, achieves a greater depth of cure through the addition of a number of different photo-initiators [159]. In particular, the addition of Ivocerin, a highly reactive photo-initiator, allows the resin to be polymerized in larger increments than when using other photo-initiators, for example camphorquinone or lucrin [160].

Clinicians should refer to manufacturers' instructions on the maximum curable depth of a material. However, without dismantling the restoration it is not possible to determine whether the curing process has been successful all the way to the bottom. Clinicians are therefore advised to take a conservative approach, using longer rather than shorter irradiation times and or placing the restoration incrementally [37].

There are a number of available techniques for assessing depth of cure. The ISO Standard for Dental Composites 4049 suggests that unset materials should be scraped straight away after irradiation, so that the depth of the set material can be measured and divided by two [161]. Other techniques commonly employ assessing the surface hardness of the top and bottom materials [162], or through hardness profile testing [120] .

1.5.2.4 Hardness

The definition of hardness is the quantifiable measure of deformation resistance, and it can be calculated according to the maximum applied load divided by the projected area of contact.[119]. Hardness refers to the material's resistance to indentation [163] which is a critical parameter for dental restorative materials. A major disadvantage when using resin composite with a low hardness value is that it will wear quickly, leading to a rough surface that can support the growth of bacterial [164]. Many laboratory tests are used to measure the surface hardness of materials. The Vickers hardness test is a universally accepted method that represents the accurate value of a surface hardness. The Vickers hardness test technique involves using a diamond indenter to indent the material. This takes the form of a square-based pyramid with an angle of 136° between opposite faces, and a test force is applied of between 1 gf and 10 kgf. Typically, the full load is applied for 10-15 s. Using a microscope, measurement is made of the two diagonals of the indentation on the sample material's surface after the load has been removed, and the average measurement is calculated. The quotient acquired after dividing the load by the square area of indentation is the Vickers hardness. This hardness quotient should be reported along with the dwell time and the test force [119]. Another way to evaluate surface hardness is the Knoop hardness test. The Knoop indenter is an elongated pyramid with a more obtuse angle, which is suitable for use with hard and brittle materials. While for metals and alloys, e.g. dental amalgam, Rockwell and Brinell hardness test is usually utilized to test the surface hardness.

1.5.2.5 Fibre orientation distribution

The orientation of the fibres within the resin is of critical importance due to the isotropic versus the anisotropic reinforcement they provide. It is more difficult to determine the orientation distribution of discontinuous (random or unidirectional) fibres than to do so for continuous (unidirectional or bidirectional) fibres, especially if the discontinuous fibres are oriented in a multidirectional fashion. The methods that are used for measuring the fibre orientation include imaging techniques such as optical microscope and scanning-electron microscope [165]. A drawback of the imaging

methods is the two-dimensional projection of the discontinuous fibres aligned in one plane. This could be resolved by providing sections of the same sample cut in different planes and analysing each of them [88].

1.5.2.6 Flexural Strength and flexural modulus

Flexural strength has been defined as '*the ability of a material to bend without deformation before it break*s "[166]. Flexural strength is one of the most crucial mechanical properties, which relates to a resin's ability to resist occlusal forces [119, 167, 168]. Resin composites need to have a high flexural strength in order to endure the recurrent bending, flexing, and twisting forces associated with chewing. The twisting forces are particularly high when the restoration comprises thin layers and/or has a minimal support of dentine.

The ISO specification to guide dental tests ISO 4049:2009 states that a resin composite's flexural strength should be tested by a 'three-point bending test', whereby 25 mm bar-shaped specimens are placed on two supported points, and various loads are applied in the middle of the bar [169, 170]. Resin composites typically exhibit similar flexural strength to amalgam , but with lower levels than ceramics [30].

Flexural strength is commonly tested using the three-point bending method. In this test, a beam-shaped sample is held from below between two supporting points, and a load is applied to the middle section of the beam with a downwards force. This action simulates a situation where the beam is in flexure. With respect to the extension-to-load curve, the maximum load is the greatest load that the material can withstand, and the linear-portion slope signifies the material's elastic property; thus, calculations of both of these are generally taken in order to determine the flexural strength and modulus. The benefit of the three-point bending technique over four-point bending is that sensitivity to surface flaws is much lower, therefore there is less attention paid to the preparation process and more focus on the property of the material [119].

The flexural modulus describes the stiffness of a material within its range of elasticity [45, 125]. The measurement of distortion under load (modulus of elasticity) is taken at the same time as the other measurements. If the modulus of elasticity is low, then

the distortion will be high, and this is clearly not desirable in dental composites. It is also not recommended to achieve high flexural strength in a material that gives way too easily and thus compromises the strength, as this would mean that the load distribution is uneven, and the chewing strength is not horizontally distributed over the periodontium. If this occurs, a high tensile load is applied to the surface of the restoration, from the occlusal pressure, and this may negatively influence the adhesion to the tooth structure. Further within the cavity, lateral expansion may be caused by occlusal load on the flexible filling materials and the tooth surface may break. Materials with a high elastic modulus are not suitable for restorative work because they would fracture too easily when subjected to stress and deformation. Rather, materials with a moderately high modulus are preferred because they have some flexibility and can withstand small deformations – an example is dentine [45]. Closely matching moduli between the restorative material and dentine, the flexural modulus of which is 17 GPa [125], could allow the stresses at the dentine -composite interface to be evenly distributed.

1.5.2.7 Fracture Toughness

Several studies show bulk fracture in composite fillings to be one of the common causes for restoration replacement [171, 172]. It is therefore imperative to make improvements to the fracture resistance of resin composites. The fracture toughness (FT) of a composite material should be improved as this is an important criterion for establishing its damage tolerance; a material with higher fracture toughness is better able to resist the initiation and propagation of cracks. The resin matrix as well as the fillers used in a dental composite can be modified to improve performance. In terms of fillers, the morphology and size are important factors in the improvement of FT. Resin composites with high aspect ratio (length/diameter) fillers have been shown to exhibit higher FT [173-176]. High aspect ratio fillers such as E-glass fibres have been used for a number of decades in dental applications [97, 176]. Fracture toughness measurement (K_{IC}) is based on the assumption that the split happens due to the presence of microscopic defects in the material, and that a crack would propagate leading to a catastrophic breakdown of the tested material [177]. This effect (crack)

can be replicated in dental composites either by moulding it into the specimen in the curing process, or by cutting it into the specimen after curing has taken place [119]. Acoustic emission analysis could be employed to aid in the analysis of the fracture toughness of a selected material. Highly sensitive microphones will receive acoustic signals from the subjected samples, thus providing real time data while testing.

1.5.2.8 Water Sorption and Solubility

One of the leading causes of resin degradation is water sorption, where the water acts as a plasticiser inducing hydrolytic degradation at the resin/filler interface [178].

Degradation starts when the solvent molecules diffuse into the resin, leading to swelling of the resin; the resin will then start leaching unreacted monomers, which in turn may cause unfavourable effects upon the oral tissues [179]. Several factors mandate the quantity of released monomers, such as nature of the solvent used, the molecule size and the structure of the monomers, and the amount of residual unreacted monomers [77, 180]. A great deal of research has gone into the process of water sorption in resin composite materials, and several researchers have identified it as a diffusion-controlled process that follows the Fickian diffusion kinetic model [181, 182] . From a theoretical perspective, the process is seen to be regulated in two different ways. The first means of regulation is the free volume factor; here, physico-chemical forces drive water molecules to collect in intermolecular spaces, or microvoids, and at resin-filler interfaces. The second is the interaction factor, whereby hydrogen bonds are formed between water molecules and particular hydrophilic groups [182].

There is considerable variation in the extent of water sorption experienced by polymer networks, depending on the type of dimethacrylate monomer involved. Sorption values are ordered as follows: TEGDMA> BisGMA> UDMA> BisEMA [29, 183]. Poly-TEGDMA exhibits much higher water sorption than poly-BisGMA, even though it has greater DC. The explanation for this is that poly-TEGDMA is that there are large spaces between the polymer clusters, thus enabling more water to be absorbed. Furthermore, poly-TEGDMA networks can be more flexible, allowing the water to swell the polymer chains to a greater degree [29]. The higher water sorption observed

in BisGMA compared to BisEMA and UDMA can be explained by the greater hydrophilicity of the monomer molecules in BisGMA. Stronger hydrogen bonds between water molecules are formed by BisGMA hydroxyl groups compared to those formed by BisEMA ether groups or UDMA urethane groups. A comparison of water sorption along with other properties of various BisGMA copolymers revealed that when TEGDMA is gradually substituted with BisEMA or UDMA in copolymerisation with BisGMA, more flexible resins can be formed that have lower water sorption [29].

Dimethacrylate monomers never achieve full conversion, as between 25% and 50% of the methacrylate groups do not react. Up to approximately 10% of the unreacted methacrylate groups exist as elutable residual monomers [136, 184]. Sideridou et al examined the amount of residual monomer eluted in water by various co-polymer and homo-polymer systems, based on BisEMA, BisGMA, UDMA, and TEGDMA [29]. The results showed the polymer which released the most unreacted monomer (14.21 μg/mm3) was the BisEMA homo-polymer, with BisGMA (10.44 μg/mm3) and UDMA (6.62 μg/mm3) homo-polymers coming next, and the lowest amount released by the TEGDMA homo-polymer (2.41 μg/mm3) [29]. Lower solubility values were exhibited by BisGMA/TEGDMA co-polymers in comparison to BisGMA/BisEMA and BisGMA/UDMA co-polymers [29]. According to Sideridou et al. (2003), DC has a significant effect on the solubility values of polymer systems; when the DC is lower, solubility and elution are increased, as well as the effect of the polymer network's flexibility and cross-link density. A material's sorption and solubility can be measured by weighing the material before and after immersing it in a storage media for different amounts of time [185, 186].

1.5.2.9 Hygroscopic expansion

Hygroscopic expansion is the phenomenon of attracting and holding water through either absorption or adsorption leading to physical change in volume.

Expansion related to water sorption experiments can be evaluated by measuring circular specimens' linear change following water storage [187, 188]. Composite materials do in fact absorb water over the course of time, despite being hydrophobic in nature. This can result in the filler-matrix bonds degrading therefore contributing to

increased wear [189], as well volume change (expansion). This expansion typically exceeds the shrinkage that occurs in all composites. Most composites level off after around three to four months in water storage, after which no more expansion takes place [188, 190]. A laboratory study has shown that deflection of the cusps of three-surface resin composites resulting from shrinkage was offset by its expansion within one month [191]. If the expansion is too powerful, this can negatively affect the reaming tooth tissue, resulting in cracks on the hard tissue, or nerve injury (pulpitis).

It is possible to monitor the hygroscopic expansion of a dental resin composite at different time points of its storage, and make the measurements with a light microscope [192]. This technique could utilize restored teeth giving a better representation of clinical situations. Unfortunately, this method utilises more expensive equipment, is more time consuming, and requires a highly skilled operator to carry out the measurements. A material's initial volume (V_1) is calculated after being cured at room temperature by measuring its thickness and diameter using mechanical callipers. The specimen's final volume (V_2) is calculated after water storage in the dark at 37°C, and the difference between the two measurements is the hygroscopic expansion [120, 193] , or a laser scan micrometer (LSM) which can identify any changes in the dimensions of the specimen. The equipment is made up of a laser-scan micrometer attached to a heavy base, with a disc-shaped specimen holder which is rotated horizontally by an electronic control unit. The diameter of the specimen can be measured by the laser to a maximum resolution of 200 nm [185].

1.6 Clinical Concerns with dental resin composite

A restoration life span which happens to be the service life or length of service is what describes the restored tooth longevity. This is quite complex as everything is dependent on the patient and the dentist, as well as material related properties [194] [195]. Furthermore, the amount of residual tooth tissue plays a crucial role determining the longevity of the restored tooth [196, 197], while the foremost factor determining the restorations service life is the patient's caries risk [198]. Other patient

related factors having impact on the restorations' longevity are: compliance of the patient, oral hygiene, age, and diet [199]. Other determining factors include treatment plan of which the view point of the dentist to have the indication for surgical intervention, the restoration size and technique, the restorative material properties and adhesive system utilised, as well as mode of curing, and occlusion [194, 200].

1.6.1 Polymerization shrinkage

Shrinkage during polymerisation is a result of polymerization stresses caused by the setting reactions that occur within the resin composite. Shrinkage occurs during the initial stage of polymerisation as the polymer network increases in hardness. This can have a number of consequences, such as cuspal deflection, postoperative sensitivity, and secondary caries. The latter can result in the fracture of the tooth and pulpal irritation. A number of methods have therefore been suggested to mitigate polymerisation shrinkage stress; these include incremental placement and techniques using low to high light-curing energy in order to lengthen the gel time [201].

The amount of polymerisation shrinkage that occurs is related to either the configuration of the cavity or the resin composite. The C-factor, which stands for 'cavity-related factor', is the ratio of bonded surfaces to unbonded surfaces, and a higher C-factor results in higher polymerisation stress. This is illustrated by class I and class V restorations, which have the highest C-factor and therefore the highest polymerisation shrinkage stresses.

1.6.2 Degradation

Composite restorative materials face a number of challenges in the mouth, from bacteria, changes in temperature, food, saliva and occlusal function. Interactions lead to processes that can degrade the material, for example biological, hydrolytic, enzymatic and mechanical biologic degradation processes. The integrity of the material's surface can be affected, as well as its physical stability and mechanical properties.

The component that mainly determines the amount of degradation in the oral environment of a resin composite is the resin monomer. As stated earlier, 25-50 % of the final polymerized network comprises unreacted methacrylate molecules, which are more likely to leach out from the composite [136].

Hydrolytic degradation occurs when a solvent accumulates in the matrix filler interface; this allows the leaching out of particles, which affects the material's physical stability and chemical structure [202]. The problems it can cause such as defective margins and micro leakage. Any materials that leach out may be toxic and affect the longevity of the restoration [136, 138].

There are a number of factors that can affect the resin composite's ability to resist water or solvent penetration. These include features of the material itself, such as the hydrophobicity of the resin matrix, and coupling agent used [203]. It has been reported that on average, by weight, the leached out particles caused by hydrolytic degradation account for 0.05-2% and the majority (50-75%) of these leach out in the first three hours [204].

1.6.3 Bulk fracture

A systematic review by Alcaraz et al. in 2014 compared the rate at which resin composite failed against that of amalgam in posterior teeth. Bulk fracture was found to be the second most common mode of failure for both materials [205]. On the other hand, in a review of the literature on resin composite restorations published between 1996 and 2003, concluded that the most common failure mode over a period of five years was the fracture of posterior composite restorations [171].

Many reviews exist on resin composite restorations in vital posterior teeth. One review compared studies conducted between 1995 and 2005 with those conducted between 2006 and 2016 [206]. Over the earlier period, reported survival rates were 89.4% compared with 86.9% for the later period, a marginal difference. The reported rates of secondary caries were also similar: 29.5% in 1995–2005, and 25.7% in 2006–2016. However, the frequency of fractures in composite and teeth was significantly higher in 2006- 2016. The possible explanation was that composites were employed in larger

restorations in this more recent period. Therefore studies have investigated potential ways to enhance the mechanical properties of particulate filled composite (PFC), through various curing techniques [141, 207], selection of resin matrices [208], and improving the filler content [30].

Chapter Two

Rational of the study and Aims and Objective

2.1 Statement of the Problems

The good aesthetic results of resin-composites coupled with their improved physical properties have led to them becoming the most commonly used materials for the restoration of both anterior and posterior teeth. Moreover, resin-composites enable a more conservative preparation, and can reinforce the tooth structure as opposed to weakling it. Although there have been improvements to dental composite properties in recent years, a number of challenges are still faced in producing the ideal composite resin.

The main objective when developing resin composites is to enhance their physical properties, and thus extend their durability within the oral cavity while maintaining their aesthetic quality. However, studies looking into survival and durability in posterior teeth have demonstrated that amalgam might be the most reliable and user friendly direct restorative material available; this finding highlights the importance of developing a deeper understanding of resin composites and the reasons for their failure in order to improve their longevity [209-211]. Damage experienced by resin composites can lead to deterioration of the matrix and/or filler as a result of interfacial debonding, microcracking, mechanical load or filler/particle fracture. Prolonged application of mechanical loads will ultimately result in progressive degradation and crack development and advancement, leading to irreparable failure of the restoration [212].

The development of an ideal composite material for use in restoring large cavities in posterior teeth has been a crucial issue in the field for many years [30]. In order to place an ideal restoration, it is essential to understand the risks factors and types of failure associated with posterior teeth. The two most common reasons for the failure of posterior restorations are bulk fracture and secondary caries [198]. A review of clinical cases of posterior composite restorations carried out between1996-2002 was conducted, and it was found that among restoration failures between 0-5 years, most were due to restoration issues (material choice or placement technique). For failures between 6-17 years, secondary caries and bulk fracture were the main reason for replacement of the restoration [171]. Longitudinal studies by Pallesen and Qvist and

Da Rosa et al, have shown that fracture causes more failures than caries [213, 214]. These results indicate that in posterior restorations of any age or lifespan, bulk fracture is a principal risk. Furthermore, recent review assessing the longevity of posterior composites in adults reported that secondary caries and restoration fracture were the main reasons for failure [215]. As one would surmise, the failure rate of a restoration is increases along with its time in use, but the failure or success of resin composites depends on a lot more than just the properties of the material. In the same way as other restorative materials, the success of resin composites depends on good technique, proper patient selection, and appropriate materials.

The NHS has calculated the cost of a composite filling as £53, with private patients paying anything from £40 to £260 [216]. Burke investigated the failure rate of teeth restorations and concluded that NHS-funded composite restorations failed on average after 4.7 years [217]. This means that patients replacing composite fillings under the NHS would need to pay £53 every 4 years.

These findings highlight the importance of developing a deeper understanding of the mechanisms that lead composites to fail; this knowledge may promote their durability [209, 218]. Furthermore, these disadvantages display the need for improved materials, and much innovation has been seen in this area [176, 219]. Fibre reinforcement was introduced in order to strengthen polymeric materials, and this was necessary because resin-composite materials exhibit some physico-mechanical deficiencies when subjected to highly demanding clinical conditions. It has been confirmed that reinforcement increases the toughness of the composite, allowing fibre reinforced composites (FRC) to be used as a foundation for severely weakened teeth [220]. During the 1990s, FRC dental composites were largely unsuccessful and the reason for this is that the fibres used for strengthening were too short (below the critical fibre length), thus the toughness and strength of the fillings were not sufficiently increased. Currently, there is one commercial glass FRC that contains fibres meeting the critical fibre length. However, the stability and mechanical properties of FRC can be negatively affected by hydrolytic and hygroscopic effects. As further improvements are made, it is essential to keep abreast of ongoing research and development in order

to compare the performance of new materials with that of the more traditional materials.

2.2 Aims and objectives

The overall aim of the project was to evaluate the physico-mechanical properties of the additionally reinforced resin composite materials, and to compare the effect of resin matrix composition, on mechanical and hygroscopic behaviour of experimental fibre reinforced composites.

Chapter 4

Aims

- To investigate the surface micro-hardness (VHN) and fracture toughness (K_{IC}) of resin-composites, with and without incorporated short fibres, after solvent storage.

Objectives

- Evaluate the effect of food-simulating solvents on surface micro-hardness, stored in distilled water, 75% ethanol 25% water, for 1d and 1 m at 37°C.
- Evaluate the effect of water storage on fracture toughness, stored for 1 d and 7 d at 37°C.

Chapter 5

Aims

- To assess the long-term water sorption and solubility and extent of hygroscopic expansion processes of resin-composites, with and without incorporated short fibres, at 37°C.

Objectives

- Evaluate water sorption, solubility, of aged specimens in water for 140 d at 37°C.
- Investigate the effect of water storage on the hygroscopic expansion, of aged specimens in water for 140 d at 37°C.

Chapter 6

Aims

- To formulate a series of experimental resin composites with short e-glass fibre reinforcement resin composites and to evaluate the degree of conversion and depth of cure.

Objectives

- To substitutes the semi-interpenetrating polymer network (Bis-GMA-TEGDMA/PMMA) with an entirely dimethacrylate resin matrix (with different Bis-EMA: UDMA mass ratio).
- To evaluate the depth of cure of Bis-GMA-UDMA/Bis-EMA (with different Bis-EMA: UDMA mass ratio) based fibre reinforced dental composite, and to assess the degree of monomer conversion.

Chapter 7

Aims

- To evaluate how water storage would influence the flexural strength, fracture toughness, sorption, solubility, and hygroscopic expansion of the experimental fibre reinforced resin composite materials.

Objectives

- To evaluate the flexural strength and fracture toughness of Bis-GMA-UDMA/Bis-EMA (with different Bis-EMA: UDMA mass ratio) based fibre reinforced dental composite, stored in distilled water, for 1d, 7d and 1 m at 37°C, and compare it to the Bis-GMA- TEGDMA/PMMA-based FRC control group.
- Evaluate water sorption, solubility, of aged specimens in water for 168 d at 37°C.
- Investigate the effect of water storage on the hygroscopic expansion, of aged specimens in water for 168 d at 37°C.

Chapter 8

- Summary, conclusions and future work recommendations.

Chapter Three

Methodology

3.1 Introduction

This research consisted of four in vitro studies which utilised a number of different techniques. The methodologies and techniques used in the studies are touched upon in their respective chapters, although the present chapter describes each of these in more detail.

For the first set of experiments in this thesis (see Chapters 4 and 5), resin composites that contained particle reinforcement and additional fibres were used, with four composites containing only particle reinforcement being used as controls. The resin composites were materials that are commercially available. The composites were selected in such a way that they represented a wide range of materials with varying types and percentages of resin and filler, to compare the properties of resin composites reinforced with fibres with composites that had only particle reinforcement. The surface micro-hardness (VHN) and fracture toughness (K_{IC}), and the long-term water sorption and desorption and extent of hygroscopic expansion processes of these resin-composites were evaluated. For the second set of experiments in this thesis (see Chapters 6, and 7), experimental fibre-reinforced composites were formulated using varying ratios of Bis-GMA-UDMA/Bis-EMA in order to explore the mechanical and physical properties of the resultant materials.

3.2 Surface micro-hardness measurement. (Chapter 4)

From all of the available hardness tests, the Vickers hardness test was chosen as the most appropriate in this instance due to its simplicity, popularity, and accuracy; regardless of the material being tested or the loading being applied, the geometry of its indentation remains the same. In chapter 4 the study aimed to assess how two solvents affected surface hardness.

The specimens were carefully made using a Teflon mould of 8 mm diameter and 2 mm thickness, taking care to avoid air becoming trapped in the uncured material. Preparation took place at room temperature (23±1°C). The mould was positioned between 1 mm thick microscopic slides and two polyester films on each side. The specimens were cured for 20 s at an output irradiance of 1200 mW/cm^2 with an Elipar

S10 LED curing light from 3M ESPE. The top surfaces of the specimens were irradiated, and 1000-grit abrasive papers were then used to finish them and smooth the edges. The specimens were measured 1h after irradiation using a Vickers Micro-hardness Instrument (FM-700, Kawasaki, Kanagawa, Japan) (Figure 3-1) and then again after being solvent stored in the dark at 37 ± 1°C for one and 30 d. Vickers hardness (VHN) was determined using a load of 300 g at 23 ± 1°C for 15 s. At each time interval three indentations were made on each specimen equal distances apart, and 1 mm adjacent indentations and specimen margins (Figure 3-2).

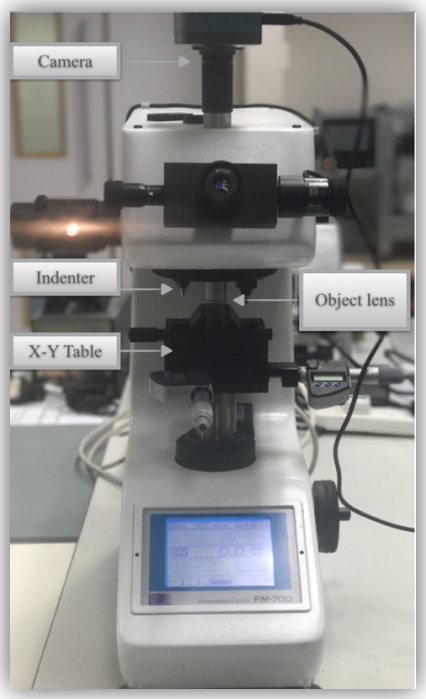

Figure 3-1 FM-700 microhardness tester.

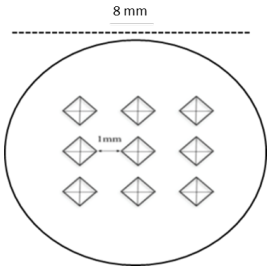

Figure 3-2: The ca.1 mm distance between Vickers indentations with 9 indentations per specimen.

3.3 Fracture toughness (KIC) measurement. (Chapters 4 & 7)

The K_{IC} measurement of a dental composite is frequently used to determine the properties of an experimental or new material. As can be seen from (Figure 3-3), the current study utilised a Universal Testing Machine (Zwick Roell 2020, Leominster, UK) to conduct the experiment. In all testing, recommendations from both British Standards (BS) and the American Society for Testing and Materials (ASTM) were followed. In the current study, the adopted method involved bending single edge-notched (SEN) specimens.

A total of six SEN specimens were produced using a polytetrafluoroethylene (PTFE)-lined brass mould (Figure 3-4), which adheres to BS 54479:1978 [221]. The specimen beam measured 3 mm x 6 mm x 34 mm, and included a sharp notch measuring 3 mm in length perpendicular to half the height of the beam. Sections of clear mylar strip were placed over the mould, followed by 1 mm thick piece of glass placed over to ensure that the specimen material was flush with the top of the mould. Each specimen underwent 120 s of photo-polymerisation using an LED curing unit that had an average tip irradiance of 1200 mW/cm^2 (Elipar S10, 3M Espe, Seefeld, Germany). A calibrated radiometer was used to verify the irradiance after each use of the LED curing unit (MARC™ Resin Calibrator, Blue-light analytics Inc, Halifax, NS, Canada). There were a number of overlapping regions of irradiation across each specimen. The specimen surface was finished through polishing with 320-grit metallographic paper, followed by wetting the pre-crack with a drop of glycerol. A sharp razor blade was used to further cut the notch with a sliding back-and-forth motion before being stored in small bottles of distilled water. Each specimen-containing bottle was then put into an incubator at 37°C (Heraeus Incubator BB 16, Heraeus Instruments, Hanau, Germany). The crack length of each specimen was then measured using a stereomicroscope (EMZ-5; Meiji Techno Co. Ltd., Japan) at 1.5x magnification to 0.1 mm accuracy (Figure 3-5). The specimen dimensions were measured using an electronic digital caliper (Powerfix, OWIM GmbH & Co., KG,

Germany) with an accuracy of 0.01 mm. The width and height were measured at the centre of the sample and at two different points.

A Universal Testing Machine (Zwick Roell 2020, 2.5kN load cell) was used to identify the fracture toughness values for each specimen through a three-point bending flexural test at 23 ± 1°C. A central load was placed onto each specimen in a three-point bending mode at a crosshead speed of 1.0 mm/s, until the fracture point of each beam had been achieved.

Furthermore, after obtaining the load value at fracture, fracture toughness values were calculated through the following formula [67]:

$$\boldsymbol{K_{IC}} = \left[\frac{PL}{BW^{1.5}}\right] Y$$

$$Y = [2.9\,(a/w)^{1/2} - 4.6\,(a/w)^{3/2} + 21.8\,(a/w)^{5/2} - 37.6\,(a/w)^{7/2} + 38.7\,(a/w)^{9/2}]$$

Where P is the load at fracture, L is the distance between the supports, W is the width of the specimen, B is the thickness of the specimen, Y is calibration function for given geometry, and a is the notch length.

Figure 3-3: Universal testing machine

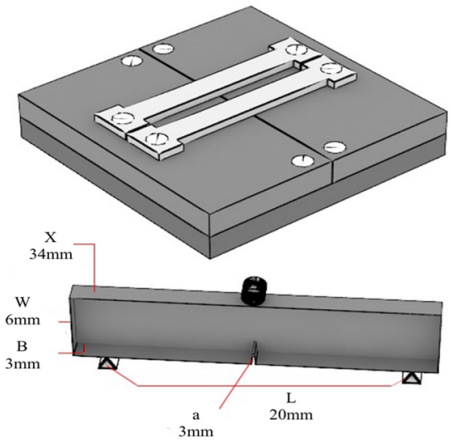

Figure 3-4: PTFE mould used for specimen, specimen dimensions and geometry.

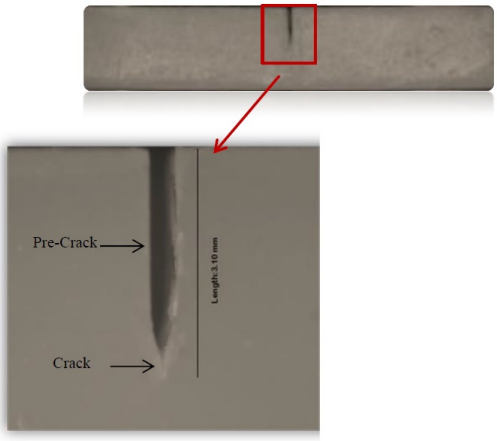

Figure 3-5: Notch length measurement under stereomicroscope with an objective lens of x 1.5

3.4 Scanning electron microscopy (SEM) (Chapters 4 & 7)

After the fracture toughness and flexural strength measurements were completed, the morphology of the fibres and the fractured composite surfaces were assessed using SEM (Quanta 650 FEG, FEI company, USA). In order to prepare the specimens for SEM, they were vacuum sputter-coated with Au/Pd alloy 60/40 with a 10 nm layer thickness using a turbomolecular-pumped coating system (Q150T ES, Quorum technologies, UK) (Figure 3-6) for 2 min, due to the non-conductive nature of the resin

composite [222]. In order to minimize the specimen charging during imaging, one side of the specimen was coated with silver tarnish (G302 Agar Scientific silver paint).

Figure 3-6: Turbomolecular-pumped coating system.

3.5 Percentage of fillers by weight using ashing in air (Chapter5)

In order to calculate the resin composite's mass percentage of inorganic filler content, the ISO 1172:1996 standard ash method was utilised [223]. For each material, two specimens were made. Teflon mould was used to prepare the specimens (2 mm thickness, 4 mm diameter) and they were placed between two sections of clear mylar strip with glass slides on each side (1 mm in thickness) and then squeezed together. An LED light curing unit with an output irradiance of 1200 Mw/cm^2 was used to irradiate the specimens for 20 s on one side (Elipar S10, 3M Espe, Seefeld, Germany). The specimens were then stored for 24 h at 37°C in an incubator (Heraeus Incubator BB 16, Heraeus Instruments, Hanau, Germany). An electric furnace (Figure 3-7) (Programat EP 5010, Ivoclar Vivadent) was used to keep a silica crucible at 630°C for 30 min (Figure 3-8). Once the crucible had been cooled to ambient temperature using a desiccator containing silica gel at 37± 1°C, a digital balance (BM-252, A&D Company, Japan) was used to determine its weight. Each of the composite specimens

was placed in the crucible and the digital balance was used again to weight the specimen, including the crucible.

In order to burn out the organic matrix, the specimen-containing crucible was placed in the electric furnace for 30 min at 630°C. Once cooled to ambient temperature using a desiccator, the crucible and residue were weighed again. The following equation was used to determine the inorganic filler content (mass %):

$$\textbf{\textit{Filler content}}\ (\%) = \frac{a_3 - a_1}{a_2 - a_1}\ \mathbf{x}\ 100$$

Where a_1 is the mass of the dry crucible, a_2 is the mass of the dry crucible plus the dried specimen; a_3 is the final mass of the crucible plus the residue after heat treatment.

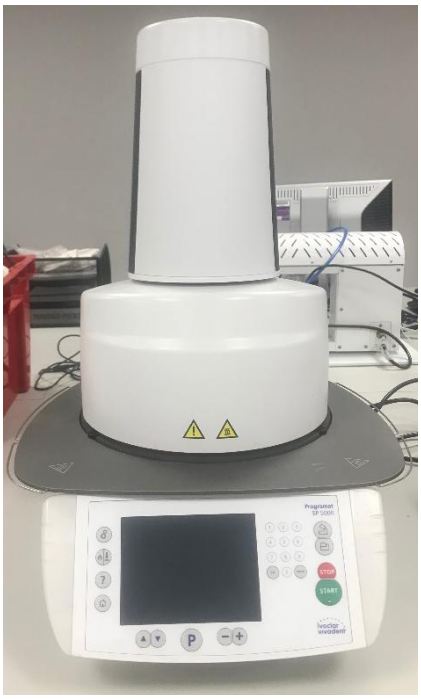

Figure 3-7: Electric furnace (Programat EP 5010, Ivoclar Vivadent)

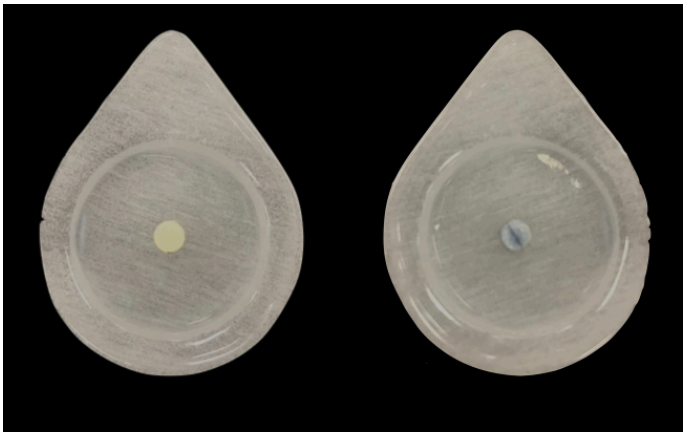

Figure 3-8: Silica crucible with composite specimen pre and after ashing

3.6 Sorption and solubility measurement. (Chapters 5 & 7)

Specimens of resin composites were made according to modified method from ISO 4049:2009 (International Standards Organisation, 2009). The thickness of specimen was modified from 1 mm to 2 mm. This increased thickness, corresponding more closely to clinical setup, allowing water sorption studies over a longer period. Using a ring mould made of brass, with a diameter of 15 mm and a thickness of 2 mm. The specimens were produced by placing each material into the brass mould, positioned beside a strip of clear mylar strip and a glass slab. The mould was filled with slightly more material than necessary, and the excess was then squeezed out by firmly pressing another mylar strip and glass slab on the top. The moulds were filled with the uncured material cautiously, in order to ensure that minimal or no voids are present in the uncured specimens. Curing then took place for 20 s at five overlapping sections of the samples (Figure 3-9) on both sides, using the aforementioned LED light curing unit. Once cured, the specimens were carefully pushed from their moulds and a sharp blade was used to remove any excess flash.

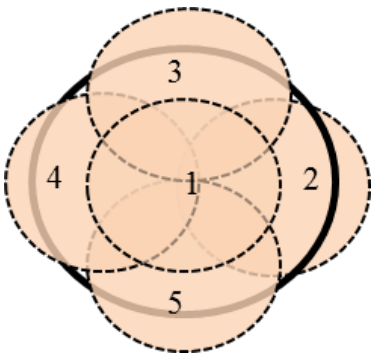

Figure 3-9: Overlapping irradiation on specimen surface

Each specimen was then placed into an individual glass vial and transferred to a desiccator along with anhydrous self-indicating silica at 37 ± 1°C, as illustrated in Figure 3-10. The specimens were placed in a second desiccator 22 hours later, and kept at room temperature (23°C ± 1) for two hours before being weighed with a calibrated electronic balance (BM-252, A&D Company, Japan) to an accuracy of 0.01mg . Repetition of this cycle until each specimen lost mass of not more than 0.1mg in 24 h ensured that post-irradiation polymerisation and dehydration was complete. The constant mass (m_1) was the specimens' initial mass.

Figure 3-10: Desiccator used in this study to store specimens during desiccation and reconditioning cycles.

Once the specimens had been dried, the dimensions for each were measured to an accuracy of 0.01mm using a digital caliper (Powerfix, OWIM GmbH & Co., KG,

Germany). The diameter of each specimen was measured twice, with measurements taken at right angles to each other. The specimens' thickness was measured both at the centre as well as at four points on the circumference, at equal distances apart. Calculation of the volume (V) of each specimen was obtained using the average mean diameter and thickness, in mm^3.

Each specimen was placed into a glass vial with 10ml of distilled water at a temperature of 37 ± 1°C in an incubator (Heraeus Incubator BB 16, Heraeus Instruments, Hanau, Germany). The specimens were weighed at various immersion times, with the recorded mass denoted as m_2. Before the measurements were taken, the specimens were removed, dried using filter paper, and air-blown. Once measurements had been taken the specimens were put back into their respective storage media, which were replaced regularly to maintain pH levels (every week). Once the storage period was over, a desiccator was used to recondition the specimens to a constant mass (m_3) using the aforementioned cycle.

The following formula was used to calculate the percentage mass change during storage in distilled water:

$$W_i(\%) = 100\left[\frac{m_{2\,(t)} - m_1}{m_1}\right]$$

Equation 3.1: Weight increase calculation formula

The following formula was used to calculate the sorption for each specimen, measured in $\mu g/mm^3$:

$$W_{So} = \left[\frac{m_{2\,(t)} - m_3}{V}\right]$$

Equation 3.2: Water sorption calculation formula

The following formula was used to calculate the solubility of each specimen, measured in $\mu g/mm^3$:

$$Sol = \left[\frac{m_1 - m_3}{V}\right]$$

Equation 3.3: Solubility calculation formula

3.7 Hygroscopic expansion measurement. (Chapters 5 & 7)

The laser scan micrometer (LSM) system (Measuring Unit LSM-503s and Display Unit LSM-6200, Mitutoyo Corporation, Japan) (Figure 3-11) is attached to a 25 mm base made from stainless steel, with rubber feet. An electronic stepper control unit rotated a disc specimen holder horizontally around a vertical axis. The LSM was connected to a PC through the Display Unit, and a USB input enabled further recording and data processing. **Table 3-1** presents the technical specifications of the LSM system.

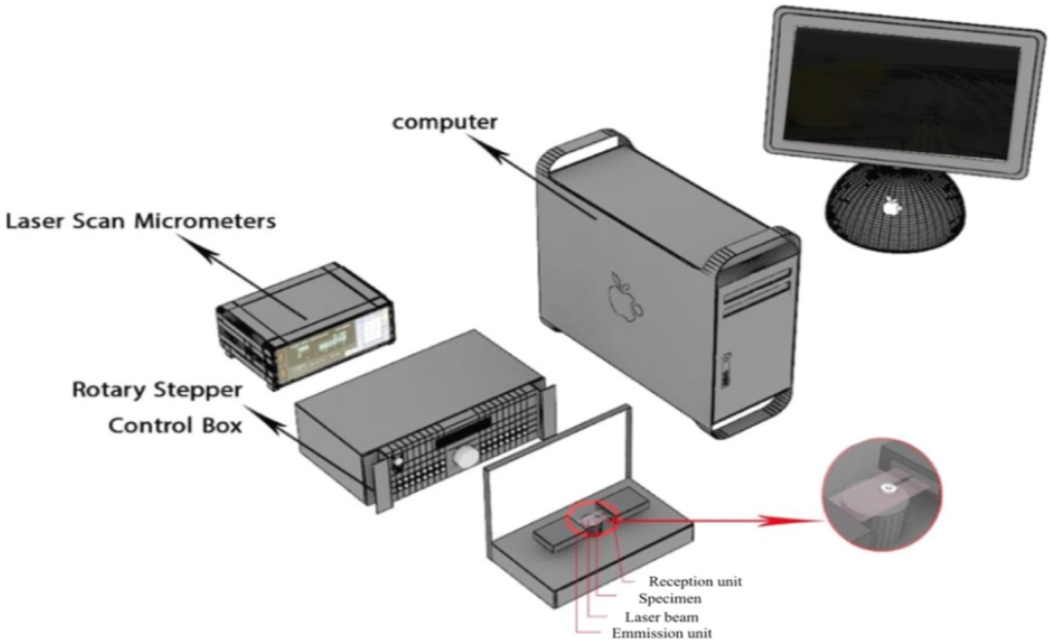

Figure 3-11: Laser scan micrometre.

The LSM system acquired the dimensional data of the specimen quickly and accurately via a parallel-scanning laser beam. Generated by a laser oscillator, this highly directional beam was positioned towards a rotating polygonal mirror and synchronised by clock pulses. The reflected beam then passed through a collimator lens, maintaining constant direction towards the specimen through the beam window. The light rays used to for measurement travel as ‘parallel beams’ towards the photo-electric detector unit, and then become obstructed partially by the specimen. The

extent to which the beam is obstructed signifies the diameter of the disc specimen. Thus, the resulting electrical output signal changes in relation to the length of time the beam was obstructed. In this experiment, the Display Unit CPU processed this change, and produced a digital display of the specimen's dimensions. The diameter of each specimen was measured to a resolution of 200nm.

The stepwise rotation of the specimen was maintained at a total of 800 steps per rotation by the stepper control unit, and the rotation speed was 28 steps per second. The laser beam scanning speed was 3200 scans per second, meaning that 91,428 diametral measurements were taken during each revolution. The average of these measurements was used, to produce 89 recorded readings per revolution. Each specimen was measured across six complete rotations in each sorption time period. The diametral measurements recorded at each time point for each specimen were acquired as overall averages of 534 data values, and these were transferred into an Excel spreadsheet. This enabled the grand mean for the five specimens per group to be calculated for each sorption time period.

Table 3-1: LSM unit specifications

Laser type	Visible semiconductor laser
Laser wavelength	650 nm
Scanning range	Up to 30 mm
Measuring range	0.3 to 30 mm
Resolution	200 nm

3.8 Formulation of model fibre reinforced resin composite (Chapters 6, and 7)

3.8.1 Surface treatment of fillers

The modification of the barium borosilicate glass particle surface was carried out using silane coupling agent 3-trimethoxysilyl propyl methacrylate (3-MPS) as a treatment,

a process which improves the chemical reaction between the resin matrix and the barium borosilicate glass fillers (BaSi) [224-229]. Zanchi et al, conducted a study in which this method was assessed, the results demonstrated that the 3%wt of 3-MPS is most effective percentage for the treatment of BaSi [230]. 60ml of ethanol solvent and 20g of borosilicate particle fillers were put into a plastic container before being placed in a speed mixer (DAC 150.1 FVZK, High Wycombe, Buckinghamshire, UK) (Figure 3-13) and mixed for 20 mins at 1500 rpm. Once the initial mixing had taken place, a sterile syringe was used to slowly add 0.6 g (3%) of the silane coupling agent 3-trimethoxysilyl propyl methacrylate to optimise the mixing of the ethanol and filler. This mixture was then put back into the speed mixer for 10 mins at 1500 rpm, before being separated equally into two tubes and put into a 4000-rpm centrifuge (Heraeus, UK) for 20 mins at 23°C (Figure 3-14). The separated ethanol was removed, and the silanated fillers put into plastic tubes and dried for 3 h in an EZ-2 Elite personal solvent evaporator machine (Genevac Ltd, SP Scientific Company, UK) at 60°C, as shown in Figure 3-15. Once dried, the silanated fillers were stored at room temperature in the laboratory. Table 3-2 shows the reinforcing materials that were used.

Table 3-2: Reinforcing materials used.

Abbreviation	Name	Refractive index	Lot number	Manufacturer
BaSi	Barium borosilicate glass with an average particle size of 0.7 μm*	1.555	EEG 101-07-/871-12	Esschem, Europe
GF	Silanated E-glass fibres with a diameter of 15 μm & length of 3mm.*	1.556	86-792	Hebei yuniu fibreglass manufacturing CO., LTD, Guangzong ,China
3-MPS	3-Trimethoxysilyl Propyl methacrylate	----	2530-85-0	Sigma–Aldrich Inc., St. Louis, USA

*According to manufacturer's information

Figure 3-12: E-glass fibres used in the experimental groups

Figure 3-13: Speed-mixer machine used.

Figure 3-14: A centrifuge machine used in the experiment.

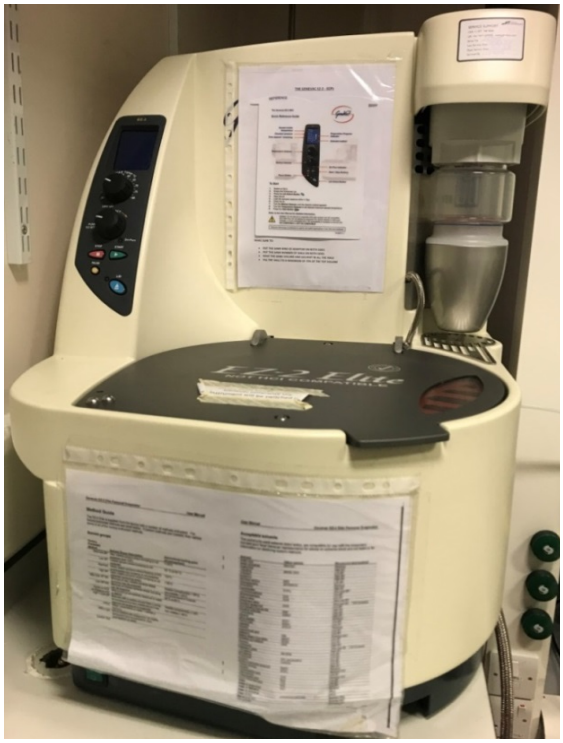

Figure 3-15: Elite personal solvent evaporator machine used.

Figure 3-16: Barium borosilicate glass sinks in water (left), the salinized Barium borosilicate glass floats (right).

3.8.2 Formulation of photo-curable monomer formulation

Four resin monomers groups were formulated: (60% bis-GMA+30 TEGDMA + 10% PMMA) for group A; 50% bis-GMA+ 37.5% bis- EMA + 12.5% UDMA for group B; 50% bis- GMA + 30% bis EMA 20% UDMA for group C; 50% bis-GMA + 25% bis-EMA + 25% UDMA for group D, 50% bis-GMA + 20% bis- EMA + 30% UDMA for group E). Table 3-3 shows the monomers that were used. The amount of the resin matrix was measured using a digital microbalance (BM-252, A&D Company, Japan) (Figure 3-17). The 4 different groups (B, C, D and E) and control group (A) were used in this study and are described in Table **3-4**.

Mixing the different monomers was done with the aid of a SpeedMixer™ (DAC 150.1 FVZK, High Wycombe, Buckinghamshire, UK) for 15 minutes at 1500 rpm for each resin formulation.

Table 3-3: Monomers used in this study. Refractive index values obtained from the manufacturer.

Abbreviation	Name	Refractive index	Lot number	Manufacturer
Bis-GMA	(2,2-bis[4-(2-hydroxy-3-methacryloxypropyloxy)phenyl] propane)	1.540	804-39	Esschem, Europe
UDMA	Urethane dimethacrylate	1.483	803-66	Esschem, Europe
Bis-EMA$_8$	Ethoxylated bisphenol-A dimethacrylate	1.518	849-17	Esschem, Europe
TEGDMA	Triethyleneglycol dimethacrylate	1.461	807-32	Esschem, Europe
PMMA	Polymethyl methyl methacrylate	----	93-097	Esschem, Europe
CQ	Camphorquinone	----	09003A	Sigma–Aldrich Inc., St. Louis, USA
DMAEMA	Dimethylaminoethyl methacrylate	1.438	BCBR4467V	Sigma–Aldrich Inc., St. Louis, USA

Figure 3-17: Microbalance used in this experiment.

Table 3-4: Matrix composition (in wt %) for the control (A) and experimental (B, C, D, E) groups

Group	Bis-GMA	TEGDMA	PMMA	Bis-EMA	UDMA	CQ	DMAEMA
A	59.5%	29.5%	9.5%	----------	----------	0.5%	1%
B	49.5%	----------	----------	37.0%	12.0%	0.5%	1%
C	49.5%	----------	----------	29.5%	19.5%	0.5%	1%
D	49.5%	----------	----------	24.5%	24.5%	0.5%	1%
E	49.5%	----------	----------	19.5%	29.5%	0.5%	1%

3.8.3 Selection of appropriate percentages of E-glass fibres

Garoushi et al, investigated a high aspect ratio discontinuous FRC by introducing short E-glass fibre (5 mm in length) at different percentages into a dimethacrylate/polymethylmethacrylate resin matrix [231]. The results showed that while 22.5 Wt% (E-glass fibre) demonstrated a greater increase in compressive and flexural strength, this did not differ significantly from 14.7 Wt% for compressive strength, 10 Wt% for flexural strength [231] (Table 3-5).

Furthermore, a Brazilian group (Fonseca et al) found that 10 Wt% E- glass fibre (3 mm in length) embedded into filled composite resin (30 wt% silica) facilitated good wetting of the fibres within the material and produced mechanical properties when compared with materials with greater fibre content [232] (Table 3-6).

In regards to the fibre length Garoushi et al [231] observed 2 to 5 mm long fibres resulting in similar values for flexural strength and modulus and compressive resistance, although the greatest values obtained in their study were in samples with 5 mm long fibres. However, 3 mm long fibres exceed the fibre critical value and have a higher potential to be randomly oriented, being the reason for which studies have used this fibre length [102, 232, 233].

Taking into account the results of these studies, the most appropriate percentage of E-glass fibre would be between 10%wt to 15%wt, therefore it was decided that a percentage of 10 Wt% of 3mm E-glass fibres was used.

Table 3-5: Results of Flexural strength and static compressive test of specimens with different fibre volume fractions in mean values [71]

Group (Fibre loading) wt%	Flexural strength Mpa	Compressive strength N
A (0%)	53 (20) [a]	971 (201) [a]
B (8.5%)	192 (24) [b]	1529 (250) [bcde]
C (10%)	226 (38) [bc]	1725 (164) [cde]
D (14.7%)	264 (50) [bc]	2201 (130) [f]
E (22%)	330 (31) [c]	2308 (175) [f]

Superscript letters indicate data sets that are not statistically different (p> 0.05)

Table 3-6: Results of Flexural strength of particulate filled specimens with different E- glass fibre wt % in mean values [232]

Group (Fibre loading wt%)	Flexural strength Mpa
A (0%)	442 (140) [c]
B (10%)	772 (446) [abc]
C (15%)	854 (297) [ab]
D (20%)	863 (418) [a]
E (30%)	459 (140) [bc]

Superscript letters indicate data sets that are not statistically different (p> 0.05)

3.8.4 Selection of appropriate percentages of glass filler (Pilot study)

3.8.4.1 Rational

A pilot study (flexural strength) was carried out in order to ascertain the most appropriate percentages of barium borosilicate glass filler, using mixtures of 60%, 65% and 70%, with 10% E-glass fibre. Four resin mixtures (A, B, C, D) (Table **3-4**) were selected to prepare the required specimens (n=3) for each group.

3.8.4.2 Materials and Methods:

E-glass fibres with twelve resin composite formulations made of 10% wt of the glass fibres, and (60%wt, 65%wt, 70%wt) of filler particles of BaSi (0.7 μm in size), as seen in Table 3-7.

Mixing the resin with the fillers were done with the aid of a SpeedMixer™ (DAC 150.1 FVZK, High Wycombe, Buckinghamshire, UK) for 15 minutes at 1500 rpm for each composite formulation.

For each of the group, a Teflon mould was used to produce three flexural strength specimens. The dimensions of the specimens were 2 mm x 2 mm x 25 mm. The specimens were irradiated five times for 20 s overlapping points on both sides of the specimen, by a LED curing unit with measured average tip irradiance of 1200 mW/cm^2 (Elipar S10, 3M Espe, Seefeld, Germany). Irradiance was verified using a calibrated radiometer after every use of the light curing unit (MARC™ Resin Calibrator, Blue-

light analytics Inc, Halifax, NS, Canada). The flexural strength, values for the specimens were identified by conducting a three-point bending flexural test using a Universal Testing Machine (Zwick/Roell-2020, 2.5kN load cell) at 23±1°C. Each specimen was subjected to a central load in a three-point bending mode, at a crosshead speed of 0.5 mm/s, until each specimen's fracture point has been achieved.

Table 3-7: Classification of the experimental groups of fibre reinforced resin composite according to their particulate wt %.

Experimental groups	Glass fibre wt%	Resin matrix wt%	Particulate fillers wt%
A1 (60% G + 30 T + 10% P)	10%	30%	60%
A2 (60% G + 30 T + 10% P)	10%	25%	65%
A3 (60% G + 30 T + 10% P)	10%	20%	70%
B1 (50% G + 37.5% E + 12.5% U)	10%	30%	60%
B2 (50% G + 37.5% E + 12.5% U)	10%	25%	65%
B3 (50% G + 37.5% E + 12.5% U)	10%	20%	70%
C1 (50% G + 30 % E + 20 % U)	10%	30%	60%
C2 (50% G + 30 % E + 20 % U)	10%	25%	65%
C3 (50% G + 30 % E + 20 % U)	10%	20%	70%
D1 (50% G + 25% E + 25% U)	10%	30%	60%
D2 (50% G + 25% E + 25% U)	10%	25%	65%
D3 (50% G + 25% E + 25% U)	10%	20%	70%

G = bis-GMA, T = TEGDMA, P = PMMA, M = bis-EMA, U= UDMA

3.8.4.3 Statistical analysis

Data for all groups were collected and analysed statistically using SPSS 22.0 (IBM SPSS Statistics, SPSS Inc., Armonk, NY, USA). Two-way ANOVA, one-way AVOVA and Tukey post-hoc tests (α=0.05) were performed to identify differences in FS (dependent variable) between different materials and BaSi % (independent variables).

3.8.4.4 Results:

Table 3-8: Results of Flexural strength of fibre reinforced resin specimens with different particulate wt % in mean values and standard deviation (SD)

Group (Resin monomer)	Flexural strength Mpa (SD)		
	60% BaSi	**65%** BaSi	**70%** BaSi
A (60% G + 30 T + 10% P)	109.6 (10.0) [a]	77.2 (10.0) [b]	Not measured*
B (50% G + 37.5% E + 12.5% U)	99.5 (6.5) [a]	109.8 (5.8) [a]	75.2(3.8) [b]
C (50% G + 30 % E + 20 % U)	124.8 (14.6) [a]	115.6 (8.6) [a]	100.8(5.9) [b]
D (50% G + 25% E + 25% U)	111.2 (18.6) [a]	75.6 (6.8) [b]	Not measured*

G = bis-GMA, T = TEGDMA, P = PMMA, M = bis-EMA, U= UDMA
For each row Superscript letters indicate data sets that are not statistically different (p> 0.05)
*For group A and D 70% of BaSi incomplete wetting of the fillers with the resin matrix hindered the evaluation as shown in Figure 3-18.

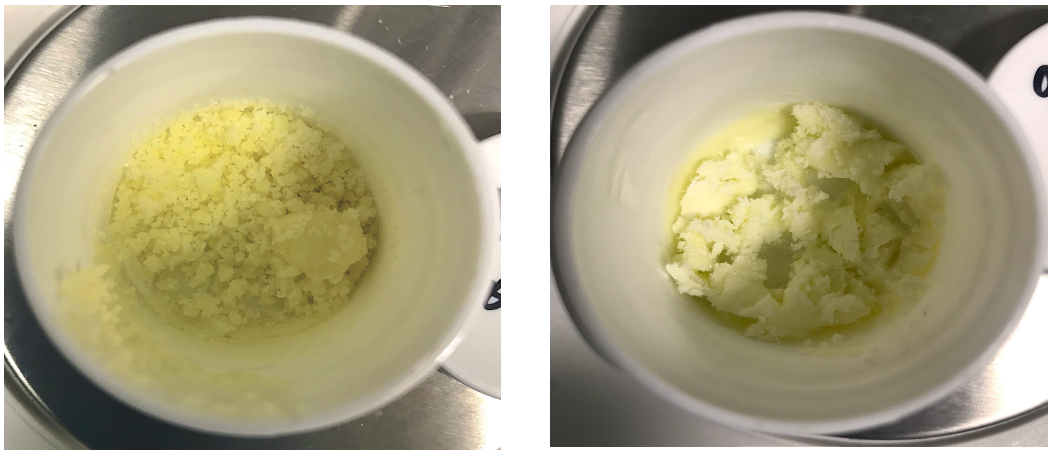

A3 **D3**

Figure 3-18: The appearance of the Photo-curable resin composite for group A3 and D3

3.8.4.5 Conclusion

The result of the pilot study indicated that the most appropriate percentage of salinized barium borosilicate glass filler is 60% with 10% E glass fibres.

Characterization of resin composites:

3.9 The refractive index measurement using Abbe's refractometer. (Chapter 6)

The Refractive index of the cured monomer mixtures was measured with an Abbe's refractometer (Bellingham and Stanley, UK). The instrument was calibrated using a silica standard (Bellingham and Stanley, UK, refractive index of 1.5160) (Figure 3-19). In order to obtain the indices of refraction of the polymer films, one drop of 1-Bromonaphthalene (contacting liquid) (Aldrich, UK, LOT 17640) was employed as an interfacial contact agent. It was placed on the refractometer's lower glass prism, and the upper hinge was pulled down into the locked position over the lower glass prism (Figure 3-20). The refractive index of the l-Bromonaphthalene was measured first, and was measured as 1.660. The silica standard was then put into position and its index of refraction was 1.5155, both of were within the standard values supported by the manufacturers. These readings took place at room temperature (23 ± 1 °C).

A Teflon mould with an internal slot measuring 32 mm x 4 mm x 2 mm was positioned on top of a clear Mylar strip with 1mm thick glass slides. The monomer mixture was then placed in the mould, a second Mylar strip with glass slide was positioned above it and the strips were pressed together. Light curing was carried out with an LED curing unit that had an average tip irradiance of 1200 mW/cm^2 (Elipar S10, 3M Espe, Seefeld, Germany). In total, the samples were photo-polymerised for 120 seconds. There were three overlapping areas of irradiation along the samples' length. A calibrated radiometer was used to confirm the irradiance for each use of the light curing unit (MARC™ Resin Calibrator, Blue-light Analytics Inc, Halifax, NS, Canada). The sample was then removed from the mould and one side was roughened with P1000 silica carbide paper, while the other side was polished with 1 μm and .25 μm diamond paste, utilising appropriate cloth wheels for 1 minute each. The polymers' RIs were measured one day later. One drop of Bromonaphthalene was placed on the polished side of the sample and the index of refraction was measured using the Abbe's refractometer and a sodium D lamp.

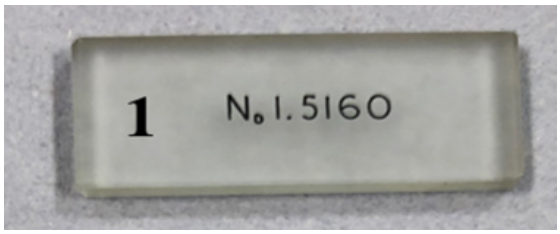

Figure 3-19: The calibration standard

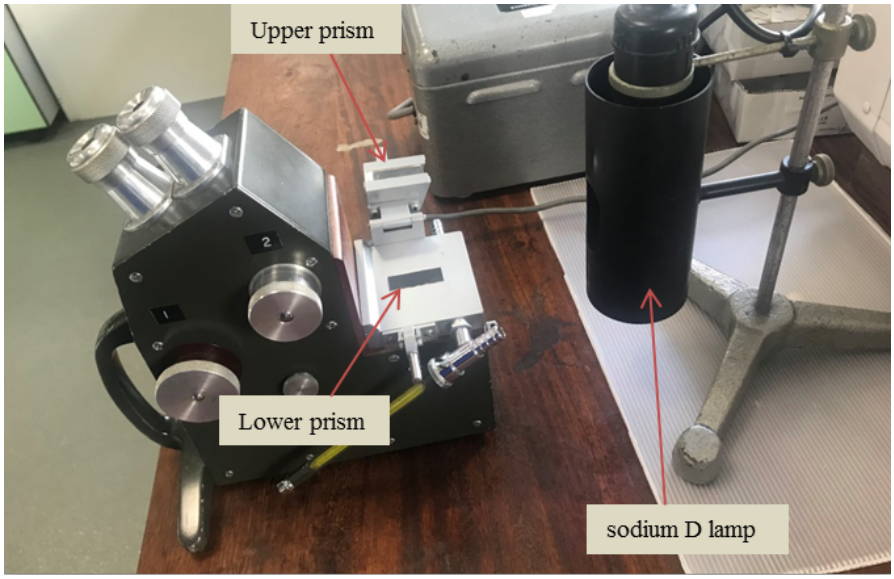

Figure 3-20: Abbe's refractometer and sodium D lamp

3.10 Degree of conversion measurement (Chapter 6)

A Fourier-transform infrared spectrometer (FTIR) (Nicolet 5700 FT-IR spectrometer (Thermo Electron company, USA) (Figure 3-21) was used to measure the DC The spectrometer was fitted with a single reflection horizontal ATR accessory with a crystal diameter of 2.5 mm (MIRacle ATR, PIKE Technologies, 6125 Cottonwood Drive, Madison). OMNIC 8.1 software (Thermo Fisher Scientific Inc) was used to generate the FTIR spectra. The conditions for the FTIR spectrometer were as follows: 4000-500 cm^{-1} wavelength, 4 cm^{-1} resolution, and 32 scans every 60s. Ethanol on lint-free tissue was used to clean the ATR crystal before each sample was measured. On

the day the specimens were taken, a background spectrum was recorded and the software was set to generate a specimen spectrum against this background.

A Teflon mould with a diameter of 6 mm and different thickness (2 mm, and 4 mm); the ATR crystal was completely covered with an uncured composite material. A clear matrix strip and transparent glass slab (1 mm in thickness) were placed over the mould and pressed by the pressure clamp. The FTIR spectra were collected for each uncured sample. Then the glass slab was removed followed by curing the specimen with a LED curing unit for 40 s at room temperature, with an average tip irradiance of 1200 mW/cm^2 (Elipar S10, 3M Espe, Seefeld, Germany). It was ensured that the light tip remained as close to the material as possible. The FTIR spectra for the cured material were obtained directly afterwards.

In order to measure the DC, we assessed the difference in the ratio of the absorbance intensities of aliphatic C=C peak at 1638 cm^{-1} and an internal standard peak of aromatic C=C at 1608 cm^{-1} of the uncured and cured samples (Figure 3-22). The equation below was used to calculate each sample's percentage DC:

$$DC\ (\%) = \left[1 - \left(\frac{1638\ cm^{-1}/Internal\ standard\ peak\ after\ cure}{1638\ cm^{-1}/Internal\ standard\ peak\ before\ cure}\right)\right] X\ 100$$

Figure 3-21: Nicolet 5700 FTIR device

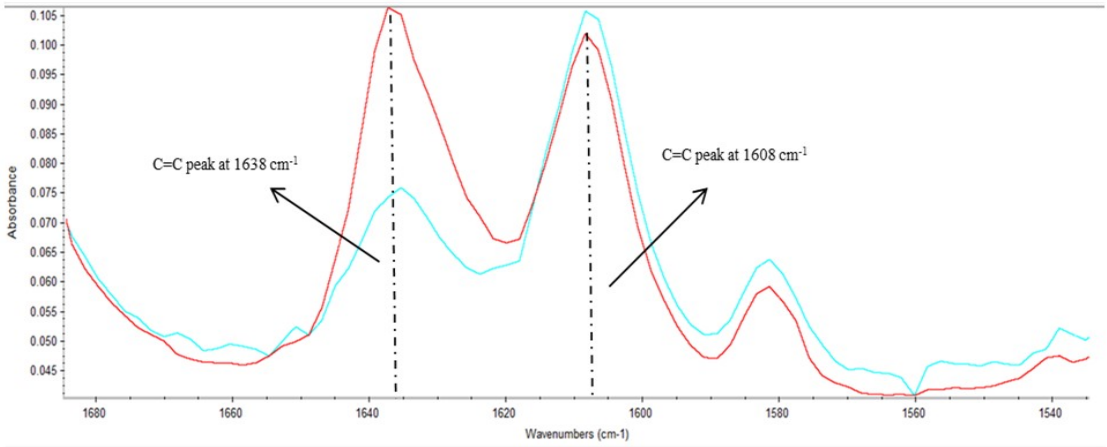

Figure 3-22: FTIR spectra of experimental FRC. The red line shows the spectra of the uncured specimen, while the blue line shows the spectra of cured specimen.

3.11 Depth of cure (DoC). (Chapter 6)

Stainless steel moulds were used to prepare three specimens of each experimental resin composite so that their surface hardness profiles could be obtained. The moulds contained a slot measuring 15 x 4 x 2 mm and a top cover (Figure 3-23). The mould was overfilled with composite, and topped with a Mylar strip and top plate, which was pressed down. Any excess material was scraped away from the top of the mould. These were all held in place with a clamp. The moulds were irradiated from one end. A visible light cure unit with a tip diameter of 10 mm was used to photo-polymerise each specimen for 40 s (Elipar™ S10, 3M ESPE, USA). The top plate and Mylar strip were taken away and the Vickers hardness number (VHN) was measured as a function of material depth at every 0.4 mm. A micro-hardness instrument (FM-700, Future Tech Corp.,Japan) was used to examine the specimens, applying a fixed load of 300 g for 15 s.

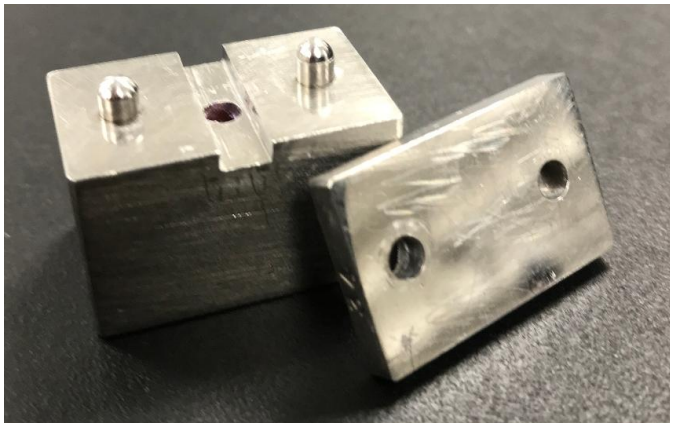

Figure 3-23: Stainless steel mould for DoC specimens.

3.12 Micro Computed Tomography (µCT): (Chapter 7)

3.12.1 SkyScan-1272 System

The SkyScan-1272 system (Bruker microCT, Kontich, Belgium) combines a computer and x-ray microscope in a compact system used for 3D investigation of objects. The computer is loaded with tomographic reconstruction software and the microscope comprises an x-ray shadow microscopic system. In order to investigate an object, three processes are carried out in a set sequence: the object is scanned, reconstructed and subject to 3D analysis. These processes are guided by the SkyScan package software.

After specimen preparation, the SkyScan unit is turned on and then the object is placed in the specimen chamber. The scanning parameters are set as appropriate. In this case, the voltage and current were set at 70kV and 142uA, respectively. A 1mm Al primary beam filter was used for the purpose of decreasing beam hardening artefacts. The objects being scanned in this research were experimental fibre reinforced composites, and these were scanned using the following parameters: image pixel size of 3µm; 0.100° rotation step, 180° sample rotation; 1800 millisecond exposure time. With these parameters, an x-ray image lasting 1800 milliseconds is taken every time the object rotates 0.100°, and this continues until a rotation of 180° has been completed. The operator determines the file name and the acquired projections images are saved in 16-bit .tiff files which are later employed for tomographic reconstruction.

3.12.2 Reconstruction and analysis

The images obtained from the SkyScan were tomographically reconstructed with NRecon software. This was also used to create 2D cross-sectional slices all along the specimen. Both 2D and 3D analysis can be carried out with the CTAn software.

3.13 Flexural strength Measurement. (Chapter 7)

Measuring flexural strength is a common test for dental composites [234], and there are a variety of ways this can be achieved based on the geometry of the specimen to be tested, the selection of load applicators and loading supports, and the specimen preparation method [235]. Testing is generally carried out using three-point bending, which requires that the specimen be of specific dimensions and is supported on two rollers spanning a certain distance, before being loaded from a point source directly above the beam specimen.

Bar-shaped specimens were prepared at room temperature for flexural strength testing using Teflon moulds with dimensions 25 mm x 2 mm x 2 mm. The resin composite was placed and adapted inside the mould before being pressed with a microscope slide (1 mm thickness). The specimens were irradiated six times for 20 s at overlapping points on both sides of the specimen, beginning at the centre. The visible light curing unit previously mentioned was used for irradiation, and afterwards SiC abrasive paper (Emery Cloth, Buckfast Tools Ltd, Manchester, UK) was used to hand-grind away any excess material. Each of the six prepared specimens were stored in distilled water and incubated at 37°C for 24 h, 7 d, and 30 d (Heraeus Incubator BB 16, Heraeus Instruments, Hanau, Germany).

The flexural strength of the specimens was measured using a three-point bending method with a crosshead speed of 0.5 mm/min and a 20 mm span [169]. The apparatus was mounted onto the universal testing machine (Zwick Roell 2020, Leominster, UK). Before testing began, a digital caliper (Powerfix, OWIM GmbH & Co., KG, Germany) was used to measure the thickness of each specimen at each end and in the centre. The median thickness was utilised for calculating the cross-sectional area. The flexural

strength FS (MPa) was calculated using the load at fracture value and specimen dimensions, as per the formula below [169]:

$$FS = \frac{3FL}{2BH^2}$$

Where F (N) is the load at fracture, L is the distance between the supports, b is the specimen width, and h is the specimen height, all in mm.

Chapter Four

Hardness and fracture toughness of resin-composite materials with and without fibres.

Abdulrahman Alshabib*, Nick Silikas, David C Watts

Published in Dental Materials

Appendix I Paper copy

4.1 Abstract

Objectives: To investigate the surface micro-hardness (VHN) and fracture toughness (K_{IC}) of resin-composites, with and without incorporated short fibres, after solvent storage.

Methods: Three resin-composites incorporating fibres, additional to particle reinforcement, were examined: everX™, NovoPro Fill™ and NovoPro Flow™. Four composites were used as controls, with only particle reinforcement: Filtek bulk Fill™, Filtek bulk one™, Filtek XTE™, and Filtek Flow XTE™. For hardness measurement, materials were cured in 2 mm thick moulds for 20 s by a LED source of average irradiance 1.2 W/cm^2. Specimens (n=6/group) were stored dry for 1 h and then in either water or 75% ethanol/water for 1 h, 1 d and 30 d at 37 ± 1°C. Vickers hardness was measured under a load of 300 g for 15 s. For fracture toughness (K_{IC}) measurements, single-edge-notched specimens (n=6/group) were prepared: (32 x 6 x 3 mm) for 3-point bending and stored for 1 and 7 d in water at 37°C. Fractured surfaces of fibre-reinforced composite were examined by scanning electron microscopy (SEM). VHN data were analysed using three-way ANOVA, one-way ANOVA and the Tukey *post hoc* test ($p \leq 0.05$). K_{IC} data were analysed by two-way ANOVA and one-way ANOVA and the Tukey post hoc test ($p \leq 0.05$). An independent t-test was used to detect differences ($\alpha=0.05$) in KIC between stored groups for each material.

Results: VHN decreased for all composites with storage time in both solvents, but more appreciably in 75% ethanol/water (an average of 20 %). K_{IC} ranged from 2.14 (everX Posterior) to 0.96 NovoPro Flow) MPa.$\mathbf{m^{0.5}}$. The longer storage period (7 d) had no significant effect on this property relative to 1 d storage.

Significance: Reinforcement with short fibres, and possibly matrix compositional differences, significantly enhanced the fracture toughness of EVX. However, for nano-fibre containing composites, there were no evident beneficial effects upon either their fracture toughness or hardness compared to a range of control composites. Water storage for 7 days of all these resin-composites produced no significant change in their K_{IC} values, relative to 1 d storage.

Key words: Resin composites, fibre reinforcement, water storage, ethanol/water, fracture toughness, surface hardness.

4.2 Introduction

Improved physical properties of resin-composites, along with their positive aesthetics, mean that they are now the most frequently used direct materials for restoring both posterior and anterior teeth. Following the Minamata convention, the agreed phase down of amalgam is expected to increase the use of resin-composites in posterior restorations [12]. Furthermore, resin-composites are able to strengthen the tooth structure rather than weakening it when compared to dental amalgam [236]. While there have been advances in dental composites in recent times, there still remain numerous challenges to achieve the optimal composite formulation. Resin-composites should withstand harsh environments, that differ between patients, as regards occlusal habits, masticatory forces, abrasive foods, temperature changes, bacteria, and salivary enzymes. The lifespan of resin-composite restoration depends highly on these factors [189, 195, 237]. It is not only the intraoral environment that impacts the longevity; the nature of the resin-composite network itself also has an effect. The crosslink density, porosity, and hydrophilicity of the network, along with the matrix/filler quality and nature of the filler system are all substantial factors [238, 239].

Intra-oral degradation is one of the major causes of failure in direct restorations. It may affect a variety of resin-composite properties, including wear resistance, microhardness, dimensional stability, colour stability, and fracture resistance [202, 212, 240]. Water sorption, temperature, and length of exposure to aqueous media all may have an impact on properties of resin-composites [202]. They can be further degraded by certain chemicals introduced into the oral environment by food and drink and from the by-products of acidogenic bacteria beneath the restoration margins [241].

Acceleration of degradation processes has been demonstrated in studies where materials are aged by immersion in solvents that simulate the oral environment [242]. This suggests that solvent sorption and resulting degradation may decrease the longevity and performance of resin-composite restorations [243]. Simulation of resin-composite degradation in the oral environment may be attempted through the use of food-simulating solvents. These may deteriorate the mechanical properties of a restoration and affect its longevity [189, 202, 244]. If a solvent and a substance share

a similar polarity, they will have a tendency towards mutually solubility or at least softening [245, 246]. For this reason, solvents with solubility parameters between 1.5 and 4.8 x 10.4 (J/m^3) may be used for the oral environmental simulation on dental composites [245, 247].

A promising type of resin-composite include fibres as reinforcement. They are aesthetic materials that incorporate glass fibres and can be used in several dental clinical applications, but predominantly in restorative dentistry [97]. They can offer enhanced mechanical properties that can be very close to those of the natural tissues [220]. The current study aimed to assess how two solvents affected surface hardness, and how water influenced the fracture toughness, of seven resin-composites with and without incorporated short fibres.

The null hypotheses were as follows:

- No difference would be observed in VHN between materials;
- No difference would be observed in VHN values after storage in solvents.
- No difference would be observed in K_{IC} between materials;
- No difference in K_{IC} between materials at 1 and 7 d of water storage at 37°C.

4.3 Materials and methods

The resin-composite materials investigated are presented in Table 4-1. These are two main groups: i) fibre containing composites and ii) Composites reinforced exclusively with particulate fillers. Both groups were chosen to represent composites used for different clinical applications with varying percentages of resin and filler.

4.3.1 Fibre length measurement

Inorganic components were extracted from NovaPro Universal composite. 0.5 g of composite paste was placed in a glass container and 20 ml of tetrahydrofuran (THF 99.9% purity, Lot: 12643750, Fisher Scientific) was added, A spatula was used to stir the THF into the composite paste for two min. The resulting mixture was then separated equally into two tubes before being centrifuged at 4500-rpm (Heraeus, UK) for 20 min at 23°C. The supernatant (separated THF), was extracted using a Pasteur-

pipette. The inorganic component was transferred to plastic tubes before being put into an EZ-2 Elite solvent evaporator (Genevac Ltd., SP Scientific Company, UK) for 3 h to dry at 60 °C. For SEM analysis, a specimen was vacuum sputter coated for two min with 60/40 Au/Pd alloy to form a 10 nm layer thickness (Q150T ES, Quorum technologies, UK). A SEM (Quanta 650 FEG, FEI company, USA) was used to obtain the images of the nano hydroxyapatite fibres. The images were processed to establish the final fibre lengths, using Image-J software [248]. A total of 50 fibres were included in the calculation.

Table 4-1: Composition of Materials investigated according to manufacturer's information.

Material		Manufacturer	Lot number	Type and shade	Filler load		Filler type	Resin matrix
Code	**Name**				Vol %	Wt %		
Fibre and Particulate reinforced composite								
NPU	**NovaPro Universal**	Nanova Inc, Missouri, USA	30001	Nano-fibre reinforced, nano-hybrid Conventional A2 shade	---	77	Barium Borosilicate Glass, Hydrophobic Amorphous Silica, Hydroxyapatite fibres.	Bis-EMA, TEGDMA, UDMA
NPF	**NovaPro Flow**	Nanova Inc, Missouri, USA	2001	Nano-fibre reinforced, nano-hybrid Flowable A2 shade	----	60	Barium Borosilicate Glass, Amorphous Silica, Hydroxyapatite fibres.	Bis-EMA, TEGDMA, UDMA
EVX	**ever X Posterior**	GC Corporation, Tokyo, Japan	1701101	Fibre reinforced BulkFill Universal shade	53.6	74.2	E-Glass short fibres, Barium Borosilicate Glass	Bis-GMA, TEGDMA, PMMA
Particulate reinforced composite								
XTE	**Filtek Supreme XTE**	3M ESPE, St.Paul USA	N836906	Nano-hybrid Conventional A2 shade	63.3	78.5	Zirconia filler Silica fillers/ Zirconia and silica clusters.	Bis-GMA, Bis-EMA, UDMA, PEGDMA
XTF	**Filtek Supreme XTE Flowable**	3M ESPE, St.Paul USA	N522058	Nano-hybrid Flowable A2 shade	46	65	Zirconia filler Silica fillers/ Zirconia and silica clusters	Bis-GMA, BisEMA, TEGDMA
FBF	**Filtek Bulk fill**	3M ESPE, St.Paul USA	N838840	Nano-hybrid Bulk fill A2 shade	58.4	76.5	ytterbium tytterbium trioride and zircon silica	DDDMA, UDMA, AUDMA
FBO	**Filtek One Bulk fill**	3M ESPE, St.Paul USA	N859232	Nano-hybrid Bulk fill A2 shade	58.4	76.5	ytterbium tytterbium trioride and zircon silica	DDDMA, UDMA, AUDMA

Bis-GMA: bisphenol-A-diglycidyl dimethacrylate; Bis-EMA: bisphenol-A-polyethylene-glycol-diether dimethacrylate; TEGDMA: triethylene glycol dimethacrylate; PMMA: polymethyl methacrylate; UDnMA: urethane dimethacrylate, DDDMA (1, 12-Dodecanediol dimethacrylate), AUDM: Aromatic urethane dimethacrylate.

4.3.2 Surface Hardness

Twelve disc-shaped specimens in Teflon moulds (8 x 2 mm) were prepared according to the instructions provided by their manufacturers for each of the seven resin-composites (Table 4-1). Each Teflon mould was placed over a clear Mylar strip with glass slides (1 mm in thickness) on each side and then squeezed together. A LED curing unit with measured average tip irradiance of 1200 mW/cm^2 (Elipar S10, 3M Espe, Seefeld, Germany) was applied directly to the specimen for 20 s. Irradiance was verified through the use of a calibrated radiometer every time the light curing unit was used (MARC™ Resin Calibrator, Blue-light Analytics Inc, Halifax, NS, Canada). Each specimen was subsequently taken from its mould and finished gently on both sides once preparation was complete. For each group a new batch of polishing discs (coarse, medium, fine); were used to remove any excess at the sides of the specimens (OptiDisc; Kerr Hawe SA, Bioggio, Switzerland) using a hand piece (15,000 rpm). Specimens of each material were assigned to one of two groups (n=6) of solvents: distilled water, or 75% ethanol/water.

The specimens were measured 1h after irradiation using a Vickers Micro-hardness Instrument (FM-700, Kawasaki, Kanagawa, Japan), and then again after being solvent stored in the dark at 37 ± 1°C for one and 30 d. Vickers hardness (VHN) was determined using a load of 300 g at 23 ± 1°C for 15 s. At each time interval three indentations were made on each specimen equal distances apart, and 1 mm adjacent indentations and specimen margins (Figure 4-1).

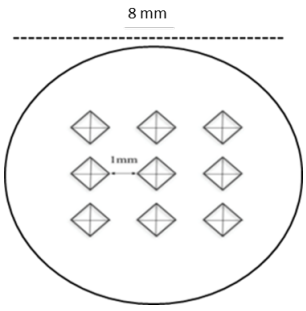

Figure 4-1**:** (A): The ca.1 mm distance between Vickers indentations with 9 indentations per specimen

4.3.3 Fracture Toughness

For each of the materials, a polytetrafluoroethylene (PTFE)-lined brass mould was used to produce 12 single edge notched (SEN) specimens. The mould conformed to British Standard 54479:1978 [221]. The specimens were photo-polymerised for a total of 120 s, by a LED curing unit (as mentioned above). Six overlapping areas of irradiation were utilized along the length of the specimens. Small volumes of composite excess at the edges of the specimen were removed using 320-grit metallographic papers before being stored in small bottles of distilled water and placed in an incubator for 24 h at 37°C. Using a stereomicroscope (EMZ-5; Meiji Techno Co. Ltd. Japan), at 1.5× magnification, the crack length was measured for each specimen to an accuracy of 0.1 mm. The specimen dimensions were measured using an electronic digital caliper (Powerfix, OWIM GmbH & Co., KG, Germany) with an accuracy of 0.01 mm. The width and height were measured at the centre of the sample and at two different points. The fracture toughness (K_{IC}), were measured by flexural loading with a Universal Testing Machine (Zwick/Roell-2020, 2.5kN load cell) at 23 ± 1°C. Each beam specimen was subjected to a central load, in a three-point bending mode, at a crosshead speed of 1.0 mm/s, until each specimen's fracture point was reached (Figure 4-2).

From the load values at fracture, fracture toughness was calculated through the following formula [67]:

$$\boldsymbol{K_{IC}} = \left[\frac{PL}{BW^{1.5}}\right] Y$$

Equation 4.1: Fracture toughness equation

$$Y = [2.9\,(a/w)^{1/2} - 4.6\,(a/w)^{3/2} + 21.8\,(a/w)^{5/2} - 37.6\,(a/w)^{7/2} + 38.7\,(a/w)^{9/2}\,]$$

Where P is the load at fracture, L is the distance between the supports, W is the width of the specimen, B is the thickness of the specimen, Y is calibration function for given geometry, and a is the notch length.

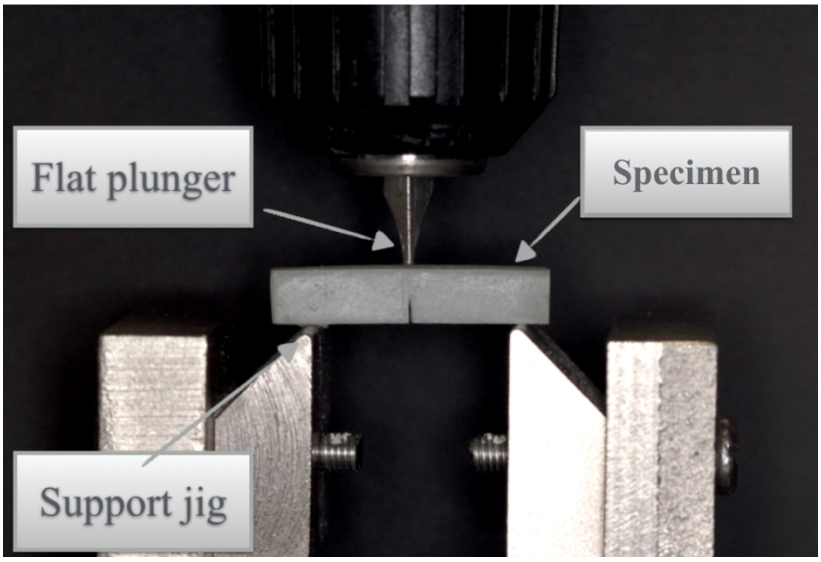

Figure 4-2: Specimen on the measurement jig of the Zwick UTM instrument (Plunger head measurements 7 mm length and 1.2 mm in width).

4.3.4 Scanning electron microscopy (SEM) of fractured specimens

Specimens were vacuum sputter coated for 2 min with 60/40 Au/Pd alloy to produce a 10 nm layer thickness (Q150T ES, Quorum technologies, UK). Then the fracture microstructure was observed for the fibre reinforced composites (EVX and NPU) using a Quanta 650 FEG-SEM (FEI company, USA).

4.4 Statistical Analysis

4.4.1 Micro-hardness

Data for all groups were collected and analysed statistically using SPSS 22.0 (IBM SPSS Statistics, SPSS Inc., Armonk, NY, USA). Three-way ANOVA, one-way ANOVA, and Tukey post hoc test (α=0.05) was performed to identify the interaction between the materials, solvent, and time (independent) and the hardness (dependent). Levene's test of homogeneity was used to analyse all data for equal variances, following the assumption of equal variance.

To investigate the relationships between hardness and filler loading Quadratic regression analysis was performed.

4.4.2 Fracture toughness

Data for all groups were collected and analysed statistically using SPSS 22.0 (IBM SPSS Statistics, SPSS Inc., Armonk, NY, USA). The *Shapiro-Wilk* test was implemented to confirm the normality of the data. Levene's test also confirmed the equality of variance. Two-way ANOVA, one-way AVOVA and Tukey post-hoc tests (α=0.05) was performed to identify differences in K_{IC} (dependent variable) between different materials and time (independent variables).

4.5 Results

4.5.1 Fibre length measurements

The measured length of the nano hydroxyapatite fibres in NovaPro Universal composite varied between 8 µm and 103 µm (average 41 µm). 64% of them ranged between 8 - 50 µm (with average length in this group being 24.3 µm), whereas 36% were between 50-103 µm (with average of 71.6 µm). Results are presented in Table 4-2.

Table 4-2: Measured fibre lengths

Group	Fibre length	
	8 - 50 µm	**50-103 µm**
Fibre lengths grouped by average length (µm).	24.3	71.6
Fibre lengths grouped by percentage values (%).	64%	36%

4.5.2 Micro-hardness

VHN data are presented for each of the composites in Table 4-3 ; Figure 4-3 and Figure 4-4 gives a graphical representation. At baseline (1 h dry storage), VHN ranged between 33.9 and 67.8, reducing to between 24.7 and 52.7 after ethanol/ water ageing. The highest VHN, both prior to and after storage, was seen in XTE, followed by NPU,

and finally NPF, which had the lowest VHN. In specimens stored in 75% ethanol/water, VHN was significantly influenced by the ageing period (decrease in VHN), where baseline readings (1h) were considerably higher than VHN measured over subsequent time periods ($p < 0.05$). VHN reduction ranged between 12.6% for NPU, to 28.8% for EVX. Conversely, specimens stored in water exhibited increased surface hardness after 24 h storage, with the exception of EVX for which no changes were observed. Nevertheless, following 30 d storage these values were significantly lower compared to 1 d measurements ($p < 0.05$), with the exception of NPU for which no significant changes were observed.

There was a positive quadratic relationships between micro-hardness and, filler loading, (Figure 4-5), with r^2 =0.97 for baseline data (1 h dry storage), r^2=0.95 for water storage and r^2=0.95 for ethanol/water storage.

Table 4-3: Vickers hardness VHN (standard deviation) of resin-composites after 1 h dry, and 1d, 30 d storage in two solvents at 37°C

Materials	Distilled water				75% Ethanol/water			
	Dry	**1 D**	**30 D**	**Change %**	**Dry**	**1 D**	**30 D**	**Change %**
NPU	55.3 (1.4) $^{a, 1}$	58.5 (1.7) $^{a, 1}$	55.6 (1.5) $^{a, 1}$	+0.5%	56.8(1.1) ^{a,1}	53.2 (1.8) $^{a, 1}$	49.6 (1.7) $^{b, 1}$	-12.6%
NPF	33.9 (1.5) $^{a, 2}$	36.1 (1.6) $^{b, 2}$	32.8 (1.2) $^{a, 2}$	-3.2%	34.0 (2.5) $^{a, 2}$	27.5 (2.1) $^{b, 2}$	24.7 (1.7) ^{b,2}	-27.3%
EVX	54.5 (2.0) $^{a ,1}$	54.4 (1.1) $^{a ,3}$	47.7 (1.6) $^{b, 3}$	-12.4%	54.4 (2.1) $^{a, 1}$	41.1 (2.3) $^{b, 3}$	38.7 (1.2) $^{c, 3}$	-28.8%
XTE	67.8 (1.6) $^{a, 3}$	69.1 (2.2) $^{a, 4}$	62.5 (1.8) $^{b, 4}$	-7.8%	68.1 (1.3) $^{a, 3}$	57.8 (2.2) $^{b, 4}$	52.7 (0.9) $^{c, 4}$	-22.6%
XTF	36.2 (1.6) $^{a, 2}$	37.3 (1.5) $^{a, 5}$	33.1 (1.3) $^{b, 5}$	-5.8%	36.1 (1.3) $^{a, 2}$	32.4 (2.1) $^{b, 5}$	29.5 (1.8) $^{b, 5}$	-18.2%
FBO	47.4 (1.5) $^{a, 5}$	50.8 (1.3) $^{b, 6}$	47.8 (1.9) $^{a, 3}$	+0.8%	46.9 (1.9) $^{a, 4}$	44.2 (2.1) $^{b, 6}$	39.4 (1.1) $^{c, 3}$	-16.9%
FBF	48.3 (0.9) $^{a, 5}$	52.4 (1.2) $^{b, 3,6}$	48.1 (1.5) $^{a, 3}$	-0.4%	47.6 (1.8) $^{a, 4}$	43.4 (2.3) $^{b, 6}$	38.5 (1.9) $^{c, 3}$	-19.1%

For each solvent the same superscript letters indicates no significant difference ($p > 0.05$).
NB each solvent is treated statistically independent.
At each time interval same number superscripts indicates no significant difference ($p > 0.05$).

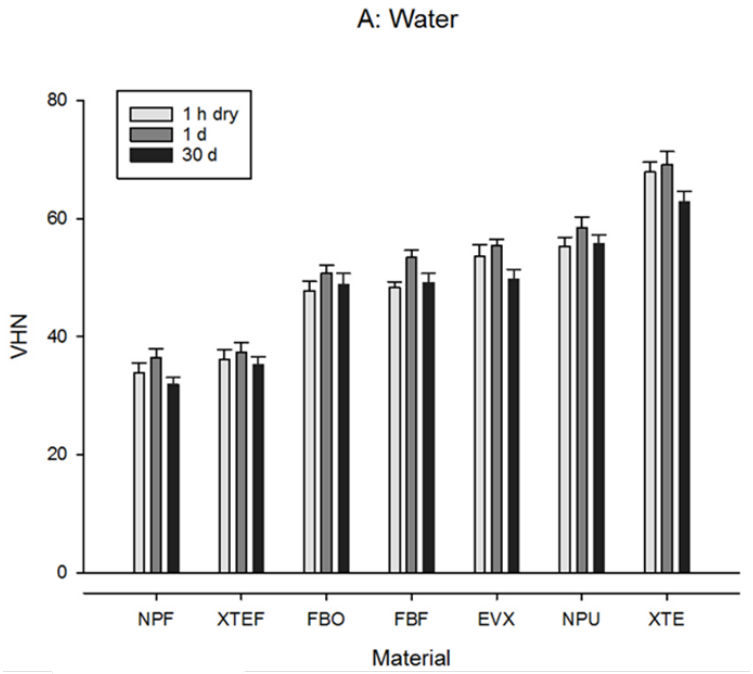

Figure 4-3: Vickers hardness (VHN) of resin-composites after 3-time intervals stored in water, 1h dry, 1d and 30 d at 37˚C showing minimal reduction.

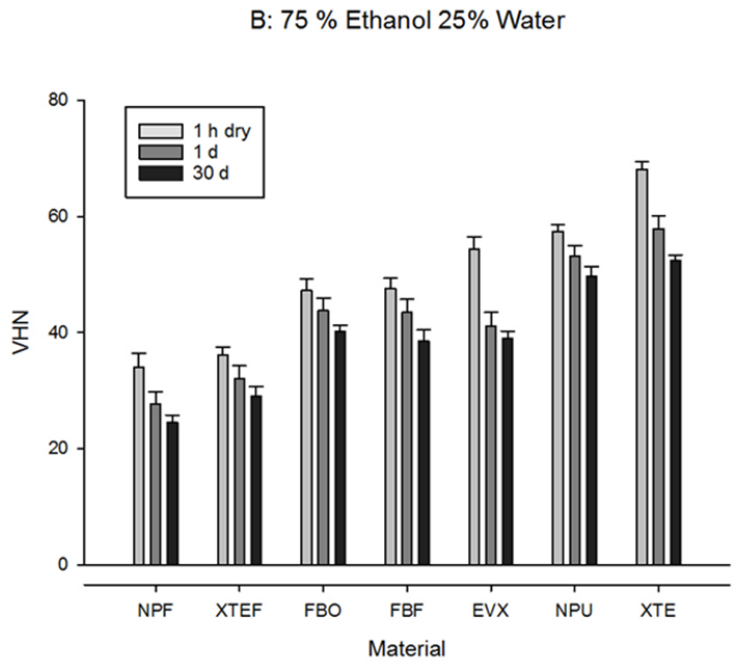

Figure 4-4 :Vickers hardness (VHN) of resin-composites after 3-time intervals stored in 75% Ethanol / water at 37˚C., 1h dry, 1d and 30 d, showing significant reduction.

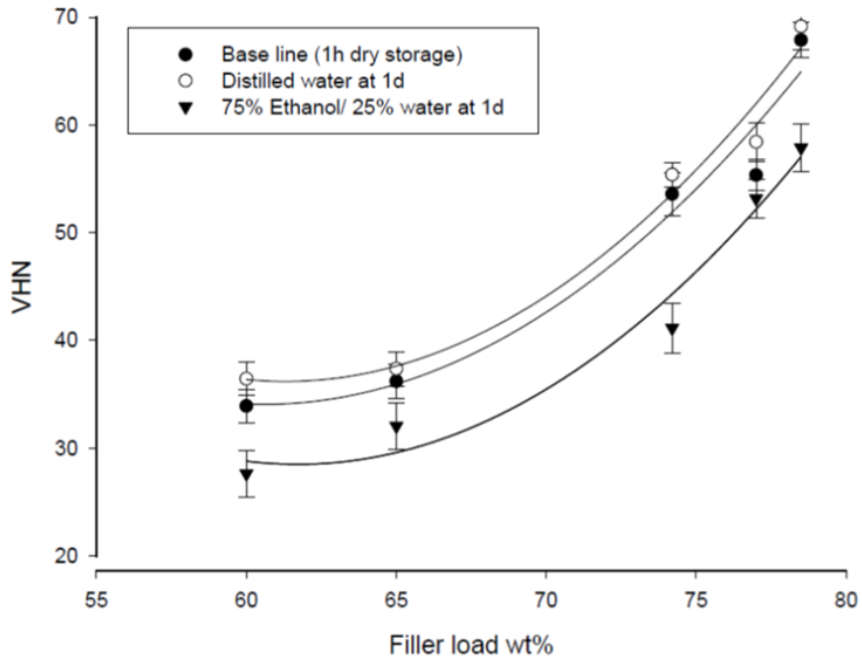

Figure 4-5: Quadratic regression analysis of the micro-hardness (VHN) and filler loading wt %.

4.5.3 Fracture toughness

K_{IC} values for the composites are presented in **Table 4-4** and shown graphically in Figure 4-6. K_{IC} ranged from 0.96 to 2.14 M.Pa $m^{0.5}$ There were statistically significant differences between resin-composites ($p < 0.05$). EVX showed the highest K_{IC}, while NPF showed the lowest (after both 1 and 7 d storage). Although mean K_{IC} increased numerically with storage time, except for EVX, there was no statistical significant change over time for the materials studied. However, there were statistically significant differences in K_{IC} between the materials ($p < 0.05$)

Table 4-4: Fracture toughness (standard deviation) of resin-composites measured

Materials	Fracture toughness KIC (M.Pa.m0.5)	
	1 D	**7 D**
NPU	1.23 (0.14) [a]	1.27 (0.15) [a, d]
NPF	0.96 (0.09) [c]	0.98 (0.13) [c]
EVX	2.14 (0.16) [b]	2.10 (0.18) [b]
XTE	1.37 (0.23) [a]	1.39 (0.17) [a]
XTF	0.97 (0.08) [c]	1.02 (0.08) [c]
FBF	1.46 (0.17) [a]	1.58 (0.30) [a ,e]
FBO	1.45 (0.09) [a]	1.47 (0.12) [a]

The same superscript small letters indicate a homogeneous subset (columns) ($p > 0.05$)

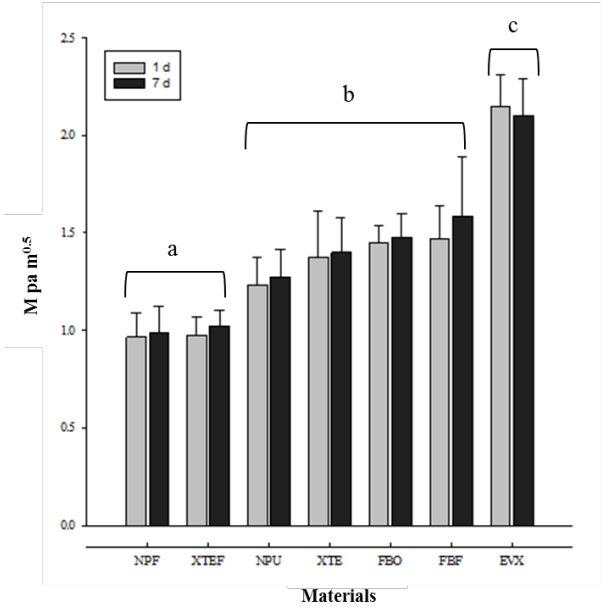

Figure 4-6: Fracture toughness (standard deviation) of composites after 1 and 7 d storage in water at 37°C. The same superscript small letters indicate a homogeneous subset (columns) ($p > 0.05$).

4.5.4 SEM examination

A representative SEM micrograph of EVX is presented at a magnification of 75 x (

Figure 4-7). Protruding fibre ends are apparent at the point of fracture of the single-edge-notched-beam specimen. In Figure 4-8, showing NPU at a magnification of 3000X, an extracted hydroxyapatite fibre bundle is seen. These hydroxyapatite fibres had a mean length of 41 μm, within the range shown in Table 4-2. The combination of particulate fillers and fibres are visible in the SEM-micrographs of the NPU composite surface.

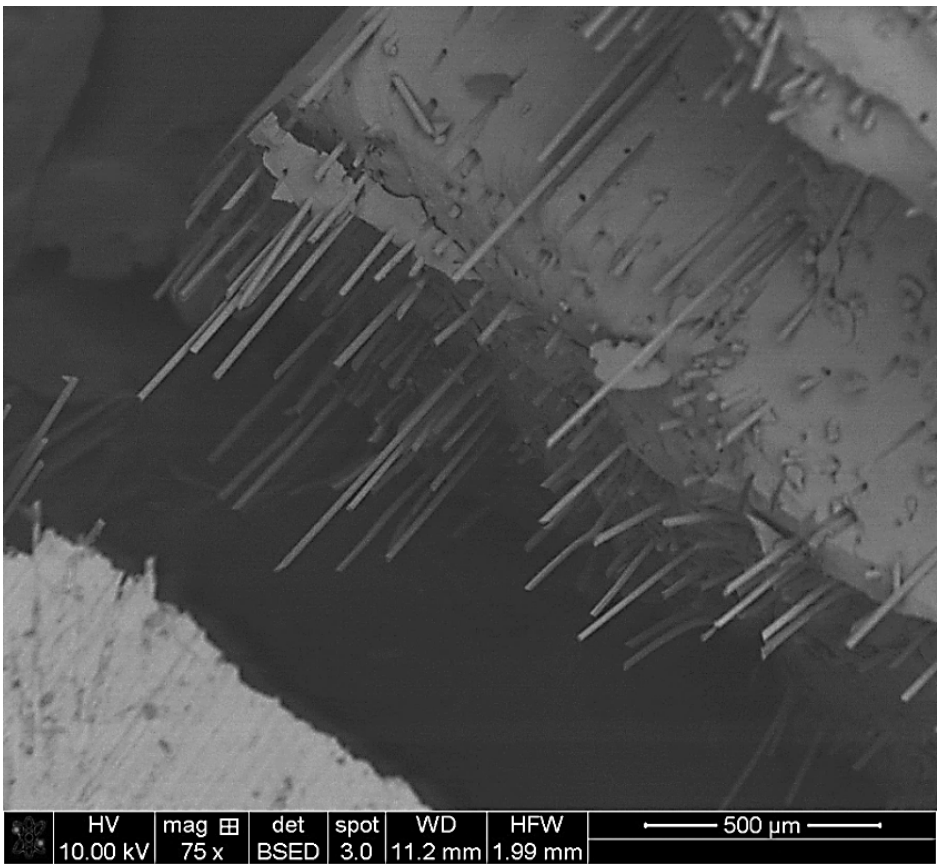

Figure 4-7: Image obtained in back scattered electron mode (x75) at a fracture site in the fibre reinforced resin-composite (everX ™) with protruding E-glass fibres.

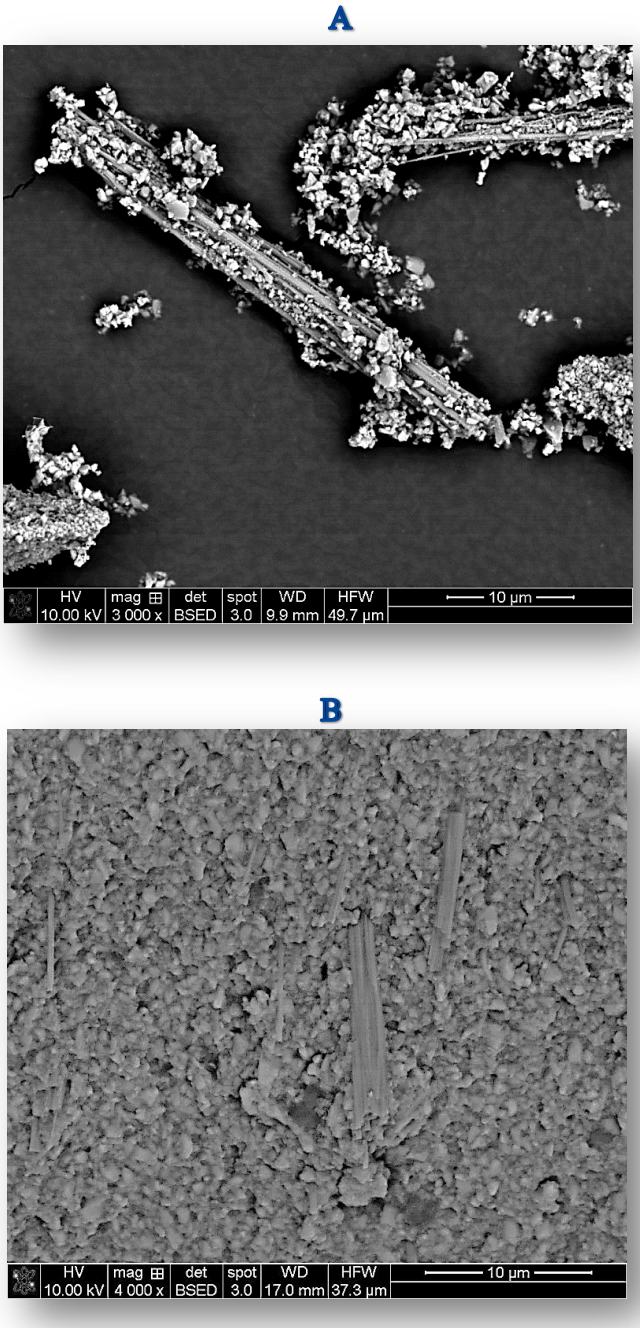

Figure 4-8 A**:** Image (x 3000) of extracted hydroxyapatite fibre bundles from fibre reinforced resin-composite (Novopro-fill™). **B:** Image obtained in back scattered electron mode (x 4000) at fracture site from fibre-reinforced resin-composite (Novopro-fill™).

4.6 Discussion

4.6.1 Micro-hardness

The first part of this study reported the effect two different solvents (water, 75% ethanol/water), on Vickers hardness of resin composites. Significant effects on hardness were observed according to materials, storage medium, and time ($p < 0.05$). Therefore, the first and second null hypotheses were rejected.

Several resin-composite factors can affect hardness including filler size, shape and fraction in the inorganic phase. Hardness generally increases with filler content [66, 249]. This is physically understandable since, as the volume-fraction of filler increases, the point is reached where particles are mutually in contact within the matrix. Beyond this point stress is transferred across the material predominantly via (hard) particle-particle interactions. Hardness is also influenced by the specific composition and structure of the organic matrix [9]. However, the physical and mechanical properties of a resin-composite can be weakened through chemical softening. The chemical composition of a resin-composite and the media to which it is exposed can therefore have a considerable effect on its properties [189].

This study reported the effect of food-simulating solvents on Vickers micro-hardness of resin-composites (distilled water, 75% ethanol/water). The top surface of the specimen was selected to measure the surface hardness. The irradiance generally reduces through the bulk of composite, owing to light being scattered by filler particles and resin matrix [250]. Thus, the top surface provides an optimum measurement due to the photo-irradiation tip of the light cure unit focusing directly on the surface.

Water sorption usually increases with resin content and monomer hydrophilicity [251]. The effect of diffusion-controlled water sorption first causes a softening of the matrix at the surface, with time needed for water to penetrate through the material bulk [252, 253]. This effect is enhanced for certain monomers, but has also been shown to be enhanced in composites with less filler concentration [254].

The surface hardness of all the restorative materials after 1 d of storage in distilled water increased relative to the baseline hardness. This is most probably due to

additional monomer post-curing via cross-linking reactions in the resin phase over time. However, storage for 30 d in distilled water decreased surface hardness of the restorative materials. This will be due to water acting as a plasticizing molecule within the composite matrix, causing a softening of the polymer resin component by swelling the network and reducing the forces between polymeric chains [74]. However, in 75% ethanol/water storage, a significant reduction was seen in VHN between 1 and 24 h and continuing over 30 days. This finding is in agreement with previous studies that reported a significant reduction in hardness after 1 d storage in ethanol [245]. The ethanol/water solution may degrade the resin and matrix/filler interface, as it easily diffuses and swells the resin matrix relieving tensile stress near the matrix/filler interface, which increases diffusion and leaching [255, 256]. Decreases in surface hardness and wear resistance after storing resin-composites in ethanol have been ascribed to chemical softening influences [257].

EVX is a glass fibre reinforced resin-composite. VHN of EVX after 30 d reduced by 9% in water and by 29% in 70:30 ethanol: water. This VHN reduction is most probably due to hydrolytic disruption between the matrix and the glass fibres. Glass fibre reinforced composites absorb more water than conventional composites, which may also be related to the hydrophilicity of the polymer network [189, 258, 259].

In this study, a positive correlation between VHN and filler loading was confirmed. This is in agreement with several studies concerned with filler loading [249, 260, 261]. NPF and XTF materials had the lowest VHN – evidently due to their low filler loading. Some nano-hybrid resin based materials have shown good mechanical properties [262]. The three nano-hybrid composites used in this experiment (XTE, FBF and FBO) showed a VHN reduction *circa* 20% after 30 d of ethanol/water storage. NPU is a hydroxyapatite fibre reinforced resin-composite, which had the least reduction (12%) in VHN among all the investigated materials after storage in 75% ethanol/water. This might be due to the high filler load with a hydrophobic resin matrix compared to the other materials. The main resin constituents of NPU are Bis-EMA and UDMA, which have demonstrated better degradation resistance during chemical aging [263].

4.6.2 Fracture toughness

For a long time, secondary caries has been reported as the most common reason for posterior resin-composite failure [195]. However, other studies have demonstrated that the most common reason for replacement of posterior restoration after five years is bulk fracture of the composite filling [171]. Restoration fracture has also been indicated as the main cause of failure in composite fillings used in larger cavities for periods of 11 years or longer [264, 265]. A meta-analysis carried out on posterior resin-composite restorations found that a minimum of 5% of restorations will fail from material fracture within a ten-year observation period [172]. The measurement of fracture toughness is, therefore, a worthwhile and often-used technique to characterize a material's resistance to fracture [119]. The result of this study showed that the K_{IC} varied significantly within the total set of materials ($p<0.05$). According to the method of application of the resin composite, the composites can be categorised into one of three bands: conventional composites (NPU and XTE), with values of 1.23 and 1.37 M.Pa $m^{0.5}$; bulk fill composites (EVX, FBO and FBF), with the highest value being 2.14 M.Pa $m^{0.5}$ for EVX; and lastly, flowable composites (NPF and XTF), with values of 0.96 and 0.97 M.Pa $m^{0.5}$, respectively. Therefore, the third null hypothesis was rejected. However, there were no statistically significant differences in fracture toughness from 1 to 7 days water storage. Therefore, the fourth null hypothesis was accepted.

The Single-Edged-Notch (SEN) beam method [266, 267] was chosen to determine fracture toughness in the current research. Such specimens are particularly sensitive to the depth and width of the notch [266] which makes it difficult to make direct comparisons between studies. Within this study, however, genuine differences in fracture behaviour of resin-composites could be established as specimen preparation and measurement conditions were constant.

Storage in water, even in the short term, can lead to deterioration in mechanical properties regardless of material type. Hydrolysis of bonds between filler and matrix is a potential mechanism for degradation by water [178, 268, 269]. A toughening effect can also occur due to the aqueous plasticization of the resin matrix [270], that may enable the specimens to be more compliant before fracturing. However, swelling

and deterioration of the cross-linked matrix within the composite, the leaching of components, and filler-matrix interface hydrolysis will ultimately result in a decline in mechanical properties [188, 270]

While prior research has identified a positive association between K_{IC} and filler load [270-272], other studies of dental composites have seen an increase in the K_{IC} with filler load up to 55 vol%, followed by a decline of K_{IC} with filler loads exceeding 55 vol% [273, 274]. The volume-fraction in the present study is not reported for some of the materials, and therefore the effect cannot be established. The shape, size, and distribution of filler particles are also relevant for mechanical properties [275].

In the present research, an improved resistance to crack propagation was seen in EVX, evidently due to this material's fibre and matrix-related properties. EVX contains fibres which are longer than the critical fibre length [83, 104, 106] which are more effective in transferring stress from the matrix. EVX has a semi-interpenetrated network (SIPN) matrix type, in which the existence of thermoplastic PMMA chains reduces the stiffness of the Bis-GMA monomer. These specific features may improve the flexural properties of the composite material and enhance its resistance to fracture development. These results are in agreement with extant literature on the topic [105, 106, 143]. The fibre length distribution of NPU fibre-reinforced composite was determined as between 8 and 103 μm, with two thirds of these fibres up to 50 um and one third up to 100 um. This contrast with the length of the EVX fibres (1,000 – 2,000 μm) may explain why EVX exhibited superior fracture toughness to NPU. This is consistent with a recent study of NPU showing that its mechanical properties were not significantly different from particulate filled composites [276]. Furthermore, bundling of the hydroxyapatite nanofibres starts to occur when the hydroxyapatite nanofibre mass fraction reaches 10 wt% [277]. At a hydroxyapatite nanofibre mass fraction of 20 wt%, the number of nanofibre bundles increased enough to create weak points in the dental resin matrix, resulting in decreased flexural strengths. Nanofibre bundling was also apparent in the SEM images of NPU (Figure 8A, B).

High K_{IC} has been seen for both FBO and FBF, which are bulk-filled nano-composites. This could be due to reduced flaw-size or an increase in monomer conversion [278]. K_{IC} can also be increased in nano-composites through enhanced bonding at the filler-

matrix interface and through high strength filler and an increased surface area to volume ratio [279]. Increasing the fracture resistance and strength of the matrix will also increase the resin-composite fracture toughness.

4.7 Conclusion

Within the limitations of this study it was concluded that:

- A glass-fibre reinforced resin composite (EVX) showed the highest K_{IC} while NPF, XTF (flowable composites) had the lowest K_{IC}.
- Reduction in surface hardness of EVX glass fibre reinforced composite in food simulating solvent (75% ethanol 25% water) supports the manufacturers' recommendations to cap this material with a conventional resin composite.
- The composite composition and the particular solvent environment both affect degradation of material properties.

4.8 Acknowledgement

GC Corporation, Tokyo, Japan for supplying everX Posterior

Chapter Five

Material behaviour of resin-composites with and without fibres after extended water storage.

Abdulrahman AlShabib*, Nick Silikas, David C Watts
Accepted in Dental Materials Journal

5.1 Abstract

Objective: To determine the long-term water sorption, desorption and hygroscopic expansion processes of resin-composites with and without incorporated short fibres.

Methods: Three resin-composites incorporating fibres, additional to particle reinforcement, were examined: everX™ (EVX), NovoPro Fill™ (NPU) and NovoPro Flow™ (NPF). Four composites were used as controls, with only particle reinforcement: Filtek bulk Fill™ (FBF), Filtek bulk one™ (FBO), Filtek XTE™ (XTE), and Filtek Flow XTF™ (XTF). Filler mass measurements were made according to ISO 1172 for which composites (n=2) were cured in Teflon moulds (2 x 4 mm) for 20 s. For water sorption and solubility measurements, 15 x 2 mm disks of each composite (n=5) were irradiated for 20 s at five sections per side by LED light delivering irradiance of 1.2 W/cm^2. Over 140 d specimens were water immersed at 37 ^{o}C, weighed at intervals, then dried for a further 42 d at 37±1°C, to determine solubility. A laser micrometer measured mean diametral expansion, as each specimen underwent sorption. A one-way ANOVA was carried out at 140 d with Tukey post-hoc tests (at $\alpha = 0.05$).

Results: Water sorptions ranged between 20.4 and 30.1 μg/mm. XTF exhibited the highest sorption, followed by EVX and NPF, for which both results were similar. Polymer matrix sorption ranged from 3.4% for NPU to 4.7% for EVX. The solubility range was between -1.4 to 4.1μg/mm; XTF had the highest solubility, with EVX demonstrating negative solubility: -1.49μg/mm. Hygroscopic expansion at 140 days ranged between 1.4% for hydroxyapatite fibre reinforced composite (NPU) and 2.2% for E-glass fibre reinforced composite (EVX).

Significance: The relatively high water sorption and expansion of the short E-glass fibre reinforced composite (EVX) supports the manufacturers' recommendations to cap this material with a conventional composite. A nano-fibre containing composite (NPU) had the most favourable sorption outcomes compared to a range of composites, which could be related to matrix compositional differences.

Key words: resin composites, fibre reinforced composite, water sorption, solubility, hygroscopic expansion, laser scan micrometer.

5.2 Introduction

The majority of resin composites are known to be chemically stable; however, chemicals present in the oral environment can be absorbed by composite polymer networks, and some of the components from the resin and filler could be released into the surrounding area [179, 280]. These occurrences are known as sorption and solubility, and these processes into and out of the network structures can result in undesirable physical and biological effects [189]. Resin composites are significantly affected by sorption and solubility in terms of longevity, as these processes affect the material's physical and mechanical properties such, colour and dimensional stability, strength, and hardness [77, 188, 189, 281].

A wide range of chemicals are found in the oral environment, including alcohol, acids and bases. The effects that these chemicals have on resin composites depend on a number of factors such as the nature of the chemicals and the length of time the material is exposed to them [189]. While the oral environment does play a significant role, the nature of the resin composite is also a factor; the filler system's nature, the porosity, crosslink density and hydrophilicity of the network, and the quality of the filler interface all have a considerable effect [9].

Long-term clinical success of a resin composite depends significantly on its dimensional changes, both during and after curing [120]. Unreacted monomer can be gradually released from these materials, water can also be absorbed and take up all of the free volume of the network structure which may lead to swelling through the separation of chains in the polymer network [282]. The elastic modulus of the polymer is known to be affected by the uptake of water, which coupled with hygroscopic expansion could potentially relax the internal stresses created by constrained shrinkage [120]. It is not as straightforward as this, however, because the expansion caused by water uptake is not controlled and can result in alternative deleterious stresses. Moreover, each of these phenomena follow very different timescales. For instance, shrinkage takes place within seconds – days at a maximum [283, 284]; on the other hand, water absorption occurs many days, and saturation typically takes weeks [188, 280]. Prior research found that material expansion is not controlled and

can lead to potential stresses on the cavity walls, which may subsequently cause micro-cracks in the restored tooth [188]. These findings demonstrate the importance and complexity of dimensional changes in resin composite, highlight their unpredictability and that these changes depend on both the material and solvent involved [120, 188, 189].

A promising type of resin-composite includes fibres as reinforcement. These fibres enhance composite properties by acting mainly as crack stoppers [74, 97]. They can offer enhanced mechanical properties that can be very close to those of the natural tissues [220]. This approach was first reported for reinforcement of polymethylmethacrylate (PMMA), which was later utilized in a different aspect of clinical dentistry [97]. Furthermore, reinforcing the resin with fibres improves the capacity of distributing the stress more efficiently when the loads are concentrated on the restoration [74]. Having said this, several factors play an important role in ensuring the efficiency of fibre reinforcement, such as fibre type and aspect ratio [167].

Several fibre materials have been used as reinforcement; carbon, for example, has been utilized in post and core systems. Unfortunately, the dark colour of the fibres restricts their clinical use as a tooth-coloured restorative material [285]. However, inorganic glasses may have favourable aesthetic, mechanical and chemical properties. Thus, glass fibres have been used as reinforcement for direct restorations [97]. Electrical/E-glass is the most commonly used glass fibre due to its low cost [97]. Due to the biocompatibility of hydroxyapatite [84], it has been used in resin composites to improve their mechanical properties. This material could be deployed in various forms, such as particulate fillers [109] or fibres [85].

According to Callister et al, short fibres with a subcritical length are not effective and significantly lower the reinforcement effect of any resin containing such [90]. This length may be defined as the minimum fibre length required for optimal stress transfer within the resin matrix [86]. It is the minimum length at which a fibre will fail, midway along its length in an fibre reinforced composite (FRC), rather than as interfacial fracture between the matrix and the fibre [87]. The critical fibre length should be 50 times greater than the diameter of the fibre to allow homogenous stress transfer within the resin matrix [87].

The present objective was to determine time-dependent water sorption and related properties of seven resin composites with and without incorporated short fibres. The null hypotheses were as follows:

• No difference in either water sorption or solubility between the evaluated resin composites after 140 d water exposure.

• No difference in hygroscopic expansion between the evaluated resin composites after 140 d water storage.

5.3 Materials and methods

The resin-composite materials investigated are presented in **Table 5-1**. Three fibre containing composites and four composites reinforced exclusively with particulate fillers. They were chosen to represent composites used for different clinical applications with varying percentages of resin and filler.

Table 5-1: Composition of Materials investigated according to manufacturers' information.

Materials		Manufacturer	Lot number	Type and shade	Filler load		Filler type	Resin matrix
Code	Name				Vol %	Wt %		
Fibre and Particulate reinforced composite								
NPU	**NovaPro Universal**	Nanova Inc, Missouri, USA	30001	Nano-fibre reinforced, nano-hybrid Conventional A2 shade	---	77	Barium Borosilicate Glass, Hydrophobic Amorphous Silica, Hydroxyapatite fibres.	Bis-EMA, TEGDMA, UDMA
NPF	**NovaPro Flow**	Nanova Inc, Missouri, USA	2001	Nano-fibre reinforced, nano-hybrid Flowable A2 shade	----	60	Barium Borosilicate Glass, Amorphous Silica, Hydroxyapatite fibres.	Bis-EMA, TEGDMA, UDMA
EVX	**everX Posterior**	GC Corporation, Tokyo, Japan	1701101	Fibre reinforced BulkFill Universal shade	53.6	74.2	E-Glass short fibres, Barium Borosilicate Glass	Bis-GMA, TEGDMA, PMMA
Particulate reinforced composite								
XTE	**Filtek Supreme XTE**	3M ESPE, St.Paul USA	N836906	Nano-hybrid Conventional A2 shade	63.3	78.5	Zirconia filler Silica fillers/ Zirconia and silica clusters.	Bis-GMA, Bis-EMA, UDMA, PEGDMA
XTF	**Filtek Supreme XTE Flowable**	3M ESPE, St.Paul USA	N522058	Nano-hybrid Flowable A2 shade	46	65	Zirconia filler Silica fillers/ Zirconia and silica clusters	Bis-GMA, BisEMA, TEGDMA
FBF	**Filtek Bulk fill**	3M ESPE, St.Paul USA	N838840	Nano-hybrid Bulk fill A2 shade	58.4	76.5	ytterbium tytterbium trioride and zircon silica	DDDMA, UDMA, AUDMA
FBO	**Filtek One Bulk fill**	3M ESPE, St.Paul USA	N859232	Nano-hybrid Bulk fill A2 shade	58.4	76.5	ytterbium tytterbium trioride and zircon silica	DDDMA, UDMA, AUDMA

Bis-GMA: bisphenol-A-diglycidyl dimethacrylate; Bis-EMA: bisphenol-A-polyethylene-glycol-diether dimethacrylate; TEGDMA: triethylene glycol dimethacrylate; PMMA: polymethyl methacrylate; UDMA: urethane dimethacrylate, DDDMA (1, 12-Dodecanediol dimethacrylate), AUDM: Aromatic urethane dimethacrylate.

5.3.1 Measurement of filler content

To measure each resin composite's mass percentage of inorganic filler, the ISO 1172:1996 standard ash method was followed [223]. For each composite (**Table 5-1**) two specimens were made (n=2). Teflon moulds were used to prepare the specimens (2 mm thickness, 4 mm diameter) and they were placed between two sections of clear Mylar strip with glass slides on each side (1 mm in thickness) and then squeezed together. An LED light curing unit with an output irradiance of 1.2 W/cm2 was used to irradiate the specimens for 20 s on one side (Elipar S10, 3M Espe, Seefeld, Germany). The irradiance was measured every time the light cure unit was utilized, using a calibrated radiometer (MARC™ Resin Calibrator, Bluelight Analytics Inc, Halifax, NS, Canada). The specimens were then stored for 24 h at 37°C. An electric furnace (Programat EP 5010, Ivoclar Vivadent) was used to keep a silica crucible at 630°C for 30 min. Once the crucible had been cooled to ambient temperature in a desiccator containing silica gel at 37± 1°C, a precision digital balance (BM-252, A&D Company, Japan) was used to determine its weight. Each of the composite specimens was placed in the crucible and the balance was used again to weight the specimen, including the crucible. To burn out the organic matrix, the specimen-containing crucible was placed in the electric furnace for 30 min at 630°C. Once cooled to ambient temperature in a desiccator, the crucible and residue were reweighed. The following equation was used to determine the inorganic filler content:

$$\textbf{\textit{Filler content}}\ (\%) = \frac{a_3 - a_1}{a_2 - a_1}\ \mathbf{x}\ 100$$

Equation 5.1: Filler content formula

Where a_1 is the mass of the crucible, a_2 is the mass of the crucible plus the specimen; a_3 is the final mass of the crucible plus the residue after heat treatment.

5.3.2 Sorption and solubility:

5.3.2.1 Specimen preparation

Using brass moulds, five disc-shaped specimens were produced for each material. The moulds, with dimensions of 15 x 2 mm, were placed between two sections of clear Mylar strip with glass slides on each side (1 mm in thickness) and then squeezed together. The thickness of specimen was modified from 1 mm to 2 mm. This increased thickness, corresponding more closely to clinical setup, allowing water sorption studies over a longer period. An LED curing unit with measured average tip irradiance of 1.2 W/cm^2 (as mentioned above) was used to irradiate five sections of each side for 20 s. The irradiance was measured every time the light cure unit was utilized, using a calibrated radiometer (as mentioned above). The specimens were taken out of their moulds with care, and 1000 grit silicon carbide paper was used to smooth out any rough edges. Following this, the specimens were placed in a desiccator containing silica gel at 37± 1°C. After a period of 24 h a precision-calibrated balance was used to weight each specimen, accurate to ± 0.01mg (BM-252, A&D Company, Japan). The cycle was duplicated repeatedly until a constant mass was acquired (m_1) – in other words, until the mass loss of the specimens was no more than 0.1 mg over 24 h.

For the thickness measurement, a digital caliper was used (Powerfix, OWIM GmbH & Co., KG, Germany) to obtain two measurements of the height. After taking the dimensions of the specimen, the volume (V) was calculated in mm^3 through the following formula:

$$\boldsymbol{V = \pi r^2 t}$$

Equation 5.2: Volume calculation formula

Where $\boldsymbol{\pi}$=3.14, **r** is the radius of cross section; **t** is the thickness of specimen

5.3.2.2 Sorption measurement

All five specimens were submerged in 10 ml of distilled water within separate glass bottles, which were sealed with polyethylene caps. The bottles were kept at 37 °C for 1 h, 3 h, and 1, 2, 3, 4, 5, 6, 7, 14, 21, 28, 56, 84, 112, and 140 d. After each time

period, a tweezer was used to take each specimen from the bottles. They were dried using filter paper before being weighed 1 min after removal from the water. The recorded mass is denoted as m_2 (t). All five specimens were then returned to aqueous storage. This was replenished every week, with the total volume of water maintained at 10 ml.

5.3.2.3 Solubility measuring

After the sorption cycle was complete, specimens were dried using a desiccator and weighed at time points of 1, 2, 3, 4, 5, 6, 7, 14, 21, 28, 35 and 42 d. Once the mass loss of the specimens was no more than 0.1 mg within any 24 h period, the constant final mass was then obtained (m_3).

Weight increase W_i (%) and water sorption W_{so} were calculated through the following formulae:

$$\boldsymbol{W_i}(\%) = 100\left[\frac{m_{2\,(t)} - m_1}{m_1}\right]$$

Equation 5.3: Weight increase calculation formula

m_1 is the conditioned mass prior to immersion in water; m_2 is the mass after to immersion in water for 140 d.

$$\boldsymbol{W_{So}} = \left[\frac{m_{2\,(t)} - m_3}{V}\right]$$

Equation 5.4: Water sorption calculation formula

m_2 is the mass after to immersion in water for 140 d, m_3 is specimens' mass after desorption, and V is the volume of the specimen.

The percentage amount of water absorbed by a composite at the end of the storage period was calculated by the following formula:

$$\boldsymbol{W_{SoC}}(\%) = \left[\frac{m_{2\,(t)} - m_3}{m_1}\right] \text{ X } 100$$

Equation 5.5: Water sorption % calculation formula

Providing sorption has occurred principally by the polymer matrix component, the following equation was used to measure the percentage amount of water the polymer matrix absorbed [286].

$$\boldsymbol{W_{SoM}}(\%) = \left[\frac{W_{So}\%}{a}\right]$$

Equation 5.6: Water sorption % in the resin matrix calculation formula

In this formula $\boldsymbol{a}$ represents the proportional weight of the polymer matrix in the composite.

The following equation was used to calculate the solubility (Sol) values:

$$\boldsymbol{Sol} = \left[\frac{m_1 - m_3}{V}\right]$$

Equation 5.7: Solubility calculation formula

5.3.3 Hygroscopic expansion

Hygroscopic dimensional changes were measured in parallel with the water sorption measurements. A custom built noncontact laser micrometer was utilised to measure the dimensional changes of the specimens [188]. After each time period had elapsed, specimens were dried using filter paper then measured 1 min after removal from the water. Mean diameter (d2) was recorded at each time interval (t), and then returned to aqueous storage. An average of 534 diametral values was recorded for each specimen at each time point.

The percentage diametral change was calculated:

$$\boldsymbol{d}(\%) = \frac{d_{(t)} - d_1}{d_1} \mathbf{x}\, 100$$

Equation 5.8: Diametral change calculation formula

In this formula d_1 represent the mean diameter before water storage, while $d_{2(t)}$ represents the mean diameter which was recorded at each time interval.

The following equation was used to calculate volumetric change, assuming isotropic expansion behaviour [287]:

$$\boldsymbol{V}\ (\%) = \left[(1 + \frac{d(\%)}{d_1})^3 - 1\right] x100$$

Equation 5.9: Volumetric change calculation formula

5.4 Statistical Analysis

SPSS v.23 (IBM, Armonk, NY, USA) was used to analyse the data. The mean and standard deviations were calculated for the water solubility, water sorption, hygroscopic expansion and mass change. One-way ANOVA was carried out at 140 d followed by Tukey *post-hoc* tests (at $\alpha = 0.05$) for the hygroscopic expansion, water sorption, and mass change. For the solubility, the same statistical test was applied to evaluate differences in weight after 42 d of desorption cycle. Pearson correlation coefficients were calculated to express the correlation between hygroscopic expansion and mass change for each material during 140 d water immersion.

5.5 Results

5.5.1 Filler content

Table 5-2 shows the mean and standard deviations of the filer wt. %, using the ashing technique, and the manufacturers reported values.

Table 5-2: Filler by weight percentage

Materials	Filler (wt %) after ashing in air	Manufacturer reported filler (wt %)
NPU	69.6 (2.3)	77
NPF	59.6 (1.3)	66
EVX	72.8 (1.2)	74.2
XTE	74.1 (1.3)	78.5
XTF	63.1 (1.1)	65
FBF	74.6 (1.4)	76.5
FBO	73.2 (1.0)	76.5

5.5.2 Sorption & Solubility

As can be seen from Figure 5-1, each of the resin composite materials exhibited a percentage mass change throughout the water sorption/desorption cycle. All of the composites demonstrated an increase in mass of various degrees by their water uptake, up to the point of equilibrium which occurred after 140 d. All of the examined composites showed a higher initial mass (*m1*) than their reconditioned mass (*m3*), with the exception of EVX whose initial mass was lower than its reconditioned mass.

At 140 d, water sorption ranged between 19.96 and 30.11 μg/mm (Table 5-3). The highest sorption was observed in XTF followed by EVX and NPF which exhibited

similar results. Conversely, XTE, NPU, FBO and FBF exhibited lower water sorption levels, with no significant differences between each other ($p \geq 0.05$).

The solubility for the resin composites was found to fall between -1.49 to 4.18 µg/ mm, as shown in Table 5-3. The most soluble materials were NPF and XTF; they had higher levels of solubility when compared with their packable counterpart. A negative solubility value was observed for EVX (-1.49 µg/ mm).

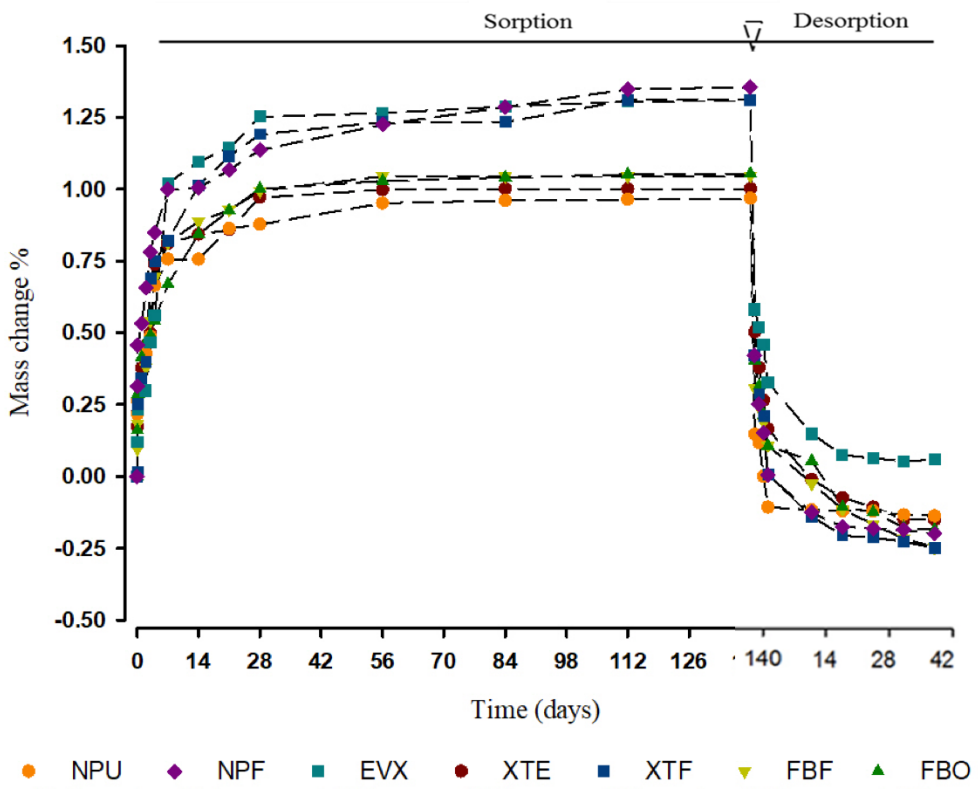

Figure 5-1: Mass change percentage with water sorption and desorption cycles

Table 5-3: Water sorption (Wso) and solubility (Sol), Water sorption in composite (Wso_C%), Water sorption in polymer matrix (Wso_M%), of resin composites after 140 d storage in distilled water at 37˚C

Materials	Wso (μg/mm³)	WsoC%	WsoM%	Sol (μg/mm³)
NPU	19.96 (3.32) [a]	1.04 (0.18) [a]	3.43(0.59) [a, b]	2.63 (0.13) [a, b]
NPF	28.88 (0.11) [b, c]	1.62 (0.13) [b, d]	3.94 (0.32) [a]	3.59 (0.44) [e]
EVX	30.00 (0.28) [b, c]	1.29 (0.05) [a, d]	4.75 (0.20) [a, c]	-1.49 (0.41) [d]
XTE	21.11 (1.62) [a]	1.17 (0.11) [a]	3.95 (0.37) [a]	3.19 (0.19) [a]
XTF	30.11 (0.28) [b, c]	1.60 (0.11) [b, c, d]	4.44 (0.33) [a]	4.18 (0.47) [e]
FBF	22.24 (3.63) [a ,b]	1.20 (0.16) [a, c]	4.55 (0.63) [a]	3.43 (1.09) [a,e]
FBO	24.70 (3.25) [a, b, c]	1.17 (0.13) [a]	4.37 (0.51) [a]	3.32 (0.57) [a,e]

The same superscript lower case letters indicate a homogeneous subset (columns) ($p > 0.05$)

5.5.3 Hygroscopic expansion

One-way ANOVA conducted after 140 d of immersion in water showed that EVX had a significantly higher hygroscopic expansion when compared to the rest of the materials. **Table 5-4** provides the mean and standard deviation for all materials for their volumetric hygroscopic expansion, taken after 140 d at 37°C. The percentage hygroscopic expansion for each material is shown in Figure 5-2.

The final hygroscopic expansions ranged between 1.40 and 2.21 % at 140 d. According to the method of application of the resin composite, the composites can be categorized into one of three bands: conventional composites (NPU and XTE), with expansions of 1.40 % and 1.54 %; bulk fill composites (EVX, FBO and FBF), with

the greatest expansion being 2.21 % for EVX; and lastly, flowable composites (NPF and XTF), with expansions of 1.70% and 1.72%, respectively.

Figure 5-2 Shows the relationship between the mass and the changes in volume over the period of 140 days revealing that the relationship was almost linear. (Appendix II)

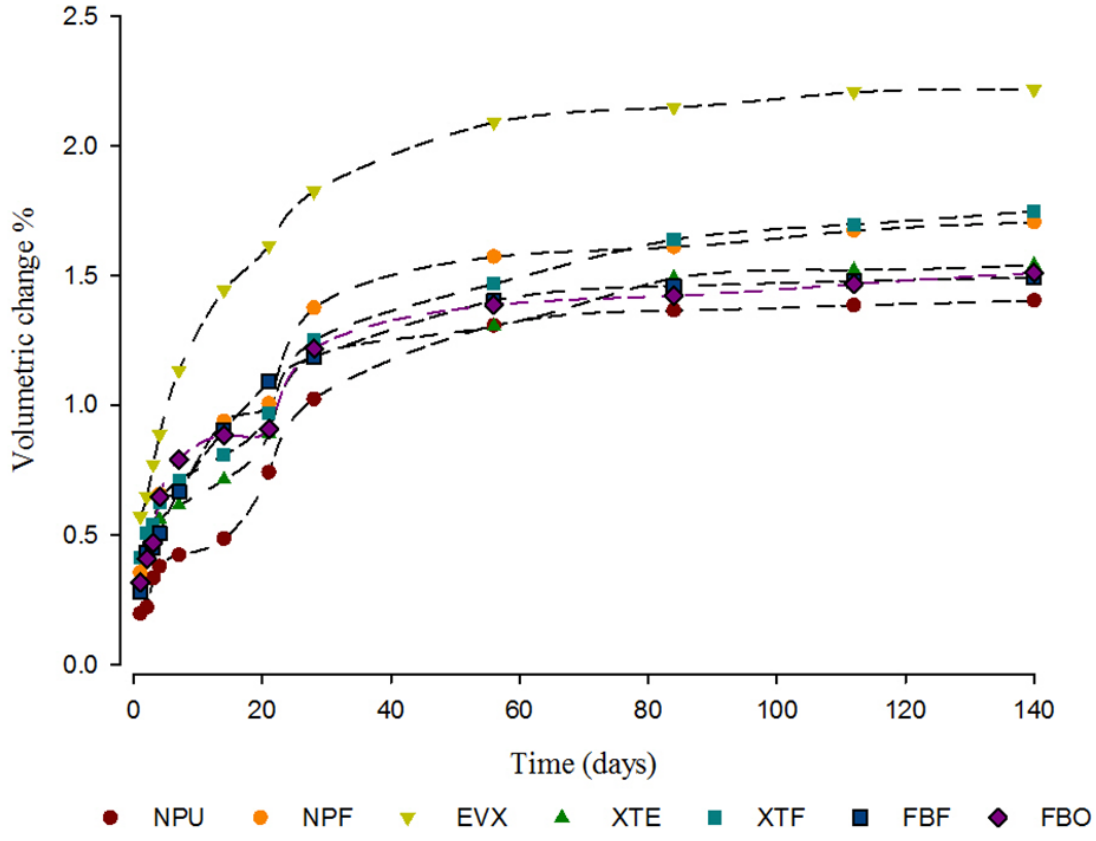

Figure 5-2: Hygroscopic expansion from 1 h to 20 w.

Table 5-4: The percentage increase in mass and volume of the investigated materials after 140 d, filler wt % after air ashinig. Pearson correlation coefficient between hygroscopic expansion and mass change during 140 d sorption period in water at 37˚C.

Materials	Mass Change %	Volumetric Change %	Pearson correlation coefficient
NPU	0.93 (0.18) [a,b]	1.40 (0.17) [a]	0.83
NPF	1.34 (0.11) [a,c]	1.70 (0.19) [a]	0.90
EVX	1.35 (0.08) [a,c]	2.21 (0.26) [b]	0.97
XTE	1.00 (0.10) [a]	1.54 (0.05) [a]	0.87
XTF	1.32 (0.14) [a,c]	1.72 (0.11) [a]	0.91
FBF	1.01 (0.12) [a]	1.49 (0.19) [a]	0.93
FBO	1.00 (0.12) [a]	1.51 (0.15) [a]	0.94

The same superscript lower-case l letters indicate a homogeneous subset (columns) ($p > 0.05$)

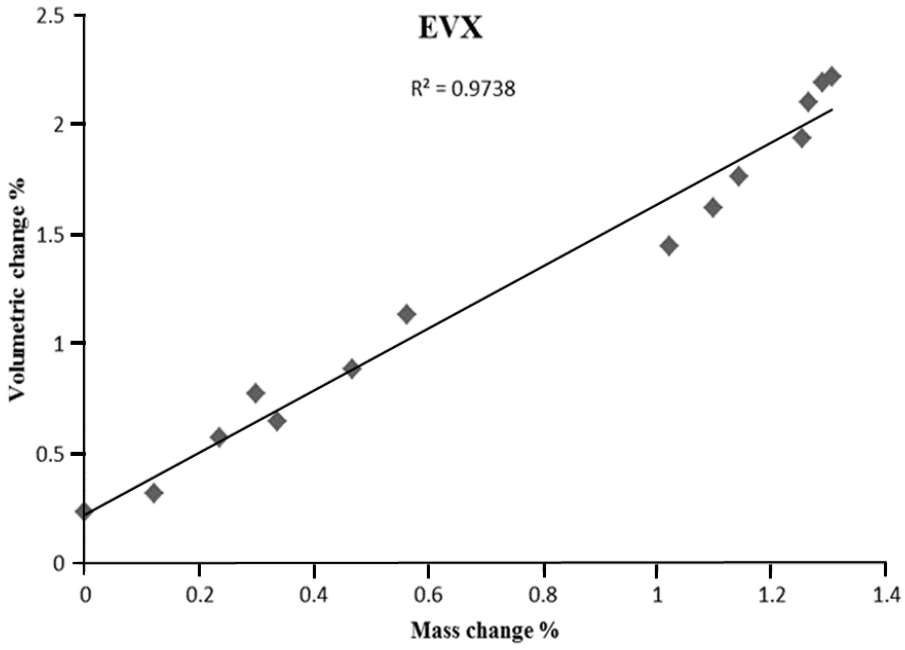

Figure 5-3: The relationship between the mass and volumetric changes during the 140d sorption period in EVX.

5.6 Discussion

This study evaluated water sorption, solubility and hygroscopic expansion of a number of resin composites immersed in water over 140 d including fibre reinforced materials. Considerable differences were identified between the materials, leading to a rejection of the first and second null hypotheses. ISO Standard 4049 permits a sorption limit of 40 μg/mm and solubility of less than 7 μg/mm after a period of 7 days storage. Each of the composite materials satisfied this standard, despite being exposed to an extended period of water sorption. Thus, the aqueous challenge was more stringent than the 7-day ISO process.

Hydrophilicity and crosslinking of the network structure are the two main factors affecting the solubility and water sorption of resin composites. Moreover, the amount of solvent taken up by the composite during the exposure period depends on both the porosity of the material itself and the nature of the filler matrix [243, 288].

Two different types of fibres incorporated in the tested materials: short E glass fibres (EVX) and Nano-hydroxyapatite fibres (NPU and NPF), which varies in their composition, configuration and amount; thus, could show different behaviour. Therefore, the focus of this study was on the main factors in overall degradation resistance: the polymeric matrix and filler amount.

The results in the present study regarding sorption values correlated negatively with the amount of filler loading (with the exception of EVX). This corresponds to the results observed in other studies [289]. The wt% of the polymeric matrix decreases as the weight percentage of filler increases, and so the water sorption also decreases as this phenomenon is known to occur within the polymeric phase [22, 290]. Although glass fillers (particulate or fibres) are known to not contribute to the sorption process, it is still possible that water is adsorbed onto their surface – this depends on the integrity of the interface between the resin matrix and the glass fillers [179].

In the case of NPF and XTF, the high sorption can be attributed to their filler content; however, when the influence of fillers was removed through the calculation of the percentage of water absorbed by the polymer matrix alone (W_{soM}) rather than by the

composite (Ws_{oC}), no significant differences were found between these materials when compared with their packable counterpart (NPU, XTE).

The properties of fibre reinforced composites deteriorate in water, similarly to Particulate filled composites. Water diffuses via the resin matrix and leaches the fibres' surface [269]. Areas with poorly impregnated fibres will be more prone to water uptake [291]. Water sorption is influenced by the hydrophilicity of the resin matrix, and the mount of the inorganic phase (fibres and the particulates) and the quality of silanization. Additionally, water uptake may be accentuated by capillary action of the fibres, resulting in mass increases [292].

EVX was shown to have the highest polymer sorption value (W_{soM}) (4.75 %) and NPU exhibited the lowest value (3.43 %) out of all the composites studied. These results confirm that water storage has a significant effect on polymeric matrix properties as noted by much previous research on dimethacrylate-based resins [77, 280, 292]. The higher sorption rate of EVX, therefore, may be explained by the highly hydrophilic PMMA and TEGDMA monomers that constitute its resin matrix. Similarly, the significantly low sorption of NPU could be associated with the fact that its main monomers are Bis-EMA and UDMA, which are highly hydrophobic. Prior studies found that Bis-EMA homopolymer has a much lower water sorption (1.8 wt%) than UDMA, Bis-GMA, and TEGDMA homopolymers (2.6, 3.05, and 6.3 wt%, respectively) [293].

logP (octanol-water partition coefficient) is a quantity that is widely employed in medicinal chemistry and pharmaceuticals to measure hydrophilicity [294]. Research on resin composites suggests that logP is an effective predictor of water sorption [295]. Alshali et al. listed the logP values of the following monomers in ascending order: TEGDMA< DEGDMA< UDMA< Bis-GMA< Bis-EMA [27]. This offers further explanation for the outcome of this study.

While no significant differences in sorption were observed between FBF and FBO, there were variations that may be accounted for by small differences between the degree of conversion for each material. Prior study has shown a negative correlation between degree of conversion and sorption, as the same filler wt% is used in both

versions of this composite [280]. During the curing process, the opacity of FBO resin increases; this attenuates light passing through the composite material, which may cause a lower degree of conversion compared to FBF [296]. Translucent resin paste has the advantage of allowing the light to travel more deeply into the material during the curing phase, thus activating the cure chemistry throughout the composite.

Incomplete dehydration of the EVX material may explain its negative solubility. This does not imply that EVX is insoluble, although it suggests that its solubility is low. Another possible explanation is that hydrolytic chemical reactions between metal oxides, glass fillers and water result in metal hydroxides forming within the composite material [297]. Additionally, water uptake may be accentuated by capillary action of the fibres, resulting in significant mass increases [292].

There was a significant variation between the final hygroscopic expansions leading to rejection of the second null hypothesis. Hygroscopic expansion happens when water diffuses into the polymer network separating the chains – particularly when the water molecules bond to hydrophilic groups within the polymer [188, 193, 292, 298]. Absorbed water can, however, often reside in free volume and micro-voids between polymer network chains, to an extent that does not increase the macroscopic volume [188, 299]. It is well established that water diffuses into the resin phase, and that the matrix expands to accommodate absorbed water [290]. Hirasawa et al. were the first to establish an association between water sorption and volumetric expansion in resin composites [300].

Water sorption thus affects the mass and dimensions of composites and previous studies highlight relationships between their volume and mass changes [188, 189]. The present study also found high correlations between percentage mass and volumetric changes (**Table 5-4**).

EVX is a resin composite material incorporating short glass fibres within a matrix of PMMA, TEGDMA, and Bis-GMA. Dental manufacturing companies introduced glass fibre reinforced materials to try to improve the strength of resin composites, especially fracture toughness and flexural strength [69, 83]. The current study observed that EVX did not behave in the same manner as the other composites, as it

exhibited the greatest volumetric changes. Research on PMMA acrylic denture-base resins indicated that, in the case of fibre-reinforced materials, the resin matrix determined material behaviour during water storage more than the glass fibres [301]. EVX polymer matrix consists of polymer PMMA and copolymer Bis-GMA/TEGDMA. The structure of Bis-GMA incorporates hydroxyl groups that raise its susceptibility to water diffusion and bonding. The sorption behaviour of Bis-GMA may also be affected by the co-monomer PMMA present in the organic matrix [292, 302]. According to its *Instructions for Use* EVX should only be used as dentine replacement and thus should be covered by a conventional particulate filled composite. However, in certain clinical situations such a procedure may not be feasible [107, 303].

NPU was found to have lower expansion, along with XTE, FBO, and FBF. If the material is hydrophobic, reduced hygroscopic expansion is known to take place [188, 292] . NPU does contain Bis-EMA, and this material is more hydrophobic than Bis-GMA [9]. It may also be that differences in polymerization can be a factor, although we have no evidence that is actually the case.

From the results of the current study, we can conclude as follows:

- There were some variations in the water sorption/desorption cycles of all the resin–matrix composites investigated. Nonetheless, they all complied with the requirements set out by ISO 4049 for water solubility and sorption, despite the sorption period.
- The greatest changes in volume and water sorption were seen in the millimeter scale glass-fibre reinforced composite (EVX), whereas the greatest stability in an aqueous environment was seen in the nano-fibre hydroxyapatite reinforced composite (NPU).

Clinical significance

Resin composites designed for various restorative purposes were evaluated in this study. Certain bulk-fill materials such as FBO and FBF can be used as single-layer restorations, while other materials need coverage using conventional hybrid

composites like EVX. The findings of this study emphasize the importance of covering this type of material, to reduce the chances of degradation through exposure to the oral environment.

5.7 Acknowledgement

GC Corporation, Tokyo, Japan for supplying everX Posterior.

Chapter Six

Characterization of Model E-Glass Fibre Reinforced Composites

Abdulrahman Alshabib*, Nick Silikas, David C Watts

6.1 Introduction

Resin composites have two main drawbacks that affect their clinical performance; secondary caries and bulk-fracture [198, 304]. Several approaches have been used to reduce polymerization shrinkage of resin-composites. Reduced shrinkage is a key factor for marginal integrity [305, 306]. Also improved mechanical properties are essential to prevent bulk-fracture. The need for strong materials stimulated investigation of ways to enhance mechanical properties of particulate filled composites [116, 307]. Professor Vallittu and his research group in Turku University have pioneered work on fibre-reinforced composites (FRC) [71, 83, 103, 308-310]. Short e-glass fibre composites everX posterior and everX flow (GC Corporation, Tokyo, Japan) have been developed as a result of their extensive research on this field [83, 103]. Short E-glass fibres incorporated into such resin composites have significantly improved the fracture toughness, where the fibres hamper crack propagation leading to higher fracture toughness of the resin-composites [77, 308]. Both linear and cross-linked polymers are utilised in everX posterior [83]. The matrix of these FRCs, with a semi-interpenetrating polymer network (SIPN), is created from a linear polymer, and a cross-linking polymer [311]. Despite significant improvements in mechanical properties for these FRCs [77, 308], there are some drawbacks to the SIPN (Bis-GMA/ TEGDMA –PMMA) system, such as water sorption and hygroscopic expansion . Further investigation into the use of Bis-EMA and urethane dimethacrylates (UDMA) as alternative components of the FRC matrix may be helpful [9, 312].

During the propagation phase of dimethacrylate polymerisation, there is a reduction in concentrations of free radicals and an increase in the viscosity. Consequently, after initiation and acceleration of the polymerization process, the reaction decelerates and further reaction becomes a self-limiting process, which explains why there cannot be a degree of conversion (DC) of 100% in photo-cured network-forming composites [21]. Residual monomers are known to be detrimental to human tissues, toxic in some cases [138]. These harmful effects include soft tissue irritation, allergic reactions, and cytotoxic effects [138, 313]. Moreover, low DC is associated with poor mechanical properties [139, 314, 315].

One of the challenges of photo-polymerised resin composites is their limited depth of cure (DoC) [316]. This limitation is attributed mainly to: (i) light attenuation inside the composite, which is in turn caused by monomers and photoinitiators' absorption. (ii) Scattering and refraction at the filler/monomer interface [129]. One of the most effective methods for improving the depth of cure is by increasing the translucency of the composite by ensuring that the indices of refraction of the matrix and fillers match as closely as possible [296].

This study substitutes the semi- interpenetrating polymer network (Bis-GMA-TEGDMA/PMMA) with an entirely dimethacrylate resin matrix Bis-GMA-UDMA/Bis-EMA), and aims to measure the refractive index, degree of conversion, and depth of cure of the model resin composites.

The null hypotheses were as follows:

- No difference would be observed in degree of conversion between the control group (A) and the experimental groups (B-E);
- There would be no differences between the control group (A) and the experimental groups(B-E), in the depth of cure.

6.2 Materials & methods:

The monomers and the reinforcing materials that were used to formulate the experimental groups are listed in Table 6-1.

Table 6-1: Monomers and reinforcing materials used in this study

Abbreviation	Name	Lot number	Refractive Index	Manufacturer
Organic Component				
Bis-GMA	Bisphenol A-glycidyl dimethacrylate	804-39	1.540	Esschem, Europe
UDMA	Urethane dimethacrylate	803-66	1.483	Esschem, Europe
Bis-EMA (EO=8)	Ethoxylated bisphenol-A dimethacrylate	849-17	1.518	Esschem, Europe
TEGDMA	Triethyleneglycol dimethacrylate	807-32	1.461	Esschem, Europe
PMMA	Polymethyl methyl methacrylate	93-097	1.49	Esschem, Europe
CQ	Camphorquinone	09003A	----	Sigma–Aldrich Inc., St. Louis, USA
DMAEMA	Dimethylaminoethyl methacrylate	BCBR4467V	----	Sigma–Aldrich Inc., St. Louis, USA
Reinforcing component				
BaSi	Barium borosilicate glass with an average particle size of 0.7 µm	EEG 101-07-/871-12	1.555	Esschem, Europe
GF	Silanated E-glass fibres with a diameter of 15 µm & length of 3mm.	86-792	1.556	Hebei yuniu fibreglass manufacturing Co., LTD, Guangzong ,China
3-MPS	3-Trimethoxysilyl Propyl methacrylate	2530-85-0	----	Sigma–Aldrich Inc., St. Louis, USA

6.2.1 Silane functionalization of barium borosilicate surfaces

60 ml of ethanol solvent and 20 g of borosilicate particle fillers were put into a plastic container before being placed in a SpeedMixer™ (DAC 150.1 FVZK, High Wycombe, Buckinghamshire, UK) and mixed for 20 min at 1500 rpm. Once the initial mixing had taken place, a sterile syringe was used to slowly add 3% (0.6 g) of the

silane coupling agent (3- trimethoxysilyl propyl methacrylate). This mixture was then put back into the speed mixer for 10 min at 1500 rpm, before being separated equally into two plastic tubes and put into a 4000-rpm centrifuge (Heraeus, UK) for 20 min at 23°C. The supernatant (separated ethanol) was removed, and the silanated fillers was placed in plastic tubes and dried for 3 h in an EZ-2 Elite solvent evaporator (Genevac Ltd, SP Scientific Company, UK) at 60°C. Once dried, the silanated fillers were stored at room temperature (23°C ±1).

6.2.2 Fabrication of filled resin composites:

Five resin matrix groups were formulated (Table 6-2). A digital microbalance (BM-252, A&D Company, Japan) was used to measure the amount of resin. Each group was mixed with CQ (0.5 wt.%) and 1 wt.% of DMAEMA in a SpeedMixer™ at 1500 rpm for 3 cycles of 5 min.

The filler phase consisted of 60 wt% silanated barium borosilicate glass and 10% wt E-glass fibre. This made the w/w percentage ratio of monomer to filler 30:70 for all composites.

The final mixture was mixed for 20 min using the SpeedMixer at 1500 rpm (5 min/cycle). The experimental resin composite groups are shown in Table 6-2.

Table 6-2: Matrix composition (in wt %) for the control (A) and experimental (B, C, D, E) 60%wt silanated barium borosilicate glass and 10%wt E-glass fibre were added. The w/w percentage ratio of monomer to filler was thus 30:70 for all composites

Groups	Bis-GMA	TEGDMA	PMMA	Bis-EMA	UDMA
A	59.5%	29.5%	9.5%	----------	----------
B	49.5 %	----------	----------	37.0%	12.0%
C	49.5%	----------	----------	29.5%	19.5%
D	49.5%	----------	----------	24.5%	24.5%
E	49.5%	----------	----------	19.5%	29.5%

6.2.3 Refractive index (RI) measurements

An Abbe refractometer (Bellingham and Stanley, UK) was used to measure the RI of the cured unfilled polymers according to ISO standard (BS EN ISO 489:1999) [317].

An Abbé refractometer measures the refractive index of a specimen using the critical angle technique. This is performed by placing a specimen onto a refracting prism using a contact liquid to ensure optical continuity and preventing reflection losses between the interfaces [318]. A monochromatic light is refracted through the specimen producing a light dark boundary. On the edge of the dark, light boundary is the critical angle of the specimen for the wavelength of the monochromatic light being used. Using Snell's law, the RI of the refracting prism, measured angle of the light dark boundary the RI of the sample can be determined [318].

The Abbe refractometer was calibrated, employing a silica calibration standard (Bellingham and Stanley Ltd., UK) and 1-Bromonaphthalene contact liquid. To match the silica calibration standard, a Teflon mould was utilised with an internal slot 20 mm x 8 mm x 31 mm. This was placed on top of a clear Mylar strip with glass slides 1mm thick.

The monomer mixture (unfilled resin) was then placed in the mould, a second Mylar strip with glass slide was positioned above it and clamped together. Light curing was carried out for 40 s with an LED curing unit that had an average tip irradiance of 1200 mW/cm^2 (Elipar S10, 3M Espe, Seefeld, Germany). In total the specimens were irradiated for 120 s, with three overlapping areas of irradiation along the specimens' length. A calibrated radiometer was used to confirm the irradiance of the light curing unit (MARC™ Resin Calibrator, Blue-light Analytics Inc., Halifax, NS, Canada). The specimen was then removed from the mould and one side was roughened with P1000 silica carbide paper (Buehler Ltd, Lake Bluff, IL, USA), while the other side was polished with 1 μm and 0.25 μm diamond paste (Buehler Ltd, Lake Bluff, IL, USA), utilising appropriate cloth wheels. The RI of the cured monomer mixtures was measured with an Abbe's refractometer after 24 h. One drop of 1 Bromonaphthalene (contacting liquid) (Aldrich, UK, LOT 17640) was placed on the polished side of the

specimen and the index of refraction was measured using the Abbe's refractometer and a sodium D lamp at 23^{o}C. Three measurements were made for each group.

6.2.4 Degree of Conversion

Five model fibre reinforced resin composite were studied (Groups A-E) (Table 6-2). A Nicolet 5700 FTIR spectrometer (Thermo Electron Company, USA) was used to measure degree of conversion (DC). The instrument was fitted with a single reflection horizontal attenuated total reflectance accessory (ATR) (MIRacle ATR, PIKE Technologies, USA). The following conditions were set while utilising the FTIR spectrometer: 32 scans, 6cm^{-1} resolution, and 4000-5000 cm^{-1} wavelength. The ATR crystal was completely covered with an uncured composite material using a Teflon mould with a diameter of 6 mm and different thickness (2 mm, and 4 mm); three specimens in total were prepared for each group, and the FTIR spectra were collected for each uncured specimen. A LED curing unit was then used to cure the specimens for 40 s at room temperature, with an average tip irradiance of 1200 mW/cm^2 (as mentioned above). It was ensured that the light tip remained as close to the material as possible. The FTIR spectra for the cured material were obtained directly afterwards.

Measurement of DC was obtained from the ratio variation in absorbance intensities of the aliphatic C=C peak (1638 cm^{-1}) and the internal standard aromatic ring peak (1608 cm^{-1}) for both the uncured and cured material.

The following equation was used to calculate the percentage DC for each specimen:

$$DC\ (\%) = \left[1 - \left(\frac{1638\ cm^{-1}/1608\ cm^{-1}\{cured\}}{1638\ cm^{-1}/1608\ cm^{-1}\{uncured\}}\right)\right] X\ 100$$

Equation 6.1: Degree of conversion equation

6.2.5 Depth of cure

Depth of cure was measured from the following parameters: i) the maximum Vickers microhardness, ii) 80% of the maximum Vickers microhardness and iii) the depth corresponding to 80% of the maximum Vickers hardness. A micro-hardness

instrument (FM-700, Future Tech Corp., Japan) was used, applying a fixed load of 300 g for 15 s.

Stainless steel moulds were used to prepare three specimens of each experimental resin composite so that their surface hardness profiles could be obtained. The moulds contained a slot measuring 15 x 4 x 2 mm and a top plate. The mould was overfilled with composite, and topped with a Mylar strip and top plate, which was pressed down. Any excess material was scraped away from the top of the mould. The mould was irradiated from one end. A light cure unit with a tip diameter of 10 mm was used to irradiate each specimen for 40 s (as mentioned above). Specimens were stored in incubator at 37°C for 24 h prior to measurement. The top plate and Mylar strip were removed and the Vickers hardness number (VHN) was measured as a function of material depth at every 0.4 mm.

6.3 Statistics

6.3.1 Degree of conversion

Data for all groups were collected and analysed statistically using SPSS 23.0 (IBM SPSS Statistics, SPSS Inc., New York, USA). Once *Shapiro-Wilk* test confirmed normality of the data. Levene's test have also confirmed the equality of variance. Two-way ANOVA, one-way AVOVA and Tukey *post-hoc* tests (α=0.05) was performed to identify differences in DC (dependent variable) between different materials and thickness (independent variables). An independent t-test was utilized for each material and thickness (2 mm vs 4 mm)

6.3.2 Depth of cure

The data for all groups were collected and analysed statistically using SPSS 23.0 (IBM SPSS Statistics, SPSS Inc., New York, USA). One-way analysis of variance, Tukey *post-hoc* tests were used to analyse the significant differences in the following parameters: (1) highest Vickers hardness number, (2) Vickers hardness number at 80%

of highest VHN, (3) The depth at 80% of highest VHN. All data were subjected to Levene's test of homogeneity of variance following the assumption of equal variances.

6.4 Result

6.4.1 Refractive index

The mean refractive indices of the unfilled polymerized monomer mixtures ranged from 1.511 to 1.528 with a very narrow standard deviation. Results are presented in **Table 6-3**. Their increasing group rank order was: B, C, D, E and A.

Table 6-3: Refractive index (RI) n_D^{23} of the experimental groups

Groups	RI
A	1.511 (0.009)
B	1.528 (0.001)
C	1.526 (0.000)
D	1.524 (0.003)
E	1.515 (0.002)

6.4.2 Degree of Conversion

Absorbance peaks at 1638 and 1608 cm^{-1} were measured and the DC determined from Equation 6.1. Mean DC values and standard deviation (SD) at each thickness (2 and 4 mm) are shown in **Table 6-4**.

At 2 mm thickness, Groups D and E had the lowest DCs of 61.8 % and 61.3 % respectively, these were significantly lower than the other three groups. Groups A and B, had the highest DCs: 67.2% and 65.6 %.

The same pattern was shown at 4 mm thickens. Group D and E were significantly lower: 59.5 %, and 55.9 % respectively, while groups A and B were significantly higher: 63.2 % and 64 % respectively.

Table 6-4: Degree of Conversion (%) mean: (SD) for experimental composites at 2 and 4mm depth

Groups	DC at 2 mm	DC at 4 mm
A	67.2 (1.4) [a,1]	63.2 (0.8) [a,1]
B	65.6 (1.1) [a,b,1]	64.0 (0.6) [a,1]
C	63.7 (0.5) [b,c1]	62.9 (1.2) [a,b,1]
D	61.8 (1.9) [c,1]	58.5 (1.2) [b,1]
E	61.3 (0.5) [c,1]	55.9 (0.8) [c,2]

At each thickness the same superscript letters indicates no significant difference ($p > 0.05$). For each material the same superscript number indicates no significant difference ($p > 0.05$).

6.4.3 Depth of Cure

Table 6-5 presents the maximum VHN, VHN at 80% of maximum VHN, and depth at 80% of maximum VHN for each of the resin composites. The results are also illustrated graphically in Figure 6-1. The maximum VHN varied from 34.0 to 43.6, whilst 80% of maximum VHN varied from 27.3 to 35.0. The depth corresponding to 80% of maximum VHN was between 3.4 and 4.4 mm. This latter measurement was taken to be depth of cure (DoC). One-way ANOVA showed that there were statistically significant differences between the materials for all of the above parameters. The greatest depth of cure was in Groups B and C (4.3 and 4.4 mm respectively), while the lowest was in Group E (3.4 mm). These groups therefore had significantly different depths of cure.

Table 6-5: Mean of max.VHN, VHN at 80% of max.VHN and depth at 80% of max.VHN for experimental composites examined.

Groups	Max VHN	VHN at 80% of Max.VHN	Depth at 80% of Max.VHN (mm)
A	43.6 (1.1) [a]	35.0 (1.0) [a]	3.9 (0.2) [a]
B	34.0 (0.9) [b]	27.3 (0.8) [b]	4.4 (0.2) [a,b]
C	35.7 (1.0) [b]	29.6 (0.9) [b]	4.3 (0.4) [a,b]
D	35.9 (0.8) [b]	29.5 (0.8) [b]	4.0 (0.2) [a]
E	41.1 (1.4) [a]	33.3 (1.0) [a]	3.4 (0.2) [a,c]

The same superscript letters indicates no significant difference ($p > 0.05$).

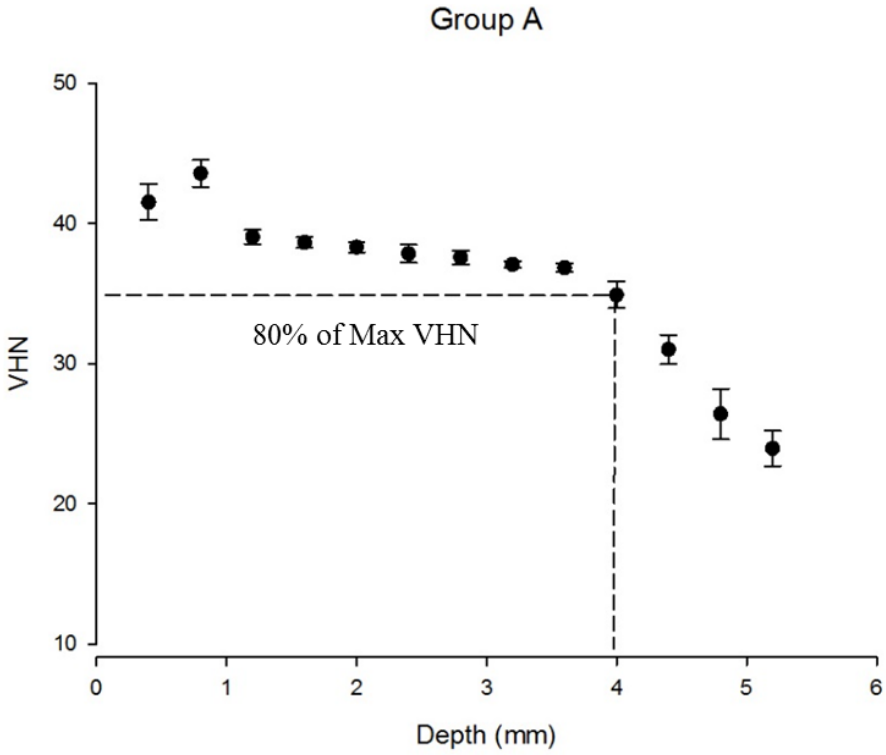
Group A
50
40
30
20
10
VHN
80% of Max VHN
0
1
2
3
4
5
6
Depth (mm)

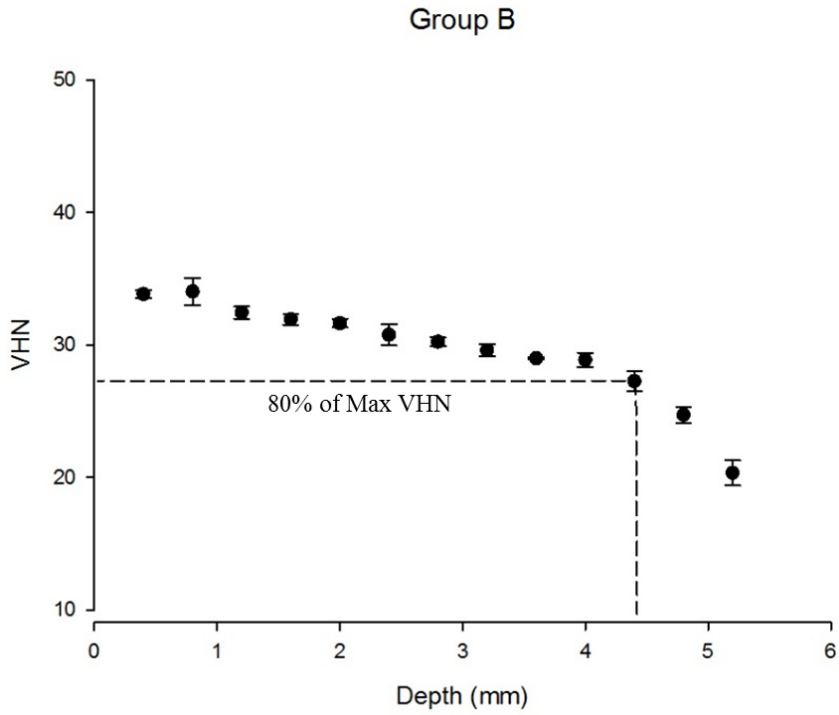
Group B
50
40
30
20
10
VHN
80% of Max VHN
0
1
2
3
4
5
6
Depth (mm)

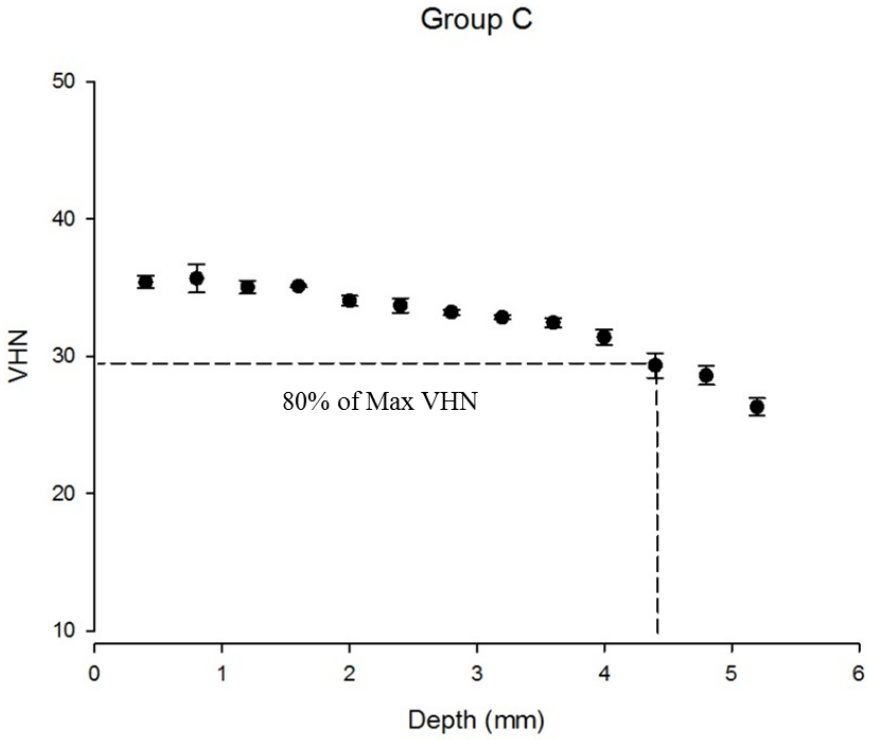
Group C
VHN
50
40
30
20
10
80% of Max VHN
0
1
2
3
4
5
6
Depth (mm)

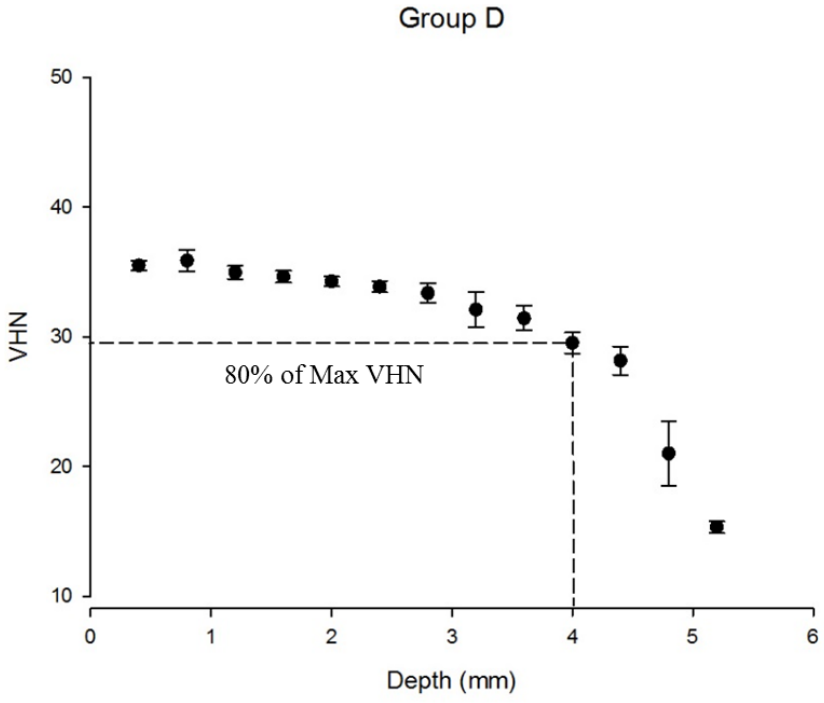
Group D
VHN
50
40
30
20
10
80% of Max VHN
0
1
2
3
4
5
6
Depth (mm)

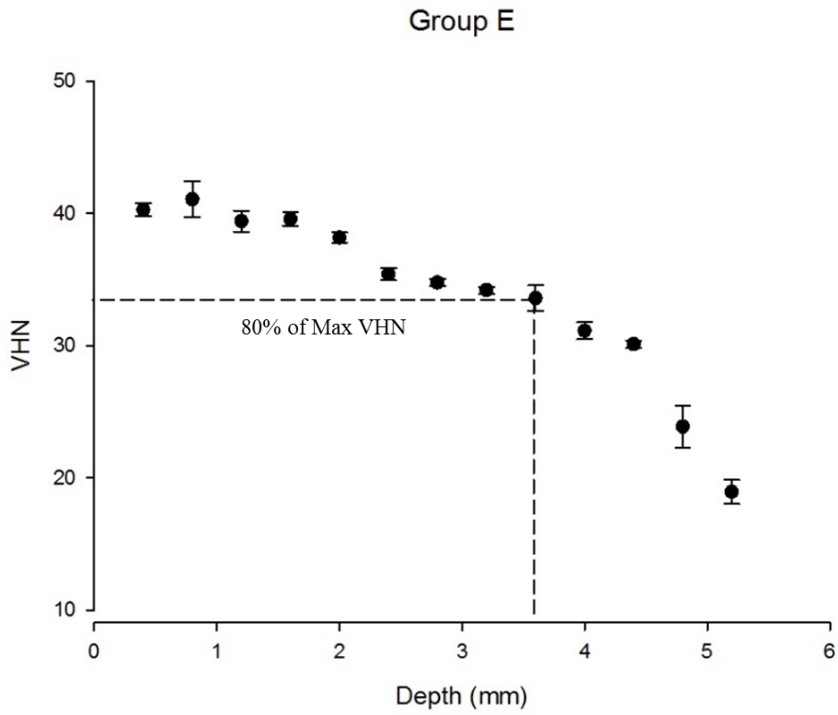

Figure 6-1: VHN at 80% of Max.VHN and depth at 80% of Max.VHN.

6.5 Discussion

This study evaluated the refractive index (RI), degree of conversion (DC), and depth of cure (DoC) of a number of experimental fibre-reinforced composites. All of the composites had the same filler type and loading, but there were variations in their resin matrices. Statistically significant differences in DC and DoC were found between the materials leading to the rejection of both null hypotheses.

6.5.1 Refractive Index

Scattering is the main cause of lower levels of light as depth increases in a 2-phase composite structure [129]. The extent of the scattering depends on the similarity or difference between each phase's refractive index. In resin composites, there is an interface with every filler particle. It is expected that if there is a close match between the refractive index of the fillers and that of the resin blend, the depth of cure will be greater, because light transmission will be higher. If this is not the case and there is a mismatch between these refractive indices, then this may affect the DoC [157, 296].

In the experimental groups refractive index rose with increasing Bis-EMA content. The changes in light transmission with different monomer mixtures observed in this work also result in different conversion and depth of cure characteristics.

6.5.2 Degree of Conversion

The importance of DC lies in the fact that its features are significantly correlated to a number of important material characteristics, such as polymerization shrinkage [319, 320], mechanical properties [321], and monomer elution [136, 322].

The DC is affected by the curing time and the level of light irradiance utilised, as different composite formulations required different amounts of total energy to polymerize. Durner *et al.* and Frauscher *et al.* reported that it is vital to allow sufficient curing time and a moderated radiance to ensure correct polymerisation of the composite – they recommended a curing time of 20 to 40 s with an irradiance of approximately 1200 mW/cm² for different nano-hybrid composites [323, 324]. Extending the curing time to over 40 s significantly increased the DC and shortening it to 5 or 10 s reduced the DC [323, 324]. A pilot study showed that when the 80% bottom-top-hardness ratio criterion was applied as a minimum acceptable threshold, groups D & E showed inadequate hardness ratio (less than 80%) at 3 mm with 20 s light exposure. At higher radiant exposure (40 s at 1200 mW/cm^2) all groups reached over 80%. It was therefore decided to utilise 40 s of light exposure for this experiment.

Commercial resin composites have shown DC to range between 50% and 75% [325, 326], with maximum conversion being reached while there is still considerable C=C unsaturation in the polymerised material. This is in line with the results of this study, as similar methacrylate double bonds were observed and attributed to the diffusion-controlled reaction mechanism associated with free-radical polymerisation [327].

The DC was higher in mixtures with TEGDMA and PMMA compared to those with UDMA and Bis-EMA at 2 mm thickness. This may be explained by some of the molecular features of these monomers. TEGDMA and PMMA (utilised in group A) were replaced with a blend of UDMA and Bis-EMA in the experimental resins (B, C, D, E). This could be explained by the greater mobility of TEGDMA and PMMA

molecules caused by its lower viscosity compared to that of UDMA/ Bis-EMA mixtures. This result is in line with the results by Goncaleves et al. whom showed that the DC decreased as TEGDMA where substituted by Bis-EMA in experimental resins [321].

Lovell *et al.* reported that the nature of the monomer molecule is significant for the DCs that are achieved. The high viscosity of Bis-GMA leads to immediate auto-acceleration, and the final conversions are then commonly less than 30% [24]. Higher DC can be achieved by incorporating monomers and decreasing system viscosity. Strong intermolecular hydrogen bonding results in the Bis-GMA monomer having high viscosity (1200 Pas) [328]. This intermolecular hydrogen bonding can be reduced significantly if derivatives of Bis-GMA are utilised, for example the Bis-EMA monomer, which is a non-hydroxylated homologous monomer of Bis-GMA [302]. This reduction in the intermolecular hydrogen bonding provides the Bis-EMA monomer with more mobility (viscosity = 3 Pas at 20°C) [321]. Moreover, in this study the Bis-EMA used has longer ethylene glycol spacers when compared to the one present in Bis-GMA, which increases its flexibility. The higher flexibility of the urethane linkage leads to lower viscosity (23 Pas at 20°C) [302] [329]. This could explain why the conversions were, although statistically different, close to the those obtained with higher Bis-EMA concentrations (group B and C).

6.5.3 Depth of Cure

The conventional method of applying resin composites is in 2 mm thick layers [330, 331]. However, due to the time-consuming nature of this method, particularly when dealing with deep posterior cavities, “bulk-fill” resin composites were developed that can be cured in 4 mm thick increments. The DoC of resin composites is an important indicator of whether or not effective polymerisation has occurred at depth in the material.

The DoC is defined as “the maximum thickness of a composite material that can be adequately cured in a single layer” [155]. The term “adequately” can be interpreted in different ways, which has led to a great deal of dispute, so there is a lack of consensus over the concept of DoC. The cure can therefore be said to be adequate if micro-

hardness greater than 80% of the maximum value are achieved [120]. Such a concept (hardness profiles) has been criticized saying that the cut-off values have been determined in a totally arbitrary way that does not correlate with any actual level of change within the composite's properties, so they have no physical meaning. However, although there seems to be no physical foundation for this cut-off point, surface hardness profiles continues to be used for the assessment of curing efficiency, many studies have cited 80% of the maximum micro-hardness value as an indication of adequate cure [156, 157].

The depth to which polymerisation can be achieved depends on how well visible light penetrates through the bulk of the material [332]. Therefore, it is important to pay attention to three particular parameters to achieve sufficient polymerisation; these are sufficient light output, duration of exposure and appropriate wavelength range of the light [333]. There are additional factors that can impact the depth of cure achieved, including the shade and translucency, distance from the tip of the light cure unit, post-irradiation period [334] and size and distribution of filler particles [335].

In this study, Groups B and C had the greatest depth-of-cure amongst materials (4.4 mm and 4.3 mm respectively); this could be as a result of the higher concentration of Bis-EMA, which was 37.5% and 29.5% in groups B and C respectively, whereas it was 19.5% in group E which had a DoC of 3.4 mm. The long spacer length in Bis-EMA indicates that the monomers have more flexibility, and system mobility is therefore enhanced [336]. Moreover, in this study, the good DoC that was observed in groups B and C may have been caused by the fact that there was a close match in the refractive indices of the polymer (1.527, 1.525 respectively) to the fibres and fillers (1.555 and 1.556 respectively). This similarity may have increased the transmission of light leading to higher DoC.

6.6 Conclusion

The resin-based composites analysed in the present study were model formulations where the monomers were systematically varied. The content of fillers, fibres and additives, were kept constant. Therefore, the risk of uncontrolled factors influencing the results were reduced. Hence, the results presented can be traced to differences in the resin matrix contents between the materials studied. Within the limitations of this study it was found that Groups B and C revealed improvements in depth of cure compared with a fibre reinforced composite with a semi-IPN-polymer matrix.

Chapter Seven

Properties of Model E-Glass Fibre Composites with Varying Matrix Monomer Ratios

Abdulrahman Alshabib*, Nick Silikas, David C Watts

Submitted to Journal of the Mechanical Behaviour of Biomedical Materials

7.1 Abstract

Objective: To evaluate properties of fibre-reinforced-composites (FRC) containing Bis-EMA/UDMA monomers but identical dispersed phase (60% wt BaSi glass power +10%wt E-glass fibre).

Methods: The following monomer mass fractions were mixed: 50% bis-GMA plus 50% of different ratios of Bis-EMA+UDMA to produce consistent formulations (Groups B-E) of workable viscosities. As control (Group A), a monomer mixture with mass fractions: 60% Bis-GMA, 30% TEGDMA, 10% PMMA (typical FRC monomers) was also studied. Flexural strength (FS), fracture toughness (KIC), water sorption (SP), solubility (SL) and hygroscopic expansion (HE) were measured. FS and KIC specimens were stored for 1, 7 d, and 30 d in water at 37°C. SP/SL specimens were water-immersed for 168d, weighed at intervals, then dried for 84 d at 37°C. Data were analysed by ANOVA.

Results: FS and KIC for groups A, D, E decreased progressively after 1 d. Groups B and C (highest amounts of Bis-EMA) did not decrease significantly. The modified matrix composites performed significantly better than the control group for SP and HE. The control group outperformed the experimental composites only for SL with up to 250 % higher SL for group E (6.9 μg/mm) but still below the maximum permissible threshold of 7.5 μg/mm.

Conclusions: Experimental composites with highest amounts of Bis-EMA showed improved hydrolytic stability and overall enhancement in several clinically-relevant properties. This makes them potential candidates for alternative matrices to a semi-interpenetrating network in fibre-reinforced composites.

Keywords: Resin composites; Ethoxylated bisphenol-A-dimethacrylate; UDMA; fibre reinforcement; flexural strength; fracture toughness; hygroscopic expansion.

7.2 Introduction

It is more than fifty years since resin composites were first employed for clinical use. Looking back, several development cycles addressed deficiencies observed in clinical practice. In the 1980s and 1990s, emphasis was placed on particulate filler systems. These led progressively to microhybrid composites that were more resistant to wear and had superior mechanical properties [30]. Over the next decade, attention turned towards reducing polymerization shrinkage to minimize the issues of interfacial gap formation, post-operative sensitivity and cuspal deflection [337]. More recently, bulk-fill composites have gained popularity as they require less time for placement into the cavity preparation [160].

Many reviews exist on resin composite restorations in vital posterior teeth. One review compared studies conducted between 1995 and 2005 with those conducted between 2006 and 2016 [206]. Over the earlier period, reported survival rates were 89.4% compared with 86.9% for the later period, a marginal difference. The reported rates of secondary caries were also similar: 29.5% in 1995–2005, and 25.7% in 2006–2016. However, the frequency of fractures in composite and teeth was significantly higher in 2006- 2016. The possible explanation was that composites were employed in larger restorations in this more recent period. Therefore studies have investigated potential ways to enhance the mechanical properties of particulate filled composite (PFC), through various curing techniques [141, 207], selection of resin matrices [208], and improving the filler content [30].

In a recent study, the physical properties of fibre reinforced composites (FRCs) were compared with various commercial *particulate filled* composites (PFCs) [77]. The results showed that the mechanical properties of FRC differed considerably from conventional and bulk-fill PFC, demonstrating superior fracture toughness. Moreover, *in vitro* fracture resistance of endodontically-treated teeth restored with various core materials was studied by Garlapati et al [338]. They concluded that fibre reinforced composites provided the highest fracture resistance. However, several factors affect the efficiency of the fibre reinforcement, including: fibre type, orientation, distribution

[308], aspect ratio [92], volume fraction [339] and the chemical bonding between fibre and resin matrix [50, 167].

Fibre orientation within the resin is of critical importance due to the isotropic *versus* anisotropic reinforcement they provide. It is more difficult to control the orientation of discontinuous fibres (unidirectional or multidirectional) than continuous (unidirectional or bidirectional) fibres, especially if the discontinuous fibres are oriented in a multidirectional manner. Methods used for evaluating fibre orientation include two-dimensional (2-D) imaging techniques such as optical and scanning-electron microscopes. A drawback of these 2-D methods is the projection of the discontinuous fibres aligned in one plane. This could be resolved by providing sections of the same sample cut in different planes and analysing each of them. However, this method is unreliable because the techniques used for specimen preparation may alter the internal structure. Non-invasive technique through the use μCT scanning could be used to analyse fibre orientation in a 3D projection.

With regard to the use of FRCs in clinical applications, the principal limitation is the few investigations of their longterm clinical performance. Most studies have concerned laboratory measurements of their material properties. The most significant weakness of FRCs is the interface between the resin matrix and the fibre. Intraoral hydrolysis and degradation can lead to failure of the restoration through weakening of this interface [340]. This may explain why there is a lack of long-term studies.

Dental fibre reinforced composites (FRCs) which are based on bis-GMA, triethyleneglycol dimethacrylate (TEGDMA), are able to form crosslinked thermoset polymer matrices for the FRC. To increase surface adhesive properties, some linear PMMA polymer has been added to the matrix. A combination of linear polymer and crosslinked polymer is utilised in a commercially available E-glass FRC (everX™ GC, Japan) [83]. Despite significant improvements in the mechanical properties for short FRC (everX™) [77], there are some drawbacks to the semi-interpenetrating polymer network (SIPN) (bis-GMA/ TEGDMA –PMMA) system, as aqueous storage has a significant negative effect on its properties [340].

Solvents can have different effects on dental composites. When stored in water for 1 or 2 months, the flexural strength of composites undergoes substantial reduction [270, 341]. Similarly, water ageing can reduce fracture toughness by 10-35% [342, 343]. However, other literature reports that flexural strength or fracture toughness do not change or may even increase when composites are stored in water [344-346].

These conflicting results may be attributed to differences in the materials and methods used, especially the composition of fillers and resins tested. Tanaka et al, studied conventional composites stored in water and found substantial 30% reductions in compressive and diametral tensile strength, flexural strength and elastic modulus. However, when similar tests were conducted on an experimental composite containing a fluorinated polymer, only the flexural strength reduced, highlighting the key role played by the resin components when investigating solvent resistance [347].

This study aims to formulate fibre-containing composites where a semi-interpenetrating polymer network (Bis-GMA-TEGDMA/PMMA) is substituted by a cross-linked resin matrix (Bis-GMA- UDMA/Bis-EMA). These experimental resin composite systems will be studied to evaluate how de-ionized water storage affects their flexural strength, fracture toughness, water sorption, solubility, and hygroscopic expansion.

The null hypotheses are that there are:

1. No differences exist between the control group (A) and the experimental groups (B-E); in flexural strength and fracture toughness after water storage at 1 d, 7 d, 30 d at 37°C.
2. No differences exist between the control group (A) and the experimental groups (B-E); in water sorption, solubility, and hygroscopic expansion after 168 d of aqueous exposure at 37°C.

7.3 Materials and methods

Monomers and the reinforcing materials used to formulate the experimental groups are listed in **Table 7-1**.

Table 7-1: Monomers and reinforcing materials used in this study.

Abbreviation	Name	Lot number	Manufacturer
Organic Component			
Bis-GMA	Bisphenol A-glycidyl dimethacrylate	804-39	Esschem, Europe
UDMA	Urethane dimethacrylate	803-66	Esschem, Europe
Bis-EMA (EO=8)	Ethoxylated bisphenol-A dimethacrylate	849-17	Esschem, Europe
TEGDMA	Triethyleneglycol dimethacrylate	807-32	Esschem, Europe
PMMA	Polymethyl methyl methacrylate	93-097	Esschem, Europe
CQ	Camphorquinone	09003A	Sigma–Aldrich Inc., St. Louis, USA
DMAEMA	Dimethylaminoethyl methacrylate	BCBR4467V	Sigma–Aldrich Inc., St. Louis, USA
Reinforcing component			
BaSi	Barium borosilicate glass: average particle size 0.7 μm	EEG 101-07-/871-12	Esschem, Europe
SiO2	Silica oxide glass: average particle size of 0.7 μm	1332-37	Donghai Changtong Silica Powder Co.Dongjai,China
GF	Silanated E-glass fibres: diam. 15 μm, length 3 mm.	86-792	Hebei Yuniu Fibreglass Manufacturing Co., Ltd, Guangzong, China
3-MPS	3-Trimethoxysilyl Propyl methacrylate	2530-85-0	Sigma–Aldrich Inc., St. Louis, USA

7.3.1 Silane functionalization of Barium borosilicate surfaces

60 ml of ethanol and 20 g of borosilicate particle fillers were put into a plastic container before being placed in a SpeedMixer™ (DAC 150.1 FVZK, High Wycombe, Buckinghamshire, UK) and mixed for 20 min at 1500 rpm. Once the initial mixing had taken place, a sterile syringe was used to slowly add 3% (0.6 g) of the silane coupling agent (3- trimethoxysilyl propyl methacrylate). This mixture was then

put back into the Speedmixer for 10 min at 1500 rpm, before being separated equally into two plastic tubes and put into a 4000-rpm centrifuge (Heraeus, UK) for 20 min at 23°C. The supernatant (separated ethanol) was removed and the silanated fillers was placed in plastic tubes and dried for 3 h in an EZ-2 Elite personal solvent evaporator (Genevac Ltd, SP Scientific Company, UK) at 60°C. Once dried, the silanated fillers were stored at room temperature (23°C ±1).

7.3.2 Fabrication of filled resin composites:

Five resin monomer matrix groups were formulated (Table 6-2). A digital microbalance (BM-252, A&D Company, Japan) was used to measure the amount of resin. Each group was mixed with CQ (0.5 wt.%) and 1 wt.% of DMAEMA in a SpeedMixer™ at 1500 rpm for 3 cycles of 5 min.

The filler phase was 60 wt% silanated barium borosilicate glass and 10% wt E-glass fibre. This made the weight percentage ratio of monomer to filler 30:70 for all composites.

The final mixture was mixed for 20 min using the SpeedMixer at 1500 rpm (5 min/cycle). The experimental resin composite groups are shown in **Table 7-2**.

Table 7-2: Matrix composition (in wt %) for the control (A) and experimental (B, C, D, E) 60%wt silanated barium borosilicate glass and 10%wt E-glass fibre were added. Making the percentage ratio of monomer to filler 30:70 for all composites.

Group	Bis-GMA	TEGDMA	PMMA	Bis-EMA	UDMA
A	59.5%	29.5%	9.5%	----------	----------
B	49.5 %	----------	----------	37.0%	12.0%
C	49.5%	----------	----------	29.5%	19.5%
D	49.5%	----------	----------	24.5%	24.5%
E	49.5%	----------	----------	19.5%	29.5%

7.3.3 Fibre length measurements

The fibre manufacturer provided nominal dimensional data on the fibres: diameter of 15 μm; length 3 mm. Experiments were made to measure the length ranges of representative fibres in a small sample.

0.5 g of E-glass fibres were dispersed in 50 ml of ethanol solution using an ultrasonic vibrator. After the evaporation of ethanol the fibres were vacuum sputter coated with Au/Pd alloy 60/40 with a 10 nm layer thickness (Q150T ES, Quorum technologies, UK) for 2 min. SEM (Quanta 650 FEG, FEI company, USA) was used to image the E-glass fibres, before being processed to establish the final fibre lengths using Image-J software [248]. A total of fifty fibres were included in the calculation.

7.3.4 Flexural strength and Modulus measurement:

Five model fibre reinforced resin composite were studied (Groups A-E). For each material, a Teflon mould was used to produce 18 specimens. The dimensions of each beam were 2 x 2 x 25 mm. A slab of glass (1mm thickness) was positioned over the mould to ensure that the material was level with the top surface of the mould. The specimens were photo-polymerised for 20 s at six overlapping sections (total of 120 s), by a LED curing unit with measured average tip irradiance of 1200 mW/cm^2 (Elipar S10, 3M Espe, Seefeld, Germany). Irradiance was verified using a calibrated radiometer after each use of the light curing unit (MARC™ Resin Calibrator, Blue-light Analytics Inc, Halifax, NS, Canada). Small areas of excess composite tended to exist at the edges of the specimen. They were removed by using 320-grit metallographic papers before being put into bottles of distilled water (n=6), and placed in an incubator at 37°C for 24 h, 7 d, 30 d. The specimen dimensions were measured using an electronic digital caliper (Powerfix, OWIM GmbH & Co., KG, Germany) with an accuracy of 0.01 mm. The width and height were measured at the centre of the sample and at two different points. The flexural strengths for the specimens were measured by conducting a three-point flexural test using a Universal Testing Machine (Zwick/Roell-2020, 2.5 kN load cell) at 23 ± 1°C. Each beam specimen was subjected to a central load in a three-point bending mode, at a crosshead speed of .5 mm/s, until each fracture point was reached.

After obtaining the fracture loads, flexural strengths (FS) were calculated through the following formula [169]:

$$\boldsymbol{FS = \frac{3FL}{2BH^2}}$$

Equation 7.1 Flexural strength equation

where *F* was the maximum load (in Newtons) at the highest point of load-deflection curve; *L* was the distance between the supports (mm); *B* was the width of the specimen (mm) and *H*, the height (mm).

The elastic modulus was calculated from the slope of the load deflection curve's linear region with the following equation [348, 349]:

$$\boldsymbol{E_f = \frac{L^3F}{4wh^3d}}$$

Equation 7.2: Elastic modulus equation

Where *w* is the width (mm), *h* is the height (mm) of the specimen, *L* (mm) is the distance between the supports and *d* (mm) is the deflection due to load *F* (N) applied at the middle of the specimen.

7.3.5 Fracture toughness:

For each material, a polytetrafluoroethylene (PTFE)-lined brass mould was used to produce 18 single edge notched (SEN) specimens. The mould conformed to British Standard 54479:1978 [221]. This included a segment of razor blade incorporated in the mould. The dimensions of the beam were 32 x 6 x 3 mm. The specimens were photo-polymerised for 20 s at six overlapping sections (total of 120 s), by a LED curing unit (as mentioned above). Small volumes of composite excess tended to exist at the edges of the specimen. They were removed using 320-grit metallographic papers followed by wetting the pre-crack with a drop of glycerol. A sharp razor blade was used to further cut the notch with a sliding back-and-forth motion before being stored in small bottles of distilled water (n=6), and placed in an incubator at 37°C for 24 h, 7 d, 30 d. Using a stereomicroscope (EMZ-5; Meiji Techno Co. Ltd. Japan), at X 1.5 magnification, the crack length was measured for each specimen to an accuracy of

0.01 mm. The specimen dimensions were measured using an electronic digital caliper (Powerfix, OWIM GmbH & Co., KG, Germany) with an accuracy of 0.01 mm. The width and height were measured at the centre of the sample and at two different points. The K_{IC}, or fracture toughness, for the specimens were measured by flexural loading with a Universal Testing Machine (Zwick/Roell-2020, 2.5kN load cell) at 23 ± 1°C. Each beam specimen was subjected to a central load in a three-point bending mode, at a crosshead speed of 1.0 mm/s, until each specimen's fracture point has been achieved.

From the load values at fracture, fracture toughness was calculated through the following formula [67]:

$$\boldsymbol{K_{IC} = \left[\frac{PL}{BW^{1.5}} \right] Y}$$

Equation 7.3 Fracture toughness equation

$$Y = [2.9\ (a/w)^{1/2} - 4.6\ (a/w)^{3/2} + 21.8\ (a/w)^{5/2} - 37.6\ (a/w)^{7/2} + 38.7\ (a/w)^{9/2}\ ]$$

Where P is the load at fracture, L is the distance between the supports, W is the width of the specimen, B is the thickness of the specimen, Y is calibration function for given geometry, and a is the notch length.

7.3.6 Scanning electron microscopy (SEM)

SEM images were taken of specimen fracture surfaces of the experimental composites. Specimens were vacuum sputter-coated with Au/Pd alloy 60/40 with a 10 nm layer thickness (Q150T ES, Quorum technologies, UK) for 2 min. Then the fracture sites were observed using a Quanta 650 FEG (FEI Company, USA).

7.3.7 Micro-CT (μCT) study of fibre orientation

A Teflon mould was used to prepare one specimen beam (3 x 6 x 34 mm) from groups B, C, and D (with 60% wt Silica oxide and 10% wt E-glass fibre) in order to render the three-dimensional images to observe the fibre orientations, radiopaque BaSi fillers were replaced with SiO_2, allowing for a distinction in X-ray opacity for the fibres. Each specimen was cured for 120 s from each side using a LED curing unit light curing

(as mentioned above). Several overlapping areas of irradiation were utilised along the length of the specimens.

After specimen preparation, the SkyScan unit (Skyscanner 1272 Bruker micro CT, Kontich, Belgium) was turned on and then the object was placed in the specimen chamber. The scanning parameters were set as appropriate. In this case, the voltage and current were set at 70kV and 142uA, respectively. A 1mm Al primary beam filter was used for the purpose of decreasing beam hardening artefacts. The objects being scanned in this research were experimental fibre reinforced composites, and these were scanned using the following parameters: image pixel size of 3μm; 0.100° rotation step, 180° sample rotation; 1800 millisecond exposure time. With these parameters, an x-ray image lasting 1800 milliseconds was taken every time the object rotates 0.100°, and this continues until a rotation of 180° has been completed. The operator determines the file name and the acquired projections images are saved in 16-bit .tiff files which are later employed for tomographic reconstruction.

After scanning, the coronal and sagittal views of each specimen were saved as 16 bit TIFF files (using N-Recon software). CTAn and CTvol software were used, respectively, to convert the images to a 3D image and then to create 3D models of the specimens. All software from Bruker AG, Germany.

7.3.8 Sorption and solubility

7.3.8.1 Specimen preparation

Using brass moulds, five disc-shaped specimens were produced for each material. The moulds (15 x 2 mm), were placed between two sections of clear Mylar strip with glass slides on each side (1 mm thick) and then squeezed together. An LED curing unit with measured average tip irradiance of 1.2 W/cm^2 (Elipar S10, 3M Espe, Seefeld, Germany) was used to irradiate five sections of each side for 20 s. The irradiance was measured every time the light cure unit was utilized, using a calibrated radiometer (MARC™ Resin Calibrator, Blue-light analytics Inc, Halifax, NS, Canada). The specimens were taken out of their moulds with care, and 1000 grit silicon carbide paper was used to smooth out any rough edges. Following this, the specimens were

placed in a desiccator containing silica gel at 37± 1°C. After a period of 24 h a precision-calibrated balance was used to weigh each specimen, accurate to ± 0.01mg (BM-252, A&D Company, Japan). The cycle was duplicated repeatedly until a constant mass was acquired (m1) – i.e. until the mass loss of the specimens was no more than 0.1 mg over 24 h.

For the thickness measurement, a digital caliper was used (Powerfix, OWIM GmbH & Co., KG, Germany) to obtain two measurements of the height. After taking the dimensions of the specimen, the volume (V) was calculated in mm^3 through the following formula:

$$\boldsymbol{V = \pi r^2 t}$$

Equation 7.4 Volume calculation formula

Where π=3.14, r is the radius of cross section; t is the thickness of specimen

7.3.8.2 Sorption

All five specimens were submerged in 10 ml of distilled water within separate glass bottles sealed with polyethylene caps. The bottles were kept at 37 °C for 1, 2, 3, 4, 5, 6, 7, 14, 21, 28, 56, 84, 112,140, and 168 d. After each time period, a tweezer was used to take each specimen from the bottles. They were dried using filter paper before being weighed 1 min after removal from the water. The recorded mass is denoted as m_2 (t). All five specimens were then returned to aqueous storage. This was replenished every week, with the total volume of water maintained at 10 ml.

7.3.8.3 Solubility

After the sorption cycle was complete, specimens were dried using a desiccator and weighed at time points of 1, 2, 3, 4, 5, 6, 7, 14, 21, 28, 56 and 84 d. Once the mass loss of the specimens was no more than 0.1 mg within any 24 h period, the constant final mass was then obtained (m_3).

Weight increase W_i (%) and water sorption W_{so} were calculated by:

$$\boldsymbol{W_i}(\%) = 100\left[\frac{m_2 - m_1}{m_1}\right]$$

Equation 7.5**:** Weight increase calculation formula

m_1 was the conditioned mass prior to immersion in water; m_2 was the mass after water immersion for 168 d.

$$\boldsymbol{W_{So}} = \left[\frac{m_2 - m_3}{V}\right]$$

Equation 7.6**:** Water sorption formula

m_2 was the mass after immersion in water for 168 d; m_3 was the mass after desorption, and V was the volume of the specimen.

The percentage water absorbed by a composite at the end of the storage period was calculated by

$$\boldsymbol{W_{So}}(\%) = \left[\frac{m_2 - m_3}{m_1}\right] \text{X } 100$$

Equation 7.7: Water sorption % formula

The following equation was used to calculate the solubility (Sol) values:

$$\boldsymbol{Sol} = \left[\frac{m_1 - m_3}{V}\right]$$

Equation 7.8: Solubility formula

7.3.8.4 Hygroscopic Expansion

Hygroscopic dimensional changes were measured in parallel with the water sorption measurements. A custom-built noncontact laser micrometer was used to measure the dimensional changes of the specimen. After each time period, specimens were dried using filter paper then measured 1 min after removal from the water. Mean diameter (d_2) was recorded at each time interval (t), and then returned to aqueous storage. An average of 534 diametral values was recorded for each specimen at each time point.

The percentage diametral change was calculated:

$$\boldsymbol{d}(\%) = \frac{d_{2(t)} - d_1}{d_1} \mathbf{x}\, 100$$

Equation 7.9: Diametral change formula

The following equation was used to calculate volumetric change, assuming isotropic expansion behaviour [287]:

$$\boldsymbol{V}\ (\%) = \left[(1 + \frac{d(\%)}{d_1})^3 - 1\right] x100$$

Equation 7.10: Volumetric change calculation formula

7.4 Statistical analysis

7.4.1 Flexural strength and fracture toughness

Data for all groups were collected and analysed statistically using SPSS 23.0 (IBM SPSS Statistics, SPSS Inc., New York, USA). Once *Shapiro-Wilk* test confirmed normality of the data. Levene's test have also confirmed the equality of variance. Two-way ANOVA, one-way AVOVA and Tukey post-hoc tests (α=0.05) was performed to identify differences in K_{IC}, Flexural strength and modulus (dependent variable) between different groups and time (independent variables). One-way analysis of variance was conducted at each time at a significance level of ($p \leq 0.05$). The Tukey *Post-hoc* test was used to determine significant differences in flexural strength, fracture toughness, and modulus between the different groups.

7.4.2 Sorption, solubility, and hygroscopic expansion

Using SPSS 23.0 (IBM SPSS Statistics, SPSS Inc., New York, USA). The mean and standard deviations were calculated for the water solubility, water sorption, hygroscopic expansion and mass change. One-way ANOVA was carried out at 168 d followed by Tukey *post-hoc* tests (at $\alpha = 0.05$) for the hygroscopic expansion, water

sorption, and mass change. For the solubility, the same statistical test was applied to evaluate differences in weight after 84 d of desorption cycle.

7.5 Results

7.5.1 Fibre length measurement

E-glass fibres length measurements ranged between 0.4 to 3.5 mm with an average length of 2.5 mm. 58% was between 2.00 – 3.5 mm (2.9 mm was the average length). 36 % of the fibres were between 1.1 – 1.9 mm (1.8 mm was the average). The remaining 6 % were between 0.3 – 1 mm with average length in this group was 0.6 mm. Results are presented in **Table 7-3**.

Table 7-3: Measured fibre lengths and aspect ratio. Fibre diameter 15 um was obtained from the manufacturer

Groups	Fibre length ranges		
	0.3-1 mm	1-2 mm	2-3.5 mm
Fibre lengths grouped by percentage values (%).	6%	36%	58%
Fibre lengths grouped by average length (mm).	0.6	1.8	2.9
Aspect ratio l/d (Average).	40	120	193

7.6 Flexural strength and modulus:

Flexural strength (FS) and Flexural moduli (FM) for the composites evaluated in this study are presented in **Table 7-4** and **Table 7-5**, and shown graphically in Figure 7-1. The highest FS both prior to and after storage was seen in group B, followed by group C, while the control group (A) had the lowest values after 30 d of water storage. However, no statistically significant difference in FS was apparent between groups.

FS was significantly influenced by the ageing period (decrease in FS), where baseline readings (1 d) were significantly higher than values measured over subsequent time periods ($p \leq 0.05$) except for group B and C which showed no statistically significant

difference. FS reduction ranged between 16 % for group B, to 29 % for group A after 30 d.

Table 7-4: Flexural strength mean and (standard deviation) (MPa)

Group	1 D	7 D	30 D	Change %
A	168.3 (13.4) [a, 1]	154.8 (17.6) [a, 1]	120.2 (22.1) [a, 2]	28.7 %
B	190.5 (22.3) [a, 1]	185.8 (27.4) [a, b, 1]	160.2 (18.1) [a, 1]	15.9 %
C	179.8 (23.3) [a, 1]	182.2 (26.0) [a, b, 1]	149.1 (16.9) [a, 1]	17.0 %
D	179.4 (17.3) [a, 1]	145.8 (14.8) [a, c, 1]	136.7 (9.4) [a, 2]	23.8 %
E	180.2 (17.0) [a, 1]	146.3 (20.8) [a, c, 1]	134.1 (32.5) [a, 2]	25.6 %

At each time interval the same superscript letters indicate no significant difference ($p > 0.05$). For each group same number superscript indicates no significant difference ($p > 0.05$).

Table 7-5: Flexural modulus mean and (standard deviation) (GPa)

Group	1 D	7 D	30 D
A	14.3 (2.6) [a]	14.0 (1.4) [a]	13.3 (1.7) [a]
B	14.7 (2.2) [a]	12.8 (1.3) [a, c]	12.9 (1.1) [a]
C	13.0 (1.9) [a]	12.1 (1.1) [a, c]	12.3 (1.1) [a]
D	12.7 (1.6) [a]	10.6 (2.0) [b, c]	11.2 (2.1) [a]
E	12.5 (1.0) [a]	10.6 (1.3) [b, c]	11.1 (1.4) [a]

At each time interval the same superscript letters indicate no significant difference ($p > 0.05$).

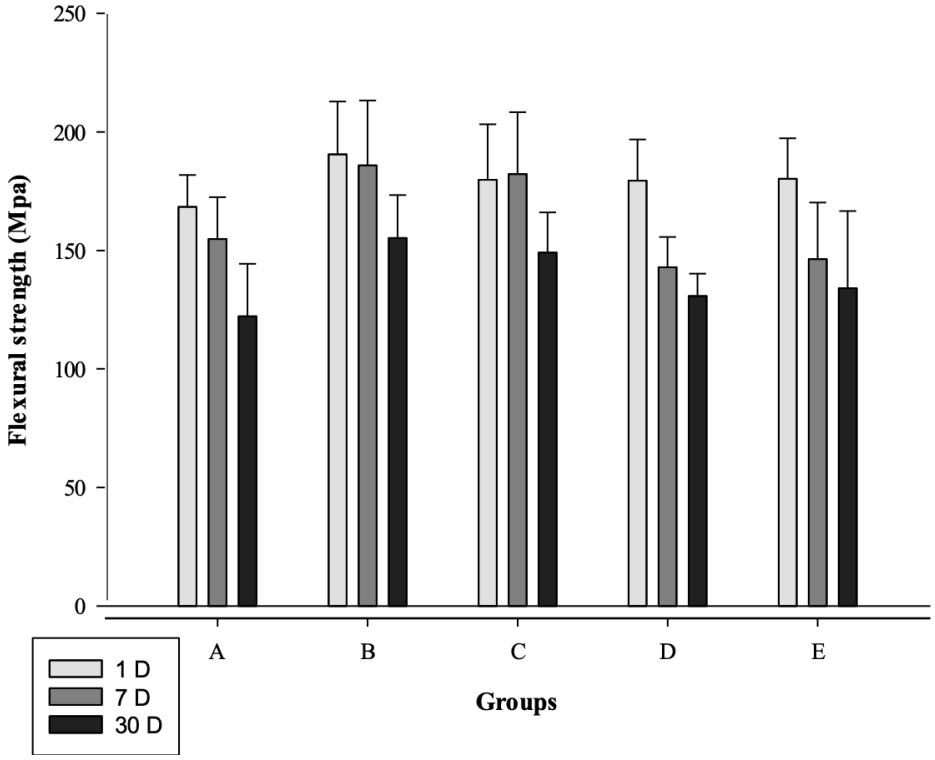

Figure 7-1: Flexural strength of composites after 30 d storage in water at 37˚C

7.7 Fracture toughness:

Fracture toughness (K_{IC}) for the resin composites are presented in **Table 7-6** and shown graphically in Figure 7-2. After 1 day water storage, K_{IC} ranged from 2.8 – 3.4 M.Pa $m^{0.5}$ reducing to between 3.0-2.3 M.Pa $m^{0.5}$ after 30 d water storage. Group B showed the highest K_{IC} 3.0 M.Pa $m^{0.5}$, while group A showed the lowest: 2.3 M.Pa $m^{0.5}$ (after 30 d). K_{IC} reduced over the ageing period. However, no statistically significant difference in K_{IC} was apparent after 30 d storage except for group A, where the reduction was 25.8 %.

Table 7-6 Fracture toughness KIC mean and (standard deviation) (M.Pa.m0.5)

Group	1 D	7 D	30 D	Reduction %
A	3.1 (0.45) ^{a,1}	2.7 (0.42) ^{a,1}	2.3 (0.38) ^{a,2}	25.8 %
B	3.4 (0.49) ^{a,1}	3.0 (0.45) ^{a,1}	3.0 (0.48) ^{a,1}	11.7 %
C	3.0 (0.68) ^{a,1}	2.8 (0.31) ^{a,1}	2.6 (0.59) ^{a,1}	13.3 %
D	2.9 (0.38) ^{a,1}	2.7 (0.15) ^{a,1}	2.5 (0.27) ^{a,1}	13.8 %
E	2.8 (0.46) ^{a,1}	2.5 (0.22) ^{a,1}	2.4 (0.45) ^{a,1}	14.2 %

At each time interval the same superscript letters indicates no significant difference ($p > 0.05$). For each group same number superscript indicates no significant difference ($p > 0.05$).

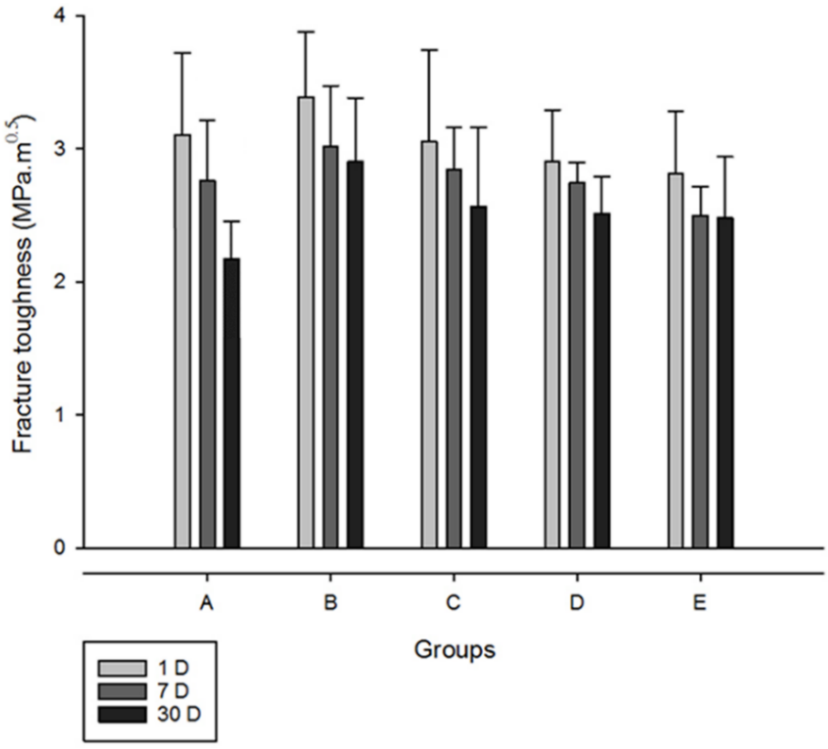

Figure 7-2 Fracture toughness of the evaluated experimental resin composites after 30 d storage in water at 37˚C

7.8 SEM of Fracture Specimens

Representative SEM micrographs of fractured specimens are shown in Figure 7-3 and Figure 7-4. These show fibre bridging, fibre pull out and fibre breakage at the point of fracture. On Figure 7-5 at a magnification of 180 X fiber alignment was observed at the crack path.

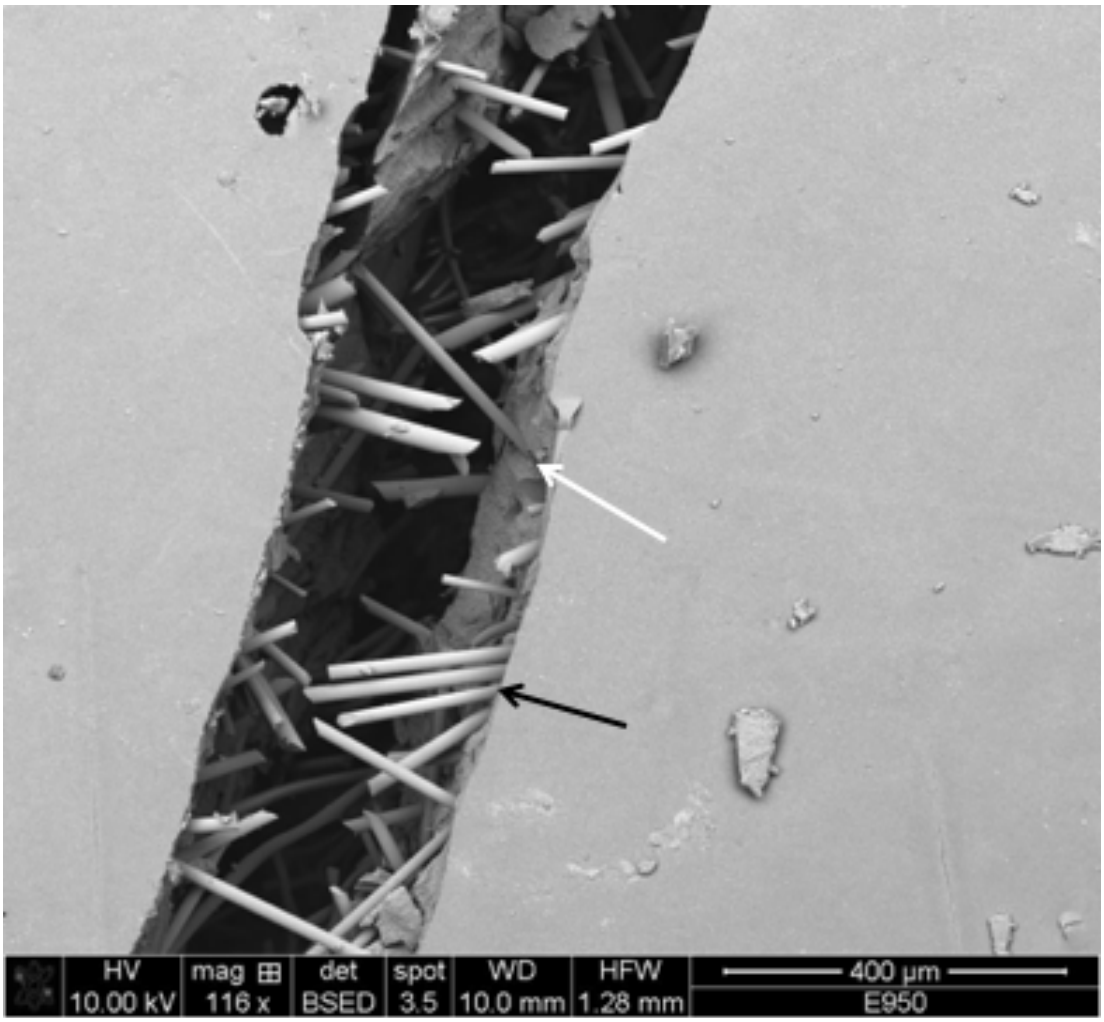

Figure 7-3*:* Fracture surface of the experimental fibre reinforced composite (group B), obtained in back scattered electron mode at ×116 magnification, showing fibre pull-out (black arrow) and fibre bridging (white arrow).

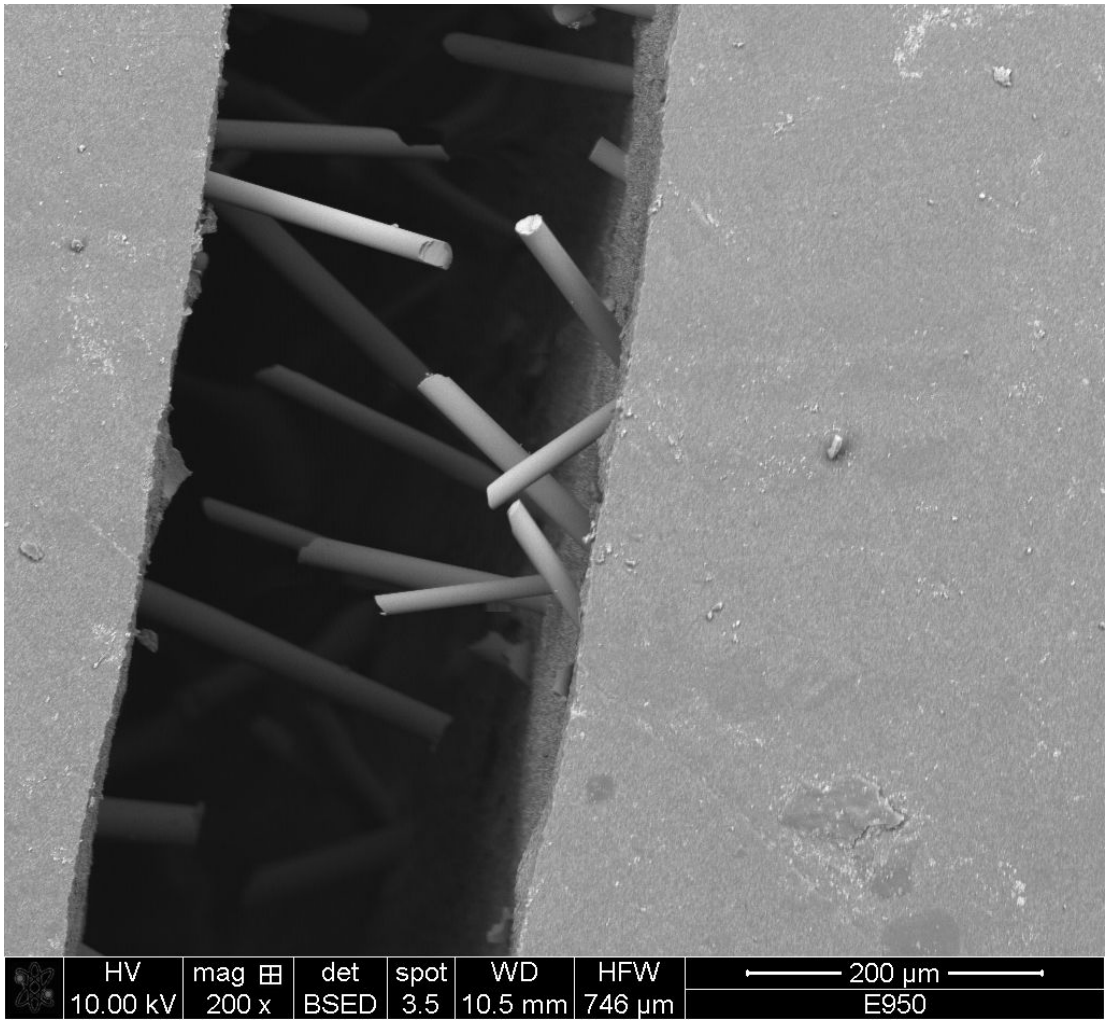

Figure 7-4: Fracture surface of the experimental fibre reinforced composite (group B), obtained in back scattered electron mode, x 200, showing random orientation of fibres.

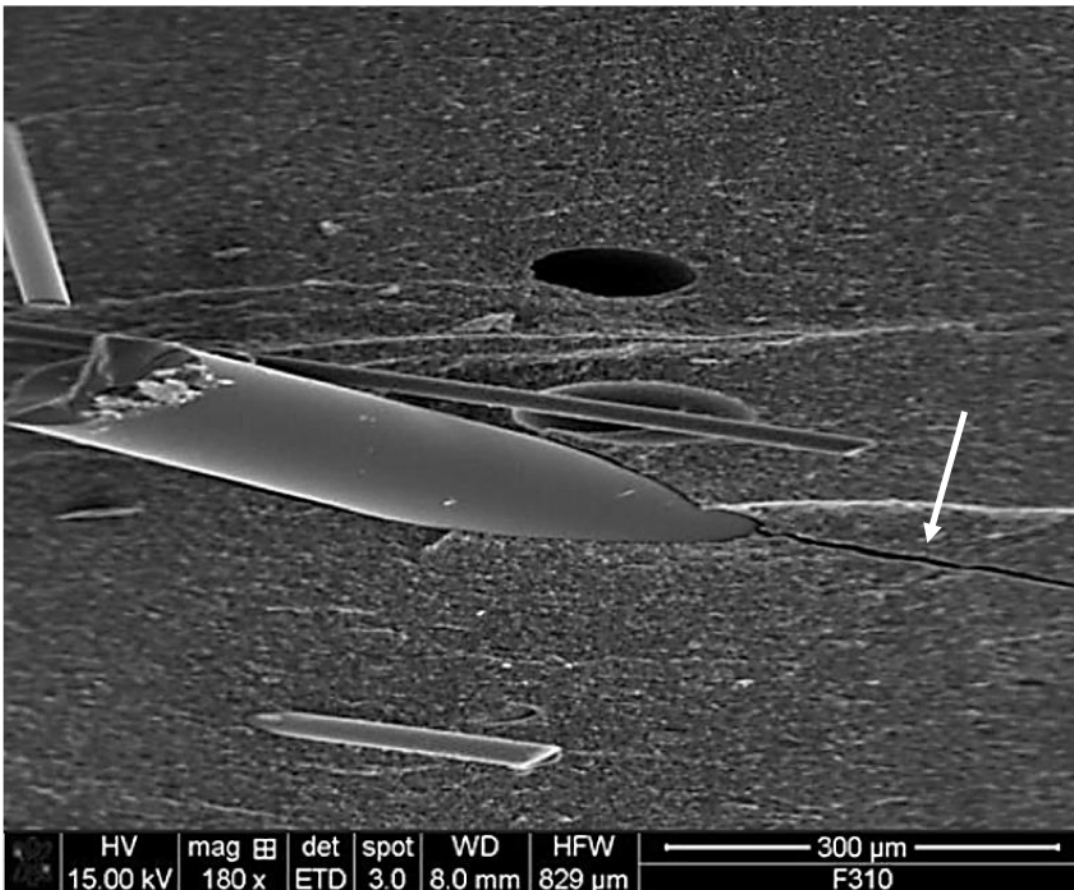

Figure 7-5: Fracture surface of the experimental fiber reinforced resin (group C). Fracture toughness specimen (×180) magnification showing the crack development (white arrow) around glass fiber within the crack.

7.9 Fibre orientation

The µCT images (Figure 7-6) showed that the short fibres were randomly aligned: a. viewed parallel to the long axis of the specimen (black arrows); b. viewed transverse (perpendicular) to the long axis of the specimen (red arrows).

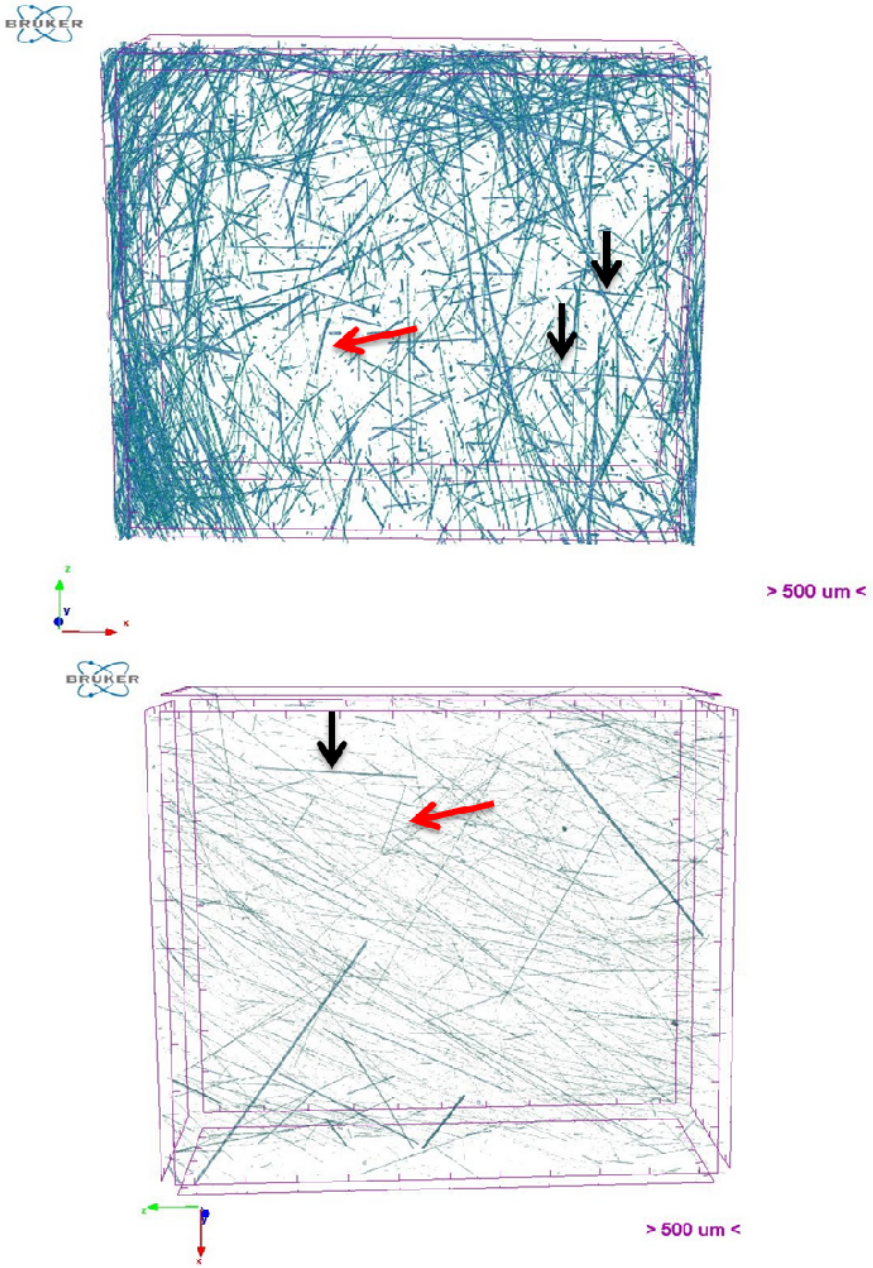

Figure 7-6 µCT images of specimens of groups B and C. Black arrows indicate parallel and red arrows indicate perpendicular fibre orientations to the long axis.

7.10 Sorption & Solubility

As can be seen from Figure 7-7, each of the resin composites exhibited a percentage mass change throughout the water sorption/desorption cycle. All of the composites demonstrated increases in mass to varying extents by their water uptake up to the point of equilibrium which occurred after 168 d.

At 168 d, water sorption ranged between 22.62 and 37.89 μg/mm (**Table 7-7**). The highest sorption was observed in group A. By contrast, groups, B, C, D and E exhibited lower water sorption, with no significant differences between these groups ($p \geq 0.05$).

The solubility for the composites ranged between 2.77 to 6.90 μg/ mm, as shown in **Table 7-7**. Groups D and E had significantly higher levels of solubility.

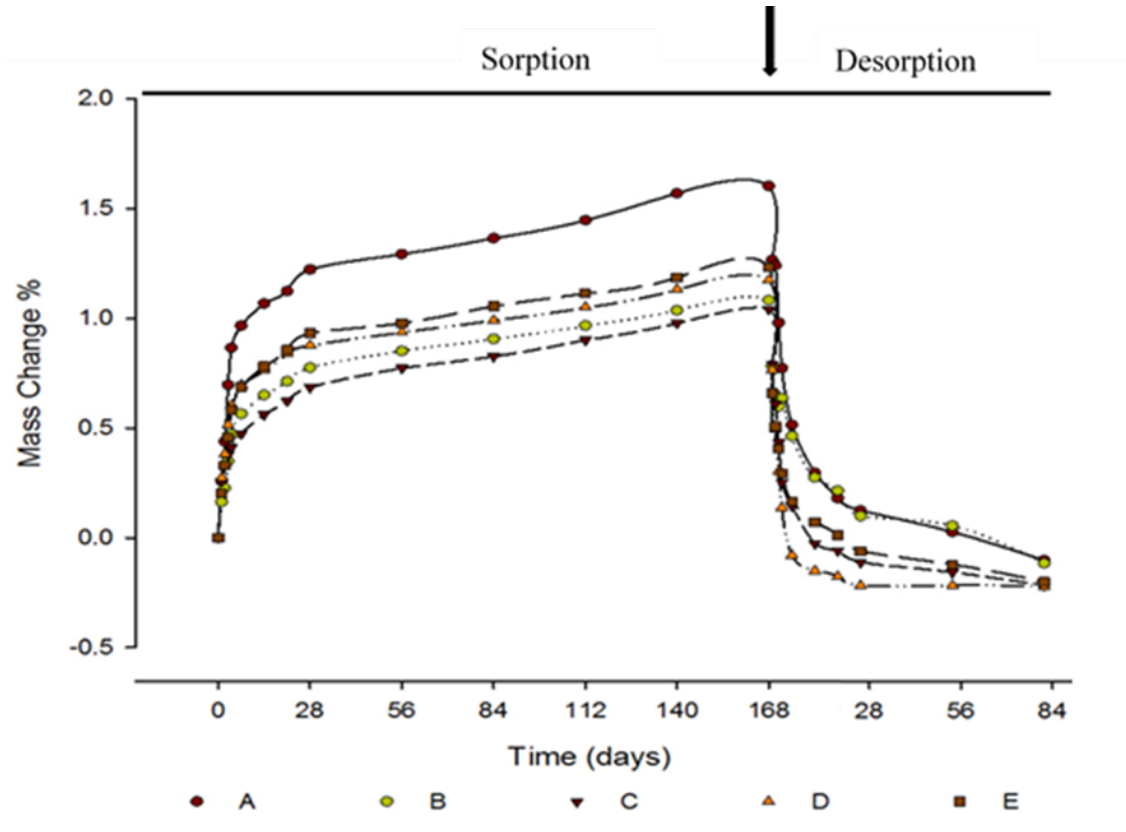

Figure 7-7: Mass changes with water sorption and desorption cycles

Table 7-7: Water sorption (WS) and solubility (SL), and percentage increase in mass and volume, of the experimental FRC after 168 d storage in distilled water at 37˚C

Materials	% Mass increase	Wso (µg/mm³)	Sol (µg/mm³)	% Volumetric increase
A	1.60 (0.30) [a]	37.89 (2.88) [a]	2.77 (0.31) [a]	1.71 (0.21) [a]
B	0.90 (0.09) [b]	22.62 (2.76) [b]	3.87 (0.46) [a]	1.23 (0.23) [b]
C	0.86 (0.15) [b]	22.70 (3.02) [b]	3.90 (1.00) [a]	1.34 (0.16) [b]
D	0.94 (0.17) [b]	25.64 (3.44) [b]	6.48 (1.13) [b]	1.32 (0.06) [b]
E	1.03 (0.15) [b]	29.60 (2.83) [b]	6.90 (1.35) [b]	1.42 (0.08) [a, b]

The same superscript lowercase letters indicate a homogeneous subset (columns) ($p > 0.05$).

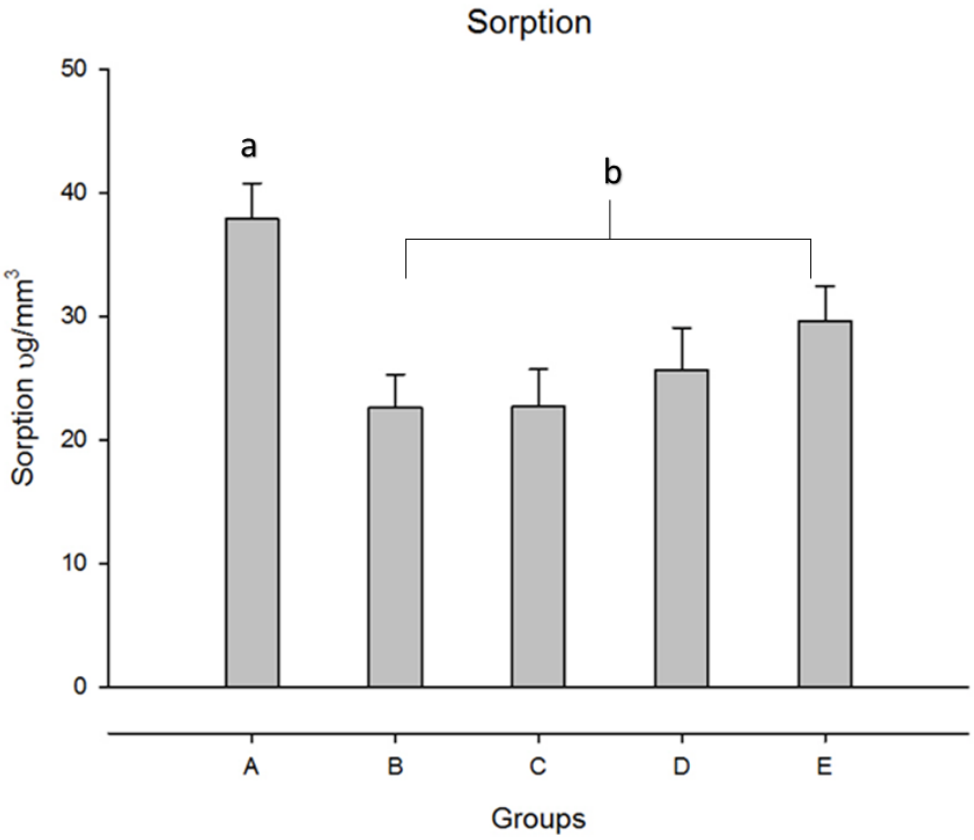

Figure 7-8: Sorption of composites after storage in distilled water for 168 days. The same lowercase letters indicate a homogeneous subset ($p > 0.05$)

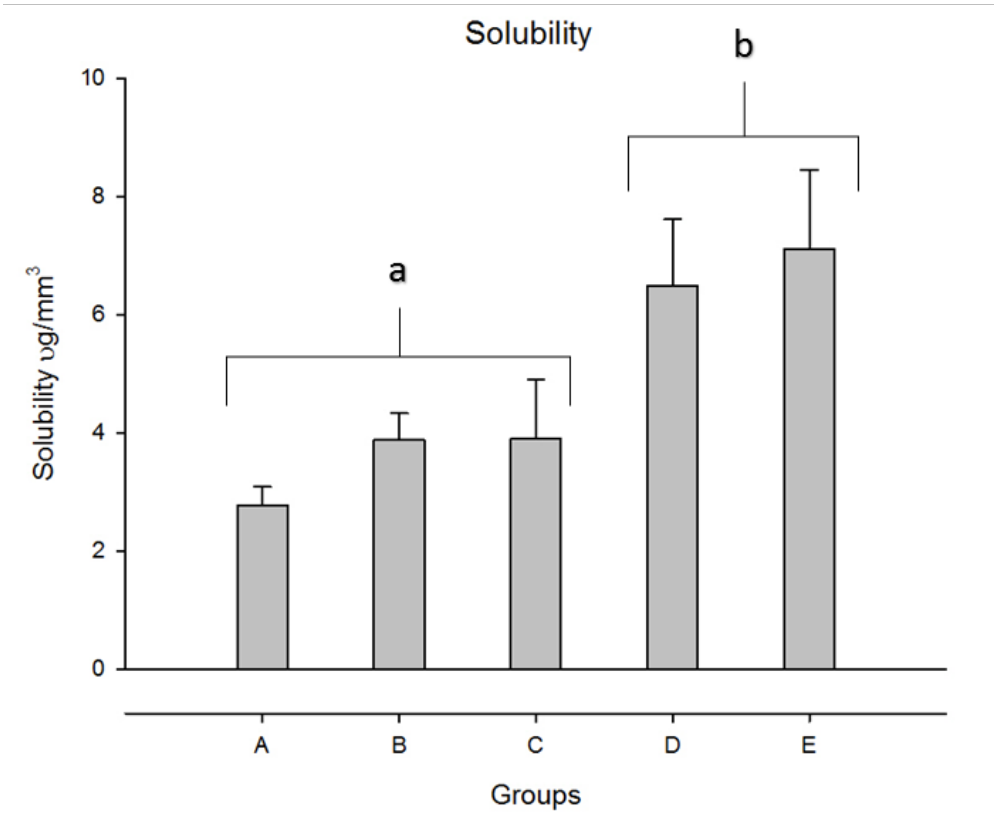

Figure 7-9: Solubility of the examined resin composites after storage in distilled water for 168 days. The same lowercase letters indicate a homogeneous subset ($p > 0.05$).

7.11 Hygroscopic expansion

One-way ANOVA conducted after 168 d of immersion in water showed that group A had a significantly higher hygroscopic expansion when compared to the rest of the materials.

The percentage hygroscopic expansion for each material is shown in **Table 7-7**.The final hygroscopic expansions ranged between 1.23 and 1.71 % at 168 d. The highest volumetric change was observed in group A. while groups, B, C, and D exhibited lower volumetric change, with no significant differences between each other ($p \geq 0.05$).

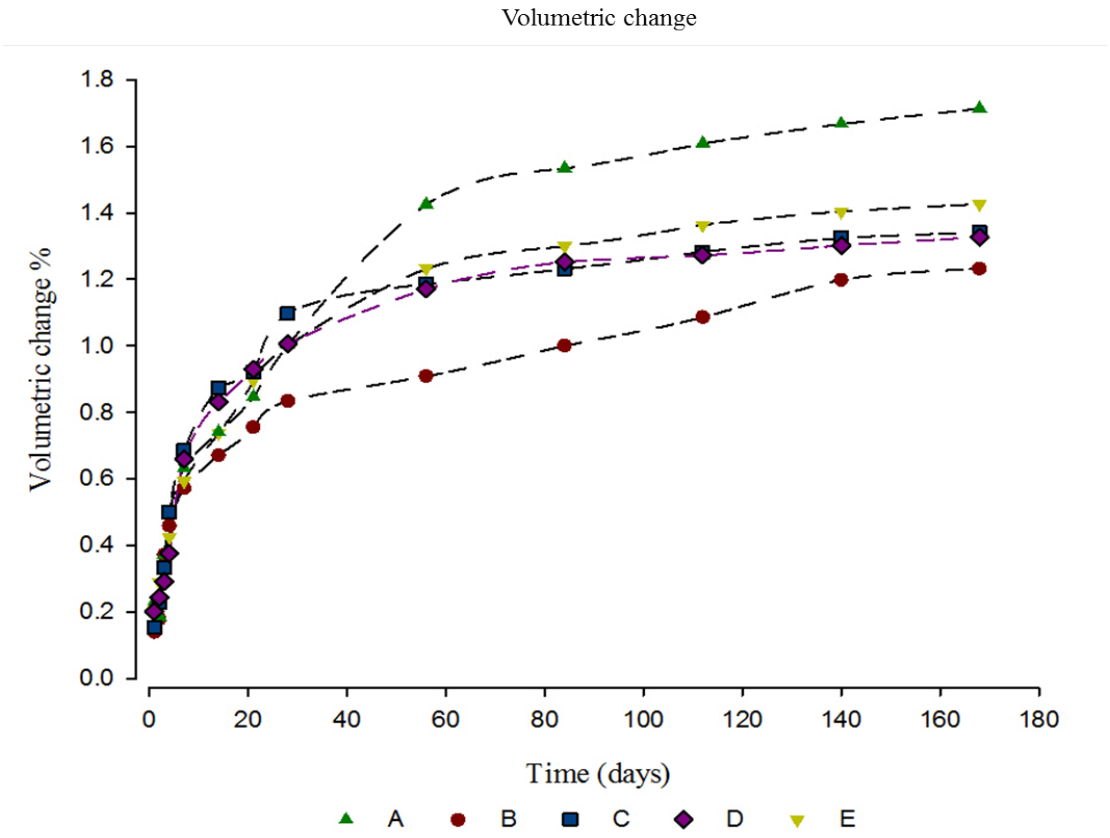

Figure 7-10 Hygroscopic expansion from 1 d to 168 d.

7.12 Discussion

This study measured the fibre length, flexural strength (FS) and fracture toughness (K_{IC}), water sorption (SP), solubility (SL) and hygroscopic expansion (HE) of experimental fibre-reinforced composites. Both mechanical and water uptake properties were significantly influenced by water storage, leading to the rejection of both null hypotheses.

7.12.1 Flexural strength and Fracture toughness

Recent reports about the clinical performance of resin composite have shown satisfactory survival rates in restorations that are small or medium in size [196, 304]. Their annual failure rates are between 1% and 3% [196, 350]. The most common causes of failure are recurrent caries and fractures [171, 196]. There is a strong

correlation between the size of the restoration and the likelihood of it failing [209]. Annual failure rates for single surface restorations are lower (0.94%) than those for four or more surface restorations (9.43%) [209].The longevity of large restorations is lower because they are more susceptible to failures relating to fractures [351]. This susceptibility to fracture may be associated with the strength of the composite material and patient-related factors such as bruxism [196].

To improve the mechanical properties and load bearing capacity of resin composite, attempts have been made to reinforce the resin phase with glass fibres [20, 69, 232]. Fibre reinforcement improves the stress distribution more effectively when loads are concentrated on the restoration [74]. Also, when combining both particles and fibres for reinforcement, improvements were found in both physical (shrinkage stress) and mechanical properties (fracture toughness) in comparison to particulate-only composites [74, 77, 352].

Previous studies have shown that discontinuous fibres have generally lower strength than with continuous fibres [85, 87]. However, when the length of the discontinuous fibres exceeds a critical value, discontinuous fibres can promote a comparable strength [92]. The aspect ratio of fibres is closely linked to the critical fibre length. This may be defined as the minimum fibre length required for optimal stress transfer within the resin matrix [86]. This length is equivalent to the minimum length at which a fibre will fail, midway along its length in an FRC, rather than by interfacial fracture between the matrix and the fibre [87]. In FRC, the critical fibre length should be 50 times greater than the diameter of the fibre, to allow homogenous stress transfer within the resin matrix [87]. The diameter of E-glass fibres used in this study was 15 μm, therefore the critical length should be over 0.75 mm. In this study the majority (94%) of the fibres were above the critical fibre length, and most of them (58%) were between 2 mm and 3.5 mm.

The experimental FRC possessed high resistance to the propagation of cracks.

Figure 7-3 illustrates the phenomenon of crack bridging (white arrow), where discontinuous fibres stretch over the edges of the crack. This reduces the strain in the notch and blunts the sharp crack. There is therefore less stress at the tip of the crack,

so crack propagation is slowed down or stopped. Furthermore, Figure 7-5 shows that propagation of the crack stopped when it came up against a fiber. It can bypass the fiber, which expends more energy and leads to a toughening effect.

Previous research has shown that the FS of resin composites was reduced when stored in water [342, 353]. But, other studies did not find a significant change in FS and K_{IC} after water storage [77, 354].These conflicting results may be due to differences in filler particle sizes, the degree of conversion or the interfaces between the filler and matrix.

In this study, storage for 30 d in water decreased FS and K_{IC} of the experimental FRC. To understand the mechanism of degradation in resin composites, synergistic pathways should be considered. For example, the cracks associated with stress crazing open up fresh surface area to reaction. Swelling and water uptake can similarly increase the number of sites for reaction. Degradation products can alter the local pH, stimulating further reaction [74]. For Group A (control group), the effect of water on this composite after 30 d was 29 % reduction in FS and 26 % in K_{IC}. An explanation is that the control FRC could have higher water sorption, which is related to the hydrophilicity of the polymer network (TEGDMA and PMMA) [189, 259, 269]. Moreover, group A had a semi-interpenetrated network (SIPN) matrix, within which thermoplastic PMMA chains are more prone to crazing and crack formation compared to thermoset polymers [355, 356].

Groups B and C showed better degradation resistance properties than the other groups of materials. Group B showed the least reduction with water-exposure among all the investigated groups (FS 12% reduction and K_{IC} 14% reduction) after 30 d of water storage. This could be due to a relatively more hydrophobic resin matrix, and higher degree of conversion especially when compared to groups (D and E). This finding is in agreement with a previous study that reported improvement in degradation resistance of Bis-GMA/Bis-EMA mixtures [208].

The placement of composite in a cavity may result in changing the fibre orientation. For instance, the filling technique and matrix viscosity can modify the fibre arrangement from the random orientation to a more planar orientation that causes

anisotropic reinforcement. The length of the fibres and size of the cavity influence the discontinuous-FRC. When cavities have smaller width compared to fibre-length during composite placement, the fibres are arranged in the cavity plane (planar-directional); hence leading to anisotropic features. Multidirectional arrangements of the fibre leading to isotropic properties are enhanced by shorter-scale fibres. To render the three-dimensional images to observe the fibre orientations, radiopaque BaSi fillers were replaced with SiO_2 which is less radiopaque when compared to BaSi, allowing for a distinction in X-ray opacity for the fibres. Specimens were fabricated with 3 mm height and 6 mm width to resemble a clinical scenario of a core build up. Random orientation of the fibres was observed suggesting that isotropic reinforcement could result in such a scenario.

7.12.2 Sorption, Solubility and Hygroscopic expansion

Sorption, through swelling, can have a positive effect, by reducing the material's polymerization stress through expansion. But it also produces negative effects as it may increase monomer leaching and accelerate material degradation [120, 357].

Under ISO Standard 4049, it is permissible for a material to possess a sorption limit of 40 μg/mm and solubility of less than 7.5 μg/mm, after it has been stored for 7 days. All of the investigated composites complied with this requirement, although the storage period was much longer, and thus the aqueous challenge more rigorous, than ISO 4049.

The results have shown that the experimental FRC have varying levels of sorption, solubility and volumetric change, depending on the type and amount of monomer used, therefore we rejected the null hypotheses. The sorption of Group A was the highest at 37.8 μg/mm³ and that of group B (containing the highest amount of Bis-EMA) was the lowest at 22.6 μg/mm³. This suggests that water storage has a significant effect on these polymeric matrices, which is in line with prior work on dimethacrylate-based composites [280, 292].

Secondary forces such as intermolecular bonds determine a number of physical properties of a material, for example its sorption, solubility and glass transition

temperature [358]. Hydrogen bonds are – cumulatively - the strongest intermolecular force, because of the great number of such bonds that may be present in some polymer/solvent systems. Bis-GMA monomer forms strong hydrogen bonds with water because the presence of –OH group. Thus, Bis-EMA and UDMA will form weaker bonds with water due to the absence of –OH group [29, 302]. Sankarapandian et al [359] also noted that lower water uptake occurred in ethoxylated monomers lacking the hydroxyl group.

Two commercially available composites, Z100 and Z250, contained copolymer bis-GMA/TEGDMA and bis-GMA/bis-EMA/UDMA, respectively. The water sorption of Z100 was 16.85 μg/mm^3 and for Z250 was 13.02 μg/mm^3 [29]. This outcome is comparable to our present study as water sorption was lower for groups (B, C, D and E) than for the control group A. The greatest relative increase in sorption was observed in the control group (with TEGDMA and PMMA), while the lowest was observed in group B (with the highest bis-EMA content). Therefore, as the content of bis-EMA decreased, the sorption increased. Composites based on bis-EMA and UDMA monomers should thus present reduced sorption than those with TEGDMA and PMMA.

The second null hypothesis was rejected because the final hygroscopic expansions showed significant variation. Group A had the highest increase (1.71%), whilst other groups had reduced expansion. Hygroscopic expansion occurs when water enters the polymer network, attracted by hydrophilic groups [188, 298]. Water diffuses through the organic matrix which expands to accommodate it [290]. Several factors influence this process: monomer structure and chemistry, the fillers employed, porosity of the network and its degree of cross-linking [360]. A material's elastic modulus is important indicator of the extent of expansion; a low modulus is required to allow the polymer phase to accommodate the expansion. The ratio of the hydrophilic attraction to elastic modulus may therefore govern to what extent the dimensions of the polymer phase can be altered. It may be clinically desirable to employ a material that expands with water sorption if this expansion counterbalances the effects of shrinkage. However, it is not desirable to have an expansion coefficient that exceeds the shrinkage value as this can lead to further stresses within the teeth.

7.13 Conclusion

Since the volume fraction and types of filler were identical in all groups, the experimental matrix compositions and monomer ratios significantly influenced the mechanical properties and evidently increased the water degradation resistance of the composites. Groups B and C had favourable outcomes in flexural strength, fracture toughness and degradation resistance. Their improved hydrolytic stability and enhancement in flexural strength may make them potential candidates for alternative matrices in fibre-reinforced composites.

7.14 Acknowledgement

We would like to thank Nick Corps at Skyscan (Bruker) for his help with X-ray tomography and analysis.

Chapter Eight

General discussion and future work

8.1 General discussion

A number of studies have proposed methods to make large posterior restorations last longer and to support the structure of the teeth that remain. One of these attempts was to employ fibre-reinforced composite (FRC) to replace dentine with enamel-replacing material (particulate filled composite (PFC)) as a surface layer, which can be considered as biomimetic bi-structured composite restorations [303, 361]. Conventional PFC has a significantly lower fracture toughness than dentine. There is high demand for materials that have a high fracture toughness as they are less prone to cracking and propagation [273]. There is therefore potential in a material that has a high toughness value, to replace dentine.

The concept of fibre reinforcement in fillings and its implementation were discussed in the literature review (Chapter 1). In brief, fibre reinforcement was introduced in order to strengthen polymeric materials, and this was necessary because resin-composite materials exhibit some physico-mechanical deficiencies when subjected to highly demanding clinical conditions. It has been confirmed that reinforcement increases the toughness of the composite, allowing fibre reinforced composites (FRC) to be used as a foundation for severely weakened teeth [220]. During the 1990s, FRC dental composites were largely unsuccessful and the reason for this is that the fibres used for strengthening were too short (below the critical fibre length), thus the toughness and strength of the fillings were not sufficiently increased. Currently, there is one commercial glass FRC that contains fibres meeting the critical fibre length and this base layer is veneered using particulate filler resin composite.

However, the stability and mechanical properties of FRC can be negatively affected by hydrolytic and hygroscopic effects. Therefore, compared to other dental materials such as dental ceramic, the usage of resin-composite restorations has been limited by some dentists due to doubts over their longevity and how they will perform. Therefore, the aim of this research was to address these uncertainties and determine how the organic component affected the performance of fibre reinforced resin-composite. This was achieved by characterizing some of the mechanical and physical properties of fibre reinforced resin-composites.

Dental fibre reinforced composites (FRCs) are based on monomer systems such as bis-GMA plus triethyleneglycol dimethacrylate (TEGDMA) and are able to form crosslinked thermoset polymer matrices for the FRC. To increase surface adhesive properties, quantities of the linear polymer PMMA have been added to the matrix. A combination of both linear and crosslinked polymer typically forms a 'semi interpenetrating polymer network (IPN) [362]. Dental FRCs can be formulated using either resin type, i.e. linear (thermoplastic) and crosslinked (thermoset) polymers. The resin system type can determine the resultant FRC properties.

A systematic approach was followed to address knowledge gaps. Eight experiments were conducted *in-vitro* to assess certain FRC properties in order to address specific research hypotheses. The Thesis consists of two parts. In part 1 (chapters 4 and 5), current commercial FRCs were evaluated and compared with established conventional resin composites. Aspects of their composition, such as fibre length were explored. In part 2 (chapters 6 and 7), insights from part 1 were used to formulate a series of model FRCs and to evaluate their properties. This was an essentially novel development and provided further insights into the relationship between composition and FRC performance. The main variable was the composition of resin matrix and particularly the types and ratio of monomers. The initial experiments (Chapters 4 and 5) studied three commercially available composites containing both particle reinforcement and fibres and four composites containing only particle reinforcement. The latter were used as controls to determine the influence of fibre reinforcement on five key properties: hardness, fracture toughness, sorption, solubility and hygroscopic expansion.

In Chapters 6, and 7 the second set of experiments were described. Utilising various ratios of Bis-GMA-UDMA/Bis-EMA, experimental E-glass fibre-reinforced composites were formulated with different structures (resin matrix compositions) and evaluated.

Chapter 4 This reported the effect of two different solvents (water, 75% ethanol/water), on Vickers hardness of composites. Significant differences were observed depending upon the variables, namely materials, storage medium, and time ($p < 0.05$).

The surface hardness of all materials after 1 d of storage in distilled water increased relative to the baseline hardness. This is most probably due to additional monomer post-curing via cross-linking reactions in the resin phase. However, storage for 30 d in distilled water decreased surface hardness of the restorative materials. This will be due to water acting as a plasticizing molecule within the matrix, swelling the polymer network and reducing the forces between polymeric chains [74]. In 75% ethanol/water, a significant reduction was seen in VHN starting between 1 and 24 h and continuing over 30 d.

everX posterior (EVX) is a glass fibre reinforced resin-composite. VHN of EVX after 30 d reduced by 9% in water and by 29% in 70:30 ethanol/water. This softening was probably due to hydrolytic disruption between the matrix and the glass fibres. Glass fibre reinforced composites absorb more water than conventional composites, which may also be related to the hydrophilicity of the polymer network [189, 258, 259].

Restoration failure may occur owing to reduced load-bearing capacity via intra-oral degradation [165]. The effect of water storage on fracture toughness (K_{IC}) has been studied for a range of materials [86, 87]. Our results showed that K_{IC} varied significantly within the total set of materials ($p<0.05$). The composites can be categorized into one of three bands: conventional composites (NPU and XTE), with the K_{IC} range 1.23 and 1.37 M.Pa $m^{0.5}$; bulk fill composites (EVX, FBO and FBF), with the highest K_{IC} 2.14 M.Pa $m^{0.5}$ for EVX; and lastly, flowable composites (NPF and XTF), with K_{IC} 0.96 and 0.97 M.Pa $m^{0.5}$, respectively.

An improved resistance to crack propagation was seen in EVX, due to its fibre and matrix-related properties. EVX contains fibres longer than the critical fibre length [104-106]. EVX has a semi-interpenetrated network (SIPN) matrix type, with thermoplastic PMMA chains that compensate for the stiffness of Bis-GMA units. These specific features may improve the flexural properties of the composite material and enhance its fracture resistance. The fibre length distribution of NPU fibre-reinforced composite was between 8 and 103 μm, with two thirds of these fibres up to 50 μm and one third up to 100 μm. This contrast with the length of the EVX fibres (1,000 – 2,000 μm) may explain why EVX exhibited superior fracture toughness to NPU.

In Chapter 5, water sorption, solubility and hygroscopic expansion were measured for a set of composites. As expected, from the results of the previous chapter, EVX composite exhibited volumetric expansion and significantly increased sorption when compared to the rest of the tested materials. With the influence of fillers and fibres were removed through the calculation of the percentage of water absorbed by the polymer matrix alone for all composites, sorption was highest in EVX, confirming that its polymeric matrix is influenced strongly by water storage.

Research on fibre-reinforced PMMA acrylic denture-base resins indicated that the resin phase determined material behaviour during water storage more than the glass fibres [301]. EVX polymer matrix consists of PMMA and Bis-GMA/TEGDMA. The structure of Bis-GMA incorporates hydroxyl groups that raise its susceptibility to water diffusion and bonding. The sorption behaviour of Bis-GMA may also be affected by the co-monomer PMMA present in the organic matrix [292, 302].

NPU was found to have lower expansion, along with XTE, FBO, and FBF. If the material is hydrophobic, reduced hygroscopic expansion is known to take place [188, 292]. NPU does contain Bis-EMA, and this material is more hydrophobic than Bis-GMA [9]. Differences in polymerization might also be a factor, although we have no evidence that is actually the case.

To enhance understanding, a study was designed to determine how far changes in monomer compositions can alter the properties of FRCs. Specific aims were to establish how matrix composition influences FRC characteristics such as their degree of conversion, mechanical properties and resistance to water aging. The monomers were formulated with Bis-GMA always included. But TEGDMA and MMA monomers were replaced by varying ratios of Bis-EMA and UDMA.

The main measurable parameter for the network structure of dimethacrylate polymers is the degree of C=C conversion (DC). The monomer chemical structure mainly determines the DC [28], but other factors are involved, such as filler content [363], and curing time [364]. In Chapter 6 the degree of conversion (DC) of the experimental FRC resin-composite materials was measured, at two clinically relevant thicknesses (2 mm, 4 mm), using Fourier transform infrared spectroscopy. At both thickness,

Groups with the highest UDMA wt% (D and E) showed the lowest DC, which were significantly lower than other materials. The control group (A) and the experimental group with high Bis-EMA wt% (B), on the other hand, showed the highest DC. The polymerization conditions were maintained the same for all the materials, so that any changes in DC were due to the composition of the material.

Insufficient polymerization can adversely affect biological and physical/mechanical characteristics of composites [138, 156]. Experimental groups with high Bis-EMA wt% (B and C), had the greatest depth-of-cure (DoC) amongst materials (4.4 mm and 4.3 mm respectively); this could be as a result of the higher concentration of Bis-EMA, which was 37.5% and 29.5% respectively, whereas it was 19.5% in group E which had a DoC of 3.4 mm. The long aliphatic spacer length in Bis-EMA means that the monomers have more flexibility, and their mobility is therefore enhanced [336]. Moreover, in this study, the higher DoC that was observed in groups B and C may have been caused by the fact that there was a close match in the refractive indices of the polymer (1.527, 1.525 respectively) to the fibres and fillers (1.555 and 1.556 respectively). This similarity may have increased the transmission of light leading to higher DoC.

Chapter 7 assessed how monomer composition influenced FRC mechanical properties after being aged in water for 30 d. The filler content, type, and proportion, were maintained across all the groups to clearly distinguish the effects of matrix composition and ratios on material mechanical properties after water aging. In terms of degradation resistance, fracture toughness and flexural strength, the best performers were Groups B and C (groups with high Bis-EMA wt%).

In the environment of the oral cavity, degradation is a complex process. It involves the dissolution and disintegration of materials in saliva, along with physical or chemical degradation caused by actions such as chewing and bacterial activity. Laboratory studies can indicate what possibly happens in vivo, but they cannot totally reproduce all the complex processes that take place in the mouth. Water sorption (WS) of dimethacrylate polymer networks depends on their chemical structure. It can be beneficial in restorative materials to have some capacity to swell; hygroscopic expansion can partially and eventually compensate for polymerisation shrinkage.

Nevertheless, the hygroscopic *expansion* of resin materials must not exceed the polymerisation *shrinkage*. A water sorption of 40 μg/mm^3 has been determined as the maximum limit for dental composites [169]. In much the same way as the material's elastic behaviour, water sorption is dependent upon several factors including the crosslink density (both covalent and non-covalent) and the chemical structure of the monomer, which influence hydrophilicity and chain elasticity. Hence, if the chains between crosslinks are longer, the crosslink density is lower, and consequently the water sorption may be higher [365].

The results from same chapter have shown that Bis-GMA/TEGDMA-PMMA and Bis-GMA/Bis-EMA-UDMA materials have varying levels of water sorption and solubility, depending on the type and amount of monomer used. The sorption value of the control group was the highest at 37.8 μg/mm³ and that of experimental composite (group C) was the lowest at 22.6 μg/mm³. This suggests that water storage has a significant effect on the properties of these polymeric matrices.

Exploring different material designs and characterizing them can improve our understanding of their physicochemical and mechanical properties. In particular, material performance can be enhanced by establishing the relationships between structure and properties at different scales. This thesis continues efforts to characterize polymer-based composites, and its findings may contribute to the development of discontinuous FRCs.

Integrating and summarizing the five chapters, it can be concluded that:

1) A commercially available glass-fibre reinforced resin composite (everX posterior) showed superior performance *in terms of fracture toughness* when compared to nano hydroxyapatite fibre and non-fibre reinforced resin composites.
2) The greatest changes *in water sorption and volumetric expansion* were seen in the millimeter scale glass-fibre reinforced composite (EVX), whereas the greatest stability in an aqueous environment was seen in the nano-fibre hydroxyapatite reinforced composite (NPU).
3) There were some variations *in the water sorption/desorption cycles* of all the resin–matrix composites investigated. Nonetheless, they all complied with the requirements set out by ISO 4049 for water solubility and sorption, despite the extended sorption period**.**
4) Bis-GMA/Bis-EMA-UDMA based resin might have the potential as an alternative to Bis-GMA/TEGDMA-PMMA based resin in glass fibre reinforced composites, when further optimized. The Bis-GMA/Bis-EMA-UDMA based resin showed *a higher degree of conversion, depth of cure, superior performance in mechanical properties (i.e., flexural strength and toughness), and less sorption* than the Bis-GMA/PMMA-TEGDMA based resin.

8.2 Future work recommendation

Progress made in biomaterials research includes technological advances in dental materials. Dental material science has two main objectives: (i) to provide an insight into the behaviour of existing materials, and (ii) to gain from this insight, practical ways to develop new materials, or to enhance those already in use.

One of the goals of a restorative material is to mimic the properties of tooth structure (enamel and dentine) to provide a durable, functional and aesthetic alternative for that which has been lost.

With CAD/CAM dentistry, the concerns over polymerization shrinkage can be mitigated with pre-cured resin-composites. Through industrial manufacturing, control can be exerted over composite fabrication and polymerization, so that properties are consistent and voids or contamination do not exist as they can in direct applications [366]. Industrial processes can also enhance the mechanical properties of resin composites, for example by using high pressure and high temperature with CAD/CAM composite blocks [366]. Resin composite used in CAD/CAM restorations do not possess such good mechanical properties as ceramics/glass-ceramics but they have a potential for direct intraoral repair and are less expensive [367].

Machinable FRCs are currently attracting interest as with indirect manufacturing it is possible to manage the production, orientation, impregnation, and polymerization of the fibres. This should enable the mechanical properties of the material to be enhanced. Trinia (Shofu, Japan) is an innovative fibre-reinforced resin composite for CAD/CAM applications. It has been described as a multi-layer material comprised of a multidirectional interlacing of fibreglass and resin [74]. The only information available about Trinia is that provided by the manufacturer, claiming a flexural strength of 393 MPa, a fracture toughness of 9.7 $MPa \cdot m^{.5}$ and an elastic modulus of 18.8 GPa. This flexural strength means that Trinia may compete with glass-ceramics and have potential for the posterior regions of the oral cavity. However, further research on the effects of water storage, compatibility with veneering composites, and in the form of long-term clinical trials is required to independently determine its characteristics and whether or not it is suitable for posterior restorations. Although the

claims made by Shofu regarding Trinia properties still need to be substantiated, they indicate that the material may be suitable for utilization in CAD/CAM restorative and prosthetic dentistry. The characteristics of this new material may mean that it is able to bridge the gap between resin composites and CAD/CAM ceramics/glass-ceramics.

At this stage, CAD/CAM resin composites have the potential to be used for long-term provisional crowns. One of the reasons for this is that they are similar to direct and indirect light-cured resin composites, plus the availability of glass ceramics, which possess excellent mechanical properties. A biomimetic inspired bilayered CAD CAM block (PFC as enamel substitute, and FRC as dentine core) with isotropic properties may also represent a new niche of research.

There are a number of possible directions for future research on FRCs. Researchers could examine the viability of incorporating bioactive minerals into the fibre reinforced resin composites or substituting a fibre binding matrix from resin base by an inorganic type. There are numerous possible combinations of resin and fibres in FRCs, so the majority of studies have examined the effect of changing just one component, assuming there was no change in the interaction between the two. ORMOCERs could have a potential in replacing the organic matrix in FRC. ORMOCERs have now progressed to the point where the difference between the matrix and dispersed phase (filler) components is no longer so stark [343].

There is vast space for further research in terms of appropriate material, specific functionality of the composite such as remineralization properties, self-heling properties, antimicrobial properties. In the future, innovations will continue and may lead to a new generation of composites. These materials will need to be able to fulfil the requirements for ease of handling and durability.

References

1. Widström, E., K. Eaton, and J. Vanobbergen, *Oral healthcare systems in the Extended European Union, partim:[Oral Health care system in] Belgium.* Oral health & preventive dentistry, 2004. **2**(3): p. 155 (157)-(159) 194.

2. Quock, R.L., *Dental Caries: A Current Understanding and Implications.* Journal of Nature and Science, 2015. **1**(1): p. 27.

3. Keyes, P. and H. Jordan, *Factors influencing the initiation, transmission and inhibition of dental caries.* Mechanisms of hard tissue destruction. Sognnaes RF, editor. New York, NY: American Association for the Advancement of Science, 1963: p. 261-283.

4. Organization, W.H., *Oral Health. Fact sheet no 318. April 2012*. 2012.

5. Stephens, R.G., S.L. Kogon, and A.M. Jarvis, *A study of the reasons for tooth extraction in a Canadian population sample.* J Can Dent Assoc, 1991. **57**(6): p. 501-4.

6. Allukian, M., Jr., *The neglected epidemic and the surgeon general's report: a call to action for better oral health.* Am J Public Health, 2000. **90**(6): p. 843-5.

7. Hung, M., et al., *Health and dental care expenditures in the United States from 1996 to 2016.* PLoS One, 2020. **15**(6): p. e0234459.

8. Donly, K.J. and M. Ruiz, *In vitro demineralization inhibition of enamel caries utilizing an unfilled resin.* Clin Prev Dent, 1992. **14**(6): p. 22-4.

9. Marghalani, H., *Resin-based dental composite materials*, in *Handbook of bioceramics and biocomposites*. 2016, Springer. p. 357-405.

10. Marshall, S.J. and G.W. Marshall, Jr., *Dental amalgam: the materials.* Adv Dent Res, 1992. **6**: p. 94-9.

11. Chemicals, U., *Global mercury assessment.* UNEP Chemicals, Geneva, 2002: p. 1-270.

12. Fisher, J., et al., *The Minamata Convention and the phase down of dental amalgam.* Bull World Health Organ, 2018. **96**(6): p. 436-438.

13. Wilson, A.D. and B. Kent, *The glass-ionomer cement, a new translucent dental filling material.* Journal of Applied Chemistry and Biotechnology, 1971. **21**(11): p. 313-313.

14. Radovic, I., et al., *Self-adhesive resin cements: a literature review.* J Adhes Dent, 2008. **10**(4): p. 251-8.

15. Sidhu, S.K. and J.W. Nicholson, *A Review of Glass-Ionomer Cements for Clinical Dentistry.* J Funct Biomater, 2016. **7**(3): p. 16.

16. Gunjal S, N.L., Raju HG *Comparative evaluation of marginal integrity of glass ionomer and resin based fissure sealants using invasive and non-invasive techniques: an in vitro study.* Indian Journal of Dental Research, 2012, May p. 1;23(3):320.

17. Hammouda, I.M., *Reinforcement of conventional glass-ionomer restorative material with short glass fibers.* J Mech Behav Biomed Mater, 2009. **2**(1): p. 73-81.

18. Ferro, K.J., et al., *The glossary of prosthodontic terms.* J Prosthet Dent, 2017. **117**(5S): p. e1-e105.

19. Bowen, R.L., *Properties of a silica-reinforced polymer for dental restorations.* J Am Dent Assoc, 1963. **66**: p. 57-64.

20. Smith, D.C., *Recent Developments and Prospects in Dental Polymers.* Journal of Prosthetic Dentistry, 1962. **12**(6): p. 1066-&.

21. Leprince, J.G., et al., *Progress in dimethacrylate-based dental composite technology and curing efficiency.* Dent Mater, 2013. **29**(2): p. 139-56.

22. Sideridou, I.D., *Polymeric Materials in Dentistry*. 2010, New York, UNITED STATES: Nova Science Publishers, Incorporated.

23. Goncalves, F., Y. Kawano, and R.R. Braga, *Contraction stress related to composite inorganic content.* Dent Mater, 2010. **26**(7): p. 704-9.

24. Lovelh, L., S. Newman, and C. Bowman, *The effects of light intensity, temperature, and comonomer composition on the polymerization behavior of dimethacrylate dental resins.* J Dent Res, 1999. **78**(8): p. 1469-76.

25. Ogliari, F.A., et al., *Influence of chain extender length of aromatic dimethacrylates on polymer network development.* Dent Mater, 2008. **24**(2): p. 165-71.

26. Durner, J., et al., *Determination of homologous distributions of bisEMA dimethacrylates in bulk-fill resin-composites by GC-MS.* Dent Mater, 2015. **31**(4): p. 473-80.

27. Alshali, R.Z., et al., *Qualitative and quantitative characterization of monomers of uncured bulk-fill and conventional resin-composites using*

liquid chromatography/mass spectrometry. Dent Mater, 2015. **31**(6): p. 711-720.

28. Sideridou, I., V. Tserki, and G. Papanastasiou, *Effect of chemical structure on degree of conversion in light-cured dimethacrylate-based dental resins.* Biomaterials, 2002. **23**(8): p. 1819-29.

29. Sideridou, I., V. Tserki, and G. Papanastasiou, *Study of water sorption, solubility and modulus of elasticity of light-cured dimethacrylate-based dental resins.* Biomaterials, 2003. **24**(4): p. 655-65.

30. Ferracane, J.L., *Resin composite--state of the art.* Dent Mater, 2011. **27**(1): p. 29-38.

31. Monsarrat, P., et al., *Survival of directly placed ormocer-based restorative materials: A systematic review and meta-analysis of clinical trials.* Dent Mater, 2017. **33**(5): p. e212-e220.

32. Cavalcante, L.M., et al., *Surface integrity of solvent-challenged ormocer-matrix composite.* Dent Mater, 2011. **27**(2): p. 173-9.

33. Maghaireh, G.A., N.A. Taha, and H. Alzraikat, *The Silorane-based Resin Composites: A Review.* Oper Dent, 2017. **42**(1): p. E24-E34.

34. Weinmann, W., C. Thalacker, and R. Guggenberger, *Siloranes in dental composites.* Dent Mater, 2005. **21**(1): p. 68-74.

35. Bacchi, A., et al., *Shrinkage, stress, and modulus of dimethacrylate, ormocer, and silorane composites.* J Conserv Dent, 2015. **18**(5): p. 384-8.

36. Furuse, A.Y., et al., *Colour-stability and gloss-retention of silorane and dimethacrylate composites with accelerated aging.* J Dent, 2008. **36**(11): p. 945-52.

37. Darvell, B.W., *Materials science for dentistry*. 10 ed. 2009: Elsevier. 842.

38. Taira, M., et al., *Analysis of photo-initiators in visible-light-cured dental composite resins.* J Dent Res, 1988. **67**(1): p. 24-8.

39. Jakubiak, J., et al., *Camphorquinone–amines photoinitating systems for the initiation of free radical polymerization.* J Polymer, 2003. **44**(18): p. 5219-26.

40. Ferracane, J.L., *Current trends in dental composites.* Crit Rev Oral Biol Med, 1995. **6**(4): p. 302-18.

41. Musanje, L., J.L. Ferracane, and R.L. Sakaguchi, *Determination of the optimal photoinitiator concentration in dental composites based on essential material properties.* Dent Mater, 2009. **25**(8): p. 994-1000.

42. Schneider, L.F., et al., *Effect of co-initiator ratio on the polymer properties of experimental resin composites formulated with camphorquinone and phenyl-propanedione.* Dent Mater, 2009. **25**(3): p. 369-75.

43. Bakopoulou, A., T. Papadopoulos, and P. Garefis, *Molecular toxicology of substances released from resin-based dental restorative materials.* Int J Mol Sci, 2009. **10**(9): p. 3861-99.

44. Price, R.B., C.M. Felix, and J.M. Whalen, *Factors affecting the energy delivered to simulated class I and class v preparations.* J Can Dent Assoc, 2010. **76**(4): p. a94.

45. Anusavice, K.J., C. Shen, and H.R. Rawls, *Phillips' science of dental materials*. 12 ed. 2013: Elsevier Health Sciences.

46. Yu, B. and Y.K. Lee, *Influence of color parameters of resin composites on their translucency.* Dent Mater, 2008. **24**(9): p. 1236-42.

47. Lung, C.Y. and J.P. Matinlinna, *Aspects of silane coupling agents and surface conditioning in dentistry: an overview.* Dent Mater, 2012. **28**(5): p. 467-77.

48. Mohsen, N.M. and R.G. Craig, *Effect of silanation of fillers on their dispersability by monomer systems.* J Oral Rehabil, 1995. **22**(3): p. 183-9.

49. Karabela, M.M. and I.D. Sideridou, *Effect of the structure of silane coupling agent on sorption characteristics of solvents by dental resin-nanocomposites.* Dent Mater, 2008. **24**(12): p. 1631-9.

50. Matinlinna, J.P., C.Y.K. Lung, and J.K.H. Tsoi, *Silane adhesion mechanism in dental applications and surface treatments: A review.* Dent Mater, 2018. **34**(1): p. 13-28.

51. Sideridou, I., D.S. Achilias, and E. Kyrikou, *Thermal expansion characteristics of light-cured dental resins and resin composites.* Biomaterials, 2004. **25**(15): p. 3087-97.

52. Hashinger, D.T. and C.W. Fairhurst, *Thermal expansion and filler content of composite resins.* J Prosthet Dent, 1984. **52**(4): p. 506-10.

53. Versluis, A., W.H. Douglas, and R.L. Sakaguchi, *Thermal expansion coefficient of dental composites measured with strain gauges.* Dent Mater, 1996. **12**(5): p. 290-4.

54. Ilie, N., et al., *Fracture toughness of dental restorative materials.* Clin Oral Investig, 2012. **16**(2): p. 489-98.

55. Ilie, N. and R. Hickel, *Investigations on mechanical behaviour of dental composites.* Clin Oral Investig, 2009. **13**(4): p. 427-38.

56. Lien, W. and K.S. Vandewalle, *Physical properties of a new silorane-based restorative system.* Dent Mater, 2010. **26**(4): p. 337-44.

57. Sabbagh, J., et al., *Characterization of the inorganic fraction of resin composites.* J Oral Rehabil, 2004. **31**(11): p. 1090-101.

58. Lutz, F. and R.W. Phillips, *A classification and evaluation of composite resin systems.* J Prosthet Dent, 1983. **50**(4): p. 480-8.

59. Heuer, G.A., et al., *A clinical comparison of a quartz-and glass-filled composite with a glass-filled composite.* The Journal of the American Dental Association, 1982. **105**(2): p. 246-247.

60. Chung, C.M., et al., *Development of a new photocurable composite resin with reduced curing shrinkage.* Dent Mater, 2002. **18**(2): p. 174-8.

61. Sillas Duarte, J., Neimar Sartori, and Jin-Ho Phark, *Achieving the Ultimate Optical Properties of Composite Resin.* Quintessence of Dental Technology, 2013: p. 39-57.

62. Peumans, M., et al., *Clinical effectiveness of contemporary adhesives: a systematic review of current clinical trials.* Dent Mater, 2005. **21**(9): p. 864-81.

63. Mitra, S.B., D. Wu, and B.N. Holmes, *An application of nanotechnology in advanced dental materials.* J Am Dent Assoc, 2003. **134**(10): p. 1382-90.

64. Ferracane, J., R. Antonio, and H. Matsumoto, *Variables Affecting the Fracture Toughness of Dental Composites, and'.* Journal of Dental Research, 1987. **66**(6): p. 1140-1145.

65. Kim, K., et al., *Microf racture mechanisms of dental resin composites containing spherically-shaped filler particles.* Journal of Dental Research, 1994. **73**(2): p. 499-504.

66. Kim, K.H., J.L. Ong, and O. Okuno, *The effect of filler loading and morphology on the mechanical properties of contemporary composites.* J Prosthet Dent, 2002. **87**(6): p. 642-9.

67. Lloyd, C. and R. Iannetta, *The fracture toughness of dental composites.* Journal of oral rehabilitation, 1982. **9**(1): p. 55-66.

68. Kundie, F., et al., *Effects of filler size on the mechanical properties of polymer-filled dental composites: A review of recent developments.* Journal of Physical Science, 2018. **29**(1): p. 141-165.

69. Garoushi, S., P.K. Vallittu, and L.V. Lassila, *Short glass fiber reinforced restorative composite resin with semi-inter penetrating polymer network matrix.* Dent Mater, 2007. **23**(11): p. 1356-62.

70. Zhang, M. and J.P. Matinlinna, *E-Glass Fiber Reinforced Composites in Dental Applications.* Silicon, 2012. **4**(1): p. 73-78.

71. Garoushi, S., et al., *Load bearing capacity of fibre-reinforced and particulate filler composite resin combination.* J Dent, 2006. **34**(3): p. 179-84.

72. Corbin, S.B. and W.G. Kohn, *The benefits and risks of dental amalgam: current findings reviewed.* J Am Dent Assoc, 1994. **125**(4): p. 381-8.

73. Kusy, R.P. and K.F. Leinfelder, *Pattern of wear in posterior composite restorations.* J Dent Res, 1977. **56**(5): p. 544.

74. Drummond, J.L., *Degradation, fatigue, and failure of resin dental composite materials.* J Dent Res, 2008. **87**(8): p. 710-9.

75. Vallittu, P.K. and C. Sevelius, *Resin-bonded, glass fiber-reinforced composite fixed partial dentures: a clinical study.* J Prosthet Dent, 2000. **84**(4): p. 413-8.

76. Ibsen, R.L., *One-appointment technic using an adhesive composite.* Dent Surv, 1973. **49**(2): p. 30-2.

77. Alshabib, A., N. Silikas, and D.C. Watts, *Hardness and fracture toughness of resin-composite materials with and without fibers.* Dent Mater, 2019. **35**(8): p. 1194-1203.

78. Murphy, J., *The reinforced plastics handbook*. 2 ed. 1998: Elsevier.

79. Viguie, G., et al., *Epoxy/carbon composite resins in dentistry: mechanical properties related to fiber reinforcements.* J Prosthet Dent, 1994. **72**(3): p. 245-9.

80. Signore, A., et al., *Long-term survival of endodontically treated, maxillary anterior teeth restored with either tapered or parallel-sided glass-fiber posts and full-ceramic crown coverage.* J Dent, 2009. **37**(2): p. 115-21.

81. Freilich, M.A., et al., *Development and clinical applications of a light-polymerized fiber-reinforced composite.* J Prosthet Dent, 1998. **80**(3): p. 311-8.

82. Norström, A.E.E., H.M. Fagerholm, and J.B. Rosenholm, *Surface characterization of silane-treated industrial glass fibers.* Journal of Adhesion Science and Technology, 2001. **15**(6): p. 665-679.

83. Garoushi, S., et al., *Physical properties and depth of cure of a new short fiber reinforced composite.* Dent Mater, 2013. **29**(8): p. 835-41.

84. Li, X., et al., *The use of carbon nanotubes to induce osteogenic differentiation of human adipose-derived MSCs in vitro and ectopic bone formation in vivo.* Biomaterials, 2012. **33**(19): p. 4818-27.

85. Chen, L., et al., *BisGMA/TEGDMA dental composite containing high aspect-ratio hydroxyapatite nanofibers.* Dent Mater, 2011. **27**(11): p. 1187-95.

86. Lee, S.M., *Handbook of composite reinforcements*. 1992: John Wiley & Sons.

87. Vallittu, P.K., *High-aspect ratio fillers: fiber-reinforced composites and their anisotropic properties.* Dental Materials, 2015. **31**(1): p. 1-7.

88. Lee, S., *Handbook of composite materials.* New York, 1993.

89. Hull, D. and T. Clyne, *An introduction to composite materials*. 1996: Cambridge university press.

90. Callister, W.D. and D.G. Rethwisch, *Materials science and engineering*. 5 ed. 2011: John Wiley & Sons NY.

91. Fonseca, R., et al., *Influence of glass fiber wt% and silanization on mechanical flexural strength of reinforced acrylics.* Journal of materials science and chemical engineering, 2014. **2014**.

92. Shouha, P., M. Swain, and A. Ellakwa, *The effect of fiber aspect ratio and volume loading on the flexural properties of flowable dental composite.* Dent Mater, 2014. **30**(11): p. 1234-44.

93. Fonseca, R.B., et al., *Effect of short glass fiber/filler particle proportion on flexural and diametral tensile strength of a novel fiber-reinforced composite.* J Prosthodont Res, 2016. **60**(1): p. 47-53.

94. Walls, A., *Applied dental materials*. 2008: Blackwell Pub.

95. Vallittu, P. *Strength and interfacial adhesion of FRC-tooth system*. in *The second international symposium on fiber-reinforced plastics in dentistry*. 2001.

96. Kallio, T., T. Lastumäki, and P. Vallittu, *Bonding of restorative and veneering composite resin to somepolymeric composites.* Dental Materials, 2001. **17**(1): p. 80-86.

97. Khan, A.S., et al., *An update on glass fiber dental restorative composites: a systematic review.* Mater Sci Eng C Mater Biol Appl, 2015. **47**: p. 26-39.

98. van Dijken, J.W. and K. Sunnegardh-Gronberg, *Fiber-reinforced packable resin composites in Class II cavities.* J Dent, 2006. **34**(10): p. 763-9.

99. Al-Turki, L.I., et al., *Contact versus flexure fatigue of a fiber-filled composite.* Dent Mater, 2007. **23**(5): p. 648-53.

100. Drummond, J.L., et al., *Fatigue behaviour of dental composite materials.* J Dent, 2009. **37**(5): p. 321-30.

101. Manhart, J., et al., *Mechanical properties and wear behavior of light-cured packable composite resins.* Dent Mater, 2000. **16**(1): p. 33-40.

102. Garoushi, S., P.K. Vallittu, and L.V. Lassila, *Fracture resistance of short, randomly oriented, glass fiber-reinforced composite premolar crowns.* Acta Biomater, 2007. **3**(5): p. 779-84.

103. Lassila, L., et al., *Characterization of a new fiber-reinforced flowable composite.* Odontology, 2019. **107**(3): p. 342-352.

104. Abouelleil, H., et al., *Comparison of mechanical properties of a new fiber reinforced composite and bulk filling composites.* Restor Dent Endod, 2015. **40**(4): p. 262-70.

105. Garoushi, S., et al., *Short fiber reinforced composite: a new alternative for direct onlay restorations.* Open Dent J, 2013. **7**: p. 181-5.

106. Lassila, L., et al., *Mechanical properties of fiber reinforced restorative composite with two distinguished fiber length distribution.* J Mech Behav Biomed Mater, 2016. **60**: p. 331-338.

107. Creugers, N.H.J., et al., *A 5-year prospective clinical study on core restorations without covering crowns.* International Journal of Prosthodontics, 2005. **18**(1): p. 40-41.

108. Garoushi, S., P.K. Vallittu, and L. Lassila, *Mechanical Properties and Wear of Five Commercial Fibre-Reinforced Filling Materials.* Chin J Dent Res, 2017. **20**(3): p. 137-143.

109. Arcis, R.W., et al., *Mechanical properties of visible light-cured resins reinforced with hydroxyapatite for dental restoration.* Dent Mater, 2002. **18**(1): p. 49-57.

110. Willems, G., et al., *A classification of dental composites according to their morphological and mechanical characteristics.* Dent Mater, 1992. **8**(5): p. 310-9.

111. Li, H., et al., *Polymer composites and fabrications thereof*. 2011, Google Patents.

112. Zhang, F., et al., *Surface modification and microstructure of single-walled carbon nanotubes for dental resin-based composites.* J Biomed Mater Res B Appl Biomater, 2008. **86**(1): p. 90-7.

113. Magnan, B., et al., *Acrylic bone cement: current concept review.* Musculoskelet Surg, 2013. **97**(2): p. 93-100.

114. Li, X., et al., *Resin composites reinforced by nanoscaled fibers or tubes for dental regeneration.* Biomed Res Int, 2014. **2014**: p. 542958.

115. Khaled, S.M., et al., *Reinforcement of resin based cement with titania nanotubes.* Dent Mater, 2010. **26**(2): p. 169-78.

116. Dafar, M.O., et al., *Reinforcement of flowable dental composites with titanium dioxide nanotubes.* Dent Mater, 2016. **32**(6): p. 817-26.

117. Kim, S.-H. and D.C. Watts, *Effect of Glass-Fiber Reinforcement and Water Storage on Fracture Toughness (K IC) of Polymer-Based Provisional Crown and FPD Materials.* International Journal of Prosthodontics, 2004. **17**(3).

118. Wetherhold, R.C., *Energy of fracture for short brittle fiber-brittle matrix composites with planar fiber orientation.* Materials Science and Engineering: A, 1989. **112**: p. 31-37.

119. Heintze, S., et al., *Laboratory mechanical parameters of composite resins and their relation to fractures and wear in clinical trials—A systematic review.* Journal of Dental materials, 2017. **33**(3): p. e101-e114.

120. Ferracane, J.L., et al., *Academy of Dental Materials guidance-Resin composites: Part II-Technique sensitivity (handling, polymerization, dimensional changes).* Dent Mater, 2017. **33**(11): p. 1171-1191.

121. Ilie, N., et al., *Academy of Dental Materials guidance-Resin composites: Part I-Mechanical properties.* Dent Mater, 2017. **33**(8): p. 880-894.

122. Silikas, N. and D.C. Watts, *Rheology of urethane dimethacrylate and diluent formulations.* Dent Mater, 1999. **15**(4): p. 257-61.

123. Lee, J.H., C.M. Um, and I.B. Lee, *Rheological properties of resin composites according to variations in monomer and filler composition.* Dent Mater, 2006. **22**(6): p. 515-26.

124. Leinfelder, K. and A. Prasad, *A new condensable composite for the restoration of posterior teeth.* Dent Today, 1998. **17**(2): p. 112-6.

125. Sakaguchi, R.L. and J.M. Powers, *Craig's restorative dental materials*. 2012: Elsevier Health Sciences.

126. Opdam, N.J.M., et al., *Consistency of resin composites for posterior use.* Dental Materials, 1996. **12**(5-6): p. 350-354.

127. Opdam, N.J., et al., *Cavity wall adaptation and voids in adhesive Class I resin composite restorations.* Dent Mater, 1996. **12**(4): p. 230-5.

128. Bayne, S.C., et al., *A characterization of first-generation flowable composites.* J Am Dent Assoc, 1998. **129**(5): p. 567-77.

129. Shortall, A.C., W.M. Palin, and P. Burtscher, *Refractive index mismatch and monomer reactivity influence composite curing depth.* J Dent Res, 2008. **87**(1): p. 84-8.

130. G, V., *Refractive index, stress-optical coefficient, and optical configuration parameter of polymers*, in *Physical Properties of Polymers Handbook*. 2007, Springer. p. 823-853.

131. Darvell, B.W., *A glossary of terms for dental materials science*. 2006: BW Darvell Pokfulam.

132. Fugolin, A., A. Bacchi, and C. Pfeifer, *Curing Reaction and Kinetics*, in *Dental Composite Materials for Direct Restorations*, Miletic.V, Editor. 2018, Springer. p. 27-42.

133. Yoshida, K. and E.H. Greener, *Effect of photoinitiator on degree of conversion of unfilled light-cured resin.* J Dent, 1994. **22**(5): p. 296-9.

134. Viljanen, E.K., M. Skrifvars, and P.K. Vallittu, *Degree of conversion of a copolymer of an experimental monomer and methyl methacrylate for dental applications.* Journal of Applied Polymer Science, 2004. **93**(4): p. 1908-1912.

135. Moraes, L.G., et al., *Infrared spectroscopy: a tool for determination of the degree of conversion in dental composites.* J Appl Oral Sci, 2008. **16**(2): p. 145-9.

136. Ferracane, J.L., *Elution of leachable components from composites.* J Oral Rehabil, 1994. **21**(4): p. 441-52.

137. Shintani, H., *Hplc Analysis of Toxic Additives and Residual Monomer from Dental Plate.* Journal of Liquid Chromatography, 1995. **18**(3): p. 613-626.

138. Goldberg, M., *In vitro and in vivo studies on the toxicity of dental resin components: a review.* Clin Oral Investig, 2008. **12**(1): p. 1-8.

139. Ferracane, J.L. and E.H. Greener, *The effect of resin formulation on the degree of conversion and mechanical properties of dental restorative resins.* J Biomed Mater Res, 1986. **20**(1): p. 121-31.

140. Asmussen, E., *Restorative resins: hardness and strength vs. quantity of remaining double bonds.* Scand J Dent Res, 1982. **90**(6): p. 484-9.

141. Lovell, L.G., et al., *The effect of cure rate on the mechanical properties of dental resins.* Dent Mater, 2001. **17**(6): p. 504-11.

142. Chung, K.H. and E.H. Greener, *Correlation between degree of conversion, filler concentration and mechanical properties of posterior composite resins.* J Oral Rehabil, 1990. **17**(5): p. 487-94.

143. Leprince, J.G., et al., *Physico-mechanical characteristics of commercially available bulk-fill composites.* J Dent, 2014. **42**(8): p. 993-1000.

144. Braga, R.R. and J.L. Ferracane, *Contraction stress related to degree of conversion and reaction kinetics.* J Dent Res, 2002. **81**(2): p. 114-8.

145. Yoon, T.H., et al., *Degree of polymerization of resin composites by different light sources.* J Oral Rehabil, 2002. **29**(12): p. 1165-73.

146. Daronch, M., F.A. Rueggeberg, and M.F. De Goes, *Monomer conversion of pre-heated composite.* J Dent Res, 2005. **84**(7): p. 663-7.

147. Price, R.B., et al., *The effect of specimen temperature on the polymerization of a resin-composite.* Dent Mater, 2011. **27**(10): p. 983-9.

148. Schrader, B., *Infrared and Raman spectroscopy: methods and applications*. 2008: John Wiley & Sons.

149. Stansbury, J.W. and S.H. Dickens, *Determination of double bond conversion in dental resins by near infrared spectroscopy.* Dent Mater, 2001. **17**(1): p. 71-9.

150. Heatley, F., et al., *Determination of extent of reaction in dimethacrylate-based dental composites using solid-state 13C masnmr spectroscopy and comparison with FTIR. spectroscopy.* Polymer., 1995. **36**(9): p. 1859-1867.

151. Atai, M., et al., *Synthesis, characterization, shrinkage and curing kinetics of a new low-shrinkage urethane dimethacrylate monomer for dental applications.* Dent Mater, 2007. **23**(8): p. 1030-41.

152. Chambers, S., et al., *Factors affecting residual unsaturation and curing rates in photocured crosslinked compositions.* Polym. Commun., 1986. **27**(7): p. 209-211.

153. Guerra, R.M., I. Duran, and P. Ortiz, *FTIR monomer conversion analysis of UDMA-based dental resins.* J Oral Rehabil, 1996. **23**(9): p. 632-7.

154. Park, J., et al., *How should composite be layered to reduce shrinkage stress: incremental or bulk filling?* Dent Mater, 2008. **24**(11): p. 1501-5.

155. Leprince, J.G., et al., *New insight into the "depth of cure" of dimethacrylate-based dental composites.* Dent Mater, 2012. **28**(5): p. 512-520.

156. Tarle, Z., et al., *Influence of irradiation time on subsurface degree of conversion and microhardness of high-viscosity bulk-fill resin composites.* Clin Oral Investig, 2015. **19**(4): p. 831-40.

157. Alrahlah, A., N. Silikas, and D.C. Watts, *Post-cure depth of cure of bulk fill dental resin-composites.* Dent Mater, 2014. **30**(2): p. 149-54.

158. Ilie, N., S. Bucuta, and M. Draenert, *Bulk-fill resin-based composites: an in vitro assessment of their mechanical performance.* Oper Dent, 2013. **38**(6): p. 618-25.

159. Vivadent, I., *Tetric EvoCeram® Bulk fill: simplifies composite restoration placement, increases efficiency.* J Compendium of continuing education in dentistry

, 2014. **35**(6): p. 432-32.

160. Chesterman, J., et al., *Bulk-fill resin-based composite restorative materials: a review.* Br Dent J, 2017. **222**(5): p. 337-344.

161. Tsai, P.C., I.A. Meyers, and L.J. Walsh, *Depth of cure and surface microhardness of composite resin cured with blue LED curing lights.* Dent Mater, 2004. **20**(4): p. 364-9.

162. Schattenberg, A., et al., *Minimal exposure time of different LED-curing devices.* Dent Mater, 2008. **24**(8): p. 1043-9.

163. Yap, A.U., et al., *Influence of dietary simulating solvents on the hardness of provisional restorative materials.* Dent Mater, 2004. **20**(4): p. 370-6.

164. Venhoven, B.A., et al., *Influence of filler parameters on the mechanical coherence of dental restorative resin composites.* Biomaterials, 1996. **17**(7): p. 735-40.

165. Norman, D.A. and R.E. Robertson, *The effect of fiber orientation on the toughening of short fiber-reinforced polymers.* Journal of applied polymer science, 2003. **90**(10): p. 2740-2751.

166. Palin, W.M., et al., *The reliability in flexural strength testing of a novel dental composite.* J Dent, 2003. **31**(8): p. 549-57.

167. Bae, J.M., et al., *The flexural properties of fiber-reinforced composite with light-polymerized polymer matrix.* Int J Prosthodont, 2001. **14**(1): p. 33-9.

168. Vakiparta, M., A. Yli-Urpo, and P.K. Vallittu, *Flexural properties of glass fiber reinforced composite with multiphase biopolymer matrix.* J Mater Sci Mater Med, 2004. **15**(1): p. 7-11.

169. Standard, I., *4049, 2009, Dentistry--Polymer-based restorative materials.* International Organization for Standardization, Geneva, Switzerland, 2009.

170. Wang, L., et al., *Mechanical properties of dental restorative materials: relative contribution of laboratory tests.* J Appl Oral Sci, 2003. **11**(3): p. 162-7.

171. Brunthaler, A., et al., *Longevity of direct resin composite restorations in posterior teeth: a review.* Clin oral investig, 2003. **7**(2): p. 63-70.

172. Heintze, S.D. and V. Rousson, *Clinical effectiveness of direct class II restorations - a meta-analysis.* J Adhes Dent, 2012. **14**(5): p. 407-31.

173. Ornaghi, B.P., et al., *Fracture toughness and cyclic fatigue resistance of resin composites with different filler size distributions.* Dent Mater, 2014. **30**(7): p. 742-51.

174. Wang, T., J.K. Tsoi, and J.P. Matinlinna, *A novel zirconia fibre-reinforced resin composite for dental use.* J Mech Behav Biomed Mater, 2016. **53**: p. 151-160.

175. Bocalon, A.C., et al., *Replacement of glass particles by multidirectional short glass fibers in experimental composites: Effects on degree of conversion, mechanical properties and polymerization shrinkage.* Dent Mater, 2016. **32**(9): p. e204-10.

176. Lassila, L., et al., *Mechanical properties and fracture behavior of flowable fiber reinforced composite restorations.* Dent Mater, 2018. **34**(4): p. 598-606.

177. Griffith, A.A., *Philosophical transactions of the royal society of london.* Series A, containing papers of a mathematical or physical character, 1921. **221**: p. 163-198.

178. Miettinen, V.M., K.K. Narva, and P.K. Vallittu, *Water sorption, solubility and effect of post-curing of glass fibre reinforced polymers.* Biomaterials, 1999. **20**(13): p. 1187-94.

179. Van Noort, R. and M.E. Barbour, *Introduction to Dental Materials4: Introduction to Dental Materials*. 2013: Elsevier Health Sciences.

180. Archegas, L.R.P., et al., *Identification and quantification of monomers released from dental composites using HPLC.* Brazilian Archives of Biology and Technology, 2009. **52**(4): p. 855-862.

181. Braden, M., E.E. Causton, and R.L. Clarke, *Diffusion of water in composite filling materials.* J Dent Res, 1976. **55**(5): p. 730-2.

182. Wei, Y.J., et al., *Diffusion and concurrent solubility of self-adhering and new resin-matrix composites during water sorption/desorption cycles.* Dent Mater, 2011. **27**(2): p. 197-205.

183. Venz, S. and B. Dickens, *NIR-spectroscopic investigation of water sorption characteristics of dental resins and composites.* J Biomed Mater Res, 1991. **25**(10): p. 1231-48.

184. Inoue, K. and I. Hayashi, *Residual monomer (Bis-GMA) of composite resins.* J Oral Rehabil, 1982. **9**(6): p. 493-7.

185. Wei, Y.J., et al., *Hygroscopic dimensional changes of self-adhering and new resin-matrix composites during water sorption/desorption cycles.* Dent Mater, 2011. **27**(3): p. 259-66.

186. Alrahlah, A., *Physical, Mechanical and Surface Properties of Dental Resin-composites*. 2013, The University of Manchester (United Kingdom).

187. Organisation., I.S., in *Technical Committee 106 - Dentistry, Sub-committee 1 - Filling and Restorative Materials,*

, I.F. 4049, Editor. 1999.

188. Alrahlah, A., N. Silikas, and D.C. Watts, *Hygroscopic expansion kinetics of dental resin-composites.* Dent Mater, 2014. **30**(2): p. 143-8.

189. Al Sunbul, H., N. Silikas, and D.C. Watts, *Surface and bulk properties of dental resin-composites after solvent storage.* Dent Mater, 2016. **32**(8): p. 987-997.

190. Heintze, S.D. and B. Zimmerli, *Relevance of in vitro tests of adhesive and composite dental materials, a review in 3 parts. Part 1: Approval requirements and standardized testing of composite materials according to ISO specifications.* Schweizer Monatsschrift fur Zahnmedizin= Revue

mensuelle suisse d'odonto-stomatologie= Rivista mensile svizzera di odontologia e stomatologia, 2010. **121**(9): p. 804-816.

191. Versluis, A., et al., *Can hygroscopic expansion compensate polymerization shrinkage? Part I. Deformation of restored teeth.* Dent Mater, 2011. **27**(2): p. 126-133.

192. Segura, A. and K.J. Donly, *In vitro posterior composite polymerization recovery following hygroscopic expansion.* J Oral Rehabil, 1993. **20**(5): p. 495-9.

193. Ruttermann, S., et al., *Polymerization shrinkage and hygroscopic expansion of contemporary posterior resin-based filling materials--a comparative study.* J Dent, 2007. **35**(10): p. 806-13.

194. Donovan, T.E., *Longevity of the tooth/restoration complex: a review.* J Calif Dent Assoc, 2006. **34**(2): p. 122-8.

195. Sarrett, D.C., *Clinical challenges and the relevance of materials testing for posterior composite restorations.* Dent Mater, 2005. **21**(1): p. 9-20.

196. Demarco, F., et al., *Longevity of posterior composite restorations: not only a matter of materials.* Dent Mater, 2012. **28**(1): p. 87-101.

197. Beck, F., et al., *Survival of direct resin restorations in posterior teeth within a 19-year period (1996–2015): a meta-analysis of prospective studies.* Dent Mater, 2015. **31**(8): p. 958-985.

198. Opdam, N.J., et al., *Longevity of posterior composite restorations: a systematic review and meta-analysis.* J Dent Res, 2014. **93**(10): p. 943-9.

199. Hickel, R. and J. Manhart, *Longevity of restorations in posterior teeth and reasons for failure.* J Adhes Dent, 2001. **3**(1): p. 45-64.

200. Shisei, K., A. Kawasaki, and Y. Hayashi, *Factors associated with the longevity of resin composite restorations.* Dental material, 2011. **30**(3): p. 374-383.

201. Ferracane, J.L., *Buonocore Lecture. Placing dental composites--a stressful experience.* Oper Dent, 2008. **33**(3): p. 247-57.

202. Martos, J., et al., *Hydrolytic degradation of composite resins: effects on the microhardness.* J Mater Res, 2003. **6**(4): p. 599-604.

203. Santerre, J.P., L. Shajii, and B.W. Leung, *Relation of dental composite formulations to their degradation and the release of hydrolyzed polymeric-resin-derived products.* Crit Rev Oral Biol Med, 2001. **12**(2): p. 136-51.

204. Ferracane, J.L. and J.R. Condon, *Rate of elution of leachable components from composite.* Dent Mater, 1990. **6**(4): p. 282-7.

205. Rasines Alcaraz, M.G., et al., *Direct composite resin fillings versus amalgam fillings for permanent or adult posterior teeth.* Cochrane Database Syst Rev, 2014(3): p. CD005620.

206. Alvanforoush, N., et al., *Comparison between published clinical success of direct resin composite restorations in vital posterior teeth in 1995–2005 and 2006–2016 periods.* Australian dental journal, 2017. **62**(2): p. 132-145.

207. Hughes, K.O., et al., *Delayed Photoactivation of Dual-cure Composites: Effect on Cuspal Flexure, Depth-of-cure, and Mechanical Properties.* Oper Dent, 2019. **44**(2): p. E97-E104.

208. Pfeifer, C.S., et al., *Bis-GMA co-polymerizations: influence on conversion, flexural properties, fracture toughness and susceptibility to ethanol degradation of experimental composites.* Dent Mater, 2009. **25**(9): p. 1136-41.

209. Bernardo, M., et al., *Survival and reasons for failure of amalgam versus composite posterior restorations placed in a randomized clinical trial.* J Am Dent Assoc, 2007. **138**(6): p. 775-83.

210. Opdam, N.J., et al., *12-year survival of composite vs. amalgam restorations.* J Dent Res, 2010. **89**(10): p. 1063-7.

211. Khangura, S., et al., *Composite resin versus amalgam for dental restorations: a health technology assessment.* 2018.

212. Lohbauer, U., R. Belli, and J.L. Ferracane, *Factors involved in mechanical fatigue degradation of dental resin composites.* J Dent Res, 2013. **92**(7): p. 584-91.

213. Da Rosa Rodolpho, P.A., et al., *22-Year clinical evaluation of the performance of two posterior composites with different filler characteristics.* Dent Mater, 2011. **27**(10): p. 955-63.

214. Pallesen, U. and V. Qvist, *Composite resin fillings and inlays. An 11-year evaluation.* Clin Oral Investig, 2003. **7**(2): p. 71-9.

215. Dagerhamn J, v.D.J., Naimi-Akbar A, Sandborgh-Englund G, Tranæus S, Nilsson M, *Longevity of posterior resin composite restorations in adults–A systematic review.* Journal of dentistry, 2015 **31;43(8)**: p. 934-54.

216. Choices, N., *Dentistry: what's available on the NHS in England-NHS Choices*. 2017.

217. Burke, F.J., et al., *Influence of the method of funding on the age of failed restorations in general dental practice in the UK.* Br Dent J, 2002. **192**(12): p. 699-702.

218. Ferracane, J.L., *Resin-based composite performance: are there some things we can't predict?* Dent Mater, 2013. **29**(1): p. 51-58.

219. Maman, P., et al., *Nano Era of Dentistry-An Update.* Curr Drug Deliv, 2018. **15**(2): p. 186-204.

220. Garoushi, S., et al., *Short fiber-reinforced composite restorations: A review of the current literature.* J Investig Clin Dent, 2018. **9**(3): p. e12330.

221. Astm, E., *399-90:" Standard test method for plane-strain fracture toughness of metallic materials.* Annual book of ASTM standards, 1997. **3**(01): p. 506-536.

222. *My Scope training for advanced research Scanning Electron Microscopy* Available from: https://myscope.training/index.html.

223. ISO, E., *1172.* Textile-glass-reinforced plastics-Prepregs, moulding compounds and laminates-Determination of the textile-glass and mineral-filler content-Calcination methods (ISO 1172: 1996), 1996.

224. Plueddemann, E.P., *Adhesion through silane coupling agents*, in *Fundamentals of adhesion*. 1991, Springer. p. 279-290.

225. Pohl, E. and F. Osterholtz, *Kinetics and mechanism of aqueous hydrolysis and condensation of alkyltrialkoxysilanes*, in *Molecular Characterization of Composite Interfaces*. 1985, Springer. p. 157-170.

226. Chen, T.M. and G.M. Brauer, *Solvent effects on bonding organo-silane to silica surfaces.* J Dent Res, 1982. **61**(12): p. 1439-43.

227. Chen, M.H., *Update on dental nanocomposites.* J Dent Res, 2010. **89**(6): p. 549-60.

228. Antonucci, J.M., et al., *Chemistry of Silanes: Interfaces in Dental Polymers and Composites.* J Res Natl Inst Stand Technol, 2005. **110**(5): p. 541-58.

229. Liu, Q., et al., *Filler-coupling agent-matrix interactions in silica/polymethylmethacrylate composites.* J Biomed Mater Res, 2001. **57**(3): p. 384-93.

230. Zanchi, C.H., et al., *Effect of the silane concentration on the selected properties of an experimental microfilled composite resin.* Applied Adhesion Science, 2015. **3**(1): p. 27.

231. Garoushi, S.K., L.V. Lassila, and P.K. Vallittu, *Short fiber reinforced composite: the effect of fiber length and volume fraction.* J Contemp Dent Pract, 2006. **7**(5): p. 10-7.

232. Fonseca, R.B., et al., *Effect of glass fiber incorporation on flexural properties of experimental composites.* Biomed Res Int, 2014. **2014**: p. 542678.

233. Garoushi, S., P.K. Vallittu, and L.V. Lassila, *Depth of cure and surface microhardness of experimental short fiber-reinforced composite.* Acta Odontol Scand, 2008. **66**(1): p. 38-42.

234. Ilie, N., et al., *Resin-based composite light-cured properties assessed by laboratory standards and simulated clinical conditions.* Oper Dent, 2013. **38**(2): p. 159-67.

235. Kumar, N., *Inconsistency in the strength testing of dental resin-based composites among researchers.* Pak J Med Sci, 2013. **29**(1): p. 205-10.

236. Watts, D.C., O.M. el Mowafy, and A.A. Grant, *Fracture resistance of lower molars with Class 1 composite and amalgam restorations.* Dent Mater, 1987. **3**(5): p. 261-4.

237. Larsen, I.B., M. Freund, and E.C. Munksgaard, *Change in surface hardness of BisGMA/TEGDMA polymer due to enzymatic action.* J Dent Res, 1992. **71**(11): p. 1851-3.

238. Elliott, J.E., L.G. Lovell, and C.N. Bowman, *Primary cyclization in the polymerization of bis-GMA and TEGDMA: a modeling approach to understanding the cure of dental resins.* Dent Mater, 2001. **17**(3): p. 221-9.

239. Martin, N., N.M. Jedynakiewicz, and A.C. Fisher, *Hygroscopic expansion and solubility of composite restoratives.* Dent Mater, 2003. **19**(2): p. 77-86.

240. Feilzer, A.J., A.J. de Gee, and C.L. Davidson, *Relaxation of polymerization contraction shear stress by hygroscopic expansion.* J Dent Res, 1990. **69**(1): p. 36-9.

241. Lee, S.Y., et al., *Leached components from dental composites in oral simulating fluids and the resultant composite strengths.* J Oral Rehabil, 1998. **25**(8): p. 575-88.

242. Shin, M.A. and J.L. Drummond, *Evaluation of chemical and mechanical properties of dental composites.* J Biomed Mater Res, 1999. **48**(4): p. 540-5.

243. Sideridou, I.D., et al., *Sorption and desorption parameters of water or ethanol in light-cured dental dimethacrylate resins.* Journal of Applied Polymer Science, 2008. **107**(1): p. 463-475.

244. Calais, J.G. and K.J. Soderholm, *Influence of filler type and water exposure on flexural strength of experimental composite resins.* J Dent Res, 1988. **67**(5): p. 836-40.

245. McKinney, J.E. and W. Wu, *Chemical softening and wear of dental composites.* J Dent Res, 1985. **64**(11): p. 1326-31.

246. Ferracane, J.L., H.X. Berge, and J.R. Condon, *In vitro aging of dental composites in water--effect of degree of conversion, filler volume, and filler/matrix coupling.* J Biomed Mater Res, 1998. **42**(3): p. 465-72.

247. Lin, C.T., et al., *Influence of silanization and filler fraction on aged dental composites.* J Oral Rehabil, 2000. **27**(11): p. 919-26.

248. Schneider, C.A., W.S. Rasband, and K.W. Eliceiri, *NIH Image to ImageJ: 25 years of image analysis.* Nat Methods, 2012. **9**(7): p. 671-5.

249. McCabe, J. and R. Wassell, *Hardness of model dental composites–the effect of filler volume fraction and silanation.* Journal of Materials Science: Materials in Medicine, 1999. **10**(5): p. 291-294.

250. Price, R.B., et al., *Effect of light source and specimen thickness on the surface hardness of resin composite.* Am J Dent, 2002. **15**(1): p. 47-53.

251. Sideridou, I.D. and M.M. Karabela, *Sorption of water, ethanol or ethanol/water solutions by light-cured dental dimethacrylate resins.* Dent Mater, 2011. **27**(10): p. 1003-10.

252. de Moraes, R.R., et al., *Effects of 6 months of aging in water on hardness and surface roughness of two microhybrid dental composites.* J Prosthodont, 2008. **17**(4): p. 323-6.

253. Finer, Y. and J.P. Santerre, *Salivary esterase activity and its association with the biodegradation of dental composites.* J Dent Res, 2004. **83**(1): p. 22-6.

254. Finer, Y. and J.P. Santerre, *Influence of silanated filler content on the biodegradation of bisGMA/TEGDMA dental composite resins.* J Biomed Mater Res A, 2007. **81**(1): p. 75-84.

255. Aguiar, F.H., et al., *Hardness and diametral tensile strength of a hybrid composite resin polymerized with different modes and immersed in ethanol or distilled water media.* Dent Mater, 2005. **21**(12): p. 1098-103.

256. Ferracane, J.L. and V.A. Marker, *Solvent degradation and reduced fracture toughness in aged composites.* J Dent Res, 1992. **71**(1): p. 13-9.

257. Pilliar, R.M., R. Vowles, and D.F. Williams, *The effect of environmental aging on the fracture toughness of dental composites.* J Dent Res, 1987. **66**(3): p. 722-6.

258. Vallittu, P.K., *Effect of 180-week water storage on the flexural properties of E-glass and silica fiber acrylic resin composite.* Int J Prosthodont, 2000. **13**(4): p. 334-9.

259. Abdel-Magid, B., et al., *The combined effects of load, moisture and temperature on the properties of E-glass/epoxy composites.* Composite Structures, 2005. **71**(3-4): p. 320-326.

260. Rueggeberg, F.A., J.W. Ergle, and D.J. Mettenburg, *Polymerization Depths of Contemporary Light-Curing Units Using Microhardness.* Journal of Esthetic and Restorative Dentistry, 2000. **12**(6): p. 340-349.

261. Wang, R., E. Habib, and X.X. Zhu, *Evaluation of the filler packing structures in dental resin composites: From theory to practice.* Dent Mater, 2018. **34**(7): p. 1014-1023.

262. De Souza, G.M., *Nanoparticles in Restorative Materials*, in *Nanotechnology in Endodontics*. 2015, Springer,cham p. 139-171.

263. Moraes, R.R., et al., *Preparation and evaluation of dental resin luting agents with increasing content of bisphenol-A ethoxylated dimethacrylate.* J Biomater Appl, 2010. **24**(5): p. 453-73.

264. Van Nieuwenhuysen, J.P., et al., *Long-term evaluation of extensive restorations in permanent teeth.* J Dent, 2003. **31**(6): p. 395-405.

265. van Dijken, J.W., *Direct resin composite inlays/onlays: an 11 year follow-up.* J Dent, 2000. **28**(5): p. 299-306.

266. Schneider, S.J., *Engineered Materials Handbook, Volume 4: Ceramics and Glasses*. 1991: ASM International.

267. Belli, R., et al., *Practical and theoretical considerations on the fracture toughness testing of dental restorative materials.* Dent Mater, 2018. **34**(1): p. 97-119.

268. Curtis, A.R., et al., *Water uptake and strength characteristics of a nanofilled resin-based composite.* J Dent, 2008. **36**(3): p. 186-93.

269. Vallittu, P.K., I.E. Ruyter, and K. Ekstrand, *Effect of water storage on the flexural properties of E-glass and silica fiber acrylic resin composite.* Int J Prosthodont, 1998. **11**(4): p. 340-50.

270. Ferracane, J., H. Berge, and J. Condon, *In vitro aging of dental composites in water—effect of degree of conversion, filler volume, and filler/matrix coupling.* Journal of biomedical materials research, 1998. **42**(3): p. 465-472.

271. Watanabe, H., et al., *Fracture toughness comparison of six resin composites.* Dent Mater, 2008. **24**(3): p. 418-25.

272. Zhao, D., J. Botsis, and J.L. Drummond, *Fracture studies of selected dental restorative composites.* Dent Mater, 1997. **13**(3): p. 198-207.

273. Kim, K.H. and O. Okuno, *Microfracture behaviour of composite resins containing irregular-shaped fillers.* J Oral Rehabil, 2002. **29**(12): p. 1153-9.

274. Kim, K.-H., et al., *Fracture toughness and acoustic emission behavior of dental composite resins.* Engineering Fracture Mechanics, 1991. **40**(4-5): p. 811-819.

275. Johnson, W.W., V.B. Dhuru, and W.A. Brantley, *Composite microfiller content and its effect on fracture toughness and diametral tensile strength.* Dent Mater, 1993. **9**(2): p. 95-8.

276. Yancey, E.M., et al., *Properties of a New Nanofiber Restorative Composite.* Oper Dent, 2019. **44**(1): p. 34-41.

277. Vidotti, H.A., et al., *Flexural properties of experimental nanofiber reinforced composite are affected by resin composition and nanofiber/resin ratio.* Dent Mater, 2015. **31**(9): p. 1132-41.

278. Kovarik, R.E. and J.W. Ergle, *Fracture toughness of posterior composite resins fabricated by incremental layering.* J Prosthet Dent, 1993. **69**(6): p. 557-60.

279. Chan, K.S., et al., *Improving fracture toughness of dental nanocomposites by interface engineering and micromechanics.* Eng Fract Mech, 2007. **74**(12): p. 1857-1871.

280. Alshali, R.Z., et al., *Long-term sorption and solubility of bulk-fill and conventional resin-composites in water and artificial saliva.* J Dent, 2015. **43**(12): p. 1511-8.

281. Jianping, F., et al., *3D finite element analysis of the damage effects on the dental composite subject to water sorption.* Acta Mechanica Solida Sinica, 2006. **19**(3): p. 212-222.

282. Drummond, J.L., et al., *Leaching and mechanical properties characterization of dental composites.* J Biomed Mater Res B Appl Biomater, 2004. **71**(1): p. 172-80.

283. Al Sunbul, H., N. Silikas, and D.C. Watts, *Polymerization shrinkage kinetics and shrinkage-stress in dental resin-composites.* Dent Mater, 2016. **32**(8): p. 998-1006.

284. Naoum, S.J., et al., *Polymerization profile analysis of resin composite dental restorative materials in real time.* J Dent, 2012. **40**(1): p. 64-70.

285. Bateman, G., D.N. Ricketts, and W.P. Saunders, *Fibre-based post systems: a review.* Br Dent J, 2003. **195**(1): p. 43-8; discussion 37.

286. Sideridou, I.D., M.M. Karabela, and E. Vouvoudi, *Physical properties of current dental nanohybrid and nanofill light-cured resin composites.* Dent Mater, 2011. **27**(6): p. 598-607.

287. Martin, N. and N. Jedynakiewicz, *Measurement of water sorption in dental composites.* Biomaterials, 1998. **19**(1-3): p. 77-83.

288. Marghalani, H.Y. and D.C. Watts, *Viscoelastic stability of resin-composites aged in food-simulating solvents.* Dent Mater, 2013. **29**(9): p. 963-70.

289. Mortier, E., et al., *Importance of water sorption and solubility studies for couple bonding agent—resin-based filling material.* Oper Dent, 2004. **29**(6): p. 669-76.

290. Braden, M. and K.W.M. Davy, *Water absorption characteristics of some unfilled resins.* Biomaterials, 1986. **7**(6): p. 474-475.

291. Vallittu, P.K., *The effect of void space and polymerization time on transverse strength of acrylic-glass fibre composite.* J Oral Rehabil, 1995. **22**(4): p. 257-61.

292. Al Sunbul, H., N. Silikas, and D.C. Watts, *Resin-based composites show similar kinetic profiles for dimensional change and recovery with solvent storage.* Dent Mater, 2015. **31**(10): p. e201-e217.

293. Sideridou, I.D., D.S. Achilias, and M.M. Karabela, *Sorption kinetics of ethanol/water solution by dimethacrylate-based dental resins and resin composites.* J Biomed Mater Res B Appl Biomater, 2007. **81**(1): p. 207-18.

294. Leo, A., C. Hansch, and D. Elkins, *Partition coefficients and their uses.* Chemical Reviews, 1971. **71**(6): p. 525-616.

295. Dickens, S.H., G.M. Flaim, and C.J. Floyd, *Effects of adhesive, base and diluent monomers on water sorption and conversion of experimental resins.* Dent Mater, 2010. **26**(7): p. 675-81.

296. Bucuta, S. and N. Ilie, *Light transmittance and micro-mechanical properties of bulk fill vs. conventional resin based composites.* Clin Oral Investig, 2014. **18**(8): p. 1991-2000.

297. Ortengren, U., et al., *Water sorption and solubility of dental composites and identification of monomers released in an aqueous environment.* J Oral Rehabil, 2001. **28**(12): p. 1106-15.

298. Sideridou, I.D., M.M. Karabela, and E. Vouvoudi, *Volumetric dimensional changes of dental light-cured dimethacrylate resins after sorption of water or ethanol.* Dent Mater, 2008. **24**(8): p. 1131-6.

299. Ferracane, J.L., *Hygroscopic and hydrolytic effects in dental polymer networks.* Dent Mater, 2006. **22**(3): p. 211-22.

300. Hirasawa, T., et al., *Materials Science: Initial Dimensional Change of Composites in Dry and Wet Conditions.* J Dent Res, 1983. **62**(1): p. 28-31.

301. Miettinen, V.M., P.K. Vallittu, and D.T. Docent, *Water sorption and solubility of glass fiber-reinforced denture polymethyl methacrylate resin.* J Prosthet Dent, 1997. **77**(5): p. 531-4.

302. Peutzfeldt, A., *Resin composites in dentistry: the monomer systems.* Eur J Oral Sci, 1997. **105**(2): p. 97-116.

303. Keulemans, F., S. Garoushi, and L. Lassila, *Fillings and core build-ups*, in *A Clinical Guide to Fibre Reinforced Composites (FRCs) in Dentistry*, V.P.a.Ö. M, Editor. 2017, Elsevier. p. 131-163.

304. Demarco, F.F., et al., *Anterior composite restorations: A systematic review on long-term survival and reasons for failure.* Dent Mater, 2015. **31**(10): p. 1214-24.

305. Watts, D.C., *The quest for stable biomimetic repair of teeth: Technology of resin-bonded composites.* Dent Mater J, 2020. **39**(1): p. 46-51.

306. Ferracane, J.L. and T.J. Hilton, *Polymerization stress--is it clinically meaningful?* Dent Mater, 2016. **32**(1): p. 1-10.

307. Maas, M., et al., *Trends in restorative composites research: what is in the future?* Brazilian oral research, 2017. **31**.

308. Bijelic-Donova, J., et al., *Mechanical and structural characterization of discontinuous fiber-reinforced dental resin composite.* J Dent, 2016. **52**: p. 70-8.

309. Dyer, S.R., et al., *Effect of fiber position and orientation on fracture load of fiber-reinforced composite.* Dent Mater, 2004. **20**(10): p. 947-55.

310. Garoushi, S., P.K. Vallittu, and L.V. Lassila, *Use of short fiber-reinforced composite with semi-interpenetrating polymer network matrix in fixed partial dentures.* J Dent, 2007. **35**(5): p. 403-8.

311. Mittal, K.L., *Adhesion aspects in dentistry*. 2009: Koninklijke Brill NV, Leiden

312. Moszner, N., et al., *A partially aromatic urethane dimethacrylate as a new substitute for Bis-GMA in restorative composites.* Dent Mater, 2008. **24**(5): p. 694-9.

313. Schweikl, H., G. Spagnuolo, and G. Schmalz, *Genetic and cellular toxicology of dental resin monomers.* J Dent Res, 2006. **85**(10): p. 870-7.

314. Ferracane, J.L., et al., *Wear and marginal breakdown of composites with various degrees of cure.* J Dent Res, 1997. **76**(8): p. 1508-16.

315. Li, J., et al., *Multiple correlations of material parameters of light-cured dental composites.* Dent Mater, 2009. **25**(7): p. 829-36.

316. Lindberg, A., A. Peutzfeldt, and J.W. van Dijken, *Effect of power density of curing unit, exposure duration, and light guide distance on composite depth of cure.* Clin Oral Investig, 2005. **9**(2): p. 71-6.

317. ISO489:1999., *Plastics- Determination of refractive index*. 1999.

318. Stanley, G., *Refractometers: Basic Principles*. 1 ed. Vol. 1. 1989: Bellingham and Stanley Ltd.

319. Dewaele, M., et al., *Volume contraction in photocured dental resins: the shrinkage-conversion relationship revisited.* Dent Mater, 2006. **22**(4): p. 359-65.

320. Yu, P., A. Yap, and X.Y. Wang, *Degree of Conversion and Polymerization Shrinkage of Bulk-Fill Resin-Based Composites.* Oper Dent, 2017. **42**(1): p. 82-89.

321. Goncalves, F., et al., *Influence of BisGMA, TEGDMA, and BisEMA contents on viscosity, conversion, and flexural strength of experimental resins and composites.* Eur J Oral Sci, 2009. **117**(4): p. 442-6.

322. Pongprueksa, P., et al., *Monomer elution in relation to degree of conversion for different types of composite.* J Dent, 2015. **43**(12): p. 1448-55.

323. Durner, J., et al., *Correlation of the degree of conversion with the amount of elutable substances in nano-hybrid dental composites.* Dent Mater, 2012. **28**(11): p. 1146-53.

324. Frauscher, K.E. and N. Ilie, *Degree of conversion of nano-hybrid resin-based composites with novel and conventional matrix formulation.* Clin Oral Investig, 2013. **17**(2): p. 635-42.

325. Alshali, R.Z., N. Silikas, and J.D. Satterthwaite, *Degree of conversion of bulk-fill compared to conventional resin-composites at two time intervals.* Dent Mater, 2013. **29**(9): p. e213-7.

326. Garoushi, S., et al., *Influence of increment thickness on light transmission, degree of conversion and micro hardness of bulk fill composites.* Odontology, 2016. **104**(3): p. 291-7.

327. Lovell, L.G., et al., *Effects of Composition and Reactivity on the Reaction Kinetics of Dimethacrylate/Dimethacrylate Copolymerizations.* Macromolecules, 1999. **32**(12): p. 3913-3921.

328. Kalachandra, S., et al., *Influence of hydrogen bonding on properties of BIS-GMA analogues.* J Mater Sci Mater Med, 1997. **8**(5): p. 283-6.

329. Davy, K.W.M., et al., *Relationship between composite matrix molecular structure and properties.* Biomaterials, 1998. **19**(22): p. 2007-2014.

330. Sakaguchi, R.L., W.H. Douglas, and M.C. Peters, *Curing light performance and polymerization of composite restorative materials.* J Dent, 1992. **20**(3): p. 183-8.

331. Pilo, R., D. Oelgiesser, and H.S. Cardash, *A survey of output intensity and potential for depth of cure among light-curing units in clinical use.* Journal of Dentistry, 1999. **27**(3): p. 235-241.

332. Pianelli, C., et al., *The micro-Raman spectroscopy, a useful tool to determine the degree of conversion of light-activated composite resins.* J Biomed Mater Res, 1999. **48**(5): p. 675-81.

333. Knezevic, A., et al., *Degree of conversion and temperature rise during polymerization of composite resin samples with blue diodes.* J Oral Rehabil, 2001. **28**(6): p. 586-91.

334. Martin, F.E., *A survey of the efficiency of visible light curing units.* J Dent, 1998. **26**(3): p. 239-43.

335. Kramer, N., et al., *Light curing of resin-based composites in the LED era.* Am J Dent, 2008. **21**(3): p. 135-42.

336. Scranton, A.B., et al., *Polymerization Reaction Dynamics of Ethylene-Glycol Methacrylates and Dimethacrylates by Calorimetry.* Polymer, 1992. **33**(8): p. 1683-1689.

337. Braga, R.R. and J.L. Ferracane, *Alternatives in polymerization contraction stress management.* Critical Reviews in Oral Biology & Medicine, 2004. **15**(3): p. 176-184.

338. Garlapati, T., J. Krithikadatta, and V. Natanasabapathy, *Fracture resistance of endodontically treated teeth restored with short fiber composite used as a core material—An in vitro study.* Journal of prosthodontic research., 2017. **61**(4): p. 464-70.

339. Berger, H., et al., *Evaluation of effective material properties of randomly distributed short cylindrical fiber composites using a numerical homogenization technique.* Journal of Mechanics of Materials and Structures, 2007. **2**(8): p. 1561-1570.

340. Scribante, A., et al., *Travel beyond Clinical Uses of Fiber Reinforced Composites (FRCs) in Dentistry: A Review of Past Employments, Present Applications, and Future Perspectives.* Biomed Res Int, 2018. **2018**: p. 1498901.

341. Øysæd, H. and I.E. Ruyter, *Composites for use in posterior teeth: mechanical properties tested under dry and wet conditions.* Journal of Biomedical Materials Research, 1986. **20**(2): p. 261-271.

342. Mair, L.H. and R. Vowles, *The effect of thermal cycling on the fracture toughness of seven composite restorative materials.* Dent Mater, 1989. **5**(1): p. 23-6.

343. Algamaiah, H., et al., *The effect of aging methods on the fracture toughness and physical stability of an oxirane/acrylate, ormocer, and Bis-GMA-based resin composites.* Clin Oral Investig, 2020. **24**(1): p. 369-375.

344. Drummond, J.L. and E.E. Savers, *In vitro aging of a heat/pressure-cured composite.* Dent Mater, 1993. **9**(3): p. 214-6.

345. Fujishima, A., et al., *Fracture toughness and fracture behavior of composite resins for posterior restorative materials.* Jpn. J. Conserv. Dent, 1991. **34**: p. 45-53.

346. Janda, R., et al., *The effects of thermocycling on the flexural strength and flexural modulus of modern resin-based filling materials.* Dent Mater, 2006. **22**(12): p. 1103-8.

347. Tanaka, J., et al., *The application of fluorinated aromatic dimethacrylates to experimental light-cured radiopaque composite resin, containing barium-borosilicate glass filler--a progress in nonwaterdegradable properties.* Dent Mater J, 1993. **12**(1): p. 1-11.

348. Asmussen, E. and A. Peutzfeldt, *Flexural strength and modulus of a step-cured resin composite.* Acta Odontol Scand, 2004. **62**(2): p. 87-90.

349. Kakuta, K., et al., *Development of metal-resin composite restorative material. Part 4. Flexural strength and flexural modulus of metal-resin composite using Ag-In alloy particles as filler.* Dent Mater J, 2002. **21**(2): p. 181-90.

350. Manhart, J., et al., *Buonocore Memorial Lecture. Review of the clinical survival of direct and indirect restorations in posterior teeth of the permanent dentition.* Oper Dent, 2004. **29**(5): p. 481-508.

351. Opdam, N.J., et al., *A retrospective clinical study on longevity of posterior composite and amalgam restorations.* Dent Mater, 2007. **23**(1): p. 2-8.

352. Garoushi, S., et al., *Polymerization shrinkage of experimental short glass fiber-reinforced composite with semi-inter penetrating polymer network matrix.* Dent Mater, 2008. **24**(2): p. 211-5.

353. Pilliar, R.M., D.C. Smith, and B. Maric, *Fracture toughness of dental composites determined using the short-rod fracture toughness test.* J Dent Res, 1986. **65**(11): p. 1308-14.

354. ÜÇTAŞLI, S., H. Wilson, and L. Zaimoglu, *Variables affecting the fracture toughness of resin-based inlay/onlay systems.* Journal of oral rehabilitation, 1993. **20**(4): p. 423-431.

355. Wollff, E., *The effect of cross-linking agents on acrylic resins.* J Australian Dental Journal, 1962. **7**(6): p. 439-44.

356. McCabe, J.F. and H.J. Wilson, *Polymers in dentistry.* J Oral Rehabil, 1974. **1**(4): p. 335-51.

357. Gopferich, A., *Mechanisms of polymer degradation and erosion.* Biomaterials, 1996. **17**(2): p. 103-14.

358. Sakaguchi, R.L., et al., *Effects of polymerization contraction in composite restorations.* J Dent, 1992. **20**(3): p. 178-82.

359. Sankarapandian, M., et al., *Characterization of some aromatic dimethacrylates for dental composite applications.* J Mater Sci Mater Med, 1997. **8**(8): p. 465-8.

360. Moszner, N. and U. Salz, *New developments of polymeric dental composites.* Progress in Polymer Science, 2001. **26**(4): p. 535-576.

361. Lassila, L., et al., *Fracture behavior of Bi-structure fiber-reinforced composite restorations.* J Mech Behav Biomed Mater, 2020. **101**: p. 103444.

362. Vallittu, P.K., *Interpenetrating polymer networks (IPNs) in dental polymers and composites.* J ADHES SCI TECHNOL, 2009. **23**(7-8): p. 961-972.

363. Halvorson, R.H., R.L. Erickson, and C.L. Davidson, *The effect of filler and silane content on conversion of resin-based composite.* Dent Mater, 2003. **19**(4): p. 327-33.

364. Pfeifer, C.S., et al., *Characterization of dimethacrylate polymeric networks: A study of the crosslinked structure formed by monomers used in dental composites.* European Polymer Journal, 2011. **47**(2): p. 162-170.

365. Barszczewska-Rybarek, I., *A Guide through the Dental Dimethacrylate Polymer Network Structural Characterization and Interpretation of Physico-Mechanical Properties.* Materials, 2019. **12**(24): p. 4057.

366. Nguyen, J.F., et al., *Resin composite blocks via high-pressure high-temperature polymerization.* Dent Mater, 2012. **28**(5): p. 529-34.

367. Ruse, N.D. and M.J. Sadoun, *Resin-composite blocks for dental CAD/CAM applications.* J Dent Res, 2014. **93**(12): p. 1232-4.

Appendices

Appendix I: Publication 1

DENTAL MATERIALS 35 (2019) 1194–1203

Available online at www.sciencedirect.com

ScienceDirect

journal homepage: www.intl.elsevierhealth.com/journals/dema

Hardness and fracture toughness of resin-composite materials with and without fibers

Abdulrahman Alshabib[a,b], *Nick Silikas*[a,*], *David C. Watts*[a,*]

[a] *School of Medical Sciences, Division of Dentistry, University of Manchester, UK*
[b] *Department of Restorative Dentistry, College of Dentistry, King Saud University, Riyadh, Saudi Arabia*

ARTICLE INFO

Article history:
Received 6 April 2019
Received in revised form
16 May 2019
Accepted 16 May 2019

Keywords:
Resin composites
Fiber reinforcement
Water storage
Ethanol/water
Fracture toughness
Surface hardness

ABSTRACT

Objective. To investigate the surface micro-hardness (VHN) and fracture toughness (K_{IC}) of resin-composites, with and without incorporated short fibers, after solvent storage.

Methods. Three resin-composites incorporating fibers, additional to particle reinforcement, were examined: everX™, NovoPro Fill™ and NovoPro Flow™. Four composites were used as controls, with only particle reinforcement: Filtek bulk Fill™, Filtek bulk one™, Filtek XTE™, and Filtek Flow XTE™. For hardness measurement, materials were cured in 2 mm thick molds for 20 s by a LED source of average irradiance 1.2 W/cm^2. Specimens (n = 6/group) were stored dry for 1 h and then in either water or 75% ethanol/water for 1 h, 1 day and 30 days at 37 ± 1 °C. Vickers hardness was measured under a load of 300 g for 15 s. For fracture toughness (K_{IC}) measurements, single-edge-notched specimens (n = 6/group) were prepared: (32 × 6 × 3 mm) for 3-point bending and stored for 1 and 7 days in water at 37 °C. Fractured surfaces of fiber-reinforced composite were examined by scanning electron microscopy (SEM). VHN data were analyzed using three-way ANOVA, one-way ANOVA and the Tukey *post hoc* test ($p \leq 0.05$). K_{IC} data were analyzed by two-way ANOVA and one-way ANOVA and the Tukey post hoc test ($p \leq 0.05$). An independent t-test was used to detect differences ($\alpha = 0.05$) in K_{IC} between stored groups for each material.

Results. VHN decreased for all composites with storage time in both solvents, but more appreciably in 75% ethanol/water (an average of 20%). K_{IC} ranged from 2.14 (everX Posterior) to 0.96 NovoPro Flow) MPa. m$^{0.5}$. The longer storage period (7 days) had no significant effect on this property relative to 1 day storage.

Significance. Reinforcement with short fibers, and possibly matrix compositional differences, significantly enhanced the fracture toughness of EVX. However, for nano-fiber containing composites, there were no evident beneficial effects upon either their fracture toughness or hardness compared to a range of control composites. Water storage for 7 days of all these resin-composites produced no significant change in their K_{IC} values, relative to 1 day storage.

* *Corresponding authors at*: University of Manchester, School of Medical Sciences, Coupland 3 Building, Oxford Road, Manchester, M13 9PL, UK.
E-mail addresses: nick.silikas@manchester.ac.uk (N. Silikas), david.watts@manchester.ac.uk (D.C. Watts).
https://doi.org/10.1016/j.dental.2019.05.017
0109-5641/

Appendix II: The relationship between the mass and volumetric changes: Chapter 4

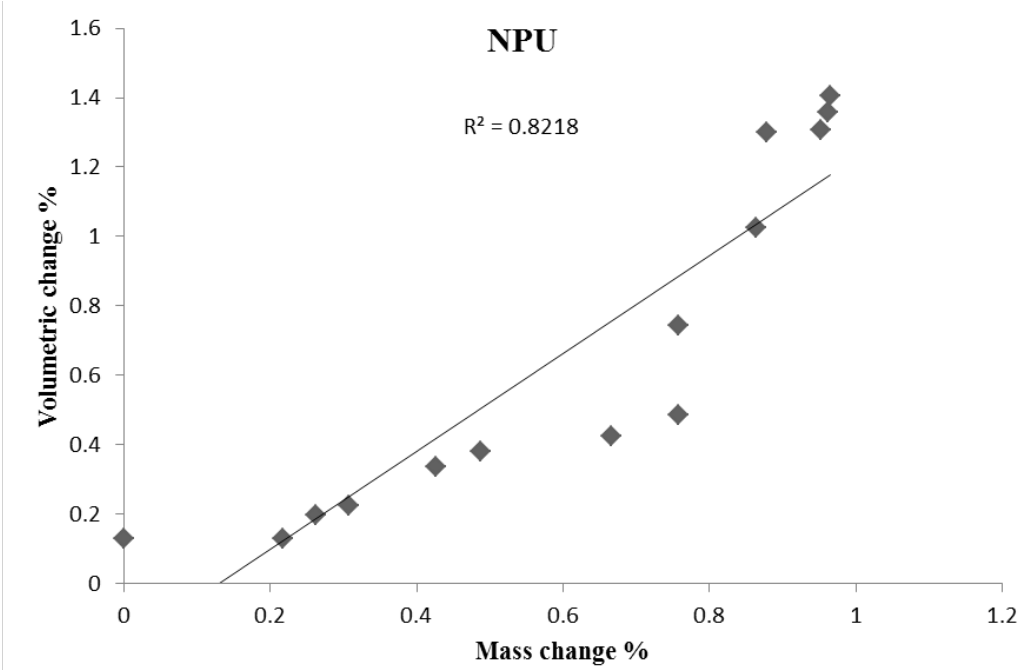

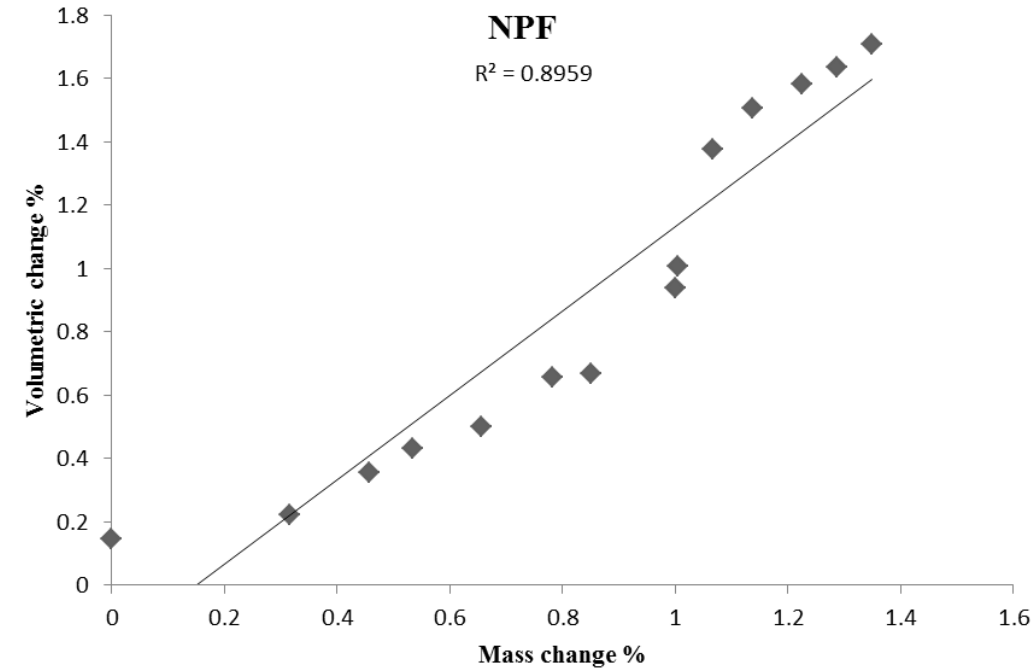

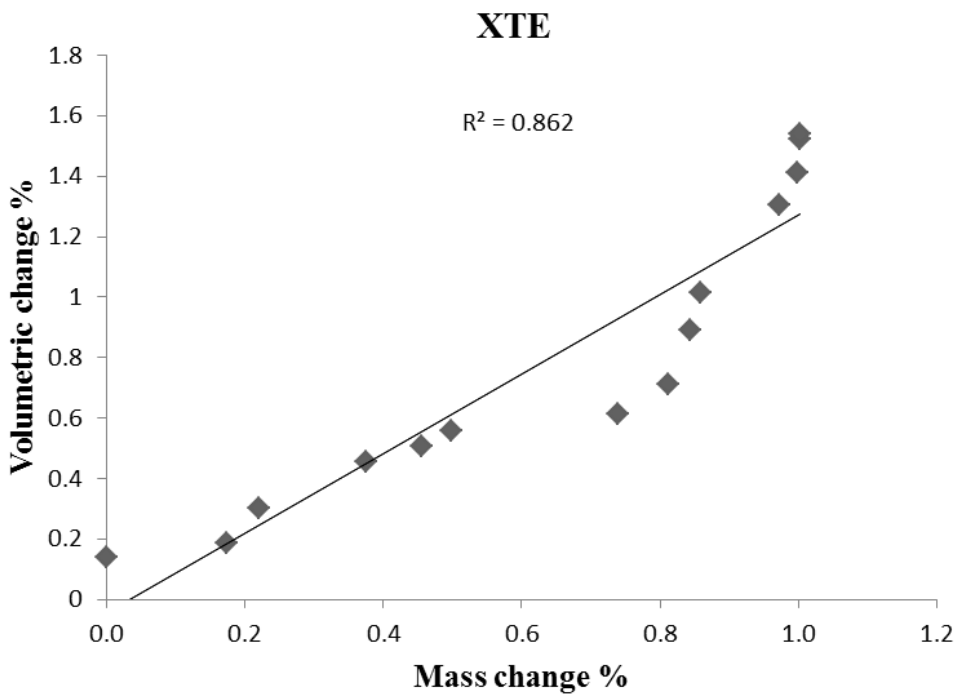
XTE
R² = 0.862
Volumetric change %
Mass change %
1.8
1.6
1.4
1.2
1
0.8
0.6
0.4
0.2
0
0.0
0.2
0.4
0.6
0.8
1.0
1.2

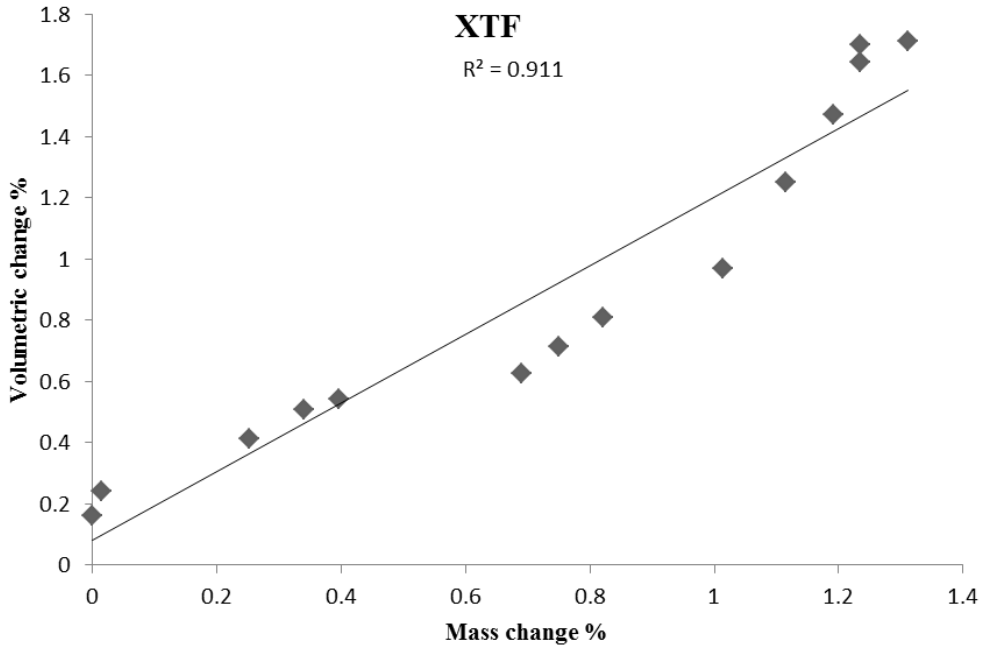
XTF
R² = 0.911
Volumetric change %
Mass change %
1.8
1.6
1.4
1.2
1
0.8
0.6
0.4
0.2
0
0
0.2
0.4
0.6
0.8
1
1.2
1.4

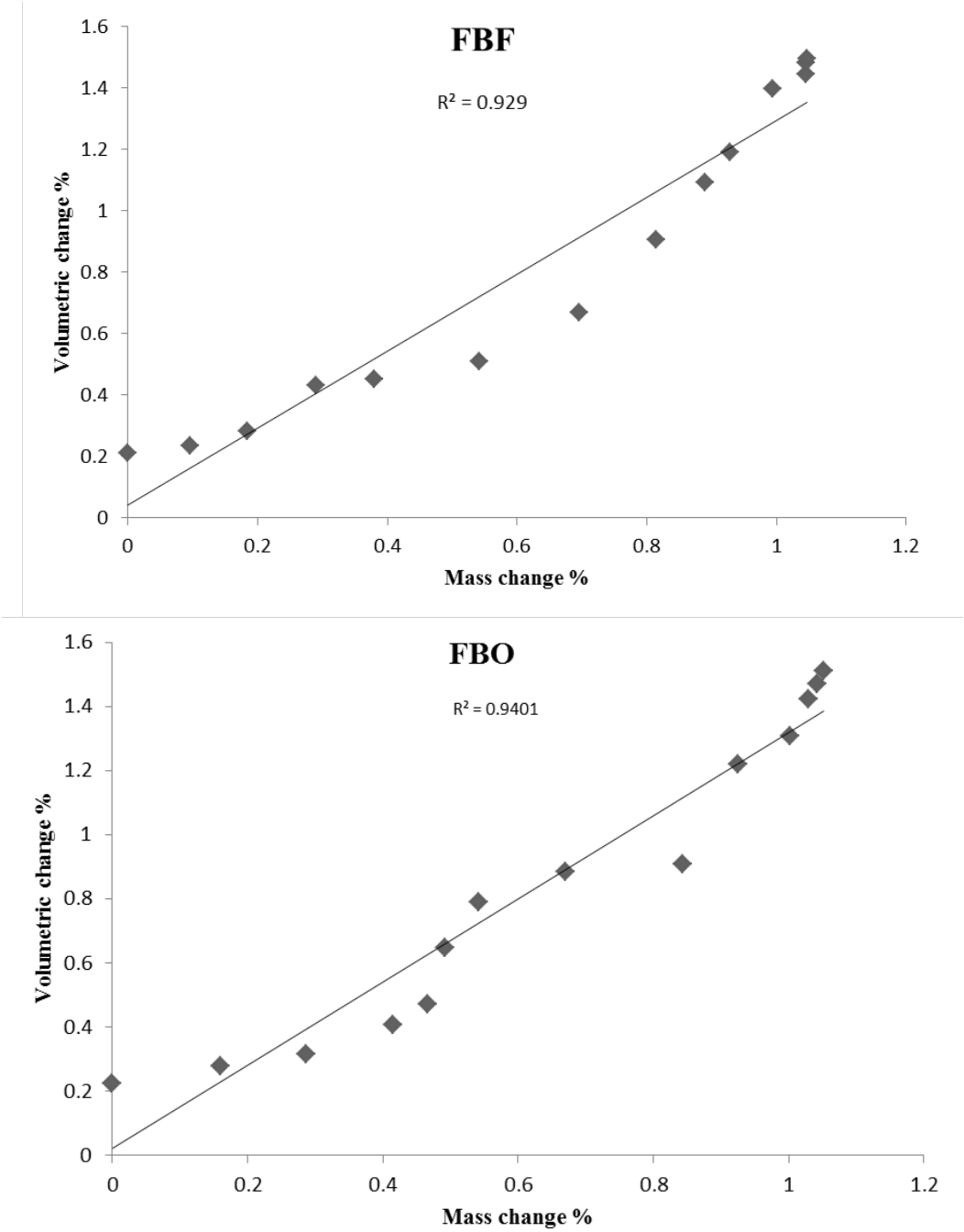

Figure 10-1 The relationship between the mass and volumetric changes during the 140d sorption period for all tested composites.

Appendix III: Publication 2

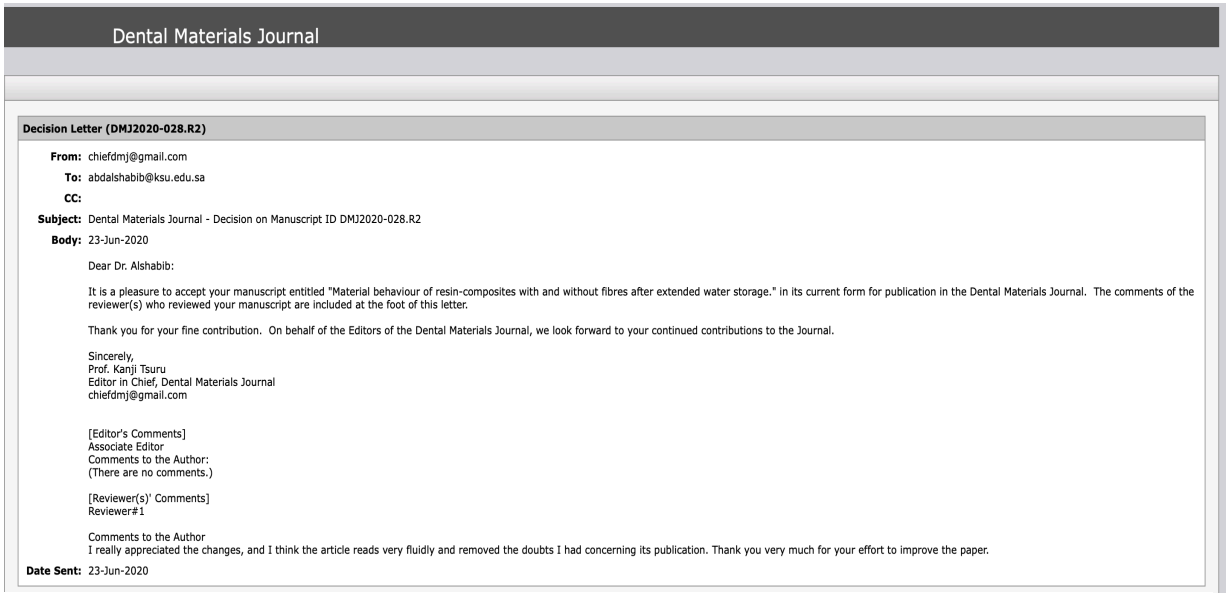

Dental Materials Journal

Decision Letter (DMJ2020-028.R2)

From: chiefdmj@gmail.com
To: abdalshabib@ksu.edu.sa
CC:
Subject: Dental Materials Journal - Decision on Manuscript ID DMJ2020-028.R2
Body: 23-Jun-2020

Dear Dr. Alshabib:

It is a pleasure to accept your manuscript entitled "Material behaviour of resin-composites with and without fibres after extended water storage." in its current form for publication in the Dental Materials Journal. The comments of the reviewer(s) who reviewed your manuscript are included at the foot of this letter.

Thank you for your fine contribution. On behalf of the Editors of the Dental Materials Journal, we look forward to your continued contributions to the Journal.

Sincerely,
Prof. Kanji Tsuru
Editor in Chief, Dental Materials Journal
chiefdmj@gmail.com

[Editor's Comments]
Associate Editor
Comments to the Author:
(There are no comments.)

[Reviewer(s)' Comments]
Reviewer#1

Comments to the Author
I really appreciated the changes, and I think the article reads very fluidly and removed the doubts I had concerning its publication. Thank you very much for your effort to improve the paper.

Date Sent: 23-Jun-2020

DENTAL MATERIALS JOURNAL 日本歯科理工学会 DMD
J-STAGE Powered by SCHOLARONE MANUSCRIPTS™

Material behaviour of resin-composites with and without fibres after extended water storage.

Journal:	*Dental Materials Journal*
Manuscript ID	DMJ2020-028.R1
Manuscript Type:	Original paper
Date Submitted by the Author:	15-May-2020
Complete List of Authors:	Alshabib, Abdulrahman; The University of Manchester School of Medical Sciences; King Saud University, School of Dentistry Hamad Algamaiah , Hamad; The University of Manchester, School of Medical Sciences ; King Saud University, School of Dentistry Silikas, Nick; The University of Manchester School of Medical Sciences Watts, David; The University of Manchester School of Medical Sciences; The University of Manchester Photon Science Institute
Keywords:	resin composites, fibre reinforced composite, water sorption, solubility, hygroscopic expansion
Categories:	Composite resin < Primary Research Field (Sub Field)